2018

Smart Classifiers and Bayesian Inference for Evaluating River Sensitivity to Natural and Human Disturbances: A Data Science Approach

Kristen Underwood
University of Vermont

SMART CLASSIFIERS AND BAYESIAN INFERENCE FOR EVALUATING RIVER SENSITIVITY TO NATURAL AND HUMAN DISTURBANCES: A DATA SCIENCE APPROACH

A Dissertation Presented

by

Kristen L. Underwood

to

The Faculty of the Graduate College

of

The University of Vermont

In Partial Fulfilment of the Requirements
For the Degree of Doctor of Philosophy
Specializing in Civil and Environmental Engineering

October, 2018

Defense Date: August 24, 2018
Dissertation Examination Committee:

Donna M. Rizzo, Ph.D., Advisor
Mandar M. Dewoolkar, Ph.D., Co-Advisor
Beverley C. Wemple, Ph.D., Chairperson
Arne Bomblies, Ph.D.
Julia N. Perdrial, Ph.D.
Cynthia J. Forehand, Ph.D., Dean of the Graduate College

ABSTRACT

Excessive rates of channel adjustment and riverine sediment export represent societal challenges; impacts include: degraded water quality and ecological integrity, erosion hazards to infrastructure, and compromised public safety. The nonlinear nature of sediment erosion and deposition within a watershed and the variable patterns in riverine sediment export over a defined timeframe of interest are governed by many interrelated factors, including geology, climate and hydrology, vegetation, and land use. Human disturbances to the landscape and river networks have further altered these patterns of water and sediment routing.

An enhanced understanding of river sediment sources and dynamics is important for stakeholders, and will become more critical under a nonstationary climate, as sediment yields are expected to increase in regions of the world that will experience increased frequency, persistence, and intensity of storm events. Practical tools are needed to predict sediment erosion, transport and deposition and to characterize sediment sources within a reasonable measure of uncertainty. Water resource scientists and engineers use multidimensional data sets of varying types and quality to answer management-related questions, and the temporal and spatial resolution of these data are growing exponentially with the advent of automated samplers and *in situ* sensors (i.e., "big data"). Data-driven statistics and classifiers have great utility for representing system complexity and can often be more readily implemented in an adaptive management context than process-based models. Parametric statistics are often of limited efficacy when applied to data of varying quality, mixed types (continuous, ordinal, nominal), censored or sparse data, or when model residuals do not conform to Gaussian distributions. Data-driven machine-learning algorithms and Bayesian statistics have advantages over Frequentist approaches for data reduction and visualization; they allow for non-normal distribution of residuals and greater robustness to outliers.

This research applied machine-learning classifiers and Bayesian statistical techniques to multidimensional data sets to characterize sediment source and flux at basin, catchment, and reach scales. These data-driven tools enabled better understanding of: (1) basin-scale spatial variability in concentration-discharge patterns of instream suspended sediment and nutrients; (2) catchment-scale sourcing of suspended sediments; and (3) reach-scale sediment process domains. The developed tools have broad management application and provide insights into landscape drivers of channel dynamics and riverine solute and sediment export.

CITATIONS

Material from this dissertation has been published in the following form:

Underwood, K. L., Rizzo, D. M. Schroth, A. W. Dewoolkar, M. M.. (2017). Evaluating spatial variability in sediment and phosphorus concentration-discharge relationships using Bayesian inference and self-organizing maps. Water Resources Research. doi: 10.1002/2017WR021353.

ACKNOWLEDGEMENTS

The river has not only been a focus of my professional and academic careers, it is an apt metaphor for life's journey - sometimes flowing fast and turbulent, other times more quiescent, allowing for contemplation and reflection. In this present eddy of life, I would like to extend my thanks to those who have inspired this body of work and helped me to complete it. Foremost, I am indebted to my advisor and mentor, Donna Rizzo, for her dedication, expert knowledge, and artful guidance. I am grateful to my co-advisor, Mandar Dewoolkar, for his generosity of spirit and expert navigation of the academic process. I appreciate the contributions of my additional committee members, Beverley Wemple, Arne Bomblies, and Julia Perdrial, who have helped to guide this research and offered critiques that have greatly improved the manuscripts. Co-authors Andrew Schroth and Mike Kline were instrumental to the research presented in Chapters 2 and 4. Andrew's insightful comments were helpful in posing a link between our results and the bloom dynamics of Lake Champlain. Mike's contributions to river science and conservation have led to much improved flood resilience for Vermont communities. My previous river work under Mike's leadership and in the company of many professional colleagues too numerous to mention was instrumental in my decision to return to graduate school to learn new statistical techniques for analysis of complex natural systems. Early in my return to academics, Joan "Rosie" Rosebush, helped me to clear the cob-webs from my neural synapses to refresh my calculus skills. I am grateful for her encouragement and expert tutelage.

The field monitoring underlying our research based in the Mad River watershed would not have been possible without the support of my colleague, now post-doctoral scholar, Scott Hamshaw. He preceded me down-river in this doctoral journey, and has been gracious to point out the “rocks” and “strainers”, guiding me toward the smooth and clear water. To other fellow graduate students, I thank you for your companionship and helpful advice along the way: Jody Stryker, Justin Guilbert, Nikos Fytilis, John Hanley, Ian Anderson, Luke Howard, Jim Montague, Saleh Alghamdi, Matt Trueheart, Jeremy Matt, Lindsay and Bobby Worley and Doug Denu. We were aided in the field and lab by many capable students and interns, including Jordan Duffy, Alex Morton, Baxter Miatke, Kira Kelley, Marisa Rorabaugh, Hanna Anderson, Thomas Bryce and Thomas Adler. It was fun to share this brief time with you and I will enjoy seeing your many contributions to the water resources fields in years to come. Landowners and stakeholders in the Mad River valley were especially welcoming, and were kind to grant us permission to sample and monitor on their properties.

Finally, this dissertation is dedicated to my parents, John and Peg, who continue to model integrity, community service, and intellectual curiosity.

.

TABLE OF CONTENTS

LIST OF FIGURES

LIST OF TABLES

CHAPTER 1. INTRODUCTION AND COMPREHENSIVE LITERATURE REVIEW

Motivation and Research Objectives

Enhanced sediment loading from rivers is a widespread phenomenon, associated with significant impacts to instream conditions as well as to receiving water bodies including both freshwater lakes and coastal estuaries (National Research Council, 2000). In the United States, more than 140,000 river miles have been identified nationally as threatened or impaired by sediment (USEPA, 2016). Sediment loading may cause a variety of impacts, including degraded instream and near-shore habitats, compromised drinking water quality, and loss of reservoir capacity. Nutrients are often associated with sediment loaded to rivers from streambank erosion and surface runoff (Dubrovsky et al., 2010; Howarth et al., 1996; National Research Council, 2000), either as a result of current land use practices or legacy accumulations (James, 2013). Excess levels of phosphorus and nitrogen, can lead to enhanced eutrophication of receiving water bodies, fish kills from hypoxia, and harmful algae blooms that may interfere with drinking-water and recreational uses and present a human health risk (Anderson et al., 2002). Over 112,000 river miles in the US have been impacted by nutrients (USEPA, 2016). In addition to sediment impacts on water quality, excessive rates of landscape erosion and channel adjustment present a challenge to society in terms of erosion hazards to infrastructure, compromised public safety, and degraded ecological integrity (Rapp & Abbe, 2003; Poff et al., 1997; Pringle, 2003).

A better understanding of sediment transport dynamics would help to identify critical catchment locations and time periods responsible for disproportionate fluxes of

sediment and associate pollutants. Knowledge of these so called "hot spots" and "hot moments" (McClain et al., 2003; Heathwaite et al., 2000) would help to inform best management practices for reductions in sediment and nutrient loading and to mitigate fluvial erosion hazards.

Water resource managers and stakeholders need tools to model and predict sediment erosion, transport and deposition and to characterize sediment sources within a reasonable measure of uncertainty and help optimize river management. However, rivers are complex, nonlinear systems (Phillips, 2003) and sediment dynamics exhibit high variability over spatial and temporal scales (Fryirs, 2013; Walling, 1983; Dubrovsky et al., 2010). Spatial variability exists in the nature, distribution and magnitude of both source areas and transport pathways. Heterogeneous properties of topography, soils, vegetation and land use influence transport and transfer pathways and mechanisms, and moderate a complex cascade (Burt & Allison, 2010) of sediment and associated nutrients through the catchment (Fryirs, 2013; Dubrovsky et al., 2010). Glacially-conditioned, mountainous rivers are particularly vulnerable to adjustment and sediment export due to their topographic setting, close coupling of hillslope and channel processes, and reworking of glacial legacy sediments (Church & Ryder, 1972; Ballantyne, 2002). Human disturbances to the landscape and river networks have also altered hydrologic and sediment connectivity within catchments with resulting controls on source and sink dynamics (Walter & Merritts, 2008; Noe & Hupp, 2005). Temporally, processes governing the flux of sediment and nutrients are driven by stochastic inputs of climate and hydrology (Benda & Dunne, 1997). Interannual changes in climate or land cover, seasonal fluctuations in hydrology, vegetation, biological uptake, and human activities on

the landscape, and event-based changes in hydrology influence both the production and transport of nutrients and sediment (Dubrovsky et al., 2010), leading to considerable variability in sediment/nutrient flux over time. Recovery times from natural and human perturbations, and in response to extreme floods (Costa & O'Connor, 1995), may extend 100 years or more in humid temperate regions (Wolman and Gerson, 1978), such as the Northeastern United States.

Given the complexity of river dynamics, stakeholders face significant challenges when trying to prioritize the allocation of limited resources to achieve reductions in sediment and pollutant loading or identifying infrastructure at enhanced risk of failure from fluvial erosion during extreme flood events. Water resource scientists and engineers use multidimensional data of varying types and quality to model sediment dynamics and answer management-related questions, and the temporal and spatial resolution of this data is growing exponentially with technological advances. For example, with the advent of automated samplers and *in situ* sensors, more studies are making use of high-frequency monitoring data (Bende-Michl et al., 2013; Isles et al., 2015). Similarly, the increasing availability of high-resolution topographic data sourced from satellite imagery, airborne and terrestrial light detection and ranging systems, and unmanned aerial systems photogrammetry (Bizzi & Lerner, 2013; Hamshaw et al., 2017), has enabled remote-sensing methods for assessing erosion and deposition in the active river corridor. This increasing availability of data has the potential to improve model predictions for improved water resource management.

These high-resolution spatial and temporal data sets (i.e., "big data") require new computational tools for data reduction and analysis (Kirchner et al., 2004) that are able to

incorporate the nonlinear nature of hydrologic and sediment/solute responses (so called "gray-box" methods of Kirchner, 2006). Physically-based, distributed models are able to forecast sediment concentration and flux; but the accuracy and calibration are resource-intensive, making such models typically less transferable among watersheds or regions (Todini, 2007). On the other hand, data-driven statistical models can be more readily implemented and have the appeal of representing system complexity in simple ways (McDonnell et al., 2007), although they are more limited in their prediction capabilities.

In consideration of the nonlinear complexity of sediment dynamics, this dissertation examines the application of machine-learning clustering or classification algorithms (so-called, smart classifiers) and Bayesian inference as two such data-driven approaches to improve our understanding of riverine sediment flux. The following questions have motivated this research:

1. Can smart classifiers, utilizing machine-learning algorithms, improve upon conventional (parametric) classification methods to mine watershed metrics and predict concentration-discharge (C-Q) relationships associated with sediment and sediment-related constituents?

2. Can Bayesian techniques model threshold effects in C-Q regressions to improve the utility of regression metrics to discern between hydrologically-dominated and biogeochemically-dominated phases of constituent export (adapted from Musolff *et al.*, 2015 and Thompson *et al.*, 2011)?

3. Can Bayesian inference be leveraged to address uncertainty in un-mixing models to discern the relative contributions of suspended sediment sources at a watershed scale?

4. Given that sediment sources and sinks along a river network are highly variable in both space and time, can "hot spots" and "hot moments" be predicted using smart classifiers?

5. Can the process of training and testing data-driven models elicit information regarding the relative importance of various hydrologic and geomorphic drivers of sediment erosion and deposition in catchments, and scale-dependent phenomena, thereby guiding water resource management priorities?

Organization of Dissertation

Following a review of the current literature, I illustrate the application of smart classifiers and Bayesian statistical techniques to multidimensional data sets characterizing riverine-sediment source and flux at three different scales: basin, catchment, and reach (Chapters 2 – 4). As a test bed for these tools, we focus our applications on the glacially-conditioned, montane regions of Vermont in the Northeastern United States. Chapter 2 examines sediment and nutrient concentration-discharge dynamics at a basin scale, using the Lake Champlain Basin study region, by applying a framework of Bayesian statistics and neural network clustering. I use a Bayesian segmented linear regression approach to identify different functional stages of sediment and phosphorus export, where "reactive" versus "hydrologically-driven" stages of constituent export are dominant. I then apply a nonparametric clustering and data

visualization approach, using a Self-Organizing Map (SOM), to yield insights into nonlinear combinations of independent variables that appear to be driving basin-scale differences in mean annual flux and concentration of sediment and phosphorus. Spatial variability in sediment and nutrient flux across the basin is reviewed, along with management implications for the tributary watersheds in the context of ecological balance in the receiving water, Lake Champlain.

At the catchment scale, in Chapter 3, I illustrate the value of Bayesian statistical techniques to address uncertainty in an un-mixing model to discriminate between surface and subsurface sources of fine particulates (clay, silt, fine sand) carried in suspension by a river. The study focuses on the Mad River watershed in north-central Vermont and compares suspended sediment flux between catchment and tributary scales during moderate-sized, mid-summer storm events, and examines summer versus autumn seasonal differences at the tributary scale.

Chapter 4 demonstrates the utility of SOMs for data visualization and interpretation to characterize and predict differences in reach-scale fluvial geomorphic form and dominant adjustment processes in response to natural and human perturbations. The process of SOM training identifies a parsimonious set of geomorphic and hydraulic variables that meaningfully separate reaches into sediment process domains constituting net sources or sinks of coarse and fine sediment on a mean annual temporal scale. The data set comprises stream geomorphic data from six Vermont catchments distributed across several biogeophysical regions, and SOM outcomes represent proof-of-concept for future automation of classifications leveraging state-wide geomorphic databases. Finally,

Chapter 5 concludes with a summary of this dissertation and identifies opportunities for future research.

An enhanced understanding of river sediment sources and dynamics is important for stakeholders, and will become more critical under a nonstationary climate, as sediment yields are expected to increase in regions of the world that will experience increased frequency, persistence, and intensity of storm events (IPCC, 2014), including the northeastern US (Collins, 2009; Guilbert *et al*. 2015; Guilbert *et al*. 2014). Data-driven statistical methods and smart classifiers, similar to those demonstrated in the chapters below, have great utility for representing system complexity, and can be readily implemented in an adaptive management context to complement process-based models.

Sediment Connectivity at the Catchment Scale

Sediment is a critical component of the physical framework of catchments and plays an important role in biogeochemical cycling of nutrients and other elements. While the classical delineation of a catchment into the source, transfer, and response zones of Schumm (1984) is useful for characterizing sediment sourcing and storage at a broad scale (Figure 1.1), greater refinement of landscape variability is needed for optimal management of water resources.

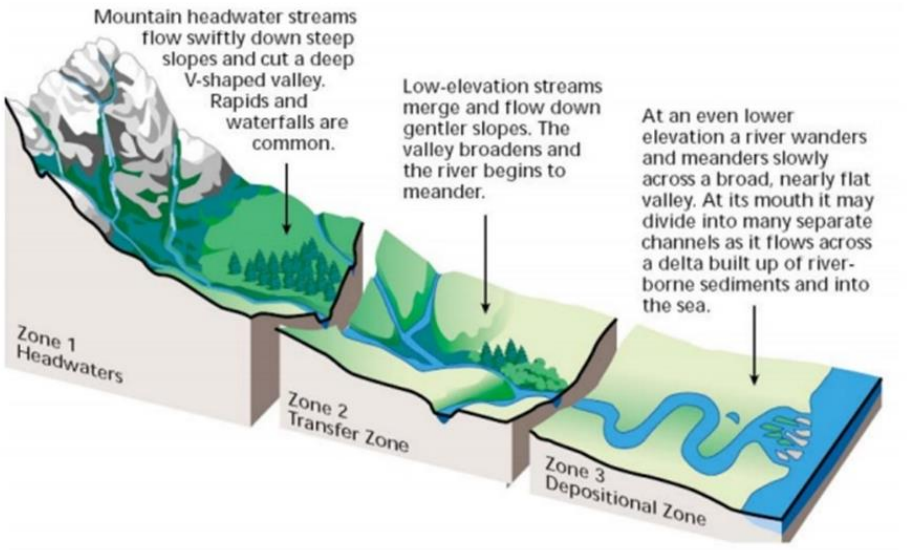

Figure 1.1. Sediment source (Zone 1), transfer (Zone 2) and response (Zone 3) regions of a catchment classified by Schumm (1984), as modified by the Federal Interagency Stream Restoration Working Group (FISRWG, 1998).

Sediment connectivity has been defined as the "connected transfer of sediment from a source to a sink in a system via sediment detachment and sediment transport, controlled by how the sediment moves between all geomorphic zones in a landscape" (Bracken, *et al.*, 2014). Sediment movement through the catchment has been conceptualized as a cascade (Dietrich & Dunne, 1978; Burt & Allison, 2010), whereby sediment is alternately stored and mobilized on its journey from the headwaters to the watershed outlet as linkages between landscape units are disconnected and reconnected, and the strength of those linkages is altered (Fryirs *et al*., 2007; Fryirs, 2013). Sediment connectivity is controlled by the physical and topographic nature of landscape units that make up a catchment, their configuration, and the dynamic flow paths between them (Hooke, 2003; Fryirs, 2013).

Thorp et al. (2006) has conceptualized the catchment as a mosaic of hydrogeomorphic units of relatively uniform composition, structure, and function that differentially impact sediment connectivity. In mountainous catchments, bedrock influences sediment connectivity by controlling the overall topography and relief, which in turn controls valley confinement, offering frequent vertical and lateral armoring in the river networks draining the landscape. In the Northeastern US, surficial sediments and soils present in the landscape reflect the glacial and post-glacial history of the region, and the diversity of sediments left behind by multiple glacial advances and retreats, temporary high-elevation lakes, and outwash channels (Stewart & MacClintock, 1969). In the current hydrologic regime, surficial sediments have been reworked to varying extents by gravitational and fluvial processes, yielding colluvial and alluvial deposits and erosional landforms.

Macro-scale hydrogeomorphic units characterizing humid-temperate, mountainous provinces include:

- **Slopes** are moderate to extremely steep (>2%) land surfaces that dominate the catchment aerial extent. In the headwaters, hillslope topography is largely controlled by the structure and composition of the underlying bedrock. Slopes can also be found at the ecotones between hydrogeomorphic units such as where terraces grade downhill to meet an adjacent floodplain, or where the floodplain transitions to the channel at a streambank.
- **Plains** are shallow-gradient (<3%) land surfaces of varying genesis and extent**. Floodplains** are low-lying land areas present along segments of the river network in catchment areas characterized by lesser longitudinal gradients and greater valley confinement ratios (>2; VCR = valley width / channel width). Floodplains are composed predominantly of contemporary or Quaternary alluvial deposits, and may be punctuated along their length by bedrock-controlled valley constrictions or channel-spanning bedrock exposures. **Terraces** are higher in elevation than floodplains and are frequently found along the margins of river valleys at the transition between hillslope and floodplain environments. Terraces are formed either by glacial processes (e.g., kame terraces, kame delta complexes, post-glacial lake deposits and deltas) or more recent fluvial processes. Abandoned stream terraces have been formed through the process of floodplain development in Quaternary or Holocene times (Stewart & MacClintock, 1969).

- **Fluvial network**- The fluvial network comprises the complete river network from disperse points of initiation in the headwaters to the catchment outlet, and includes the subunits of the active channel/ hyporheic zone, the parafluvial zone and the riparian zone. Ephemeral or perennial elements of the fluvial network traverse and connect all of the other hydrogeomorphic unit types composing the catchment. The fluvial network is dominated by alluvial sediments; however it is not uncommon for glacial tills to be exposed along the banks of headwater streams, and for stream segments to impinge upon hillslopes or terraces composed of glacio-lacustrine, glacio-fluvial sediments or bedrock.

Flow paths connect these hydrogeomorphic units, and represent linkages between sediment sources and sinks. They operate both within and between hydro-geomorphic units – at local and zonal scales (Harvey, 2002) and can be classified on a continuum between diffuse (e.g., distributed overland flow) and concentrated (e.g., ephemeral or perennial channel) (Poeppl, et al., 2012; Croke et al., 2005). Source-sink linkages can also be classified on a continuum from fully-connected to disconnected over varying timescales (Harvey, 2002; Fryirs et al., 2007).

Sediment flow paths in humid temperate regions are driven both by gravitational processes (e.g., debris slides and debris flows) and by hydrologic processes (e.g., rill and gully erosion, streambank erosion) – with aeolian processes constituting a driver of relatively minor significance in the current regime. Sediment flow paths are predominantly a function of hydrologic connectivity, as saturation overland flow regimes dominate (Dunne and Black, 1970; Croke et al., 2013; Bracken & Croke, 2007). Given

the latitude and elevation of mountainous catchments of the Northeast, solid states of water and related processes (frost, freeze-thaw cycles, snow pack, anchor ice, ice jams) provide additional controls on hydrologic (and sediment) connectivity (Turcotte et al., 2011; Prowse & Culp, 2003).

Flow paths operate in four dimensions – vertical, lateral, longitudinal and temporal (hydrologic) (Ward, 1989). On slopes, processing of sediment in the vertical dimension is minimized in favor of the lateral and longitudinal directions, given the shallow depths to confining layers and steep gradients. Vertical processing is predominant on terrace units of glacial-fluvial origin (e.g., kame terraces, delta and fan deposits), given the planar surfaces and the highly permeable nature of sediments comprising the terraces. In contrast, vertical processing of sediment on terraces of glacio-lacustrine origin is minimal due to the predominance of fine-grained silts and clays comprising these terraces and their low infiltrative capacity (e.g., hydrologic soil groups C and D; USDA, 1986). Floodplains are dominated by lateral and longitudinal flow paths. In the fluvial network of mountainous catchments, longitudinal transport of sediment, including the upstream-to-downstream linkages and tributary-to-main stem linkages (Fryirs, 2007), is a dominant flow path, though significant sediment is processed in the lateral dimension through interactions with the parafluvial and riparian subunits.

At a given point along a flow path, the power to entrain and transport sediment is directly proportional to the gradient of that path and the contributing area. At a broader scale, the juxtaposition of slopes and plains and the sequencing of these hydrogeomorphic units along the flow path will govern the dominant process of sediment transport: either erosional or depositional. Transitioning from a plain to a downhill slope,

stream power increases and the process would tend toward erosional (as mediated by the erosion resistance of the boundary materials which itself is a complex function of many variables including composition, grain size, and vegetation) (Figure 1.2a). Conversely, when transitioning from a downhill slope to a plain, stream power decreases, transport capacity decreases, and deposition is induced (Figure 1.2b). The configuration and sequencing of hydrogeomorphic units and flow paths along the fluvial network are unique to a given catchment and to a specified hydrologic domain.

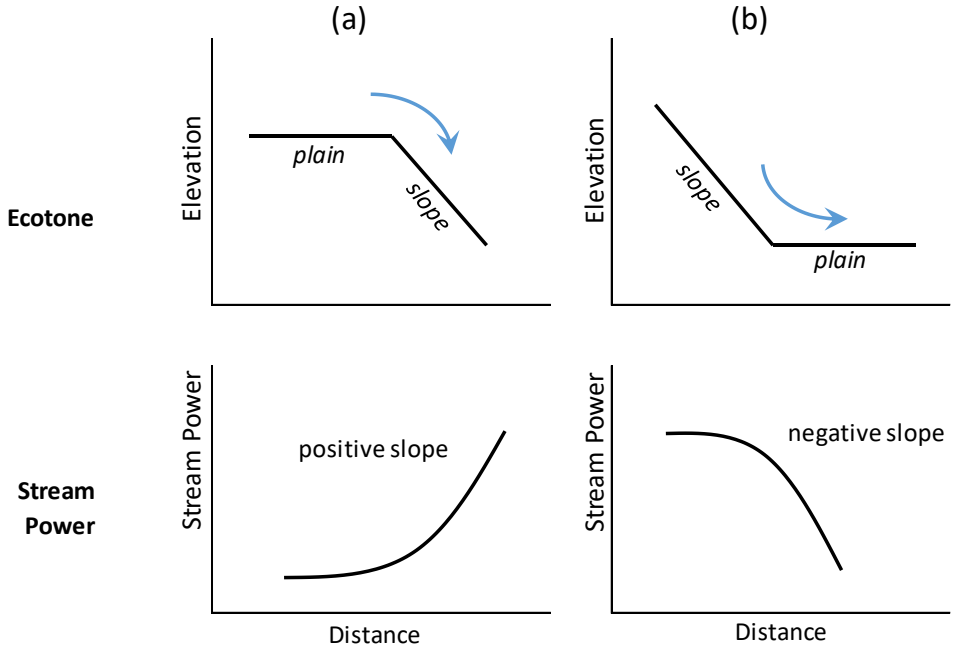

Hydrogeomorphic Unit	Erosional Feature	Depositional Feature
slopes:	landslides, rills	debris cones/ alluvial fans
plains:	gullies	deltas, terraces
fluvial network:	headcuts, cut banks	aggradational bars, slackwater deposits

Figure 1.2. Conceptual diagram of processes active at the ecotone between hydrogeomorphic units that manifest in erosional or depositional features.

Hot spots and hot moments

The rate of sediment transfer can be especially important at the boundaries between hydrogeomorphic units (or ecotones), constituting a disproportionately high rate of transfer, or "hot spot" (McClain, 2003). Through hot-spot processes, a relatively small areal percentage of the catchment may be responsible for a majority of the eroded sediment volume. For example,

- **Landslides** commonly form at the ecotone between hillslopes and channels (Figure 1.a). Landslides are episodic, and most often controlled by the interacting forces of gravity and hydraulic shear from streamflow at the toe of the slope. Microscale hydrology (e.g., saturation effects on pore pressure and failure mechanisms) and nature and degree of vegetative cover also play mediating roles.
- **Eroding streambanks** form at the ecotone between floodplains (or terraces) and channels. Streambanks yield sediment through a combination of gravitational (vertical) forces and shear (lateral/longitudinal) forces – mediated by vegetative effects (roughness) and micro-scale hydrology (e.g., matric potential).
- **Gullies** commonly form at the ecotone between terraces and floodplains. Steep terrace side slopes result in increased transport capacity; soils comprising these terraces are often unconsolidated and erodible, or may be comprised of finer grains (glaciolacustrine).
- **Rills** form along slopes where overland flow is concentrated and runoff velocity exceeds the threshold of erosion of the underlying sediment (mediated by vegetation).

- **Knickpoints** (head-ward migrating head cuts) form in coarse bed sediment within the fluvial network where a local increase in slope has manifest as a result of local erosion or deposition patterns (mediated by large woody debris and/or bedrock exposures).

These critical source areas (Heathwaite *et al*., 2000) – where sediment (or sediment-bound pollutant) sources overlap with an activated hydrologic transport pathway(s) - may also vary in time (hot moments; McClain, 2003). Within a normal flow year, the bankfull flow event (~$Q_{1.5}$) is responsible for a majority of the sediment mobilized through the river network. Gullies along terrace side slopes are initiated or enlarged during summer convective storms by intense rainfall and runoff. Extreme events may represent a hot moment on a multi-annual time scale, that are responsible for mobilizing additional sediment. For example, Tropical Storm Irene (August 2011) was a >200-year event that resulted in significant rejuvenation of landslides and alluvial fan deposits along New England's stream channels and floodplains (Yellen *et al*., 2014; Dethier, 2016).

Cold spots and cold moments

Various landforms may impede hydrologic and sediment flow paths; these "cold spots" operate at various spatial scales and may be composed of glacial or paraglacial sediments (Church & Ryder, 1972). Cold spots may persist as either long-term sinks or short-term stores of sediment (Meade, 1982; Fryirs, 2013), and the length of these cold moments is highly variable. The role of cold spots and cold moments in the overall sediment cascade will be a function of their position in the catchment relative to other landscape units (e.g., context, degree of [de]coupling) as well as the hydrologic domain

(from event to regime scales) (Harvey, 2002; Michaelides & Wainright, 2002; Hooke, 2003; Fryirs, *et al.*, 2007). With the onset of a flow event of sufficient magnitude, all or portions of these sediment *sinks* located proximal to active (or newly-activated) hydrologic flowpaths may become *sources* of sediment – thus, cold spots can be readily transformed into hot spots.

Various macro-to micro-scale landscape features can serve as impediments to hydrologic and sediment flow paths (Bracken & Croke, 2007) - termed "buffers, barriers and blankets" by Fryirs *et al.* (2007):

- **Buffers** are "landforms that prevent sediment from entering the channel network" serving as impediments to lateral and longitudinal flow paths (Fryirs et al., 2007). Floodplains and terraces can serve as buffers, particularly when they are positioned between a hillslope source of sediment and the channel at the transition from steep, valley-confined settings and much lower-gradient, unconfined settings. These deposition zones often take the form of alluvial fans or debris cones (Figure 1.2b) that were originally deposited during a previous, more intense hydrologic regime (Bierman et al., 1997). In the current regime, extreme storm events result in episodic rejuvenation of these landforms (Jennings, 2001; Bierman et al., 1997). Macro-scale buffers are generally found in the middle to lower reaches of a watershed. At the meso- to micro-scale, discontinuous pockets of floodplain can serve as localized buffers along headwater tributaries in discrete locations where valley confinement and longitudinal gradients are relaxed. Sediment can be tied up in these buffer features for significant timeframes (up to

10^3 years), and overtopping or reworking of these landform sediments generally requires an extreme flood event (Fryirs *et al.,* 2007).

- **Barriers** are landforms or features that disconnect sediment transport in the longitudinal direction (Fryirs et al., 2007). Natural barriers include macro- to micro-scale features operating in the floodplain and fluvial network, and include bedrock nickpoints or gorges and bedrock-controlled valley pinch points that control local base levels in the longitudinal profile of the channel. Aggradation is induced upstream of these features generating sediment stores that persist over long time scales (10^3 years) and contribute to floodplain genesis. These features are highly resistant to erosion and can be considered permanent over historic timescales. At smaller timescales (up to 10^2 years) and localized spatial scales within the active channel and parafluvial zone, sediment stores are built behind channel-spanning large woody debris jams and boulder grade controls. These features are common in forested headwater channels where the channel widths are generally less than the typical height of trees and where bedrock-cascade and boulder step/pool channel bedforms are common (Benda et al, 2005; Montgomery & Buffington, 1997). Sediment slugs (often generated by colluvial processes along closely-coupled hillslopes) can also serve as transient barriers to sediment connectivity and will eventually be reworked by future high-flow events. Channel segments of markedly reduced transport capacity (e.g., braided channels, or single-thread channels with high width/depth ratios) can also cause discontinuities in downstream sediment transport. These channel forms are common at transitions from hillslopes to floodplains or from hillslopes to alluvial

fans or other terrace features. Debris jams, sediment slugs, and braided channel segments are frequently reworked and can induce sudden channel avulsions or break-outs in higher-flow conditions (Montgomery & Buffington, 1997; Williams & Costa, 1998; Fryirs *et al.*, 2007).

- **Blankets** are features that influence sediment movement in the vertical dimension at the surface-subsurface interface, in floodplains and in the fluvial network (Fryirs et al., 2007). In the floodplain, blankets can include such meso- to micro-scale features as sediment sheets or slackwater deposits which may persist for up to hundreds of years and are reworked periodically by higher-flow or extreme events. In the fluvial network, blankets may include channel-bed armoring in the stream, or fine-grained sediment infill in the channel bed or local depressions of the stream or parafluvial zone. These features of the active channel and parafluvial zone are more frequently reworked. Cobble or gravel bed armoring will persist until a flow of sufficient transport capacity can breach the armoring (10^0 to 10^2 years). Fine-grained stores of sediment on bars in the channel or in localized depressions in the parafluvial zone (e.g., bankfull-accesible flood chutes) are easily reworked by flows of sufficient stage (event-based to decadal timescales) and thus represent shorter-term stores of sediment. Between mobilizing events, these fine-grained blanket features reduce the exchange rates of water and thereby influence sediment / nutrient/ element cycling in the hyporheic zone.

Sediment (dis)connectivity and the sediment delivery ratio

The degree to which sediment flow paths are connected, and not blocked by buffers, barriers and blankets, will determine the extent of the catchment which is directly contributing sediment to the fluvial network and the efficiency with which that sediment is being conveyed to the catchment outlet over a given timeframe. The "effective catchment area" (Harvey, 2002) – or sum of the activated hydrologic (and sediment) transport pathways - varies with time (event, season, water year, climate/hydrologic regime) (Poff *et al.*, 1997; Thoms & Parsons, 2003) and is further conditioned by magnitude and frequency patterns (Wolman & Miller, 1960) and antecedent states.

Variable source area concepts advanced by Dunne & Black (1970) suggest that runoff contributing areas vary temporally in accordance with changing magnitude and intensity of precipitation, regulated by antecedent degree of soil saturation (Walling, 1971; Moore *et al.*, 1976). An expanding variable source area may re-connect previously disconnected sediment (pollutant) source areas leading to changes in the effective catchment area with regard to sediment delivery.

As a consequence of this spatial and temporal variability in sediment sourcing and transport, sediment load exported from a catchment is less than the load delivered to the downstream receiving water (Williams, 1983). If the sediment cascade is integrated to the basin scale, one can represent the suspended sediment yield from a glacially-conditioned landscape as an exhaustion model (Figure 1.3; after Ballantyne, 2002). This model assumes an exponential decay of sediment from the landscape, which is predicated on the assumption of a finite store of sediment and a stationary climatic regime. Sediment transfer rates decline over time as the sediment stores are depleted and/or as

vegetation matures on the landscape leading to reduced entrainment of sediment. The decline of sediment yields is more pronounced for small, headwater basins that have steeper slopes, minimal floodplains, and whose channel network is more closely coupled with hillslopes. Whereas at points in the basin with a larger cumulative drainage area, the rate of decline in sediment yield is much more gradual. In this way, suspended sediment yields at a given time since glaciation (t_1 in Figure 1.3a) can be higher in the lowland part of a basin than they are in the headwaters. This is a pattern reflected in glacially-conditioned basins of northwestern North America (Church and Slaymaker, 1989) but has yet to be defined for previously-glaciated basins of the Northeastern US.

With continued climate change, higher magnitude and duration of runoff will generate increased stream power leading to increased gullying, and erosion of sediments from the land surface, roads, ditches, landslides and streambanks. Long-term sinks or shorter-term stores of sediment will be increasingly converted to sources of sediment at the growing interface between hydrogeomorphic units. Source and sink roles of river corridor features will also vary temporally with differing magnitude and stage of hydrologic events. During a flow event of sufficient magnitude, all or portions of those sediment (and nutrient) *sinks* located proximal to active or newly-activated flow paths may become *sources* of sediment (Fryirs *et al.*, 2007, Harvey, 2002) and associated nutrients. The exact distribution of sources and sinks across the catchment may be difficult to predict, but it may be possible to estimate net sediment yields on a basin scale. Figure 1.3b depicts a system wide perturbation (e.g., extreme storm event) that preferentially impacts the headwater reaches of a nested basin, leading to a sudden rejuvenation of sediment erosion, as areas of glacial sediment previously disconnected

from the channel are accessed by higher flows. It is likely that increased frequency, intensity and magnitude of storms in coming decades (Guilbert et al, 2015) will rejuvenate erosion processes in headwater regions where hillslopes are closely coupled with stream channels. Such a pattern was evident, for example, during Tropical Storm Irene in the Connecticut River basin (Yellen *et al*., 2014).

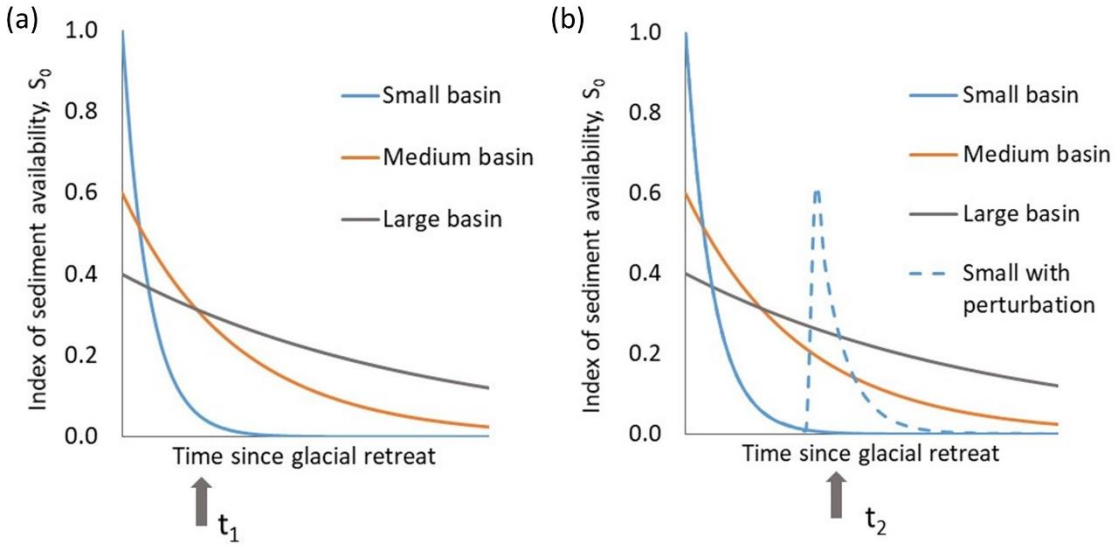

Figure 1.3. Sediment exhaustion model in a nested basin, after Ballantyne (2002) depicting (a) the differential sediment export from headwaters versus lowlands; and (b) the effects of a perturbation (e.g., extreme flood) impacting the headwaters, leading to renewed sediment yields.

Sediment Erosion, Transport and Deposition within Stream Networks

In the humid temperate climate of the Northeast, land areas that are the most hydrologically connected to the stream network will be the predominant contributor of water and sediment (and associated nutrients) (Dunne & Black, 1970; Harvey, 2002; Fryirs, 2013). This hydrologically-connected region, composed of the channel, floodplain, riparian zone and hyporheic zone, has been termed the river corridor (National Research Council, 2002). Patterns of sediment flux and channel adjustment

within the river corridor exhibit high variability across spatial and temporal scales (Walling, 1983; Fryirs, 2013), as a function of both watershed-level and reach-level processes that alter flow and sediment inputs, combined with reach-scale modifiers of stream power and boundary resistance. Many factors, including the geologic setting, climate and hydrology, vegetation, and land use, combine in nonlinear ways (Benda & Dunne, 1997; Fryirs, 2013) to govern reach-scale adjustments in channel dimensions, profile and planform over time. The present channel form is the manifestation of various channel-floodplain processes occurring over a range of flows (Pickup & Rieger, 1979). Thus, both the spatial and temporal context (Wohl, 2018) are important determinants of the present channel-floodplain form and dominant adjustment process(es) that characterize a given process domain.

Working in Northwest US, Montgomery and Buffington (1997) identified reach types for mountainous catchments that range on a continuum from supply-limited to transport-limited (Figure 1.4), within the broader catchment classifications of source, transfer and response zones (Schumm, 1984).

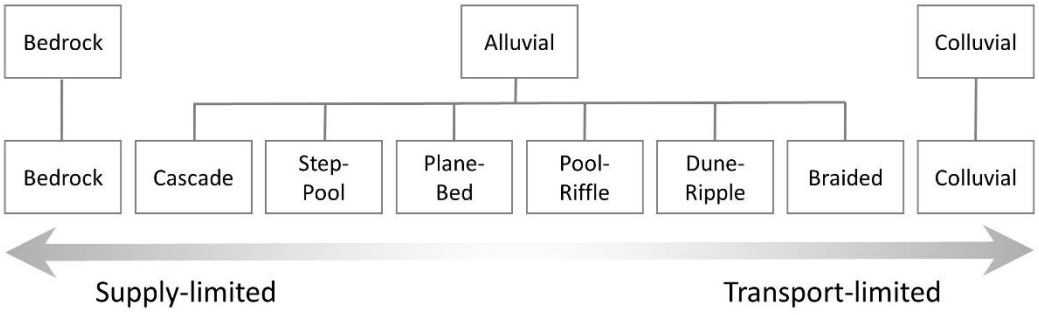

.

Figure 1.4. Continuum of stream types in mountainous rivers after Montgomery & Buffington (1997).

Watershed and channel stressors

Over geologic and historic time frames, river corridors are subjected to natural and human disturbances, or stressors, that operate at both watershed and channel scales to influence the sediment source, transport and deposition conditions of these reaches. Watershed-scale stressors in temperate humid climates of the Northeastern US commonly include glacial and post-glacial processes (Bierman et al, 1997), historic deforestation in the 19th century followed by reforestation in the 20th century (Foster & Aber, 2004) and increasing urbanization (Booth, 1990). Additionally, since the 1970s, regions of the northeast have experienced an increasing trend in precipitation intensity, frequency and persistence (Collins, 2009; Guilbert et al., 2015) and associated increasing trends in streamflow (Hodgkins & Dudley, 2011). Channel-scale stressors may include: channelization and straightening to remove meanders; selective removal of large boulders and woody debris; gravel mining; dredging and windrowing, berming and armoring; and floodplain encroachments by railroads, roads, and urban development (Kline & Cahoon, 2010; Noe & Hupp, 2005). Depending upon their magnitude, extent, and the resistance offered by boundary conditions, watershed and channel stressors can lead to enhanced degrees channel adjustment.

Channel evolution models

The sequence of vertical and lateral channel adjustments in response to natural and human stressors have been described in terms of channel evolution models (Schumm, *et al*., 1984; Simon and Hupp, 1986; Rosgen, 2006), which outline a trajectory of channel change that can be interpreted both in time and space. Common to each of these models is the possibility of a quasi-equilibrium state where the stream power produced by the

volume and slope of the water come into balance with the resistance created by the quantity and caliber of the sediment under transport and that offered by geologic and vegetative boundary conditions (Lane, 1955). Such a condition would describe the channel in Stage 1 of Figure 1.5, after Schumm, Harvey and Watson (1984), where the channel is vertically well-connected to its surrounding floodplain.

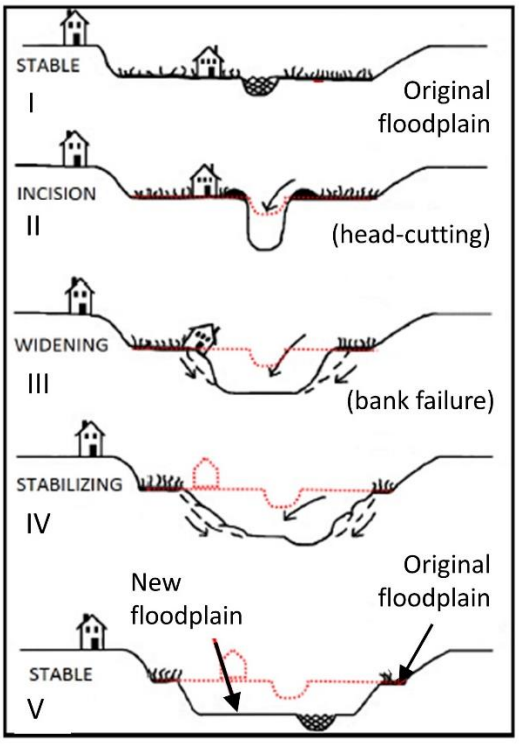

Figure 1.5. Schematic of a channel evolution model for an unconfined, alluvial channel after (Schumm et al., 1984) modified from (VTDEC, 2016).

This model then depicts a channel evolving through three unstable forms before returning to a quasi-equilibrium state at Stage V. Stage II results when a watershed or channel disturbance changes the balance between sediment supply and sediment transport capacity, leading to degradation or scouring of the bed. A stressor of sufficient magnitude may cause upstream migration of this incision process (or, head-cutting), leading to a vertical disconnection of the channel from the floodplain. As a consequence,

streambank heights exceed the critical height, and are induced to fail under geotechnical forces, which leads to widening (Stage III). Because an over-widened channel has an increased wetted perimeter, reduced hydraulic radius, and a decreased competence to transport sediment, widening gives way to aggradation as the dominant process in Stage IV. Eventually, the channel narrows and forms an incipient floodplain, often at a lower elevation than the original Stage I channel.

Channel evolution models most often describe stages of channel response to a single stressor or disturbance. In reality, rivers are integrating a myriad of stressors overlapping in time and space, and may adjust to an external stressor(s) in complex ways based on: the magnitude, intensity and duration of stressor; lag effects; intrinsic and extrinsic thresholds; self-reinforcing or self-limiting feedbacks; and the presence of antecedent conditions or contingencies (Bull, 1979; Chappell, 1983; Phillips, 2003; Toone et al., 2014). This has led others to suggest multiple scenarios of channel succession (e.g., Rosgen, 2006).

Noting the present stage of a channel in the context of a given channel evolutionary model is useful for identifying a probable trajectory of change in the face of projected increases in magnitude, frequency, and duration of extreme events or additional human-caused watershed and channel disturbances. Various field assessment techniques have been developed to classify river reaches in terms of their stability or sensitivity to adjustment, following the assumption that dominant adjustment process and degree of stability can be inferred from observations of channel form (Pfankuch, 1975; Nanson & Croke, 1992; Rosgen, 1996; Montgomery & Buffington, 1997; Raven et al, 1998 [River Habitat Survey]; Brierley & Fryirs, 2005; Rinaldi *et al*., 2013). Typically, these protocols

involve compilation of metrics and descriptors from a combination of remote-sensing work and direct field observations and surveys. Insights gained from these assessments have led to the theory that river networks comprise a longitudinal array of hydro-geomorphic units of relatively uniform composition, structure, and function, or "process domains" that differentially impact sediment connectivity (Montgomery, 1999; Brardonini & Hassan 2007; Lisenby and Fryirs, 2016).

Occurrence of a given reach-based sediment regime is the manifestation of various governing variables operating in nonlinear, complex ways. Classification schemes thus should consider both the vertical and lateral dimensions of sediment (dis)connectivity in the context of varying degrees of channel confinement by valley walls (hillslope-channel coupling in narrowly-confined to semi-confined settings) and the vertical-lateral connectivity to floodplain (floodplain-channel coupling in unconfined settings). The spatial arrangement of reach-based sediment regime can then be considered in the longitudinal, or stream-network, context.

Sediment process domains

Montgomery (1999) has offered the concept of sediment process domains to describe recognizable and predictable zones of the fluvial network "characterized by distinct suites of geomorphic processes" that "govern physical habitat type, structure, and dynamics" and which are manifest in response to patterns of disturbance. The process domains of Montgomery (1999) focused primarily on natural disturbance regimes to include effects of flooding, debris flows, mass failures and avalanches (Figure 1.6) and were developed for unglaciated catchments. The process domain framework was later extended to glacially-conditioned landscapes for mountainous catchments of British

Columbia (Brardonini & Hassan, 2006) and catchments of lower relief in the Laurentian Great Lakes (Phillips & Desloges, 2014a), using slope-area analysis. The concept has been invoked: to help explain sediment dynamics in bedrock canyons of the Colorado Rocky Mountains (Wohl, 2010); to distinguish sediment patterns in headwater reaches with alluvial versus glacial provenance in the same study area (Livers & Wohl, 2015); and to define channel adjustment typologies as a function largely of width-to-depth ratio, drainage area, stream power and substrate size in (Lisenby and Fryirs, 2016). Various metrics have been explored in these studies to classify river networks into fluvial process domains, using Frequentist statistical techniques and maximum-likelihood models, as discussed in the next sections. Typically, multiple topographic, geomorphic and hydraulic variables are required to distinguish between domains (Livers and Wohl, 2015).

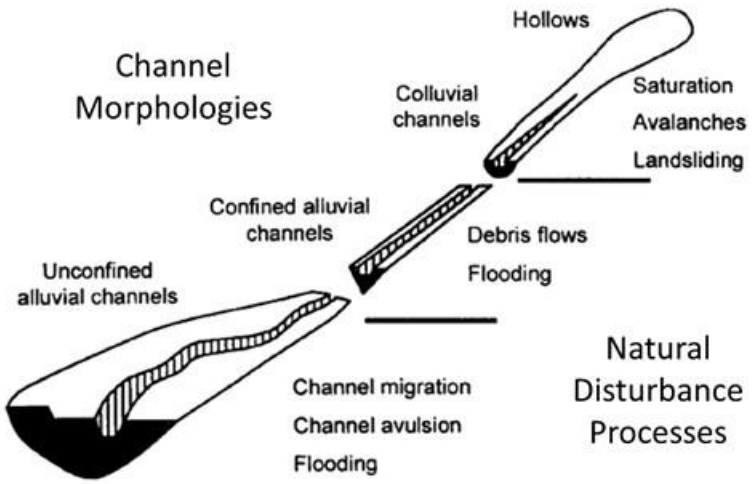

Figure 1.6. Fluvial sediment process domains (modified after Montgomery, 1999).

To integrate multivariate hydraulic and geomorphic data in a classification system of reach-based fluvial process domains, water resource managers are in need of computational tools and predictive models to enhance our understanding of sediment

transport processes at both reach and network scales, and how these processes drive (and are driven by) channel evolution.

Linear Methods for Data Analysis and Classification

Linear methods employed in data science for data reduction and clustering or classification aim to separate observations into two or more classes based on a linear combination of features. Methods are numerous and include discriminant analysis (DA), principal components analysis (PCA), and logistic regression. Various forms of the Generalized Linear Model (Nelder & Wedderburn, 1972) have also been used to infer relationships between response variable(s) and explanatory variables to gain insights into a system, including linear regression, multiple linear regression, log-linear regression, One-way ANOVA, and the t-test.

These parametric statistical techniques have been applied to infer relationships between riverine sediment flux and various physical and biogeochemical characteristics of catchments. A comprehensive review is beyond the scope of this dissertation, but a few examples are presented below.

Bivariate methods

At a catchment scale, the parsimonious sediment (and nutrient) rating curve - i.e., $\log(C) = \log(\beta_0) + \beta_1 \log(Q)$ - has been used to examine between-watershed differences in sediment and solute production (e.g., Walling, 1977; Vogel et al., 2005). Sediment and nutrient regression parameters have been interpreted to suggest drivers of underlying processes (Syvitski et al., 2000; Asselman, 2000; Godsey et al., 2009; Basu et al., 2011). While prediction does not necessarily suggest causation, the coefficient ($\log \beta_0$) and

exponent (β_1) in this linear model can be interpreted to suggest something about the system properties (Asselman, 2000; Syvitski et al., 2000) and encapsulate the "biogeochemical filtering" of the watershed in question (Gall et al., 2013). The intercept of the linear regression model represents the background sediment (or solute) concentration delivered from the catchment source regions and explained by variables other than changing discharge proximal to the gaging location. In the context of sediment transport modeling, the regression intercept reflects the capacity of the watershed to produce and transport fine sediment (Asselman, 2000). It has been characterized as an "index of sediment supply" (Wang et al., 2008) or a "baseline supply parameter" (Krishnaswamy et al., 2000), and may be a function of particle size and weathering intensity in the source catchment, as moderated by vegetative controls or human disturbances.

On the other hand, the regression slope parameter reflects the rate at which the energy of flowing water is transferred to its physical surroundings to entrain and transport sediment (or sediment-bound constituents) and to accomplish geomorphic change (Krishnaswamy et al., 2000; Wang et al., 2008). The regression slope can be thought of as an index of the river's erosive power, with higher values (i.e., steeper slopes) indicating greater sediment transport capacity, and may also reflect the degree to which additional sources of sediment (or sediment-related constituents) become available to the river at higher flow stages (Asselman, 2000). Flatter regression slopes can be characteristic of rivers where sediment continues to be transported even under lower discharge conditions – as a function of either ample supply or easily-entrained particle size in the source areas, or both (Asselman, 2000).

Similarly, researchers have examined bivariate relationships to infer drivers for coarse sediment erosion, transport and deposition at a reach scale. For example, valley morphology has been identified as a controlling variable for the depositional versus erosional tendencies of river reaches (Weber and Pasternak, 2017). Recently, derived measures of reach-based stream power (including reach-to-reach ratios or differentials) have been examined for possible correlations to field-based or remotely-sensed measures of geomorphologic form to better understand and classify process and sediment transport regime. Yochum et al. (2017) used a cumulative logit model to predict six ordinal classes of geomorphic change from channel gradient and differential specific stream power (SSP) and total stream power (TSP). Similarly, Parker et al (2014) have used a ratio of downstream-reach to upstream-reach SSP to predict erosion or deposition dominance, where reaches were defined by a zonation algorithm applied to SSP values calculated at 50 m intervals. Working in VT and CO streams across a range of confinement conditions and slopes, Gartner et al (2015) demonstrated that TSP gradients were useful predictors of lateral sediment inputs (mass-wasting and bank erosion along increasing TSP gradients) and exports (e.g., floodplain deposits along decreasing TSP gradients).

Multivariate methods

Because riverine sediment dynamics result from a complex interaction of hydrologic, hydraulic, and biogeochemical factors, they are best modeled using multivariate statistical methods and models. At a catchment scale, linear un-mixing models have been employed to unravel the disparate sources of sediment production and transport (Collins & Walling, 2002; Walling, 2013). To estimate the relative proportions of various terrestrial sediment sources contributing to the load of suspended sediment at a

catchment outlet, researchers have utilized a wide variety of tracer types, from geochemical constituents (Collins et al., 1997), to fallout radionuclides (Walling & Woodward, 1992), to sediment color (Martinez-Carreras, 2010), to stable isotopes of C and N (Fox & Papanicolaou, 2008), or a combination of multiple types in a "composite fingerprint" (Walling et al., 1993; Koiter et al., 2013). Typically, a subset of tracers with power to differentiate between sources is identified using Kruskal-Wallis-H test followed by stepwise discriminant function analysis (Collins et al. 1997). A multivariate un-mixing model is then employed to: (i) link the tracer signature of the suspended sediment transported to the outlet (target material) back to the tracer signature(s) of the source-type sediments; and in so doing, (ii) determine the relative proportions of each sediment source (i.e., source apportionment). The model is a mass balance equation:

$$Y = \sum_{k} S_k \, x \, P_k$$

subject to the following constraints:

$$\sum_{k=1}^{K} P_k = 1 \quad \text{and} \quad P_k \geq 0,$$

where *Y* is the tracer concentration measured in the target (suspended solids at the catchment outlet), *S* is the tracer concentration in source-area sediments, *P* is the proportional sediment contribution of each modeled source, and *k* is an index of source areas (Cooper et al., 2014). Since S and Y are known quantities for a given suite of tracers, and P is unknown, an inverse mass balance problem is solved (Fox & Papanicolaou, 2008). Frequentist un-mixing models utilizing Maximum Likelihood

optimization methods have been widely applied (Collins et al., 1997) to minimize the sum or squared residuals (SSR), computed as:

$$\text{SSR} = \sum_{j=1}^{J} \left[Y_j - \sum_{k=1}^{K} S_{j,k} P_k \right]^2,$$

In the above equations, *Y* is the tracer concentration measured in suspended solids; *S* is the modeled tracer concentration in source-area sediments, *j* is a tracer index, *k* is an index of source areas; and *P* is the proportional sediment contribution of each modeled source (Cooper et al., 2014).

The outcome of a least-squares optimization is a set of estimates for model parameters that make the observed results (tracer concentrations in the target) most probable. With any un-mixing model, there is uncertainty in the source apportionment results, related to natural variability or errors introduced by sampling methods, laboratory methods, as well as the chosen model structure and parameterization. This uncertainty is not well captured by the point estimates and associated confidence intervals generated through conventional, Frequentist methods.

At the reach scale, Brardonini & Hassan (2007) applied multivariate discriminant analysis (DA) paired with PCA to channel and floodplain metrics for dimension reduction and classification of process domains, identifying a variation on the downstream continuum of stream types of Montgomery & Buffington (1997), related to legacy glacial landforms in British Columbia. Phillips and Desloges (2014) used k-means clustering, PCA, and DA to analyze geomorphic parameters and classify alluvial channels from a glacially-conditioned setting in southern Ontario. Their analysis (limited

to low-gradient, single-thread, channels in unconfined settings) identified four broad channel-floodplain types.

Traditionally, linear un-mixing models and simple and segmented regression models have been favored for their relative parsimony and simplicity. However, least-squares methods are susceptible to influence by outliers, and these Frequentist methods are subject to limitations where model parameters do not conform to Gaussian distribution, or where input data are sparse. Consequently, data-driven, nonparametric modeling approaches have been adopted with increasing frequency.

Non-Parametric, Nonlinear, Data-driven Methods for Classification

Nonparametric statistical techniques are a helpful alternative to parametric methods of classification, since they relax the requirements that data follow a given distribution and offer greater robustness to outliers. Recent advances in computational power have overcome one of their disadvantages (computational time) compared to GLM classification methods.

Nonparametric methods for clustering and classification have emerged in the literature with applications to modeling sediment and nutrient dynamics in rivers. For example, "functional stages" of sediment and nutrient export were defined using hierarchical clustering techniques to result from unique combinations of source strength and connectivity, entrainment or mobilization conditions, and transport mechanisms; and these functional stages were found to vary in both space and time (Bende-Michl et al., 2013). At a reach scale, Bizzi & Lerner (2013) used a classification tree to define four classes of erosion or deposition dominance based on channel confinement and differential

values of total stream power (TSP) and specific stream power (SSP). Similarly, a tree was applied by Livers and Wohl (2015) within each of two process domains (glacial, fluvial) to determine variables with power to distinguish stream types after Montgomery & Buffington (1997), including slope, channel geometry, stream power and substrate size. With the wide-spread availability of commercial and open-source software tools, hierarchical clustering methods and classification trees are simple to apply, but can be subject to overfitting and may not be easily transferable to other data sets or regions. Moreover, both parametric and conventional nonparametric statistical techniques are often of limited efficacy when applied to data of varying quality, mixed data types (continuous, ordinal, nominal), censored or sparse data. Data-driven methods including machine-learning algorithms and Bayesian statistical approaches have advantages over these more conventional methods for data reduction and visualization, and for addressing uncertainty.

Machine-learning clustering and classification

The Self-Organizing Map (SOM) is a type of neural network (or machine-learning algorithm) with advantages for clustering or classification of multivariate observations and for exploratory data analysis and visualization of complex, nonlinear systems. A detailed description of the SOM algorithm and computational considerations are provided in Chapter 4. SOMs have advantages over other methods for data visualization and interpretation (Alvarez-Guerra, et al., 2008), and have demonstrated superior performance over parametric methods where data contain outliers or exhibit high variance (Mangiameli et al., 1996). SOMs have been used to classify or cluster multivariate environmental data, including instream species richness (Park et al., 2003),

fish community distribution patterns (Stojkovica et al., 2013), alluvial fan types (Karymbalis et al., 2010), lake chemistry data associated with harmful algal blooms (Pearce et al., 2011, 2013), estuary sediment samples (Alvarez-Guerra et al., 2008), and watershed-based ecoregions (Tran et al., 2003). Research applications of SOMs to hydrologic and geomorphic data have been more limited. Ley and others (2011) applied SOMs to hydrologic time series data to classify runoff response, and riverine habitats were classified using an SOM by Fytilis and Rizzo (2013). Rarely, however, have neural networks been used to cluster observations at basin or reach scales into groups exhibiting similar sediment (and nutrient) export regimes or similar erosion and deposition characteristics (Besaw et al., 2009) – and this paucity of riverine research applications motivated the research presented in Chapters 2 and 4.

Bayesian approaches

As an alternative to maximum-likelihood / Frequentist modeling methods, new methods have emerged that apply Bayes rule to make inferences about a system. Bayes rule states that the probability of a model, given the observed data (i.e., the posterior: p[Model|Data]) can be calculated as the product of the prior belief in the model (i.e., p[Model]) and a quotient of the likelihood (p[Data|Model]) and the marginal likelihood (p[Data]:

$$p(Model|Data) = \frac{p(Data|Model) * p(Model)}{p(Data)}$$

The posterior distribution on model parameters is approximated using Markov Chain Monte-Carlo methods. Vague priors can be established for model parameters so that the posterior distributions are influenced most by the data themselves (Gelman et al., 2004).

On the other hand, for sparse, or unbalanced data sets, the priors can be informed by prior study or a preponderance of expert opinion.

Given their advantages, and with the advent of faster computational abilities, Bayesian methods have been increasingly applied to the study of hydrology and riverine sediment and nutrient dynamics: to estimate values of regression parameters for simple linear models of stage-discharge relationships (Moyeed and Clark, 2005); an eight-parameter load rating curve for nutrients (Vigiak and Bende-Michl, 2013), and for the identification of threshold position in segmented regression models for nitrogen-discharge patterns (Alameddine et al., 2011; Qian and Cuffney, 2012; Qian and Richardson, 1997).

At the catchment scale, Bayesian statistical methods have increasingly been used in un-mixing models to discern relative sources of suspended sediment export (Fox and Papanicolaou, 2008; Koiter et al., 2013, D'Haen et al., 2013; Dutton et al., 2013; Barthod et al., 2015). Cooper and others (2014) note that a "Bayesian approach is advantageous over Frequentist methods as it enables all known and residual uncertainties associated with the mixing model and the data set to be coherently translated into parameter probability distributions in a hierarchical framework." Additional advantages of the Bayesian framework include the flexibility to incorporate prior information (Owens et al., 2015). More details of the Bayesian un-mixing model are provided in Chapter 3.

References

Alameddine, I., S. S. Qian, and K. H. Reckhow (2011), A Bayesian changepoint-threshold model to examine the effect of TMDL implementation on the flow-nitrogen concentration relationship in the Neuse River basin, *Water Res.*, 45, 51–62, doi:10.1016/j.watres.2010.08.003.

Alvarez-Guerra, M., C. González-Piñuela, A. Andrés, B. Galán, and J. R. Viguri (2008), Assessment of Self-Organizing Map artificial neural networks for the classification of sediment quality, *Environment International*, 34(6), 782-790, doi:10.1016/j.envint.2008.01.006.

Anderson D.M., Glibert P.M., Burkholder J.M. (2002), Harmful algal blooms and eutrophication: nutrient sources, composition, and consequences, *Estuaries*, 25, 704–726

Asselman, N. E. M. (2000), Fitting and interpretation of sediment rating curves, *J. Hydrology*, 234, 228-248, doi:10.1016/S0022-1694(00)00253-5.

Ballantyne, C. K. (2002), Paraglacial geomorphology, *Quaternary Science Reviews*, 21, 1935-2017.

Barthod, L.R.M., Liu, K., Lobb, D.A., Owens, P.N., Martinez-Carreras, N., Koiter, A.J., Petticrew, E. L., McCullough, G.K., Liu, C., Gaspar, L., 2015, Selecting color-based tracers and classifying sediment sources in the assessment of sediment dynamics using sediment source fingerprinting. J. Environ. Qual., 44: 1605-1616.

Basu, N. B., S. E. Thompson, and P. S. C. Rao (2011), Hydrologic and biogeochemical functioning of intensively managed catchments: A synthesis of top-down analyses, *Water Resour. Res.*, 47, W00J15, doi:10.1029/2011WR010800.

Benda, L., and T. Dunne (1997), Stochastic forcing of sediment supply to channel networks from landsliding and debris flow, *Water Resour. Res.*, 33, 2849-2863.

Benda, L., M. A. Hassan, M. Church, and C. L. May (2005), Geomorphology of steepland headwaters: the transition from hillslopes to channels, *Journal of the American Water Resources Association*, 41(4), 835-851.

Bende-Michl, U., K. Verburg, and H. P. Creswell (2013), High-frequency nutrient monitoring to infer seasonal patterns in catchment source availability, mobilization and delivery, *Environ. Monit. Assess.*, 185, 9191-9219.

Bennett, G.L., P. Molnar, B.W. McArdell, and P. Burlando (2014), A probabilistic sediment cascade model of sediment transfer in the Illgraben, *Water Resources Research*, 50, 1225-1244.

Besaw, L. E., D.M. Rizzo, M. Kline, K.L. Underwood, J.J. Doris, L.A. Morrissey, K. Pelletier, (2009), Stream classification using hierarchical artificial neural networks: A fluvial hazard management tool, *Journal of Hydrology*, 373, 34-43, doi:10.1016/j.jhydrol.2009.04.007.

Bierman, P., A. Lini, P. Zehfuss and A. Church, 1997, Postglacial ponds and alluvial fans: recorders of holocene landscape history, *GSA Today*, 7(10), 1-8.

Bizzi, S., and Lerner, D.N., 2013, The use of stream power as an indicator of channel sensitivity to erosion and deposition processes: River Research and Applications, v. 31, p. 16–27, doi:10.1002 /rra.2717.

Booth, D.B., 1990. Stream-channel incision following drainage basin urbanization. Water Resour. Bull. Am. Water Resour. Assoc. 26 (3), 407–417, doi: 10.1111/j.1752-1688.1990.tb01380.x

Borselli, L., P. Cassi, D. Torri (2008), Prolegomena to sediment and flow connectivity in the landscape: A GIS and field numerical assessment, *Catena*, 75, 268-277.

Bracken, L. J., L. Turnbull, J. Wainwright, P. Bogaart (2014), Sediment connectivity: a framework for understanding sediment transfer at multiple scales, *Earth Surf. Process. Landforms*, doi: 10.1002/esp.3635.

Bracken, L .J. and J. Croke (2007), The concept of hydrological connectivity and its contribution to understanding runoff-dominated geomorphic systems, *Hydrological Processes*, 21, 1749-1763, doi: 10.1002/hyp.6313.

Brardinoni, F., and M. A. Hassan (2006), Glacial erosion, evolution of river long profiles, and the organization of process domains in mountain drainage basins of coastal British Columbia, *J. Geophys. Res*., 111, F01013, doi:10.1029/2005JF000358.

Brierley, G.J., K. A. Fryirs, (2005.), Geomorphology and River Management: Applications of the River Style Framework. Blackwell, Oxford, p. 398.

Bull, W.B. (1979), Threshold of critical power in streams. *Bull. Geol. Soc. Am*., 90, 453–464.

Burt T. and R. Allison (2010), Sediment cascades: an integrated approach. New York, NY: John Wiley & Sons.

Cavalli, M., S. Trevisani, F. Comiti, L. Marchi, 2013. Geomorphometric assessment of spatial sediment connectivity in small Alpine catchments. Geomorphology, 188 (31-41).

Church, M. and J. Ryder, 1972, Paraglacial sedimentation: A consideration of fluvial processes conditioned by glaciation. Geological Society of America Bulletin, 83: 3059-3072.

Church, M., O. Slaymaker (1989), Disequilibrium of Holocene sediment yield in glaciated British Columbia, Nature, 337, 452-454.

Chappell, J. (1983), Thresholds and lags in geomorphologic changes, *Australian Geographer*, 15, 358–66.

Clark, G.M., D.K. Mueller, and M.A Mast. 2000. Nutrient concentrations and yields in undeveloped stream basins of the United States. Journal of the American Water Resources Association 36(4):849–860.

Collins, M. J. (2009). Evidence for Changing Flood Risk in New England Since the Late 20th Century. *Journal of the American Water Resources Association, 45*(2), 279-290. doi: DOI: 10.1111/j.1752-1688.2008.00277.x

Collins, A.L., and D. E. Walling (2002), Selecting fingerprint properties for discriminating potential suspended sediment sources in river basins, *J. Hydrology*, 261, 218.

Collins, A.L., D. E. Walling, G.J.L. Leeks (1997), Source type ascription for fluvial suspended sediment based on a quantitative fingerprinting technique, *Catena*, 29, 1–27, doi:10.1016/S0341-8162(96)00064-1.

Cooper, R. J., T. Krueger, K. M. Hiscock, and B. G. Rawlins (2014), Sensitivity of fluvial sediment source apportionment to mixing model assumptions: A Bayesian model comparison, *Water Resour. Res*., 50, 9031–9047, doi:10.1002/2014WR016194.

Costa, J.E. and J. E. O'Connor (1995), Geomorphically effective floods. In Natural and Anthropogenic Influences in Fluvial Geomorphology, Costa JE, Miller AJ, Potter KW, Wilcock PR (eds). American Geophysical Union: Washington, DC; 45–56.

Croke, J., Mockler, S., Fogarty, P. and Takken, I., 2005. Sediment concentration changes in runoff pathways from a forest road network and the resultant spatial pattern of catchment connectivity. Geomorphology, 68, 257-268.

Croke, J., K. Fryirs, C. Thompson, 2013. Channel-floodplain connectivity during an extreme flood event: implications for sediment erosion, deposition, and delivery. Earth Surface Processes and Landforms, 38 (1444-1456).

Clark, G.M., D.K. Mueller, and M.A Mast. 2000. Nutrient concentrations and yields in undeveloped stream basins of the United States. Journal of the American Water Resources Association 36(4):849–860.

Dethier, E., F. J. Magilligan, C. E. Renshaw, and K. H. Nislow (2016), The role of chronic and episodic disturbances on channel-hillslope coupling: the persistence and legacy of extreme floods, *Earth Surface Processes and Landforms*, *41*(10), 1437-1447, doi: 10.1002/esp.3958

Dietrich, W.E. and T. Dunne, 1978. Sediment budget for a small catchment in mountainous terrain. *Zeitschrift fvr Geomorphologie, Supplementeband*, 29 (191-206).

Dubrovsky, N.M., Burow, K.R., Clark, G.M., Gronberg, J.M., Hamilton P.A., Hitt, K.J., Mueller, D.K., Munn, M.D., Nolan, B.T., Puckett, L.J., Rupert, M.G., Short, T.M., Spahr, N.E., Sprague, L.A., and Wilber, W.G. 2010. The quality of our Nation's waters—Nutrients in the Nation's streams and groundwater, 1992–2004: U.S. Geological Survey Circular 1350.

Dunne, T. and R.D. Black (1970), Partial Area Contributions to Storm Runoff in a Small New England Watershed, *Water Resources Research*, 6(5), 1296-1311.

Dutton, C., A.C. Ainsfield, H. Ernstburger. (2013). A novel sediment fingerprinting method using filtration: application to the Mara River, East Africa, J. Soils Sediments, 13: 1708-1723.

Ferguson, R.I. (1981), Channel forms and channel changes. In British Rivers, Lewin J. (ed). Allen and Unwin: London: 90-125.

Finlayson, D. P., and D. R. Montgomery (2003), Modeling large-scale fluvial erosion in geographic information systems, *Geomorphology*, 53(1): 147-164. doi:10.1016/S0169-555X(02)00351-3

FISRWG. 1998. Stream Corridor Restoration: Principles, Processes, and Practices. Federal Interagency Stream Restoration Working Group, U.S. Department of Commerce, National Technical Information Service. http://www.nrcs.usda.gov/technical/stream_restoration.

Foster, D.R. & Aber, J.D. (2004). Forests in Time: The Environmental Consequences of 1,000 Years of Change in New England. New Haven, CT: Yale University Press. 477 pp. ISBN: 0–300–09235–0.

Fox, J. F. & A. N. Papanicolaou (2008), An un-mixing model to study watershed erosion processes, *Advances in Water Resources*, 31, 96.

Frumhoff, P. C., McCarthy, J. J., Melillo, J. M., Moster, S. C., & Wuebbles, D. G. (2007). *Confronting Climate Change in the U.S. Northeast: Science, Impacts, and Solutions*. Cambridge, MA: Union of Concerned Scientists

Fryirs, K.A., G.J.Brierley, N. J. Preston, and M. Kasai (2007), Buffers, barriers and blankets: The (dis)connectivity of catchment-scale sediment cascades, *Catena*, 70 (49-67).

Fryirs, K, 2013. (Dis)Connectivity in catchment sediment cascades: a fresh look at the sediment delivery problem. Earth Surface Processes and Landforms, 38, 30-46.

Fytilis, N. and D. M. Rizzo (2013), Coupling self-organizing maps with a Naıve Bayesian classifier: Stream classification studies using multiple assessment data, *Water Resour. Res.*, 49, 7747–7762, doi:10.1002/2012WR013422.

Gall, H. E., J. Park, C. J. Harman, J. W. Jawitz, P. S. C. Rao (2013), Landscape filtering of hydrologic and biogeochemical responses in managed catchments, *Landscape Ecology*, 28, 651–664, doi:10.1007/s10980-012-9829-x.

Gartner, J. D., W. B. Dade, C.E. Renshaw, F.J. Magilligan and E. M. Buraas (2015), Gradients in stream power influence lateral and downstream sediment flux in floods, *Geology*, 43(11), 983-986, doi:10.1130/G36969.1.

Gelman, A., Carlin, J. B., Stern, H. S., Rubin, D. B. (2004), *Bayesian Data Analysis*, Chapman & Hall/CRC, Boca Raton, FL.

Godsey, S. E., J. W. Kirchner, D. W. Clow (2009), Concentration–discharge relationships reflect chemostatic characteristics of US catchments, *Hydrol. Processes*, 23, 1844-1864, doi: 10.1002/hyp.7315.

Groisman, P. Y., Knight, R. W., & Karl, T. R. (2001). Heavy Precipitation and High Streamflow in the Contiguous United States: Trends in the 20th Century. *Bulletin of the American Meteorological Society, 82*(2), 219-246Harvey, A. M., 2002. Effective timescales of coupling within fluvial systems. Geomorphology, 44, 175-201.

Guilbert, J., B. Beckage, J. M. Winter, R. M. Horton, T. Perkins, and A. Bomblies (2014), Impacts of projected climate change over the Lake Champlain Basin in Vermont, *J. Appl. Meteorol. Climatol.*, 53, 1861-1875, doi:10.1175/JAMC-D-13-0338.1.

Guilbert, J., A. K. Betts, D. M. Rizzo, B. Beckage, and A. Bomblies (2015), Characterization of increased persistence and intensity of precipitation in the Northeastern United States, *Geophys. Res. Lett.*, 42, 1888–1893, doi:10.1002/2015GL063124.

Hamshaw, S. D., T. Bryce, D. M. Rizzo, J. O'Neil-Dunne, J. Frolik, and M. M. Dewoolkar (2017), Quantifying streambank movement and topography using unmanned aircraft system photogrammetry with comparison to terrestrial laser scanning, *River Research and Applications*, *33*(8), 1354-1367, doi: 10.1002/rra.3183.

Harvey, A.M., 2002. Effective timescales of coupling within fluvial systems. Geomorphology 44, 175–201.

Hayhoe, K., Wake, C. P., Huntington, T. G., Luo, L., Schwartz, M., Sheffield, J., . . . Wolfe, D. (2007). Past and future changes in climate and hydrological indicators in the U.S. Northeast. *Climate Dynamics, 28*, 381-407.

Heathwaite, A. L., A. N.Sharpley, and W. J. Gburek. 2000. Integrating phosphorus and nitrogen management at catchment scales. J. Environ. Qual 29:158-166.

Hecht-Nielson, R. 1987. Counterpropagation Networks. *Applied Opt*. 26(23)

Hodgkins, G. A., & Dudley, R. W. (2011). Historical summer base flow and stormflow trends for New England rivers. *Water Resources Research, 47*. doi: 10.1029/2010WR009109.

Hooke, J., 2003. Coarse sediment connectivity in river channel systems: a conceptual framework and methodology. Geomorphology, 56 (79-94).

Howarth, R.W., Billen, G., Swaney, D., Townsend, A., Jaworski, N., Lajtha, K., Downing, J.A., Elmgren, R., Caraco, N., Jordan, T., Berendse, F., Freney, J., Kudeyarov, V., Murdoch, P., and Zhu Zhao-Liang, (1996), Regional nitrogen budgets and riverine N & P fluxes for

the drainages to the North Atlantic Ocean: natural and human influences: Biogeochemistry v. 35, p. 75-139.

Huntington, T. G., Sheffield, J., & Hayhoe, K. (2007). *Impacts of Climate Change on Wintertime Precipitation, Snowmelt Regime, Surface Runoff and Infiltration in the Northeastern USA during the 21st Century*. Paper presented at the 64th Eastern Snow Conference, St. John's, Newfoundland, Canada.

Huntington, T. G., Richardson, A. D., McGuire, K. J., & Hayhoe, K. (2009). Climate and hydrological changes in the northeastern United States: recent trends and implications for forested and aquatic ecosystems. *Canadian Journal of Forest Research, 39*, 199-212.

Huntington, T. G., Sheffield, J., & Hayhoe, K. (2007). *Impacts of Climate Change on Wintertime Precipitation, Snowmelt Regime, Surface Runoff and Infiltration in the Northeastern USA during the 21st Century*. Paper presented at the 64th Eastern Snow Conference, St. John's, Newfoundland, Canada.

Intergovernmental Panel on Climate Change, 2014, Climate Change 2014: Impacts, Adaptation and Vulnerability: Summary for Policymakers, downloaded from: http://ipcc-wg2.gov/AR5/images/uploads/WG2AR5_SPM_FINAL.pdf

Isles, P. D. F., C. D. Giles, T. A. Gearhart, Y. Xu, G. K. Druschel, and A. W. Schroth (2015), Dynamic internal drivers of a historically severe cyanobacteria bloom in Lake Champlain revealed through comprehensive monitoring, *J. Great Lakes Res.*, 41(3), 818–829, doi:10.1016/j.jglr.2015.06.006.

James, L. A. (2013). Legacy sediment: Definitions and processes of episodically produced anthropogenic sediment. *Anthropocene, 2*, 16–26.

Jarvie, H. P., M. D. Jurgens, R. J. Williams, C. Neal, J. J. L. Davies, C. Barrett, and J. White (2005), Role of river bed sediments as sources and sinks of phosphorus across two major eutrophic UK river basins: the Hampshire Avon and Herefordshire Wye, *J. Hydrology*, 304(1-4), 51-74, doi:10.1016/j.jhydrol.2004.10.002.

Jennings, K.L., 2001, Depositional Histories of Vermont Alluvial Fans: MS Thesis, University of Vermont, Burlington, VT.

Karl, T. R., & Knight, R. W. (1998). Secular trends of precipitation amount, frequency, and intensity in the United States. *Bulletin of the American Meteorological Society, 79*, 231-241

Karymbalis, E., K. Gaki-Papanastassiou and M. Ferentinou (2010), Fan deltas classification coupling morphometric analysis and artificial neural networks: The case of NW coast of Gulf of Corinth, Greece, *Hellenic Journal of Geosciences*, 45, 133-146.

Kirchner, J. W. (2006), Getting the right answers for the right reasons: Linking measurements, analyses, and models to advance the science of hydrology, *Water Resour. Res*., 42, W03S04, doi:10.1029/2005WR004362.

Kirchner, J. W., X. H. Feng, C. Neal, and A. J. Robson (2004), The fine structure of water-quality dynamics: The (high-frequency) wave of the future, *Hydrol. Processes*, 18, 1353– 1359, doi:10.1002/hyp.5537.

Kline, M., & Cahoon, B. (2010). Protecting River Corridors in Vermont. *Journal of the American Water Resources Association, 1*(10). doi: 10.1111/j.1752-1688.2010.00417.x

Kohonen, Teuvo, 1990, The Self-Organizing Map., *Proceedings of the IEEE*, 78 (9): 1464 – 1480.

Koiter, A.J., D.A. Lobb, P.N. Owens, E.L.Petticrew, K. Tiessen, S. Li (2013), Investigation the role of scale and connectivity in assessing the sources of sediment in an agricultural watershed in the Canadian prairies using sediment source fingerprinting, J. Soils Sediments, 13: 1676-1691.

Krishnaswamy, J., M. Lavine, D. D. Richter, and K. Korfmacher (2000), Dynamic modeling of long term sedimentation in the Yadkin River Basin, *Adv. Water Resourc.*, 23(8), 881-892, doi:10.1016/S0309-1708(00)00013-0.

Lake Champlain Basin Program, 2012, State of the Lake and Ecosystem Indicators Report, downloaded from: http://www.lcbp.org/wp-content/uploads/2013/05/SOL2012-web.pdf

Lane, E.W. 1955. The Importance of Fluvial Morphology in Hydraulic Engineering, American Society of Civil Engineering, Proceedings, 81, paper 745: 1-17.

Leopold, L.B., Maddock, T., 1953. The Hydraulic Geometry of Stream Channels and Some Physiographic Implications. Professional Paper 252. US Geological Survey, Washington, DC.

Ley, R., M. C. Casper, H. Hellebrand, and R. Merz (2011), Catchment classification by runoff behaviour with self-organizing maps (SOMs), *Hydrol. Earth Syst. Sci.*, 15, 2947-2962, doi:10.5194/hess-15-2947-2011.

Lisenby, P. E., and K. Fryirs (2016), Catchment- and reach-scale controls on the distribution and expectation of geomorphic channel adjustment, *Water Resour. Res*., 52, 3408–3427, doi:10.1002/2015WR017747.

Livers, B. and E. Wohl (2015), An evaluation of stream characteristics in glacial versus fluvial process domains in the Colorado Front Range, *Geomorphology*, 231, 72–82.

Mangiameli, P., S. K. Chen, and D. West (1996), A comparison of SOM neural network and hierarchical clustering methods, *Eur. J. Oper. Res*., 93(2), 402–417, doi:10.1016/0377-2217(96)00038-0.

Martinez-Carreras, N., A. Krein, F. Gallart, J.F. Iffly, L. Pfister, L. Hoffmann, and P.N. Owens. 2010. Assessment of different colour parameters for discriminating potential suspended sediment sources and provenance: A multi-scale study in Luxembourg. Geomorphology 118:118–129. doi:10.1016/j.geomorph.2009.12.013

McClain, M.E, E. W. Boyer, C. L. Dent, S. E. Gergel, N. B. Grimm, P. M. Groffman, S. C. Hart, J. W. Harvey, C. A. Johnston, E. Mayorga, W. H. McDowell, and G. Pinay. 2003, Biogeochemical Hot Spots and Hot Moments at the Interface of Terrestrial and Aquatic Ecosystems, *Ecosystems*, 6: 301-312.

McDonnell, J. J., M. Sivapalan, K. Vache´, S. Dunn, G. Grant, R. Haggerty, C. Hinz, R. Hooper, J. Kirchner, M. L. Roderick, J. Selker, and M. Weiler (2007), Moving beyond heterogeneity and process complexity: A new vision for watershed hydrology, *Water Resour. Res*., 43, W07301, doi:10.1029/2006WR005467.

Meade, R.H., 1982. Sources, sinks and storage of river sediment in the Atlantic drainage of the United States. Journal of Geology, 90: 235-252.

Michaelides ,K., A. Chappell, 2009, Connectivity as a concept for characterizing hydrological behavior. Hydrological Processes, 23 (517-522).

Montgomery, D. R. (1999), Process domains and the river continuum, *Journal of the American Water Resources Association*, 35(2), 397–410.

Montgomery, D.R. and Buffington, J.M., 1997, Channel-reach morphology in mountain drainage basins: Geological Society of America Bulletin, 109 (5): 596-611.

Moyeed, R. A., and R. T. Clark (2005), The use of Bayesian methods for fitting rating curves, with case studies, *Adv. Water Resourc.*, 28, 807-818, 10.1016/j.advwatres.2005.02.005.

Musolff, A., C. Schmidt, B. Selle, and J. H. Fleckenstein (2015), Catchment Contols on Solute Export, *Adv. Water Resourc.*, 86, 133-146, doi:10.1016/j.advwatres.2015.09.026.

Nanson, G.C. and J.C. Croke (1992), A genetic classification of floodplains, *Geomorphology*, 4(6), 459-486.

National Research Council, 2000, Clean coastal waters understanding and reducing the effects of nutrient pollution: Washington, D.C., National Academy Press, 405 p.

National Research Council (2002), Riparian Areas: Functions and Strategies for Management, Natl. Acad. Press, Washington, D. C.

Nelder, J. A., and R. W. M. Wedderburn (1972), Generalized linear models, *Journal of the Royal Statistical Society: Series A (General)*, 135(3), 370-384.

Noe, Gregory B. and Cliff R. Hupp, 2005, Carbon, Nitrogen, and Phosphorus Accumulation in Floodplains of Atlantic Coastal Plain Rivers, USA. Ecological Applications, 15(4): 1178-1190.

Owens, P. N., W.H. Blake, L.Gaspar, D. Gateuille, A.J. Koiter, D.A. Lobb, E.L. Petticrew, D.G.Reiffarth, H.G. Smith, J.C. Woodward (2018), Fingerprinting and tracing the sources of soils and sediments: Earth and ocean science, geoarchaeological, forensic, and human health applications, Earth-Science Reviews, 162, 1-23, doi: 10.1016/j.earscirev.2016.08.012.

Park, Y.-S., R. Cereghino, A. Compin, and S. Lek (2003), Applications of artificial neural networks for patterning and predicting aquatic insect species richness in running waters, *Ecological Modelling*, 160, 265-280, doi:10.1016/j.ecoinf.2015.08.011.

Parker, C., C.R. Thorne, and N. J. Clifford (2014), Development of ST:REAM: a reach-based stream power balance approach for predicting alluvial river channel adjustment, *Earth Surface Processes and Landforms*, doi: 10.1002/esp.3641.

Pearce, A. R., D. M. Rizzo, and P. J. Mouser (2011), Subsurface characterization of groundwater contaminated by landfill leachate using microbial community profile data and a non-parametric decision making process, *Water Resour. Res*., 47(6), W06511, doi:10.1029/2010WR009992.

Pearce, A. R., D. M. Rizzo, M. C. Watzin, and G. K. Druschel (2013), Unraveling Associations between Cyanobacteria Blooms and In-Lake Environmental Conditions in Missisquoi Bay, Lake Champlain, USA, Using a Modified Self-Organizing Map, *Environ. Sci. Technol.*, 47, 14267−14274, doi:10.1021/es403490g.

Pfankuch, D. J. (1975), Stream reach inventory and channel stability evaluation. U.S. Department of Agriculture Forest Service. Region 1. Missoula, Montana.

Phillips, J.D. (2003), Sources of nonlinearity and complexity in geomorphic systems. *Progress in Physical Geography*, 26, 339–361, doi:10.1191/0309133303pp340ra.

Phillips, R.T.J., J. R. Desloges (2014a), Glacially conditioned specific stream powers in low-relief river catchments of the southern Laurentian Great Lakes, *Geomorphology,* 206, 271–287, doi:10.1016/j.geomorph.2013.09.030.

Phillips, R.T.J., J. R. Desloges (2014b), Alluvial floodplain classification by multivariate clustering and discriminant analysis for low-relief glacially conditioned river catchments, *Earth Surf. Process. Landforms*, doi:10.1002/esp.3681.

Pickup, G., Rieger, W.A., 1979. A conceptual model of the relationship between channel characteristics and discharge. Earth Surface Processes 4, 37–42.

Poeppl, Ronald E., M. Keiler, K. Von El Verfeldt, I. Zweimueller, and T. Glade (2012), The Influence of Riparian Vegetation Cover on Diffuse Lateral Sediment Connectivity and Biogeomorphic Processes in a Medium-Sized Agricultural Catchment, Austria. Geografiska Annaler: Series A, Physical Geography, 94 (4), p 511-529.

Poff, N. L., J. D. Allan, M. B. Bain, J. R. Karr, K. L. Pres-tegaard, B. D. Richter, R. E. Sparks, and J. C. Stromberg. 1997. The natural flow regime: a paradigm for river con-servation and restoration. BioScience 47:769-784.

Pringle, C. (2003). What is hydrologic connectivity and why is it ecologically important? *Hydrological Processes*, *17*, 2685–2689.

Prowse, T.D., J. M. Culp (2003), Ice breakup: a neglected factor in river ecology, *Can. J. Civ. Eng*., 30, 128–144, doi:10.1139/L02-040.

Qian, S. S, and T. F. Cuffney (2012), To threshold or not to threshold? That's the question, *Ecological Indicators*, 15, 1–9, doi:10.1016/j.ecolind.2011.08.019.

Qian, S. S., and C. J. Richardson (1997), Estimating the long-term phosphorus accretion rate in the Everglades: a Bayesian approach with risk assessment, *Water Resour. Res*., 33, 1681-1688, doi:10.1029/97WR00997.

Rapp C., Abbe T. (2003) A Framework for Delineating Channel Migration Zones. Washington State Department of Ecology & Washington State Department of Transportation: Ecology Final Draft Publication #03-06-027. https://fortress.wa.gov/ecy/publications/documents/0306027.pdf

Ratcliffe, N.M., Stanley, R.S, Gale, M.H., Thompson, P.J., and Walsh, G.J., 2011, Bedrock Geologic Map of Vermont: U.S. Geological Survey Scientific Investigations Map 3184,

Raven, P.J., N. Holmes, F.H. Dawson, P.J.A. Fox, M. Everard, I.R. Fozzard, K.J. Rouen (1998), River Habitat Quality: the physical character of rivers and streams in the UK and Isle of Man. River Habitat Survey Report No. 2, Environment Agency.

Rinaldi, M., N. Surian, F. Comiti, M. Bussettini (2013), A method for the assessment and analysis of the hydromorphological condition of Italian streams: the Morphological Quality Index (MQI), *Geomorphology*, 180-181, 96–108.

Rizzo, D. M. and D.E. Dougherty, 1994, Characterization of aquifer properties using artificial neural networks: Neural kriging. *Water Resources Research* 30 (2): 483-497.

Rosgen, D. (1996), Applied Fluvial Morphology, Wildland Hydrology Books, Pagosa Springs, CO. ISBN 0 965 32890 2.

Rosgen, D., 2006. Watershed Assessment for River Stability and Sediment Supply, WARSSS. Wildland Hydrology Books, Ft. Collins, Colorado, ISBN 13: 978-0979130809.

Schumm, S.A. 1984. The Fluvial System. New York, NY: John Wiley and Sons.

Schumm, S.A., Harvey, M.D., and Watson, C.C., 1984. Incised Channels Morphology, Dynamics and Control. Water Resources Publications: Littleton, CO.

Schumm SA, Rea DK (1995) Sediment yield from disturbed earth systems. Geology, 23, 391-394.

Shanley, J. B., & Chalmers, A. (1999). The effect of frozen soil on snowmelt runoff at Sleepers River, Vermont. *Hydrological Processes, 13*, 1843-1858.

Shanley, J. B., & Denner, J. C. (1999). The hydrology of the Lake Champlain Basin. In T. O. Manley & P. L. Manley (Eds.), *Lake Champlain in transition-From research toward restoration* (Vol. 1, pp. 41-66): American Geophysical Union, Water Science and Application.

Simon, A. and Hupp, C., 1986, Channel evolution in modified Tennesee channels in Proceedings of the 4th Federal Interagency Sedimentation Conference, Las Vegas US Government Printing Office, Washington, DC, 571-582.

Springston et al, 2011, Fluvial Geomorphology of the Middlebury River Watershed: Geologic Controls, Assessment of Stream Channel Stability, and River Corridor Restoration. Trip B5. Guidebook for Field Trips in Vermont and Adjacent New York. New England Intercollegiate Geological Conference.

Stewart, D.P. and P. MacClintock, 1969, The Surficial Geology and Pleistocene History of Vermont. Vermont Geological Survey Bulletin No. 31.

Stojkovica, M., V. Simic, D. Milosevic, D. Mancev, T. Penczak (2013), Visualization of fish community distribution patterns using the self-organizing map: A case study of the Great Morava River system (Serbia), *Ecological Modelling*, 248, 20-29, doi:10.1016/j.ecolmodel.2012.09.014.

Syvitski, J. P., M. D. Morehead, D. B. Bahr, and T. Mulder (2000), Estimating Fluvial Sediment Transport: The Rating Parameters, *Water Resour. Res.*, 36(9), 2747-2760, 10.1029/2000WR900133.

Thompson, S. E., N. B. Basu, J. Lascurain Jr., A. Aubeneau, and P. S. C. Rao (2011), Relative dominance of hydrologic versus biogeochemical factors on solute export across impact gradients, *Water Resour. Res*., 47, W00J05, doi:10.1029/2010WR009605.

Thoms, M.C., M. Parsons (2003), Identifying spatial and temporal patterns in the hydrological character of the Condamine-Balonne River, Australia, using multivariate statistics, *River Res. Applic*., 19, 443-457, doi: 10.1002/rra.737.

Thorp, J. H., M. C. Thoms, M. D. Delong (2006), The Riverine Ecosystem Synthesis: Biocomplexity in river networks across space and time, *River Res. Applic*., 22, 123-147, doi: 10.1002/rra.901.

Todini, E. (2007), Hydrological catchment modelling: past, present, and future, *Hydrol. Earth Syst. Sci*., 11(1), 468-482, doi:10.5194/hess-11-468-2007.

Toone, J., S. Rice, and H. Piégay (2014), Spatial discontinuity and temporal evolution of channel morphology along a mixed bedrock-alluvial river, upper Drôme River, southeast France: Contingent responses to external and internal controls, *Geomorphology*, 205, 5–16, doi:10.1016/j.geomorph.2012.05.033.

Tran, L. T., C. G. Knight, R. V. O'Neill, E. R. Smith, and M. O'Connell (2003), Self-Organizing Maps for Integrated Environmental Assessment of the Mid-Atlantic Region, *Environmental Management*, 31(6), 822-835.

Turcotte, B., B. Morse, N. E. Bergeron, A. G. Roy, (2011), Sediment transport in ice-affected rivers, *J. Hydrology*, 409, 561-577, doi: 10.1016/j.jhydrol.2011.08.009.

US Department of Agriculture, 1986. *Urban hydrology for small watersheds*. Technical Release 55 (TR-55) (Second Edition ed.). Natural Resources Conservation Service, Conservation Engineering Division.

US Environmental Protection Agency, 2016, "National Summary of State Information" for available water quality data reported by the States to EPA under Section 305(b) and 303(d) of the Clean Water Act. Downloaded July 2016 from: https://iaspub.epa.gov/waters10/attains_nation_cy.control.

de Vente, Joris, J. Poesen, M. Arabkhedri, G. Verstraeten, 2007, The Sediment Delivery Problem Revisited. Progress in Physical Geography, 31(2): 155-178.

Vermont Department of Environmental Conservation, 2016, Vermont Rivers & Roads Field Manual: A Guide for Considering the River and Habitat in the Design, Construction and Maintenance of Transportation Infrastructure in Vermont, available at: http://dec.vermont.gov/sites/dec/files/wsm/rivers/docs/2016_ RiverAndRoadFieldManual.pdf.

Vigiak, O., and U. Bende-Michl (2013), Estimating bootstrap and Bayesian prediction intervals for constituent load rating curves, *Water Resour. Res*., 49, 8565–8578, doi:10.1002/2013WR013559.

Vogel, R. M., B. E. Rudolph, and R. P. Hooper (2005), Probabilistic Behavior of Water-Quality Loads, *J. Environ. Eng.*, 131(7),1081-1089, doi:10.1061/(ASCE)0733-9372(2005)131:7(1081).

Wang, H., Z. Yang, Y. Wang, Y. Saito, and J.P. Liu (2008), Reconstruction of sediment flux from the Changjiang (Yangtze River) to the sea since the 1860s, *J. Hydrology*, 349, 318-332, doi:10.1016/j.jhydrol.2007.11.005.

Ward, J.V., 1989. The four-dimensional nature of lotic ecosystems. Journal of the North American Benthological Society, 8, p. 2-8.

Walling, D. E. (1977), Assessing the accuracy of suspended sediment rating curves for a small basin, *Water Resour. Res.*, 13, 531–538.

Walling, D.E. (1983), The Sediment Delivery Problem, *J. Hydrology*, 65, 209-237.

Walling, D.E. (2013), The evolution of sediment source fingerprinting investigations in fluvial systems, *J. Soils Sediments*, 1310, 1658-1675.

Walling, D.E. and J.C. Woodward (1992), Use of radiometric fingerprints to derive information on suspended sediment sources. *In* Erosion and sediment transport monitoring programmes in river basins. Publ. 210. IAHS, Wallingford, UK.

Walling, D.E., J. C. Woodward, A.P. Nicholas, (1993), A multiparameter approach to fingerprinting suspended sediment sources. In: Tracers in Hydrology, IAHS Publication No. 215, 329–338.

Walter, R.C.,Merritts, D.J., 2008. Natural streams and the legacy of water-powered mills. Science. 319 (5861), 299–304.

Weber, M. D. and G. B. Pasternack (2017), Valley-scale morphology drives differences in fluvial sediment budgets and incision rates during contrasting flow regimes, *Geomorphology*, 288, 39-51, doi:10.1016/j.geomorph.2017.03.018.

Williams, G.P., and Costa, J.E., 1998, Geomorphic measurements after a flood: *In* Baker, V.R., Kochel, R.C., and Patton, P.C., eds., Flood geomorphology: Wiley Interscience, NY: New York, p. 65-77.

Wohl, E. (2018), Geomorphic context in rivers, *Progress in Physical Geography*, 1–17, doi: 10.1177/0309133318776488.

Wohl, E. (2010), A brief review of the process domain concepts and its application to quantifying Wohl, E., 2010b. Mountain Rivers Revisited. American Geophysical Union Press, Washington, D.C.

Wolman, M. G., and R. Gerson (1978), Relative scales of time and effectiveness of climate in watershed geomorphology, *Earth Surf. Process. Landf.*, 3, 189-208, doi: 10.1002/esp.3290030207.

Wolman, M.G. and J.P. Miller, 1960. Magnitude and Frequency of Forces in Geomorphic Processes. J. Geology, 68: 54-74.

Yellen, B., J. D. Woodruff, L. N. Kratz, S. B. Mabee, J. Morrison, and A. M. Martini (2014), Source, conveyance and fate of suspended sediments following Hurricane Irene. New England, USA, *Geomorphology*, *226*, 124-134, doi: 10.1016/j.geomorph.2014.07.028.

Yochum, S. E., J. S. Sholtes, J. A. Scott, B. P. Bledsoe (2017), Stream power framework for predicting geomorphic change: The 2013 Colorado Front Range flood, *Geomorphology*, 292, 178-192, doi:10.1016/j.geomorph.2017.03.004.

CHAPTER 2. EVALUATING SPATIAL VARIABILITY IN SEDIMENT AND PHOSPHORUS CONCENTRATION -DISCHARGE RELATIONSHIPS USING BAYESIAN INFERENCE AND SELF-ORGANIZING MAPS

Abstract

Given the variable biogeochemical, physical, and hydrological processes driving fluvial sediment and nutrient export, the water science and management communities need data-driven methods to identify regions prone to production and transport under variable hydro-meteorological conditions. We use Bayesian analysis to segment concentration-discharge linear regression models for total suspended solids (TSS) and particulate and dissolved phosphorus (PP, DP) using twenty-two years of monitoring data from eighteen Lake Champlain watersheds. Bayesian inference was leveraged to estimate segmented regression model parameters and identify threshold position. The identified threshold positions demonstrated a considerable range below and above the median discharge – which has been used previously as the default breakpoint in segmented regression models to discern differences between pre- and post-threshold export regimes. We then applied a Self-Organizing Map (SOM), which partitioned the watersheds into clusters of TSS, PP and DP export regimes using watershed characteristics, as well as Bayesian regression intercepts and slopes. A SOM defined two clusters of high-flux basins, one where PP flux was predominantly episodic and hydrologically-driven; and another in which the sediment and nutrient sourcing and mobilization were more bimodal, resulting from both hydrologic processes at post-threshold discharges and reactive processes (e.g., nutrient cycling or lateral/vertical exchanges of fine sediment) at pre-threshold discharges. A separate DP SOM defined two high-flux clusters exhibiting a bimodal concentration-discharge response, but driven by differing land use. Our novel framework shows promise as a tool

with broad management application that provides insights into landscape drivers of riverine solute and sediment export.

Introduction

The river network is an integrator of spatiotemporal variability in catchment properties. Stakeholders face significant challenges to model the export of sediment and nutrients based on concentration-discharge relationships measured at a catchment outlet, and to prioritize the allocation of limited resources to achieve reductions in sediment and pollutant loading. Given the regulatory context of Total Maximum Daily Loads (TMDLs) in the US and the Water Framework Directive in the European Union, there has been a recent focus on quantifying loads of solutes and sediment. Yet as research becomes increasingly interdisciplinary in nature, a more holistic approach to investigating catchment dynamics has returned emphasis to concentration-discharge relationships and what they may reveal about biogeochemical filtering processes at multiple spatiotemporal scales (*Basu et al.,* 2011; *Gall et al.,* 2013). Better understanding of concentration-discharge dynamics will help identify critical catchment locations and time periods ("hot spots" and "hot moments") responsible for disproportionate fluxes of solutes and sediment, inform best management practices, and thereby optimize overall reductions in loading at broader temporal and spatial scales (*McClain et al.,* 2003; *Heathwaite et al*., 2000).

Practitioners need models that predict spatiotemporal variability in concentration-discharge relationships and their linkage to catchment characteristics and processes - and at the same time deal with large amounts of data that vary in type and spatial-temporal resolution. Physically-based, distributed models are able to forecast constituent

concentration and flux, but accuracy and calibration are resource-intensive, making such models typically less transferable among watersheds or regions (*Todini*, 2007). On the other hand, data-driven models can be more readily implemented and have the appeal of representing system complexity in simple ways (*McDonnell et al.*, 2007), although they are more limited in their prediction capabilities. Ideally, stakeholders are guided by a combination of model types. With the advent of automated samplers and *in situ* sensors, an increasing number of studies have leveraged high-frequency monitoring data to develop conceptual models that further refine our understanding of temporal and spatial patterns in concentration-discharge dynamics (e.g., *Lloyd et al*., 2016; *Bende-Michl et al.*, 2013).

Parametric statistical techniques have been applied to infer relationships between water quality and various biogeochemical characteristics of catchments using concentration (C) –discharge (Q) or load-discharge relationships. The parsimonious sediment (and nutrient) rating curve - i.e., $\log(C) = \log(\beta_0) + \beta_1 \log(Q)$ - has been used to examine between-watershed differences in sediment and solute production (e.g., *Walling*, 1977; *Vogel et al.*, 2005). Sediment and nutrient regression parameters have been interpreted to suggest drivers of underlying processes (*Syvitski et al.*, 2000; *Asselman*, 2000; *Godsey et al.*, 2009; *Basu et al.*, 2011). While prediction does not necessarily suggest causation, the coefficient ($\log \beta_0$) and exponent (β_1) in this linear model can be interpreted to suggest something about the system properties (*Asselman*, 2000; *Syvitski et al*., 2000) and encapsulate the "biogeochemical filtering" of the watershed in question (*Gall et al*., 2013). The intercept of the linear regression model represents the background sediment (or solute) concentration delivered from the catchment source

regions and explained by variables other than changing discharge proximal to the gaging location. In the context of sediment transport modeling, the regression intercept reflects the capacity of the watershed to produce and transport fine sediment (*Asselman*, 2000). It has been characterized as an "index of sediment supply" (*Wang et al*., 2008) or a "baseline supply parameter" (*Krishnaswamy et al*., 2000), and may be a function of particle size and weathering intensity in the source catchment, as moderated by vegetative controls or human disturbances.

On the other hand, the regression slope parameter reflects the rate at which the energy of flowing water is transferred to its physical surroundings to entrain and transport sediment (or sediment-bound constituents) and to accomplish geomorphic change (*Krishnaswamy et al*., 2000; *Wang et al*., 2008). The regression slope can be thought of as an index of the river's erosive power, with higher values (i.e., steeper slopes) indicating greater sediment transport capacity, and may also reflect the degree to which additional sources of sediment (or sediment-related constituents) become available to the river at higher flow stages (*Asselman*, 2000). Flatter regression slopes can be characteristic of rivers where sediment continues to be transported even under lower discharge conditions – as a function of either ample supply or easily-entrained particle size in the source areas, or both (*Asselman*, 2000). Previous studies have used the slope value from a concentration-discharge regression to classify catchments on a continuum between accretionary (> 0) and dilutionary (< 0) (*Basu et al*., 2010; *Gall et al.*, 2013). *Godsey et al.*, (2009) proposed that chemostatic watershed responses (i.e., constant concentration with increasing discharge) could be defined by an absolute value less than 0.2 (i.e., near-zero regression slope). Subsequent work (*Thompson et al.*, 2011; *Basu et*

al., 2010), however, clarified that at low slope values, constituent concentrations can still exhibit considerable variance around a central tendency (i.e., chemodynamic response). Moreover, as the slope value approaches zero, concentration becomes decoupled from discharge as an explanatory variable; the coefficient of determination (r^2) value becomes nonsignificant, and the linear regression slope loses importance in the interpretation of the concentration-discharge relationship.

Instead, the coefficient of variation (CV) ratio (i.e., CV of concentration vs. CV of discharge) has been promoted to characterize the concentration-discharge relationship on a continuum from episodic (chemodynamic) to chemostatic (*Thompson et al.*, 2011). Thompson *et al.,* (2011) classified North American catchments with varying hydrologic, geologic, topographic and land use settings based on a bivariate plot of CV ratio and normalized constituent export for total phosphorus and total suspended solids (among other constituents). Those watersheds with higher normalized export exhibited chemostasis (low CV ratios), which can be attributed to legacy stores of nutrients with an anthropogenic source (*Basu et al*., 2011) or geogenic constituents (*Godsey et al*., 2009). Building on this approach, Musolff *et al.* (2015) used a bivariate plot of CV ratios and regression slope to cluster humid temperate catchments into five constituent export regimes. Categories ranged from strongly chemodynamic responses, termed "threshold-driven" (with strongly positive regression slopes) or "reactive" (with smaller absolute values of the regression slope, either positive or negative), to less chemodynamic responses with a concentration-discharge correlation that is either weak ("chemostatic") or strong, ranging from accretionary (termed "mobilization") to "dilution" driven.

These studies employed slope and intercept parameters developed from simple linear regression models. Often, however, concentration-discharge (C-Q) relationships show variability across the discharge distribution (Zhang *et al*., 2016) or exhibit threshold effects (*Meybeck and Moatar*, 2012) that would be better modeled with a segmented regression. Segmented linear C-Q responses may result from temporal or spatial discontinuities in sediment and solute transport - either from natural conditions (e.g., bedrock nickpoints, or sudden reduction in gradient) or human modifications (e.g., dams) (*Wang et al*., 2008; *Toone et al*., 2014; *Williams and Wolman*, 1984). A segmented linear pattern may also result from sudden depletion of sediment/solute supply relative to discharge, or dilution effects (*Shanley et al*., 2011; *Meybeck and Moatar*, 2012).

Solute-export plots developed on slope and intercept parameters from simple regression models in the style of *Musolff et al.* (2015) or *Thompson et al.* (2011) may not adequately characterize solute export conditions for basins that exhibit significant threshold effects (Figure 2.1). Segments before and after a threshold will have different slope and intercept values, suggesting different sediment/solute export regimes (or functional stages) for pre- and post-threshold flow conditions. Application of a segmented regression method will not only improve model fit, it can provide greater insight into landscape drivers of the C-Q response, and suggest management strategies appropriate to different functional stages (*Bende-Michl et al*., 2013).

However, it can be difficult to determine the optimal discharge value for the onset of threshold effects, and to identify the nature of the transition as either stepped, transitional or continuous (*Qian and Cuffney*, 2012). *Moatar et al*., (2017) have presented a review of nine, single-threshold, C-Q patterns based on fixed segmentation at

the median discharge value on a log-log plot (*Meybeck and Moatar*, 2012), although they acknowledge the actual inflection point in the slope of the C-Q relationship may vary from the median Q value. Methods have been developed to define a threshold using both parametric (*Ryan et al.*, 2002 - bootstrapping) and Bayesian techniques (*Alameddine et al.*, 2011; *Qian and Cuffney*, 2012; *Qian and Richardson*, 1997); but relatively few studies have focused on determining the hydrologic, hydraulic and biogeochemical processes that may account for these threshold effects, or dominate during pre- and post-threshold phases (*Wang et al.*, 2008; *Ryan et al.*, 2002; *Moatar et al.*, 2017).

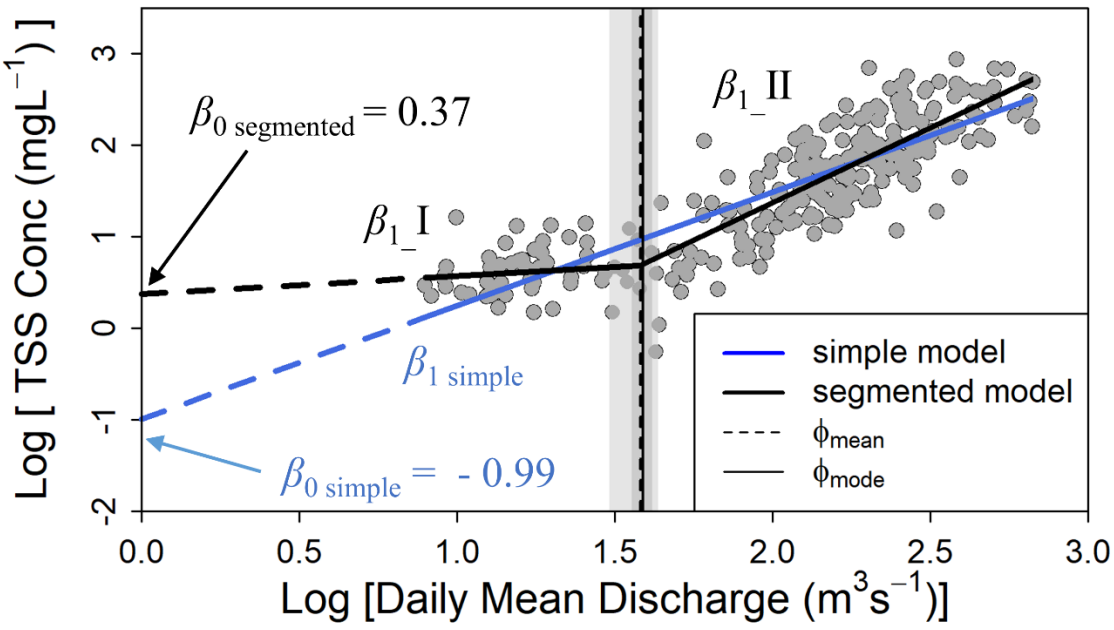

Figure 2.1. Comparison of best-fit simple (blue line) and segmented (black line) regression models for log_{10}-transformed Total Suspended Solids (TSS) concentration vs daily mean discharge data for Winooski River (n=261) for 1992-2015. Data points were fit with Bayesian linear regression methods. Threshold (ϕ) of segmented model depicted as solid vertical line (mode) and dashed vertical line (mean) with gray shading indicating the 95% credible interval of the posterior distribution. Regression parameters are annotated, including the intercept (β_0) for each model, and pre-threshold ($\beta_{1_}$I) and post-threshold slopes ($\beta_{1_}$II) of the segmented model.

We use a Bayesian regression method in this work to facilitate selection of the threshold position, and quantify the uncertainty on the estimated threshold, as well as other regression parameters. Generation of a posterior joint distribution for each model parameter, and the ability to define a credible interval for the estimate at a chosen probability level, permits explicit estimation of uncertainties associated with the model selection and the data (e.g., variance introduced by sampling and analytical methods (*Qian et al.*, 2005)). This approach provides more information than a Frequentist approach to simple (or segmented) regression that generates a single point estimate of the central tendency of model parameters. Bayesian frameworks have the added advantage of allowing for non-normal distribution of residuals and greater robustness to outliers (*Gelman et al.*, 2004). Bayesian methods have been applied to estimate values of regression parameters for simple linear models of stage-discharge relationships (*Moyeed and Clark*, 2005); an eight-parameter load rating curve for nutrients (*Vigiak and Bende-Michl*, 2013), and segmented regression models for nitrogen-discharge patterns (*Alameddine et al*., 2011; *Qian and Richardson*, 1997).

C-Q dynamics result from a complex interaction of hydrologic, hydraulic, and biogeochemical processes. “Functional stages” of sediment and nutrient export have been defined using hierarchical clustering to result from unique combinations of source strength and connectivity, entrainment or mobilization conditions, and transport mechanisms; and these functional stages vary in both space and time (*Bende-Michl et al*., 2013). Self-organizing maps (SOMs) are data-driven, nonparametric techniques well-suited for classifying or clustering data of varying types (e.g., continuous, ordinal, nominal), scales and distributions. SOMs have advantages over other methods for data

visualization and interpretation (*Alvarez-Guerra, et al*., 2008), and have demonstrated superior performance over parametric methods where data contain outliers or exhibit high variance (*Mangiameli et al.*, 1996). SOMs have been used to classify or cluster multivariate environmental data, including instream species richness (*Park et al.*, 2003), fish community distribution patterns (*Stojkovica et al*., 2013), alluvial fan types (*Karymbalis et al.*, 2010), lake chemistry data associated with harmful algal blooms (Pearce *et al.*, 2011, 2013), estuary sediment samples (*Alvarez-Guerra et al.*, 2008), watershed-based ecoregions (*Tran et al.*, 2003), and riverine habitats (*Fytilis and Rizzo*, 2013). While SOMs have been applied to hydrologic time series data to classify runoff response (*Ley et al.*, 2011), the authors are not aware of research that has applied a neural network to cluster basins into sediment and nutrient export regimes.

In this work, we combine the application of a Bayesian segmented linear regression technique paired with an SOM to cluster patterns in C-Q relationships as a function of catchment properties for a humid-temperate study area located in a previously-glaciated, mountainous region of the Northeastern US. The purpose of this research was two-fold: (1) to model threshold effects in C-Q regressions using Bayesian techniques to enhance the utility of regression metrics to suggest watershed variability in hydrologically- and biogeochemically-driven impacts on C-Q dynamics; and (2) examine the ability of various watershed metrics to predict C-Q relationships and characterize between-watershed comparisons of sediment and nutrient flux or concentration.

Methods

Study Area

The study area consists of 18 tributary basins of Lake Champlain that drain portions of Vermont and New York in the northeastern US, as well as the province of Quebec in Canada (Figure 2.2). In recent decades, this largely mesotrophic lake has been impacted by an increasing frequency of harmful algal blooms in its eutrophic bays, and is the subject of a TMDL for phosphorus (*Smeltzer et al*., 2012). Eighteen of the Lake Champlain tributaries have been monitored for more than 25 years (*Medalie et al.,* 2012) and were selected for this study for their sufficient duration of flow gaging and water quality records (*Kennard et al*., 2010). The selected basins range in size from 137 to 2,754 km^2 and represent a wide range of geologic settings and land cover / land use conditions.

The Lake Champlain Basin (LCB) was previously glaciated, and spans biogeophysical regions from the Green Mountains in Vermont to the Adirondack Highlands in New York, separated by the Champlain Valley Lowland in the north-central basin and Taconic Mountains and Vermont Valley in the south end of the basin merging with the Hudson Valley Lowland (*Stewart and MacClintock*, 1969). Elevations in the study basins range from 1,339 m at Mount Mansfield in the Winooski Basin of Vermont, and 1,629 m at Mount Marcy in the Ausable River basin of New York, to 29 m at the average water level of Lake Champlain. The climate is characterized as humid temperate, with mean annual precipitation (MAP) ranging from over 1,270 mm along the north-south trending spine of the Green Mountains to a low of 813 mm in the Champlain

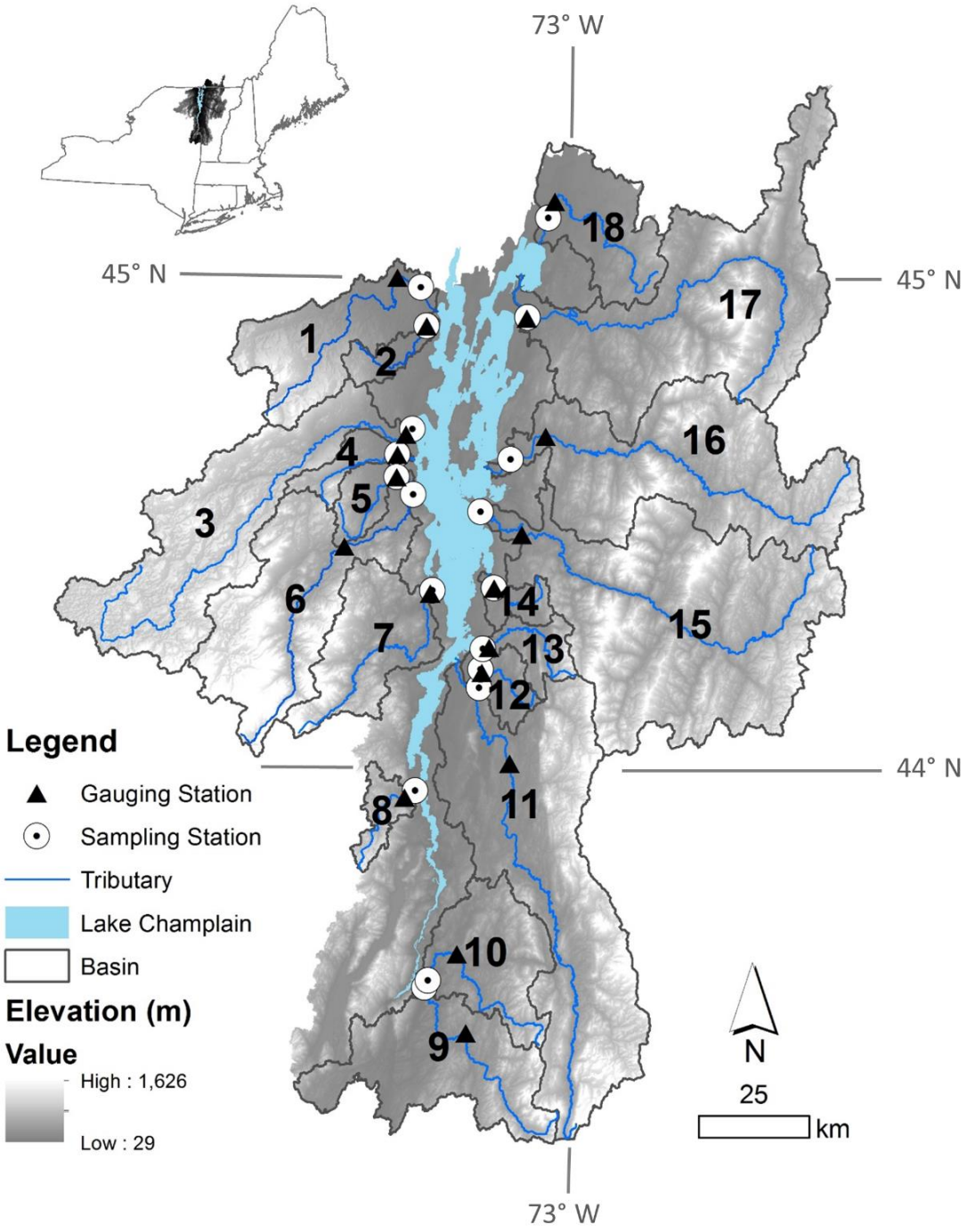

Figure 2.2. Locations of the 18 study area watersheds in the Lake Champlain Basin. Watershed identifications are keyed to Table 1.

Valley (*Randall*, 1996). Within a typical year, a majority of the runoff from Lake Champlain tributaries occurs between ice-out and late spring (*Shanley and Denner*, 1999). The hydrologic regime is characterized by variable hydrologic source areas attributed to saturation-excess flow regimes (*Dunne and Black*, 1970). Flow in some of the basins is regulated to varying degrees by hydroelectric dams that operate in run-of-river mode (Supplemental Table 2.S1). In recent years, these basins have been impacted by extreme events, including Tropical Storm Irene (August 2011) in central and southern Vermont and floods of 1996 and 1998 in northeastern New York.

Watershed Characteristics

Various hydrologic, topographic, geologic and land use characteristics were developed for the 18 tributary basins (Table 2.1). Land use in the selected watersheds ranges from 3.3 to 54% agricultural and 33 to 89% forested. Urban land uses, including transportation corridors, range from 4.4 to 14% (*Troy et al*., 2007). Flow-normalized total suspended solids (TSS), particulate phosphorus (PP), and dissolved phosphorus (DP) flux and concentration data for each basin were compiled from *Medalie* (2014) for each available year (1990 - 2012 for PP and DP; 1992 – 2012 for TSS). PP was derived as the difference of measured total and DP (filtered to < 0.45 µm). Flow-normalization was achieved using *Weighted Regressions on Time, Discharge, and Season* (*Hirsch et al.*, 2010); and data thus reflect interannual variability in constituent flux and concentration attributed to factors other than flow variability. To facilitate between-watershed comparisons, mean annual constituent flux was normalized by basin area to generate a mean annual, flow-normalized, yield (in $mT/km^2/yr$ for TSS and in $kg/ km^2/yr$ for PP and DP; Table 2.S2).

Table 2.1. Physical characteristics of Study Area watersheds, Lake Champlain Basin

Map Key	Tributary	Total Drainage Area [a] (km^2)	Mean Annual Precip-itation [b] (mm)	Peak Flow Anomaly [c] (-)	Basin Relief [d] (m)	Drainage Density [e] (km/km^2)	Percent of Hydrologic Soil Group A & B Soils [f] (%)	Land Use [g]			
								Water/ Wetland (%)	Forest (%)	Agri-culture (%)	Dev-eloped (%)
6	Ausable	1,334	1,164	16.0	1,598	1.08	26.5	3.0	89.1	3.3	4.5
7	Bouquet	708	1,051	14.7	1,446	1.18	30.0	1.5	87.4	6.3	4.6
1	Great Chazy	778	848	11.8	1,139	1.54	38.7	3.7	68.7	21.9	5.6
16	Lamoille	1,870	1,198	10.7	1,309	1.89	24.4	2.3	39.1	44.4	14.2
14	LaPlatte	137	1,002	21.9	468	2.05	8.1	2.2	75.5	13.9	8.2
13	Lewis	207	1,074	19.1	736	2.32	28.5	4.2	61.6	25.6	8.2
5	Little Ausable	193	850	21.2	619	1.23	55.0	1.4	71.5	19.4	7.8
2	Little Chazy	140	917	14.1	429	1.37	45.1	3.5	58.4	30.7	7.3
12	Little Otter	188	974	14.7	380	3.08	15.2	3.4	33.0	54.0	9.4
9	Mettawee	1,063	1,228	17.7	1,117	1.36	25.6	2.7	59.1	29.3	8.9
17	Missisquoi	2,232	1,050	11.3	1,146	1.57	33.3	1.9	73.0	18.8	6.2
11	Otter	2,442	1,239	3.5	1,260	1.99	27.8	3.3	62.9	25.7	8.0
18	Pike	662	1,184	12.0	681	1.23	71.4	2.3	52.6	37.7	7.0
10	Poultney	719	1,120	15.3	800	1.65	13.0	5.0	66.0	20.9	8.0
8	Putnam	160	1,103	17.6	678	1.33	36.2	4.2	87.2	3.8	4.4
4	Salmon	175	913	20.1	693	1.42	55.4	2.2	77.9	11.0	9.0
3	Saranac	1,589	1,070	6.1	1,451	0.93	26.6	9.8	81.0	3.9	5.3
15	Winooski	2,754	1,163	10.3	1,307	1.77	18.1	1.5	76.6	9.9	11.7

a Source: (WBD) 1:24,000 scale

b PRISM data for 1981 - 2010 obtained through USGS Streamstats of Vermont (*Olson*, 2014) and New York (*Lumia et al*., 2006)

c Ratio of mean annual peak flow to mean annual flow for the period from 1990-2012 (except Little Ausable (wy1992-2012) and Pike (wy2001-2015))

d Source: 10m Digital Elevation Models

e Total length of National Hydrography Dataset (NY, Que) or Vermont Hydrography Dataset stream network mapped in each basin, normalized by basin area

f Sources: SSURGO (NY and VT), Canadian National Soil Database (Que), and STATSGO02 (Franklin County portion of the Saranac River basin in NY)

g Source date: 2001; Developed category includes Open-Urban and Roads; Agriculture includes Brush/Transitional; from (*Troy et al.*, 2007)

Additionally, slope (β_1) and intercept ($\log_{10}(\beta_0)$) values from Bayesian linear regression models were developed for the time series of TSS, PP, and DP concentration (C) – discharge (Q) data (see next section). These data were included as indicators of the sediment and nutrient export regimes of the watersheds (*Vogel et al.*, 2005; *Asselman*, 2000). C-Q data were sourced from long-term monitoring data sets of instantaneous concentrations (*VTDEC*, 2015) and daily mean flows (*USGS*, 2016). Velocity- and depth-integrated composite samples were collected approximately monthly, targeting a mixture of flow conditions (*VTDEC*, 2015). PP/DP and TSS were sampled approximately 12 and 10 times per year, respectively. In the few cases (1.8% for TSS, 0.3% for DP/PP) where constituents were reported below the detection limit (i.e., 1 mg/L for TSS, 5 µg/L for DP/PP), a value one half the respective detection limit was substituted. C and Q data were $\log_{10}$–transformed to meet homoscedasticity assumptions for application of linear models.

Coefficient of Variation (CV) of the C and Q time series (non-transformed), were each calculated as the series standard deviation, σ, normalized by the series mean, μ:

$$CV = \frac{\sigma}{\mu}.$$

A CV ratio was then generated to evaluate the temporal inequality between CV of the two variables, C and Q:

$$\frac{CV_C}{CV_Q} = \frac{\sigma_C}{\mu_C} * \frac{\mu_Q}{\sigma_Q}.$$

Pre- and post-threshold values (i.e., Segment I and II of the segmented regression model; Figure 2.1) were treated independently.

A flow duration curve for each basin was constructed from existing USGS records of mean daily Q for years 1990 through 2015 (*Medalie*, 2014; *USGS*, 2016; *Centre d'Expertise Hydrique Québec*, 2016). The threshold value determined from Bayesian linear regression (next section) was normalized in two ways to enable between-basin comparisons of the threshold magnitude: (a) as a ratio to the median Q; and (b) expressed as a quantile of flow based on the flow duration curve.

Bayesian Linear Regression

Model Development

Segmented rating curves were developed via Bayesian linear regression (BLR) methods on the time series of C data (TSS, PP, DP) and mean daily Q data from the 18 tributaries for years 1990 through 2015. BLR provided a framework for identifying thresholds (*Qian and Cuffney*, 2012), and defining credible intervals around the estimated values for threshold, intercept, and pre- and post-threshold slopes (Figure 2.1). Bayesian models also permitted the seamless back-transformation of error terms addressing bias introduced when using log-transformed regressors (*Stow et al*., 2006; *Koch and Smillie*, 1986), and allowed for the explicit estimation of sources of uncertainty in the C-Q relationships (*Schmelter et al*., 2012). Concentration was modeled as a power function of discharge:

$$C_t = \beta_0 \, Q_t^{\beta_1} \ ,$$

where C is the sediment or solute concentration, and Q is the river discharge for a specified time interval, *t*. Rating curves were developed as the logarithm (base 10) of instantaneous concentration, C, regressed on the $\log_{10}$ of daily mean discharge, Q:

$$log_{10}C_t = \ log_{10}\beta_0 + \ \beta_1 log_{10}(Q_t) + \ \varepsilon.$$

$\text{Log}_{10}(\beta_0)$ - commonly simplified to β_0 - is the model intercept and β_1 is the slope of the regression line, which describes the predicted change in log-C with each incremental increase in log-Q. The error term, ε, then reflects scatter about the regression line and encapsulates all other sources of variance in sediment (nutrient) C with Q, such as differences in constituent availability due to seasonal effects and antecedent conditions. This error term also includes measurement error of model parameters. The following segmented linear regression model was applied to all time series data:

$y \sim N(\mu_y, \sigma_y^2)$, where:

$$\mu_y = \begin{cases} \beta_0 + \beta_1 x + \varepsilon_1 & if\ x < \phi\ (Segment\ I) \\ \beta_0 + (\beta_1 + \delta) x + \varepsilon_2 & if\ x \geq \phi\ (Segment\ II) \end{cases}$$

and where y refers to the response variable ($\log_{10}$ C); x is the explanatory variable ($\log_{10}$ Q); μ_y and σ_y^2 are the mean and variance of the response variable, respectively; ϕ is the threshold value of Q; δ is the change in slope past the threshold; and ε is the model error. For those watersheds not exhibiting a strong threshold C-Q response, the above model collapses to a simple linear regression, signified by a near-zero value for δ. The Bayesian framework includes prior knowledge on model parameters (i.e., $\beta_0, \beta_1, \mu, \sigma^2$, ϕ, δ) through the specification of parameter distributions. Vague priors were established for all parameters so that the posterior distributions would be influenced most by the data themselves (*Gelman et al.,* 2004).

Model Diagnostics and Evaluation Criteria

The posterior distributions on the pre-threshold (β_1_I) and post-threshold (β_1_II) regression slope parameters for each BLR model run were evaluated as either flat, inclined positively (accretionary), or inclined negatively (dilutionary). If the 95%

credible interval (CI) on the posterior distribution of the mean of β_1 included a zero value, the segment slope was deemed flat, or near-zero. The posterior quantiles on the delta (δ) parameter of the model were also examined to determine whether the 95% CI excluded a value of zero. Inclusion of a zero value in the CI for δ would suggest no significant difference between the slopes of Segments I and II, and a simple regression model might equally-well characterize the C-Q relationship. A decision tree for model assignment is included in supplemental Figure 2.S1.

Post-hoc analysis of model assignments was performed comparing means of basin characteristics by model type using one-way Analysis of Variance (ANOVA) methods followed by Tukey Honest Significant Differences (HSD) tests between individual group means. For those variables that were not normally distributed (as tested by Shapiro-Wilks method), nonparametric methods were applied (Kruskal-Wallis). Model assignments were also compared on a univariate basis for correlations to physical and hydrological variables, applying Pearson methods (or the nonparametric Spearman's rank method when underlying data were not normally distributed). Statistical tests were performed in JMP (v. 12.0, SAS Institute, Cary, North Carolina).

Model Computation

BLR model fitting and parameter estimation were carried out using Markov-chain Monte Carlo (MCMC) methods. A Gibbs sampler was used to obtain samples from the posterior distribution and estimate the mean, mode, quantiles and credible intervals for each model parameter. MCMC sampling was implemented in R (*R Core Development Team,* 2016) using JAGS (*Plummer,* 2003) through interfaces developed in software packages, including "rjags" (*Plummer,* 2016), "runjags" (*Denwood,* 2016), and "coda"

(*Plummer et al*., 2006). R code for the BLR model is provided in the supplementary material. Sampling was conducted with four parallel chains initialized with random number generators, for 100,000 iterations with a thinning factor of 10, after discarding the initial 5,000 iterations for adaptation and burn-in phases. Convergence was confirmed by visual examination of trace plots and the Gelman-Ruben statistic (*Gelman and Rubin*, 1992); i.e., potential shrink reduction factor less than 1.1. Measures of chain stability and accuracy included Monte-Carlo standard errors (or estimated SD of the sample mean in the chain) and effective sample size (or number of iterations normalized by autocorrelation of chains).

SOM Model Development

Supplementary material (Figure 2.S2) contains a conceptual diagram of the SOM used to cluster the study area basins into distinct sediment and nutrient flux regimes based on physical and hydrological variables. Individual observations (vector of input variables, in this case, physical characteristics of the watersheds such as MAP, basin relief, drainage density, *etc*.) are clustered into output categories (in this case, dominant annual-average sediment or nutrient flux). Details of the SOM algorithm, computational methods, and cluster validation techniques are provided in supplementary materials.

The final input data comprise seventeen variables, including metrics describing hydrologic, topographic, geologic and land use characteristics of the 18 tributary basins (Table 1) and selected parameters derived from regressions of C on Q for TSS, PP and DP. Inputs were range normalized (*Alvarez-Guerra et al*., 2008) as follows:

$$norm(x_i) = \frac{(x_i - \min(x_i))}{(\max(x_i) - \min(x_i))}.$$

Clusters were examined *post hoc* for their ability to predict loading, by comparing mean annual TSS/PP/DP concentration, flux, and yield (Table 2.S2) between clusters. Flux and yield values were log-transformed to ensure normality for application of ANOVA methods. For each input variable, the intra-cluster mean (on a normalized scale) was plotted against the overall mean, and the magnitude and direction relative to the overall mean was examined to better understand variables driving the clustering.

Results and Discussion

Models of Concentration-Discharge Dynamics Revealed by BLR

BLR methods identified six general C-Q patterns for the LCB watersheds out of the nine classifications proposed by *Moatar et al*., (2017) (Figure 2.3a, Tables 2.S3a, b, c). For TSS, the best fit of C-Q data for six of the basins was provided by Model A (i.e., an upward-inclined pre-threshold segment, and upward inclined post-threshold segment, or "up-up" pattern), while ten basins exhibited a Model D (flat-up) response and two were classified as Model B (up-flat). Given the close correlation of PP to TSS (average $R^2 = 0.81$; range: 0.50 to 0.93), model assignments for PP C-Q patterns were nearly identical, with four exceptions. The PP model differed from the TSS model for Mettawee, Little Ausable, and Pike (all D models) and Salmon (A; Table 2.S3b). A majority of the C-Q responses for DP was classified as Model D (12); additional DP responses were classified as Model G (3), E (2) or C (1), characterized by a down-up, flat-flat, or up-down pattern, respectively.

Our BLR methods permitted the definition of subclasses on the C-Q Model A and I, extending the classification of *Moatar et al*., (2017) (Figure 2.3b and 2.3c).

Examination of the posterior for model parameter, δ, allowed us to determine if regression slopes were credibly different before and after the indicated threshold. A steeper post-threshold slope (relative to the pre-threshold value) classified the response as either Model A2 (accretionary) or I2 (dilutionary); a lesser post-threshold slope defined Model A3 or I3. In the case of no credible difference between the slopes of Segments I and II (i.e., 95% CI includes zero), the model type was classified as either A1 (accretionary) or I1 (dilutionary). For TSS and PP, respectively, 28% and 22% of our basins were distinguished as having a Model A2 C-Q response.

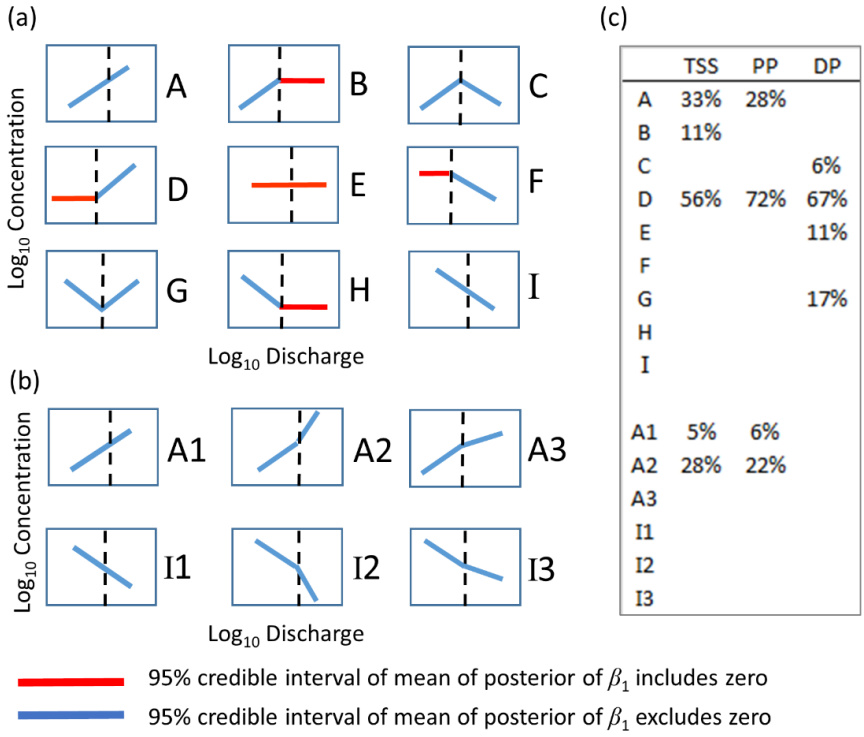

(c)

	TSS	PP	DP
A	33%	28%	
B	11%		
C			6%
D	56%	72%	67%
E			11%
F			
G			17%
H			
I			
A1	5%	6%	
A2	28%	22%	
A3			
I1			
I2			
I3			

Figure 2.3. Identification of segmented regression models of $log_{10}C$-$log_{10}Q$ relationships, including (a) conceptual models of nine types identified by *Moatar et al*. [2017], modified to depict a variable threshold position (vertical dashed line) and colored indication of dominant export regime of pre- or post-threshold segment: hydrologic (blue) and reactive (red) ; (b) variations on Models A and I suggested by this study and discerned through examination of posterior distribution of model parameters for BLR; and (c) relative abundance of model types exhibited by study area watersheds for TSS, PP, and DP.

A degree of uncertainty in model assignment arose in five cases for DP and two for PP. For all model types other than A1, E, and I1, the posterior on the delta (δ) parameter should exclude zero (Figure 2.S1). However, this was not always the case. For example, the DP C-Q response for Little Otter was assigned to Model D based on a 95% CI for the pre-threshold slope that included zero and for the post-threshold slope that excluded zero. However, the 95% CI for δ spanned zero, suggesting no significant difference between the slope values, and that a simple model (A1) could fit the data nearly as well. Similarly, Model A1 could have been substituted for Model D for Poultney (DP), Boquet (DP), Great Chazy (DP), Pike (PP), and Putnam (PP); and Model E rather than H could have fit the DP data nearly as well for Putnam (Model E rather than H). Several factors may have contributed to this uncertainty. Little Otter and Putnam are small basins that tend to exhibit weaker C-Q correlations (*Syvitski et al.*, 2000). Uncertainty in the DP model assignments may have arisen due to the generally weaker correlation of this solute to Q (i.e., lower β_1 values), as compared to sediment. Finally, in the cases of Poultney and Putnam, representativeness of the C-Q time series may have influenced model assignment, as the highest flows are somewhat underrepresented in the available records for these basins (Table 2.S4).

Overall, the C-Q responses for TSS and PP were dominated by positive slopes including Models A (33 and 28%, respectively) and D (56%, 72%). We attribute this accretionary pattern to the relative abundance of suspended sediments in these post-glacial basins and to legacy stores of phosphorus. A threshold effect in the C-Q response for TSS (and by extension, PP and other sediment associated constituents) is not uncommon (*Hicks*, 2000; *Meybeck and Moatar*, 2012). A similar distribution of TSS

models (62% D and 21% A) was observed by *Moatar et al*., (2017) in a sampling of 293 gaging stations in French basins ranging from 50 to 110,000 km^2. The C-Q responses for DP in our study area basins were also dominated by positive slopes. Dilutionary effects were relatively uncommon and limited to DP Models C and G for our LCB study area. In this regard, our results differed from those of *Moatar et al*. (2017), who evaluated a close analog to DP, namely, PO_4^{3-}. The majority of their basins exhibited a stable or declining C trend with Q (Models E, H, or I), while our basin responses were dominated by an accretionary hydrologic response for DP at high flows (67% Model D and 17% G). Our model assignments may not be directly comparable, since we applied Bayesian inference of the 95% CI on the posterior of β_1, and Moatar *et al*., (2017) used an absolute value of 0.2 for β_1 to distinguish accretionary or dilutionary behavior from a stable response. However, our β_1_II values (mean of posterior distribution) for DP ranged from 0.22 to 0.46, with one exception: 0.13 for Little Otter. Figure 2.S3 illustrates pre- and post-threshold values for our 18 basins with whiskers denoting the 95% CI on parameter estimates relative to the traditional value of 0.2.

Regression Slopes

Pre-Threshold

For TSS, ten basins had a flat or nearly-flat pre-threshold segment (Model D); values of β_1_I for these basins ranged from -0.28 to 0.48 (Figure 2.4a). However, the 95% CI of the posterior distribution of β_1_I spanned zero, suggesting that a zero value is also possible. Six basins exhibited a C-Q pattern with a moderately- to strongly-inclined pre-threshold slope (either Model A1 or A2) with β_1_I values ranging from 0.28 to 0.87, and with the 95% CI on these estimates excluding a zero value. The mean β_1_I value (μ

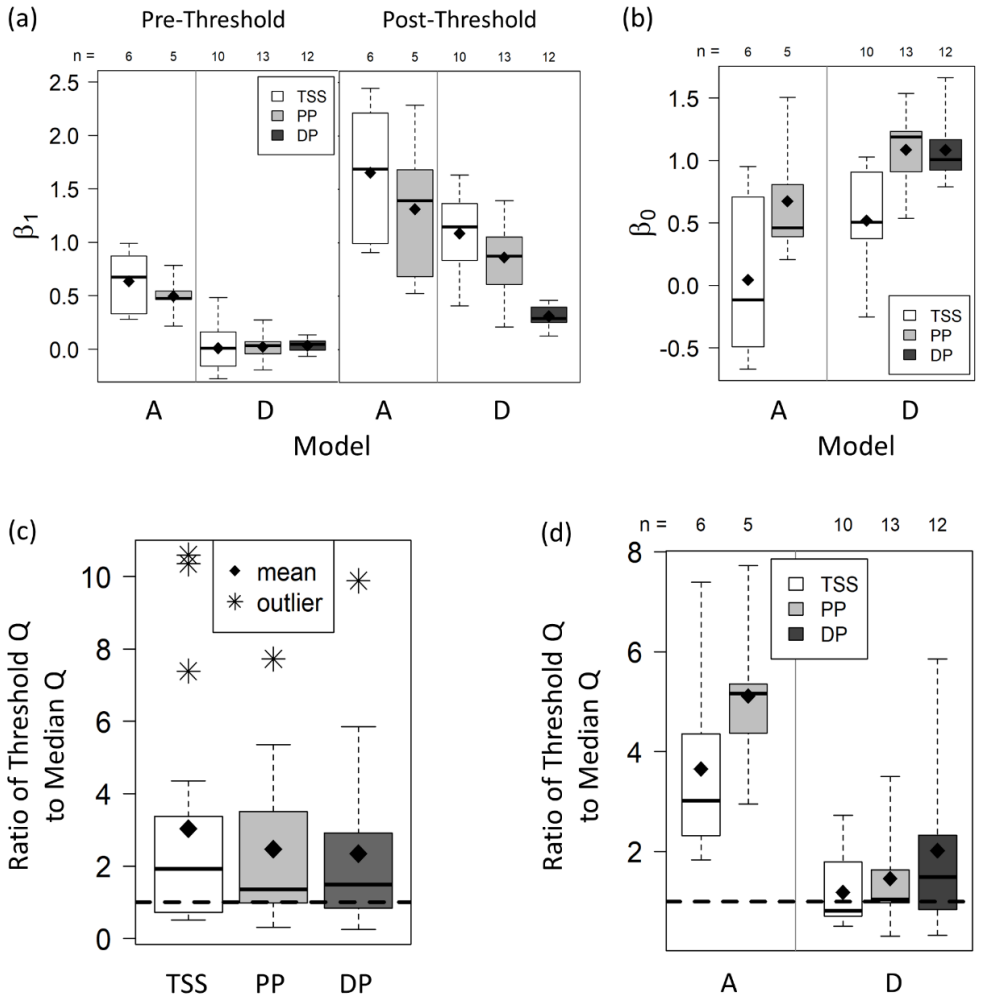

Figure 2.4. Box plots of: (a) β_1 and (b) β_0 regression parameters by constituent (TSS, PP, and DP) for the most frequently-encountered $log_{10}C$-$log_{10}Q$ relationships in the Lake Champlain Basin (Models A and D). Letter symbols denote C-Q regression model type after Figure 3. Bottom panels display the ratio of threshold Q to median Q **(c)** by constituent and **(**d**)** by constituent for Model types A and D.

= 0.57) for Model A2 basins was significantly different (ANOVA, $p<0.05$) and greater than the mean β_1_I value for Model D basins (μ = - 0.01). The one Model A1 and two Model B basins had β_1_I values in a range comparable to the Model A2 basins (Table S3a). Similarly, for PP, the β_1_I values for Model A2 basins (μ = 0.42; range: 0.21 to 0.54; n=4) were significantly different (ANOVA, $p<0.05$) and higher than values for

Model D basins (μ = 0.02; range: -0.19 to 0.27, n=13). The one Model A1 basin had a β_1_I value comparable to the Model A2 basins. For DP, pre-threshold slopes were largely flat or declining. Model D fit a majority of the basins, with β_1_I values (μ = 0.03; range: -0.07 to 0.13; n=12) comparable to those of PP and TSS (Figure 2.4a).

Post-Threshold

For both TSS and PP, the range of values for post-threshold slope, β_1_II, was higher for Model A basins than D basins (Figure 2.4a). For TSS, the group mean value for Model A2 basins (μ = 1.8; range: 0.99 to 2.4; n = 5) was greater than Model D basins (μ = 1.1; range: 0.41 to 1.6; n = 10; ANOVA, $p<0.10$). Two Model B basins had statistically-significant ($p<0.10$) lower post-threshold slopes than either A2 or D basins, with β_1_II values of -0.28 and 0.5. For PP, Model A2 basins (μ = 1.5; range: 0.68 to 2.3; n = 4) were greater than Model D basins (μ = 0.86; range: 0.21 to 1.4; n = 13; ANOVA $p<0.10$). For DP, post-threshold slopes (μ = 0.31; range: 0.13 to 0.46; n=12) were less than TSS and PP, although still weakly accretionary. Our Model D values for β_1_II (mean of posterior distribution) ranged from 0.22 to 0.46, with one exception: 0.13 for Little Otter.

Regression Intercepts

Mean values of β_0 were not significantly different between model groups (ANOVA, $p > 0.05$), but PP and DP model intercepts were higher than TSS intercepts (Figure 2.4b). When considering sediment-related constituents for all 18 basins on a univariate basis (Spearman's rank correlation, $p<0.10$), the TSS and PP β_0 values correlated negatively to basin relief (-0.469, -0.542) and positively to drainage density (0.511, 0.452). The intercept values for the solute, DP, were negatively correlated to total

drainage area, MAP, and basin relief (-0.550, -0.480, -0.689). Additionally, the percent land cover in agricultural use showed a significant positive correlation (0.488) to DP β_0 value. Intercept values for all three constituents (TSS, PP, DP) showed strong positive correlations to mean concentrations of total calcium (0.608, 0.701, 0.641), and mean total calcium (TCa) concentration, itself, was strongly correlated, in a negative sense, to total drainage area (-0.647) and basin relief (-0.845).

Findings for TSS are somewhat inconsistent with some other studies, which identify basin area as a significant factor inversely correlated to the regression intercept for sediment (*Syvitski et al.,* 2000; *Nash*, 1994). For example, in a study of 57 North American river gaging stations (on 49 rivers) with upstream drainage areas ranging from 720 to 1,680,000 km^2, Syvitski *et al*. (2000) reported a negative correlation between mean annual discharge (MAQ; as a proxy for basin size) and β_0, with MAQ explaining up to 65% of variance in β_0. With the addition of basin relief, the explained variance in the intercept increased by 5% to 70%. Our study found a moderately strong negative correlation to Total Drainage Area (Pearson r = -0.507) for PP, but this relationship was weaker for TSS (r = -0.362). Differences between our results and those of *Syvitski et al*. (2000) may be related to the wide range of basin sizes examined in the latter study. If their data set is restricted to basins of comparable size (i.e., less than 5,000 km^2, n = 11), a similar negative correlation value is obtained (r = -0.413). Notably, all the intercept values calculated by *Syvitski et al.* (2000) were less than zero, while our intercept values included a mix of positive and negative values. *Syvitski et al*. (2000) values were based on simple linear regressions, which may underestimate the β_0 value in threshold-affected watersheds. Employing segmented regressions has allowed for a less constrained

interpretation of β_0 relative to other basin variables, wherein the β_0 value is less tied to the magnitude of β_1. In other words, under the constraint of simple linear regression, an increase in β_1 will necessarily be associated with a decrease in β_0 (*Warrick*, 2014; *Asselman*, 2000). Under a segmented model fit, the magnitude of β_0 is less constrained by collinearity with the post-threshold slope, β_1_II (see Figure 2.1), and thus more useful for characterizing export dynamics.

Threshold magnitude and frequency

Model types were further reviewed for differences in threshold magnitude and frequency by examining the threshold value expressed as a ratio to the median Q (Tables 2.S3a, b, c) and computing the percentage of time that the threshold is exceeded. Notably, threshold positions identified for TSS/PP/DP models by our BLR methods, demonstrated a considerable range below and above the median Q (Figure 2.4c). The threshold position expressed as a ratio to the median Q was particularly high for two TSS Model B basins, one TSS Model A2 basin, PP Model A1, and DP Model E (comprising the outliers in Figure 2.4c).

The ten TSS Model D basins (μ = 1.2; 0.5 to 2.7) generally had lower threshold positions than Model A2 basins (μ = 4.0; 2.3 to 7.4; Figure 2.4d) and group means were statistically different (Wilcoxon rank-sum, $p<0.05$). Consequently, the percentage of time that the TSS threshold was exceeded was greater for Model D basins (17 to 72%) than for Model A2 basins (2 to 20%), (Wilcoxon, $p<0.05$). Thus, D basins are spending a relatively large amount of time in a functional stage characterized by positive C-Q correlation. The one A1 basin had a threshold position similar to the A2 basins. Two Model B basins (Little Ausable and Salmon) had very high threshold positions, exceeded

less than 2% of the time, beyond which C-Q data transitioned from a positive correlation to a flat response. The PP C-Q response reflected a similar pattern, with Model D basins exhibiting significantly lower threshold positions than Model A2 basins. No significant difference between DP models was observed for threshold ratios, which ranged widely from 0.2 to 9.9 times the median Q. DP Model D basins had a similar central tendency and range of threshold ratio as their TSS and PP counterparts (Figure 2.S3b).

On a univariate basis, the TSS and PP threshold ratios were positively correlated to the slope of the pre-threshold segment (0.712, 0.571, Wilcoxan, $p<0.05$), since Model A2 basins (with higher threshold positions) are characterized by inclined pre-threshold slopes while Model D basins (with lower threshold positions) have near-flat pre-threshold slopes. DP threshold ratios were positively correlated to the post-threshold regression slope - a reflection of the fact that a majority of those basins with thresholds above the median Q were classified as either Model D or G, which demonstrate a positive C-Q relationship for the post-threshold segment.

Sediment and solute export regimes

Regression and variance metrics can be used to classify sediment and nutrient export regimes of catchments on a continuum from chemodynamic to chemostatic, and from positive to negative correlation of the log C-Q relationship. We have adapted the bivariate plot of β_1 and CV ratio suggested by *Musolff et al.* (2015) as a convenient way to compare our results to theirs, and to highlight the advantages of a segmented regression model for discerning variable export regimes for pre- and post-threshold flow stages. *Musolff et al.* (2015) identified two overlapping zones for chemodynamic response of TSS and total phosphates, denoting export regimes dominated by "threshold-

driven" and "reactive" processes, with the latter straddling the $\beta_1 = 0$ line (Figure 2.5a). Their conceptual model defined "threshold-driven" responses as being episodic in nature with a strongly-positive relationship between C and Q (i.e., high β_1 value). These are systems in which C variability is driven predominantly by Q variability, and both *Musolff et al*. (2015) and *Thompson et al*. (2011) mapped TSS to this category. To avoid confusion, and for consistency with *Moatar et al*., (2017), we have used a more generalized term - "hydrologic"-ally-driven (Figure 2.5) – for rivers that plot to this zone, since use of the term "threshold-driven" by *Musolff et al.* (2015) does not appear to suggest a prerequisite that all watersheds of this zone exhibit a distinct threshold(s) in the C-Q pattern. For example, a Model A, E or I response could plot to this zone. In contrast, "reactive" responses reflect processes that are more independent of fluctuating Q and that are characterized by rapid instream cycling (*Musolff et al.,* 2015). Musolff *et al*. (2015) and Thompson *et al*. (2011) identified ammonium and phosphates in this category, citing the importance of biologically- and chemically-mediated processes in controlling C. Similarly, *Moatar et al*., (2017) identified a weak C-Q relationship ("reactive" response) for TSS at flows below the median Q, and suggested the importance of biochemical processes in regulating TSS concentration at these low-flow stages. In the context of sediment and sediment-related constituents, we expand the definition of "reactive" export regimes to include the array of biologically-, chemically- and *physically*- mediated processes that are responsible for the removal (uptake) or return (release) of constituents from advective transport (*Fisher et al.,* 1998). Thus, for PP and TSS, "reactive" could include non-chemical and non-biological processes that are largely decoupled from Q, such as lateral and vertical exchanges of fine sediment and associated

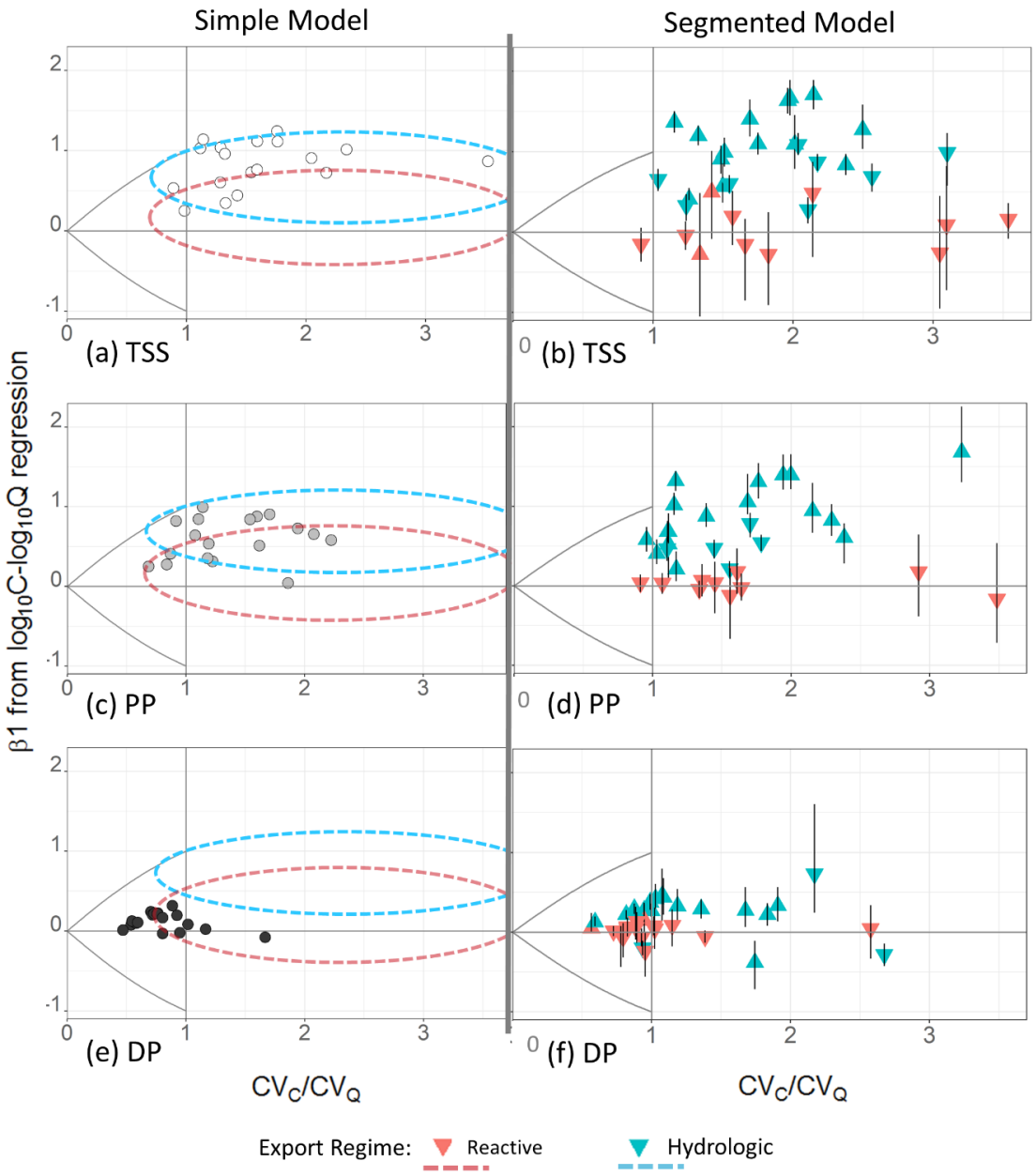

Figure 2.5. Plot of regression slope (β_1) vs. CV ratio to visualize export regime for TSS (top panels), PP (middle), and DP (bottom) from 18 LCB watersheds, respectively, (using presentation style of *Musolff et al.* (2015)). Simple regression data are presented in panels a, c and e; segmented regression data are presented in panels b, d, and f, with metrics for pre-threshold data (down-directed triangle) plotted separately from post-threshold data (up-directed triangle). Vertical whiskers span the 95% credible intervals around the estimate of β_1 defined by BLR. Bounds in the upper left and lower right of each panel are defined solely by CV_Q and β_1 (not CV_C), and have been derived from the mean and standard deviation of Q from Boquet data (see *Musolff et al.*, (2015) for further discussion).

constituents between the water column and the stream bed, channel margin deposits, disconnected flood chutes or floodplain (*Boano et al*., 2014; *Karwan and Saiers*, 2009; *Skalak and Pizzuto*, 2010).

Figure 2.5 illustrates bivariate plots for TSS, PP, and DP from our 18 LCB tributaries based on simple linear regression (Figure 2.5a, c, e) and segmented regression (Figure 2.5b, d, f). Overall, a stronger C-Q relationship is suggested by data points derived from a segmented regression than is revealed by the simple regression results (supplementary Text 2.S3), leading to greater dispersion on the β_1 / CV ratio plot. (Select data points with very high β_1 or CV values plot off the chart and are not represented in Figure 2.5 for image clarity). For TSS and PP, post-threshold data generally have higher, positive β_1 values and thus plot above the pre-threshold points, which tend to assemble close to the horizontal line marking a zero value for β_1. In the case of DP, the points assemble closer to the zero line, reflecting the generally lower β_1 values for this solute.

Figures 2.5b, 2.5d and 2.5f also help visualize the uncertainty on the pre- and post-threshold β_1 parameter explicitly estimated from our BLR approach, and how this was leveraged to classify model types (Figure 2.3a and 2.3b) as well as assign a "reactive" or "hydrologic"-ally-driven export regime (*Musolff et al*., 2015). The posterior distribution of the β_1_I (or β_1_II) parameter available from the BLR was examined, and if the 95% CI spanned a value of zero, the point was classified as "reactive" and color-coded red. Otherwise, the point was classified as "hydrologic"-ally-driven and coded blue.

For TSS and PP, the C-Q relationship of the pre-threshold stage in some cases plots to the "reactive" zone, rather than the "hydrologically-driven" zone (i.e., the Model

D basins). During the low-flow functional stage, C dynamics are nearly independent from Q (i.e., r^2 values for logC-logQ regressions are very low); and therefore, β_1 metrics provide minimal information for interpretation (*Thompson et al*., 2011). These basins are distinguished from the Model A1 and A2 basins in which the pre-threshold points were classified as "hydrologic"-ally-driven (color-coded blue) and β_1 values defined some credibly positive slope, ranging on a continuum from modestly to substantially accretionary. For TSS, two basins exhibited a "reactive" post-threshold slope (Model B). For both basins (Salmon and Little Ausable), the indicated threshold is high (greater than 10 times the median Q), and the pattern may reflect particle exhaustion at these highest discharges. In the case of Little Ausable, the apparent C-Q pattern may also be a function of having poor sample representation from these highest flow ranges (Table 2.S4). For DP, a majority of the pre-threshold stages were classified as "reactive" (Models D or E); a few basins demonstrated a hydrologically-driven response at low flows – either accretionary (Model C) or dilutionary (Model G). Similarly, most basins exhibited a hydrologically-driven post-threshold response (Model D or G), although a few were either dilutionary (Model C) or stable (Model E). Two basins have a pre- or post-threshold value that is negative and greater in absolute value than 0.2 (Otter Model C and Little Chazy Model G).

Previous researchers (*Thompson et al.*, 2011; *Basu et al*., 2010; *Musolff et al*., 2015) have suggested an absolute value of 0.2 for the regression slope as a "cut-off" to distinguish between reactive and hydrologic response. Bayesian inference provides an alternative, data-driven approach for interpretation of the regression slope parameter, which also offers insight into the uncertainty of model assignment. Interestingly, most of

our model assignments employing BLR conformed to this rule of thumb, with accretionary or dilutionary responses defined by a mean of the posterior on $\beta 1$ values > |0.2|. Generally speaking, the uncertainty of the β_1 estimate, or length of whiskers defined by the Bayesian credible interval, is greater in magnitude for the pre-threshold slopes than the post-threshold slopes for all three constituents. This finding may reflect seasonal shifts in "reactive" vs. "hydrologic" process dominance at these low flows, as moderated by factors such as temperature, plant growth, and aquatic biota. For example, recent research, aided by high-frequency sampling, suggests that the transition between functional stages is dynamic and driven largely by meteorological variables such as antecedent moisture or rainfall intensity, rather than being predominantly a function of basin-scale physical features (*Bieroza and Heathwaite*, 2015; *Bende-Michl et al*., 2013). Additionally, interannual shifts in threshold position may be contributing to uncertainty in the β_1 estimate (e.g., due to river system responses to extreme events, changing land use patterns or progressive implementation of watershed restoration projects and best management practices) (*Zhang et al.*, 2016).

Thus, while previous research has suggested that TSS and PP C-Q patterns are consistently hydrologically-driven at a basin scale (*Musolff et al*., 2015), our BLR approach suggests that TSS and PP export regimes can exhibit more complexity. In some threshold-affected systems, low discharge ranges may comprise a distinct functional stage that is more dominated by reactive processes, including and facilitated by lateral and vertical exchanges of fine sediment within the hyporheic and parafluvial zones which temporarily remove constituents from advective flow. In this context, the river corridor can be viewed as a reactor facilitating changes in particulate P concentration, as opposed

to just a vessel for transport (*Withers and Jarvie*, 2008; *Harvey and Gooseff*, 2015; *Mullholand et al.*, 1997).

The variance in threshold position among watersheds is a reflection of the duration of time that each watershed stays in a particular functional stage of sediment/nutrient flux. For example, although not a focus of this current study, the seasonal distribution of flows that exceed the PP threshold may influence the relative annual flux among basins. A cursory review of 1990-2015 discharge data indicates that the PP Model D basins spend a majority of their time (>50%) in the pre-threshold, reactive, functional stage during the months of June through October (Figure 2.S5). Most of the basins are also dominantly in this reactive functional stage during the month of February (all except Poultney). Some of the Model D basins (Great Chazy, Little Otter, Mettawee, and Winooski) spend a majority of all months except April in this reactive functional stage; these are basins with a particularly elevated threshold position exceeded between 13 and 29% of the time on an annual basis. The latter three basins have some of the highest mean annual concentrations of PP (Table 2.S2). Future application of our novel approach will examine seasonal variation in threshold position and functional stages of nutrient and sediment export.

SOM Clustering of Watersheds for PP and DP

By pre-classifying our eighteen LCB tributaries into distinct C-Q patterns, relying on Bayesian inference, we have improved the utility of regression metrics to suggest between-watershed differences in drivers and capacity for system export of sediment and phosphorus. This expanded set of regression metrics can be included, alongside other basin metrics, as inputs to a SOM for grouping our humid temperate basins by constituent

export regime. Our main intent was to discern whether the combination of watershed characteristics and export regime was responsible for greater or lesser flux of PP and DP to Lake Champlain. For example, it is conceivable that a basin that exhibits a strong sediment/PP C-Q response but has low overall P source strength due to land cover patterns, may generate low overall flux to LCB. Conversely, a basin with high sediment and P source strength may generate low flux to LCB if there are aspects of topography, climate, or geomorphic setting that enhance storage or attenuation of sediment/ PP within the river network leading to a weaker C-Q response (i.e., lower β_1). Therefore, we included both watershed characteristics (i.e., precipitation, discharge, soils, land cover, etc.) and export regime metrics as inputs to a PP SOM and DP SOM, in order to model these nonlinear, epistatic relationships, and cluster the basins by overall average annual flux of TSS and PP to Lake Champlain.

For each constituent, the 18 basins were assigned to three distinct clusters and multivariate input data (Tables 2.1 and 2.S3a, b, c) have been reduced to a 2-D lattice for visualization: a 3x6 lattice for PP (Figure 2.6a) and a 4x4 lattice for DP (Figure 2.7a). The column-to-row ratio for theses lattices approximated the ratio of the first two principal components of the input data (5.7/ 3.4 for PP; 4.3/3.2 for DP; PCA on correlations), as per *Cereghino and Park* (2009). Clustering outcomes were slightly different for each constituent (Figures 2.6b, 2.7b), driven by differing combinations of input variables (Figures 2.6c, 2.7c).

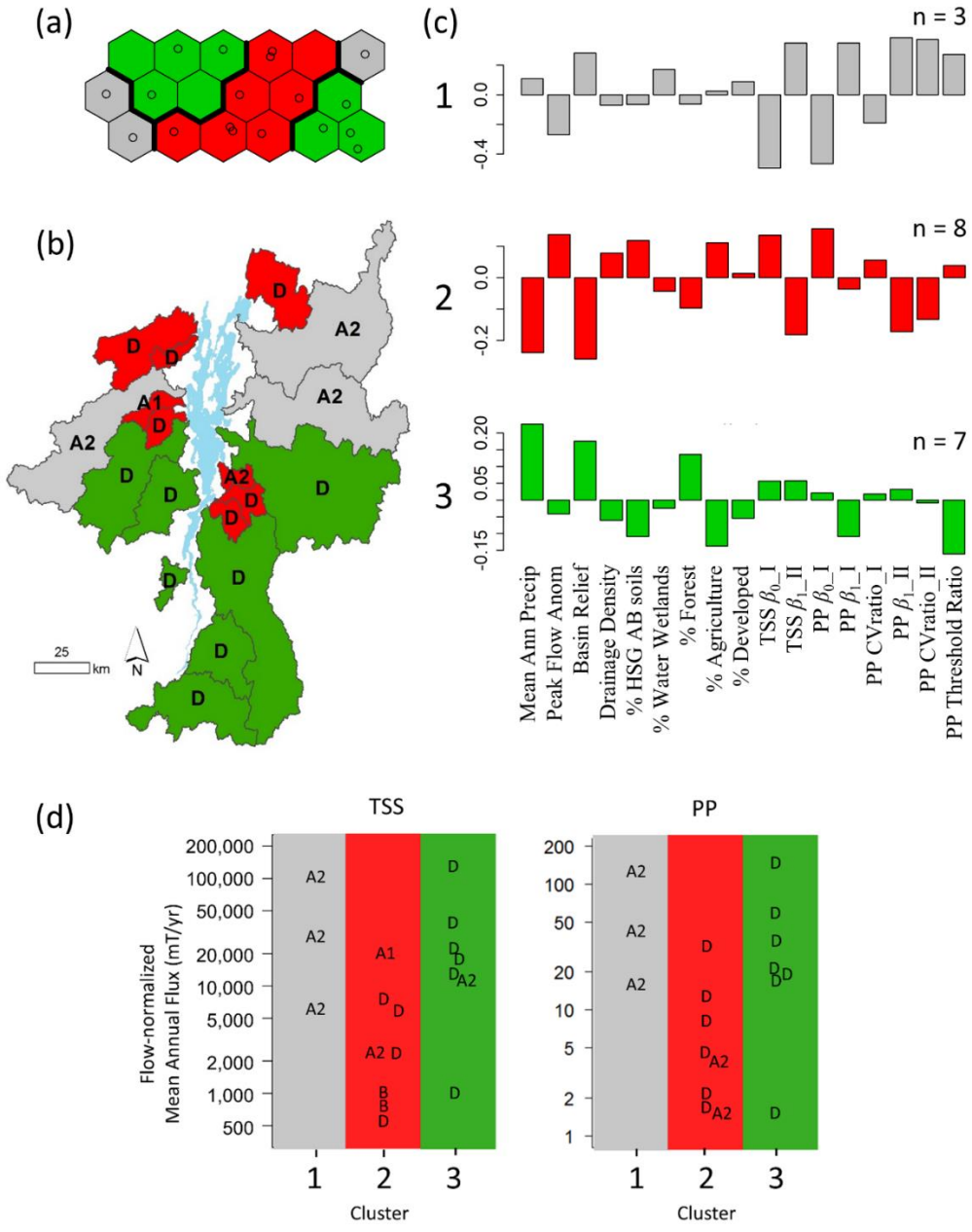

Figure 2.6. Particulate Phosphorus SOM clustering outcomes for Lake Champlain Basin tributaries, including **(**a**)** SOM lattice (see Supplementary Figure 2.S2 and Text 2.S2); (b) basin location map color-coded by SOM cluster assignment and keyed to C-Q regression model types; (c) variable bar plots by cluster (n = number of basins per cluster; y-axis represents range-normalized values; refer to Section 2.4). Note: for clarity of presentation, variable plots have been rendered using different vertical scales. Panel (d) depicts mean annual flux of TSS (left) and PP (right) in metric tons per year (mT/year) by SOM cluster. Color shading relates to clusters in panels a - c. Letter symbols denote C-Q regression model type after Figure 2.3. Flux estimates are from *Medalie* (2014).

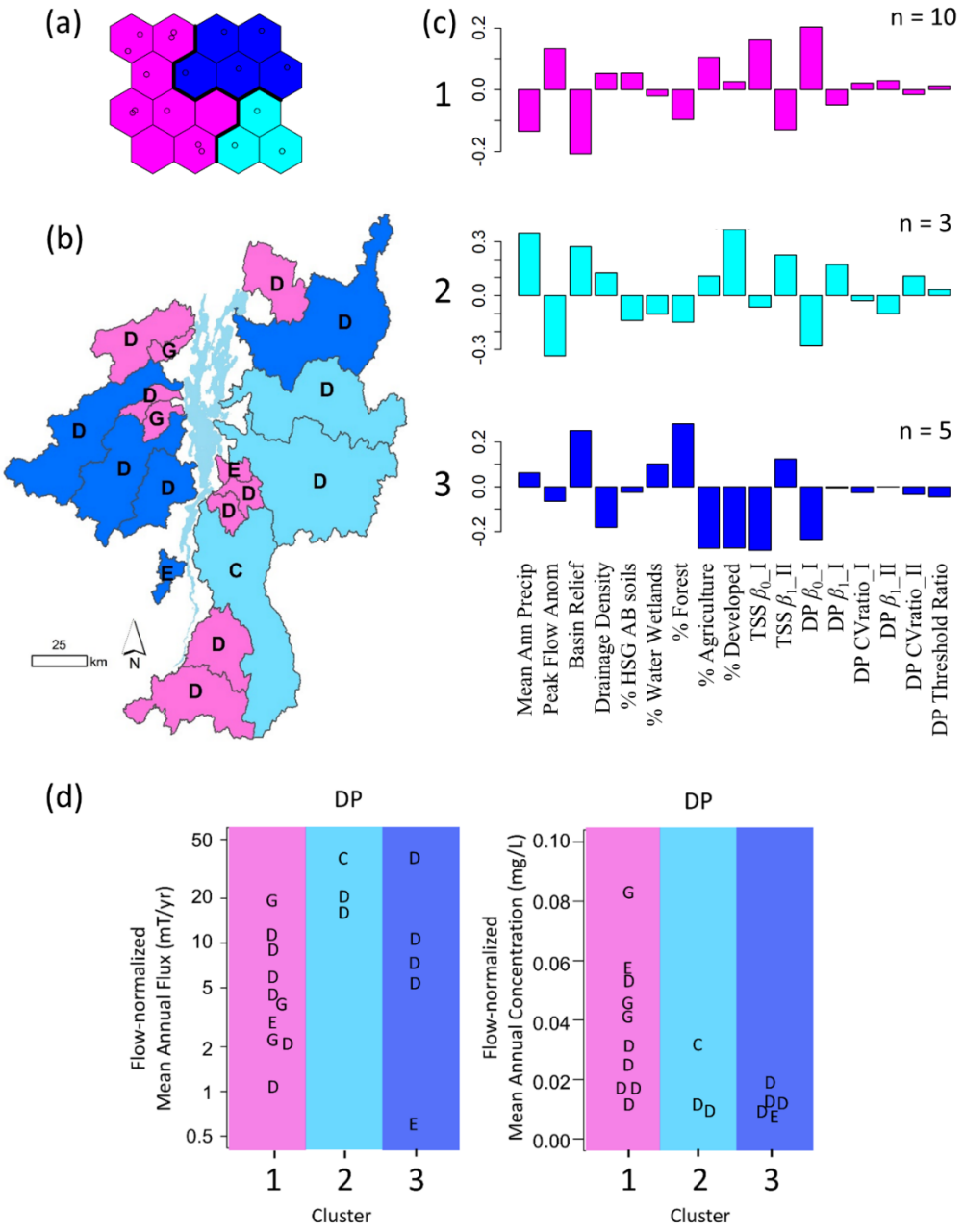

Figure 2.7. Dissolved Phosphorus SOM clustering outcomes for Lake Champlain Basin tributaries, including (a) SOM lattice; (b) basin location map color-coded by SOM cluster assignment and keyed to C-Q regression model types; (c) variable bar plots by cluster (n = number of basins per cluster; y-axis represents range-normalized values; refer to Section 2.4). Note: for clarity of presentation, variable plots have been rendered using different vertical scales. Panel d depicts mean annual flux in metric tons per year (left) and concentration in milligrams per liter (right) of DP by SOM cluster. Color shading relates to clusters in panels a - c. Letter symbols denote C-Q regression model type after Figure 3. Flux and concentration estimates are from *Medalie* (2014).

PP SOM Results

ANOVAs revealed significant differences between mean cluster values for flow-normalized flux of both TSS and PP ($p<0.10$; Figure 2.6d), but not for mean annual concentration or yield ($p > 0.10$). *Post-hoc* testing applying Tukey HSD showed that the mean flux values for Clusters 1 and 3 were higher than, and statistically different from, Cluster 2 for both PP and TSS ($p<0.10$). Larger basin sizes were generally associated with greater flux of TSS and PP. However, Clusters 1 and 3 comprised basins of similar size, but clustered separately.

Cluster 1 and 3 basins each exhibit strong threshold effects in the C-Q response for both TSS and PP: Model A2 for Cluster 1 and Model D for Cluster 3, except Mettawee in Cluster 3, which was classified as Model A2 for TSS. While both Cluster 1 and 3 basins demonstrated higher-than-average flux of PP and TSS (Figure 2.6d), a different combination of variables appears to be driving this pattern in each case (Figure 2.6c). These two clusters share some variables in common – including, higher-than-average values for basin relief and MAP.

Variables that distinguish these two higher-loading Clusters (1 and 3) from each other (i.e., variables that trend in opposite directions from the overall mean) include the regression intercepts for both TSS and PP and the post-threshold response for PP (Figure 2.6c). Cluster 1 (Model A2) basins appear to have greater transport capacity (larger β_1_II values) relative to Cluster 3 (mostly Model D) basins (Figure 2.4d). However, threshold position as a ratio to the median Q was higher for Cluster 1 than 3 basins, although not significantly so (ANOVA/ Tukey HDS, $p > 0.10$). This would mean that transport of sediment and sediment-bound P occurs disproportionately during less-frequent, higher-

magnitude flows in these Model A2 basins – i.e., they exhibit a more episodic C-Q response than Model D basins, and could be considered supply-limited with respect to TSS and PP (*Thompson et al*., 2011; *Basu et al*., 2011). Importantly, Model A2 basins also have steeper pre-threshold slopes relative to Model D basins. Therefore, small discharge events are more impactful on TSS and PP export than similar magnitude events in Model D basins.

Cluster 1 basins appear to have a much lower range of β_0 values for each constituent than their Cluster 3 counterparts, reflecting a lower baseline supply of suspended sediment and particle-bound P in the former group. The lower-than-average β_0 values for TSS and PP (as well as the higher-than-average β_1 values previously noted) in Cluster 1 basins (Saranac, Lamoille, and Missisquoi) may also be related to instream impoundments (Table 2.S1) and the possible storage of fine sediments and PP behind dams at least during low to moderate flow stages. For example, *Wang et al.,* (2008) noted a stepped decrease in the intercept parameter for C-Q regressions developed for TSS time series data on the Yangtze River in China, as instream impoundments were constructed to support generation of hydropower. At the same time, they attributed observed increases in β_1 to the increased erosive power in the lower reaches of the Yangtze River in China, resulting when upstream impoundments sequestered sediments and led to decreased downstream concentrations of suspended sediments (so-called, "hungry water" effects of *Kondolff* (1997)). Elevated β_1 values in impounded rivers have also been attributed to effects of diminished sediment storage capacity of instream reservoirs (*Zhang et al*., 2016).

Cluster 3 basins tend to be dominated by lower-infiltration soils (exhibit lower percentages of HSG A and B soils). This is likely a reflection of their geographic position with near-lake areas located in the Champlain Valley or Vermont Valley/ Taconic biophysical regions. These regions are associated with silt and clay deposits from postglacial freshwater and brackish-water lake episodes that inundated the valley to higher stages than the present Lake Champlain (*Stewart and MacClintock*, 1969). Similarly, *Medalie* (2013) noted a significant correlation between physiographic province and both concentration (Kruskal-Wallis $p = 0.092$) and flux ($p = 0.045$) of total phosphorus. This difference between Cluster 1 and Cluster 3 basins is particularly illustrated when comparing the Winooski basin (Cluster 3) to Lamoille and Missisquoi basins (Cluster 1). Despite similar size, relief, MAP, and impoundment / flow regulation status, these basins clustered differently for PP, driven in large part by differences in β_0 values which resulted in their assignment to different regression model types (e.g., Winooski, TSS_ $\beta_0 = +0.37$, Model D vs. Lamoille and Missisquoi values of -0.67 and -0.29, Model A2). This higher-than-average baseline supply of sediment (and PP) for Winooski basin, could reflect the fact that, on a basin scale, Winooski has a somewhat greater dominance of lower-infiltration soils (lower percentage of HSG A and B soils) than Lamoille or Missisquoi (Table 2.1). This pattern may also reflect differential source regions and connectivity of PP and TSS (*Doyle et al*., 2005) and may be a function of between-watershed differences in the dominant geomorphic state of the channel (aggradational vs. incisional) (*Kline and Cahoon*, 2010; *Roy and Sinha*, 2014) and duration of recovery time for vegetative boundary conditions following extreme flood events (*Wolman and Gerson*, 1978).

Post-threshold CV ratios for PP (and TSS) were elevated in Cluster 1 basins relative to the average for each of the other clusters. This pattern hints at the importance of less frequent, higher-magnitude storms in producing suspended sediment and sediment-bound P in these basins. Also, in our study area, impounded and/or regulated rivers did tend to have lower CV_Q values than non-regulated rivers (Wilcoxan, $p<0.10$), which would contribute to somewhat elevated CV ratios for both TSS and PP, and further promote the importance of low-frequency, higher-magnitude storms for sediment and sediment-bound P export (*Meade*, 1982).

Cluster 2 basins had lower flux of TSS and PP than Clusters 1 and 3 (Figure 2.6d). Cluster 2 basins are generally smaller in size (137 to 778 km^2) with C-Q relationships representing a mix of Model types (A1, A2, B, D). They have higher background supplies of TSS and PP (elevated β_0 values), and are generally of lower relief with lower MAP. Mean values for relief and MAP are significantly different (ANOVA, $p<0.05$) and lower for Cluster 2 than Cluster 1 (and 3). Cluster 2 basins exhibit lower-than-average post-threshold β_1 values for both TSS and PP, perhaps related to lesser stream power that would be expected from the combination of smaller basin size, lower relief and lesser MAP. Cluster 2 basins are also characterized by less-than-average forest cover and somewhat greater-than-average percentage of agricultural land use (although land use is not a significant factor driving clustering). Interestingly, while Cluster 2 basins overall contribute smaller loads of TSS and PP than Cluster 1 or 3 basins (likely related to their smaller size), they are characterized by a mean annual PP concentration range that is higher than that of the Cluster 1 basins (though the overall cluster means are not significantly different at $\alpha = 0.10$) and statistically different than

mean PP concentration for Cluster 3 (ANOVA, $p<0.05$). This result may be due to the fact that even at low flow ranges, these basins have sufficient power to entrain and mobilize fine particles and associated P from legacy stores (i.e., elevated β_0 values) derived from the erodible glacio-lacustrine soils and sediments of the Champlain Valley.

DP SOM Results

The DP SOM also clustered basins into three groups, but the group composition varied somewhat from that generated by the PP SOM (Figure 2.7). Log-transformed DP (and TSS) flux values for Clusters 2 and 3 were higher than Cluster 1, although statistically significant only between groups 2 and 1 (ANOVA/ Tukey HSD, $p<0.10$). Notably, these are nearly the same basins that comprised the high-flux clusters for PP, with the exception of Poultney and Mettawee (compare Figures 2.6 and 2.7). In contrast, DP concentrations were higher for Cluster 1 than Clusters 2 and 3, and the means between Clusters 1 and 3 were significantly different ($p<0.05$) (Figure 2.7d). There were no significant differences between mean cluster values for DP yield ($p > 0.10$).

The higher-flux basins of Clusters 2 and 3 tended to have higher-than-average basin relief and MAP, which can be attributed in part to their larger total drainage area (Figure 2.7b). Cluster 2 basins were larger than Cluster 3 basins, which themselves were larger than Cluster 1 basins, and the difference between group means was statistically significant (ANOVA/Tukey HSD, $p<0.05$). Basins in Clusters 2 and 3 also tended to have lower than average regression intercept values, suggesting lower baseline supplies of DP. Interestingly, they also exhibited higher values for the slope parameter on the post-threshold segment of the TSS C-Q regression. This may reflect enhanced sediment transport capacity of these basins, given their higher-than-average relief, which itself is

correlated to greater MAP (Pearson r = 0.480 for all 18 basins). To some degree, elevated β_1_II values may also reflect greater availability of TSS sources (e.g., enhanced floodplain connection) at higher flow stages (*Asselman*, 2000). We speculate that higher availability of TSS, could lead to reduced DP flux as a result of sorption (i.e., nutrient cycling).

Land use appears to contribute to differences between higher-flux Clusters 2 and 3 and suggests alternate sources of DP. Cluster 2 basins tended to be more developed and less forested, while the opposite was true for Cluster 3 basins, and the difference between cluster means was significant in each case ($p<0.10$ for forested, $p<0.01$ for developed). Cluster 2 basins (Otter, Winooski and Lamoille) include the urban centers of greater Burlington, Montpelier, Rutland and Middlebury, which are serviced by wastewater treatment facilities. The mean value of post-threshold regression slopes for Cluster 2 basins is greater than Cluster 1 basins, though not significant ($p = 0.18$), suggesting a more hydrologically-driven transport of DP for these basins.

The lower-flux basins of DP Cluster 1 are characterized by lower-than-average relief and MAP. In contrast to the other basins, they have elevated β_0 values for both TSS and DP, indicating higher baseline supplies of these constituents. Higher DP β_0 values may also be a reflection of the higher-than-average agricultural land use in Cluster 1 basins. Although it was not an input to the SOM, the mean concentration of total calcium (TCa) appears to have been a latent variable driving clustering of basins for DP. Cluster 1 had significantly higher mean TCa than Cluster 2 and 3 basins (ANOVA/ Tukey HSD, $p<0.05$). Elevated TCa concentrations and TSS β_0 values for TSS in Cluster 1 basins may both be a reflection of their geographic position within the Champlain Valley or

Vermont Valley/ Taconic biophysical regions, characterized by carbonate bedrock and erodible glacio-lacustrine sediments. Thus, DP in these Cluster 1 basins may be attenuated through sorption to, or biogenic co-precipitation with, calcite-bearing particles (*Moatar et al*., 2017). While Cluster 1 basins are responsible for generally lower flux of DP to Lake Champlain (due largely to their smaller size), they do however, exhibit higher DP concentrations than either Cluster 2 or 3 basins (Figure 2.7d).

Sediment and solute export regimes revealed by SOM clustering

Nonparametric SOM clustering results suggest that different functional stages of C-Q are responsible for the flux of sediment and nutrients to Lake Champlain from different basins. For TSS and PP, two unique clusters of high-flux basins were identified. In the first group, sediment and sediment-bound P flux is hydrologically-driven and disproportionately occurring during relatively infrequent, high-magnitude runoff events. During hydrologically- and hydraulically-dominated functional stages, TSS and PP are entrained and mobilized as a result of stream bed scour, streambank collapse, rill erosion, gully formation, floodplain scour (where hydrologically connected), and mass movement of strath terraces or closely-coupled hillsides (*Baker*, 1977; *Nanson*, 1986; *Benda and Dunne*, 1997; *Trimble*, 1997; *Walling and He*, 1999; *Walling et al.*, 1999). In the stream channel, sediment and solute transport would be more dominated by advective forces in a downstream direction than by diffusive or dispersive forces in either a lateral or vertical direction (*Ward*, 1989). Accretionary and hydrologically-dominated patterns may also result from progressive or sudden release of sediments from instream impoundments at high flows (*Meade*, 1982; *Wang et al*., 2008). The inclined pre- and post-threshold stages of these Model A2 watersheds may reflect suspended sediments liberated from a two-

phase bedload transport regime where sediments accumulated in the channel between storm events are more readily moved, while the second phase consists of additional fines liberated from disturbance of a coarse streambed armor layer (*Jackson and Beschta*, 1982; *Ryan et al*. 2002; *Reid et al*., 1997), or as stabilizing biofilms or aquatic vegetation are breached (*Lawler et al*., 2006). Alternatively, this pattern may simply reflect expansion of the variable source area with increasing stage (*Dunne and Black*, 1970; *Asselman*, 2000).

In the second group, the sourcing and mobilization of sediment and P are more bimodal, resulting from both hydrologic processes at post-threshold discharges and reactive processes (such as nutrient cycling or lateral/vertical exchanges of fine sediment) that dominate at pre-threshold discharges. For these basins exhibiting a "reactive" export regime in pre-threshold flow stages (i.e., near-flat trends in C with increasing Q), the vertical and lateral components of flow appear to gain influence relative to longitudinal (i.e., downstream) components. This may be due, in part, to lesser overall magnitudes of discharge, but may also reflect different hydrogeomorphic patterns in these rivers (i.e., an enhanced degree of floodplain connection, greater diversity of channel and bed forms, greater percentage of instream storage from impoundments or channel-contiguous wetlands than their "hydrologically-driven" counterparts). Research suggests that biogeochemical and physical processes other than advection dominate these reactive functional stages, such as: hyporheic exchange (*Karwan and Saiers*, 2009); vertical exchange or filtering (*Boano et al*., 2014); lateral exchange with fine-grained channel margin deposits (*Skalak and Pizzuto*, 2010; *Withers and Jarvie*, 2008); microscale bedform migration (*Pizzuto*, 2014; *Harvey et al.*, 2012); and attenuation in instream

wetlands (e.g., *Qian and Richardson*, 1997), impoundments (*Wang et al.*, 2008), or transient storage areas behind large woody debris jams (*Wohl and Beckman*, 2014). Lagged groundwater recharge from antecedent storms (*Bieroza and Heathwaite*, 2015) may cause short-term dilutionary effects that contribute to variability in pre-threshold TSS and PP C patterns. It is also possible that some of the more elevated concentrations result, not from reactive processes, but from hydrologically-driven sediment transport when the turbidity measured at the basin outlet has been generated by localized storms from distal areas of the basin (*Lawler et al*., 2006; *Bieroza and Heathwaite*, 2015). We speculate that this reactive functional stage of sediment/nutrient flux could also include bioturbation by wildlife (e.g., beavers and benthic organisms) as cited in *Boano et al.*, (2014) and humans (e.g., active ditching of first order streams that deliver suspended sediments during low-flow time periods), based on direct observations from these basins.

DP export to Lake Champlain from high-flux basins appears to result largely from a mix of hydrologic processes at post-threshold discharges and reactive processes (nutrient cycling) at pre-threshold discharges. Hydrologic phases of transport appear to be dominantly accretionary in nature. This result contrasts somewhat with findings of *Moatar et al.*, (2017) who noted chemostatic or dilutionary responses in a majority of their study basins. The accretionary response in our study area may reflect sourcing and mobilization of DP: (1) from impoundments at high flow stages; (2) from wastewater treatment facilities or combined sewer outflows at higher discharges; (3) from increased connections to channel-contiguous wetlands at higher flow stages; (4) or from tile drainage systems. Two high-flux DP clusters appear to be distinguished by basin-scale land use, with developed uses associated to one cluster, and agricultural uses more

prevalent in the other. Still, post-threshold β_1 values for DP are generally much lower than β_1 values for PP (Figure 2.4a). This observation is also reflected in the lower overall flux estimates for DP as compared to PP (i.e., compare Figure 2.6d to 2.7d).

Conclusions and Implications

We have outlined a methodological approach to expand upon previous classification schemes for sediment and solute export from catchments (*Musolff et al*., 2015; *Thompson et al*., 2011; Zhang *et al*., 2016; *Moatar et al*., 2017), with a focus on suspended solids and particulate and dissolved phosphorus. Using the Lake Champlain Basin to examine concentration-discharge dynamics, our method leveraged information from Bayesian inference to achieve estimation of segmented regression model parameters, and identify threshold position to avoid potential bias in manual threshold selection. Notably, threshold positions identified by our BLR methods, demonstrated a considerable range below and above the median Q – which has been used by previous researchers (*Moatar et al*., 2017; *Meybeck and Moatar*, 2012) as a default break-point to classify segmented C-Q regression models and discern differences between pre- and post-threshold export regimes. The BLR approach identified different functional stages of TSS, PP and DP export, in that a probability distribution on pre- and post-threshold regression slopes from a segmented regression model could be interpreted to discern between "reactive" and "hydrologically-driven" stages of constituent export. We extended the term "reactive" export regime to include the array of biologically-, chemically- and physically-mediated processes that are responsible for the uptake or release of constituents from advective transport.

Additionally, this study has applied a nonparametric clustering and data visualization approach, using an SOM, to yield insights into nonlinear combinations of independent variables that appear to be driving basin-scale differences in mean annual flux and concentration of sediment and phosphorus. Though further testing with greater numbers of basins would be useful, the SOM results helped define two unique clusters of high-flux basins for TSS and PP. In the first group, sediment and sediment-bound P flux is hydrologically-driven and disproportionately occurring during relatively infrequent, high-magnitude runoff events. In the second group, the sourcing and mobilization of sediment and P are more bimodal, resulting from both hydrologic processes at post-threshold discharges and reactive processes (such as nutrient cycling or lateral/vertical exchanges of fine sediment) that dominate at pre-threshold discharges. The former functional stage generates an acute flux response and may be more consequential in the context of loading to the lake (e.g., TMDLs and sediment budgets). However, the latter functional stage generates a more chronic concentration response that may be of greater concern in the context of ecological balance in the receiving waters (*Bende-Michl et al*., 2013). For example, in a hydrodynamically and ecologically diverse receiving water like Lake Champlain (*Xu et al*., 2015a, 2015b), understanding and predicting the magnitude, timing and location of these episodic vs. chronic inputs of nutrients is critical to projecting riverine load impacts on lake water quality and ecosystems across both time and space (*Giles et al*., 2016; *Isles et al*., 2017). Shallow segments of the lake, where P availability and ecosystem productivity are most impacted by benthic P loading (*Isles et al*., 2015), large PP loads from episodic high-flow events can remain potentially bioavailable for years to decades; but chronic inputs will also accumulate over time and

persist in these environments (*Isles et al*., 2017, *Zia et al.*, 2016). Deeper sections of the lake could be more impacted by chronic inputs of DP, as even during large events, particulate phosphorus quickly settles to depths where it is no longer potentially bioavailable to phytoplankton, and the short term (days to months) cycling of potentially dissolved riverine nutrients tends to govern nutrient ratios and bioavailability (*Isles et al*., 2017).

Insights into landscape drivers of concentration-discharge patterns provided by this BLR-SOM approach can also aid water resource managers. For example, different management strategies would be warranted for each of the high-flux basin clusters for PP, based on differences in the identified export regimes. Emphasis could be placed on diverting, detaining and attenuating storm-water flows and restoring and enhancing connections to floodplains and channel-contiguous wetlands in PP Cluster 3 (Model A2) basins, where flux is more episodic in nature, hydrologically-driven and disproportionately occurring during relatively infrequent, high-magnitude runoff events. Whereas, source reduction and other best management practices to buffer and disconnect sediment and PP source regions from the stream network would be more appropriate in PP Cluster 1 (Model D) basins characterized by greater baseline (legacy) supplies of these constituents. Similarly, DP clustering results that distinguish groups of high-flux basins by association with different land use patterns, may suggest differences in DP source types (e.g., point vs diffuse) and focus restoration or remediation efforts, accordingly. A better understanding of between-watershed differences in the functional stages of constituent export is also important in a nonstationary climate to anticipate spatially and temporally variant sensitivities to increased frequency, persistence, and

intensity of storm events (*Guilbert et al.,* 2015) and projected increases in dry summer conditions (*Guilbert et al.,* 2014).

This data-driven, nonparametric approach to classification of export regimes can be particularly useful in an adaptive management context, as analysis is easily updated with new estimates of physical and chemical data. Computation methods (Section 2.3.2) can be adapted to handle censored data (*Kruschke*, 2015). The Bayesian framework offers particular flexibility for study areas with sparse C-Q data. Our methods used vague priors on parameter estimates, so that the data would drive the estimates (*Gelman et al*., 2004). However, this technique could also be used with informative priors for watersheds with limited C-Q data. For example, analysis could apply the basin-scale posterior range for regression parameters as a prior on BLRs to estimate C-Q relationships at a sub-watershed scale, provided that biogeophysical characteristics of the two scales are similar. In a temporal context, our basin-scale estimates could be used as prior information in a hierarchical model of C-Q regressions by season (subject of a pending future publication).

While application of these techniques to other hydroclimatic regions and different spatial and temporal scales would yield insights into C-Q patterns unique to those areas, the overall BLR-SOM framework and methodology should be transferable among regions. The Bayesian model is sufficiently flexible to estimate parameters for C-Q responses with multiple thresholds, and the BLR approach could be extended to model additional solutes with different C-Q patterns. With increasing availability of high-frequency concentration and discharge monitoring data from *in situ* sensors, automation of the BLR-SOM approach

could permit near-real-time estimation of export regimes, of value to water quality management and stakeholder communities.

Acknowledgements

This material is based upon work supported by the National Science Foundation under Vermont EPSCoR Grant Nos. EPS-1101317 and NSF OIA 1556770. Any opinions, findings, and conclusions or recommendations expressed in this material are those of the author(s) and do not necessarily reflect the views of the National Science Foundation or Vermont EPSCoR. The authors are grateful to the Vermont Agency of Natural Resources and New York State Department of Environmental Conservation for water quality data sets used in this analysis (https://anrweb.vermont.gov/ dec/_dec/ LongTermMonitoringTributary.aspx), Hydrologic data sets were obtained from the Centre d'Expertise Hydrique Québec for the Pike station (http://www.cehq.gouv.qc.ca/ hydrometrie/historique_donnees/fiche_station.asp?NoStation=030424) and the United States Geological Survey National Water Information System for the US stations (https://doi.org/10.5066/F7P55KJN).

Supporting Information

This supplementary document contains text, figures and tables to further explain and document the manuscript's methodological framework including the segmented Bayesian Linear Regression model and Self-Organizing Map used to classify concentration (C) – discharge (Q) data for Total Suspended Solids (TSS), particulate phosphorus (PP) and dissolved phosphorus (DP) from 18 tributaries of the Lake Champlain Basin, northeast USA. Items are presented in order of their introduction within the main manuscript.

Appendix 2.S1

R script for determination of segmented Bayesian Linear Regression model parameters: Just Another Gibbs Sampler (JAGS) model

Modified from root script for simple linear regression which accompanies *Kruschke* [2015].

```
#------------------------------------------------------------------------------------------------------
source("DBDA2E-utilities.R")                    # functions provided with Kruschke, 2015

#------------------------------------------------------------------------------
genMCMC = function( data , xName="x" , yName="y" ,
                    numSavedSteps=40000 , saveName=NULL ) {
  require(rjags)
#------------------------------------------------------------------------------
  # Define the data
  y = data[,yName]
  x = data[,xName]
  #Ntotal = length(y)

  # Specify the data in a list, for JAGS:
  dataList = list(
    x = x ,
    y = y
  )
  #------------------------------------------------------------------------------
  # Define the model
  modelString = "

  # Specify the data:
  data {
```

```
        Ntotal <- length(y)
        range <- max(x)-min(x)
        low <- min(x) + 0.15*range                # constrain lower end of threshold value
        hi <- max(x) - 0.20*range                 # constrain higher end of threshold value
}

# Specify the model:
model {
   #Likelihood
   for (i in 1:Ntotal){
        y[i] ~ dnorm(yMean[i], tau.y[K[i]])
        yMean[i]<-beta0 +
            (beta1 + delta*step(x[i]-x.change[i]) )*(x[i]-x.change[i])
          x.change[i] <- (1-pp)*low+pp*hi                    #calculation of flow threshold
          K[i]<- step(x[i]-x.change[i])+1
     }
     beta0.true <- beta0 - x.change[1]*beta1
     beta1.star <- beta1 + delta

  # Priors – define noninformative priors
     for ( K in 1:2 ) {
          tau.y[K] <- pow(sigma.y[K],-2)
          sigma.y[K] ~ dunif(0,4)
     }
     delta ~ dnorm(0,0.0001)
     pp ~ dbeta(1,1)                                       #uniform beta distribution
     beta0 ~ dnorm(0,0.0001)
     beta1 ~ dnorm(0,0.0001)

} #model close parens
" # close quote for modelString

# Write out modelString to a text file
writeLines( modelString , con="TEMPmodel.txt" )

#------------------------------------------------------------------------
# INITIALIZE THE CHAINS.

init1 <- list(beta0 = rnorm(1), beta1 = rnorm(1), delta = rnorm(1),
            sigma.y = runif(2, 0, max(x)), pp = rbeta(1, 1, 1) )
init2 <- list(beta0 = rnorm(1), beta1 = rnorm(1), delta = rnorm(1),
            sigma.y = runif(2, 0, max(x)), pp = rbeta(1, 1, 1) )
init3 <- list(beta0 = rnorm(1), beta1 = rnorm(1), delta = rnorm(1),
            sigma.y = runif(2, 0, max(x)), pp = rbeta(1, 1, 1) )
init4 <- list(beta0 = rnorm(1), beta1 = rnorm(1), delta = rnorm(1),
```

```
            sigma.y = runif(2, 0, max(x)), pp = rbeta(1, 1, 1) )

  initsList = list(init1, init2, init3, init4)

  #------------------------------------------------------------------------
  # RUN THE CHAINS
  parameters = c( "beta0" ,  "beta1" , "tau.y", "sigma.y", "x.change",
                "delta", "beta1.star", "beta0.true", "deviance"  )
  adaptSteps = 1000
  burnInSteps = 4000
  nChains = 4
  thinSteps = 10
  nIter = ceiling( ( numSavedSteps * thinSteps ) / nChains )

  # Create, initialize, and adapt the model:
  jagsModel = jags.model( "TEMPmodel.txt" , data=dataList , inits=initsList ,
                      n.chains=nChains , n.adapt=adaptSteps )
  # Burn-in:
  cat( "Burning in the MCMC chain...\n" )
  update( jagsModel , n.iter=burnInSteps )
  # The saved MCMC chain:
  cat( "Sampling final MCMC chain...\n" )
  codaSamples = coda.samples( jagsModel , variable.names=parameters ,
                          n.iter=nIter , thin=thinSteps )

  # Extract and capture Deviance Information Criteria (DIC)
  cat( "Extracting DIC Information...\n" )
  myDIC = dic.samples(jagsModel, n.iter = 5000, type = 'pD')
  capture.output(myDIC, file=paste(saveName,"dic.txt",sep=""))

  if ( !is.null(saveName) ) {
    save( codaSamples , file=paste(saveName,"Mcmc.Rdata",sep="") )
  }
  return( codaSamples )
} # end function

#-------------------------------------------------------------------------------------------------------
```

Appendix 2.S2 Self-organizing Map

2.S2.1 SOM Implementation and Computation

A SOM (*Kohonen*, 1990) maps multidimensional data to a low-dimensional feature map, typically a 2-D lattice (Figure S2). The SOM architecture preserves the topology of the input data, meaning that samples with similar input variables will map to a similar location on the 2-D feature map. SOM algorithms can either be unsupervised, in which a given number of clusters are not determined *a priori*, or supervised, wherein a specific number of output classes or clusters is specified. The unsupervised SOM (used here) operates on a competitive algorithm, whereby a vector (**X**) is chosen at random from the standardized (and transformed, where applicable) input data set. In a first iteration, the distance, or dissimilarity, between **X** and the set of random weight vectors assigned to each node of the lattice is computed; Euclidean distance is typically used (*Kohonen*, 2013), and was used here. All variables in the input vector, **X**, are used to determine similarity (though, these variables can themselves be weighted (e.g., by PCA) to be more dominant in the tuning process). The weight vector most similar to **X** is identified as the best matching unit (BMU). Weight vectors of the units within a defined neighborhood centered on the BMU are each updated, by adding the distance between **X** and the weight vector of each node, adjusted by a factor, alpha, which is defined as the learning rate. The effect is that each adjusted weight becomes more similar to the input vector. These steps are repeated for a user-defined number of iterations until the algorithm converges. Typically, both the size of the updating neighborhood and the learning rate are decreased linearly with progressive iterations, moving from a coarse to fine tuning process. The distance (or dissimilarity) between weight vectors at

convergence is then examined to define clusters of similar weights. Several methods are possible, and often hierarchical clustering is used (*Vesanto and Alhoniemi,* 2000) as was the case in this study.

2.S2.2 SOM Implementation and Computation

To arrive at the final list of SOM input features, various hydrologic, topographic, geologic and land use characteristics of the 18 tributary basins, as well as magnitude frequency metrics were compiled and examined using traditional statistical methods (e.g., Pearson and Spearman Rank correlations, PCA) for their cross-correlations and relationship to sediment and nutrient flux. The input data set was streamlined to remove redundant variables during preliminary SOM runs. For example, both mean annual runoff, and percent of precipitation as runoff had similar influence as MAP, in terms of driving clustering of LCB watersheds, and were subsequently dropped in favor of MAP. The number of SOM input variables was constrained by the number of observations (i.e., no more than 18 – corresponding to the number of longterm monitoring stations being modeled).

The final input data comprise seventeen variables, including metrics describing hydrologic, topographic, geologic and land use characteristics of the 18 tributary basins (Table 1) and selected parameters derived from regressions of C on Q for TSS, PP and DP. Inputs were range normalized (*Alvarez-Guerra et al*., 2008) as follows:

$$norm(x_i) = \frac{(x_i - \min(x_i))}{(\max(x_i) - \min(x_i))}.$$

Given the potential for conditional bias between select input variables, a hexagonal lattice topology was selected (*Kohonen*, 2001). SOM training was performed in 200 iterations. The learning rate was set initially at 0.05 and decreased linearly to 0.01. The neighborhood size decreased linearly from a radius encompassing two-thirds of the lattice, to a value of 0 at one-third of the iterations - at which point the algorithm was only updating the BMU (analogous to k-means clustering). Clustering was performed using an unsupervised SOM in R applying the "kohonen" package (*Wehrens and Buydens*, 2007, v. 3.0.2 released 2017).

2.S2.2 SOM Cluster Validation

Cluster validation was evaluated using a nonparametric F statistic (*Anderson*, 2001) aided by the "adonis" function in the "vegan" package in R (*Oksanen et al*., 2017). The F statistic expresses a ratio of between-cluster variance (or cluster separation) to within-cluster variance (or compactness of clusters), and is maximized when the former is maximized and the latter is minimized. Several SOM runs were performed with varying numbers of lattice nodes lattice configurations, and number of clusters, with the additional constraints that final grid size (# nodes) should approximate a value of $5\sqrt{n}$ following the heuristic of *Vesanto et al.* (2000), yet not exceed the number of input variables. A maximum F statistic was used to identify the "correct" number of clusters for the input data set. Within a subset of various lattice configurations for this "correct" number of clusters, quantization error (QE) was minimized to identify the number and configuration of lattice nodes with best resolution (*Kohonen*, 2001), achieving a local minimization of QE (*Cereghino and Park*, 2009).

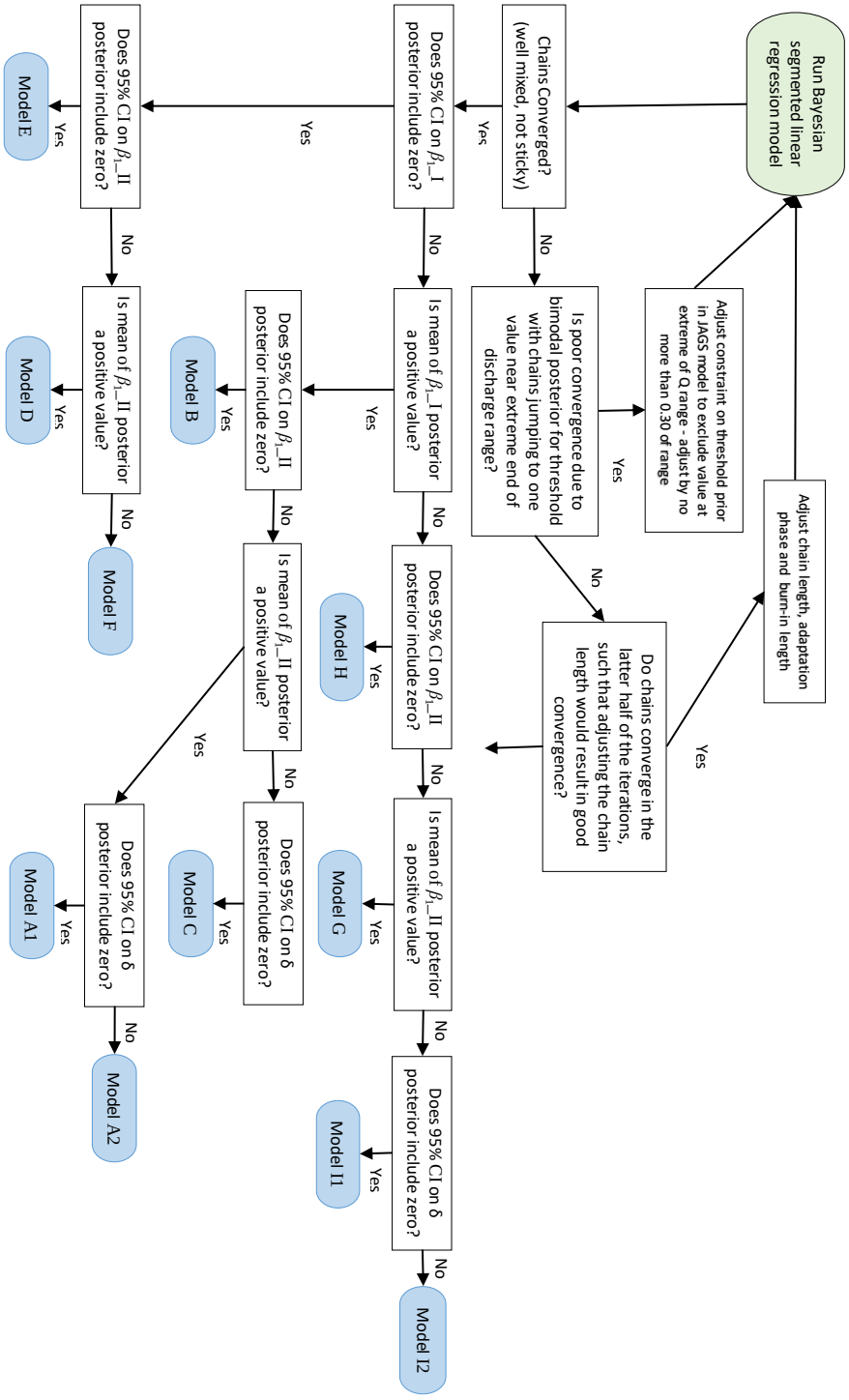

Figure 2.S1. Decision tree for classification of concentration-discharge model types after *Moatar et al.*, [2017] with reference to the posterior distribution quantiles for model parameters from Bayesian Linear Regression.

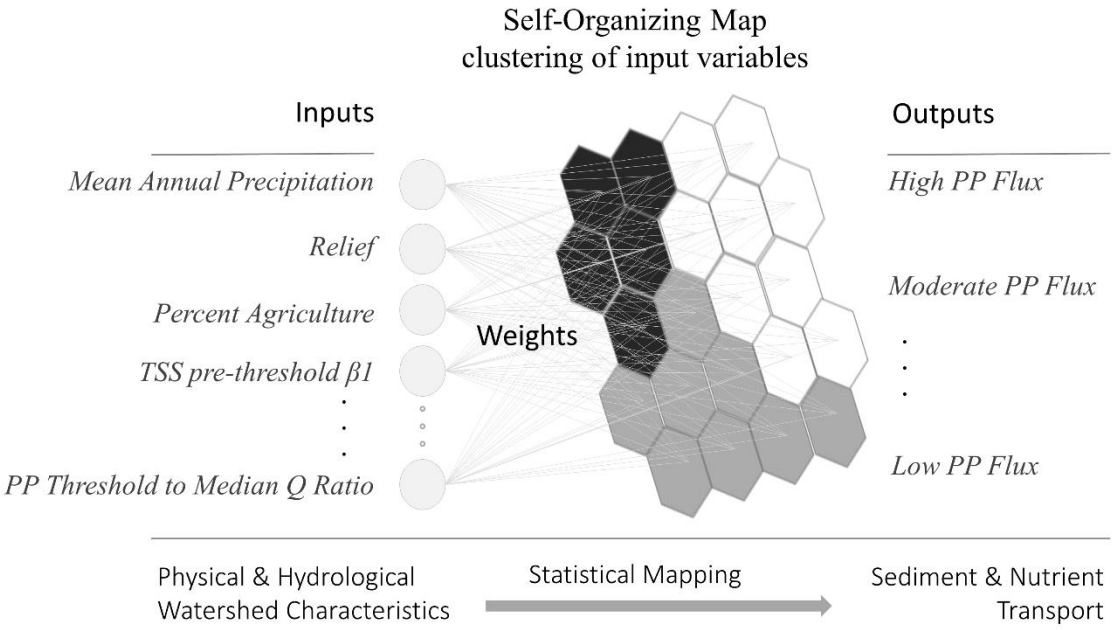

Figure 2.S2. Conceptual diagram of Self-Organizing Map used to cluster study area watersheds into distinct sediment and nutrient flux regimes based on physical and hydrological variables.

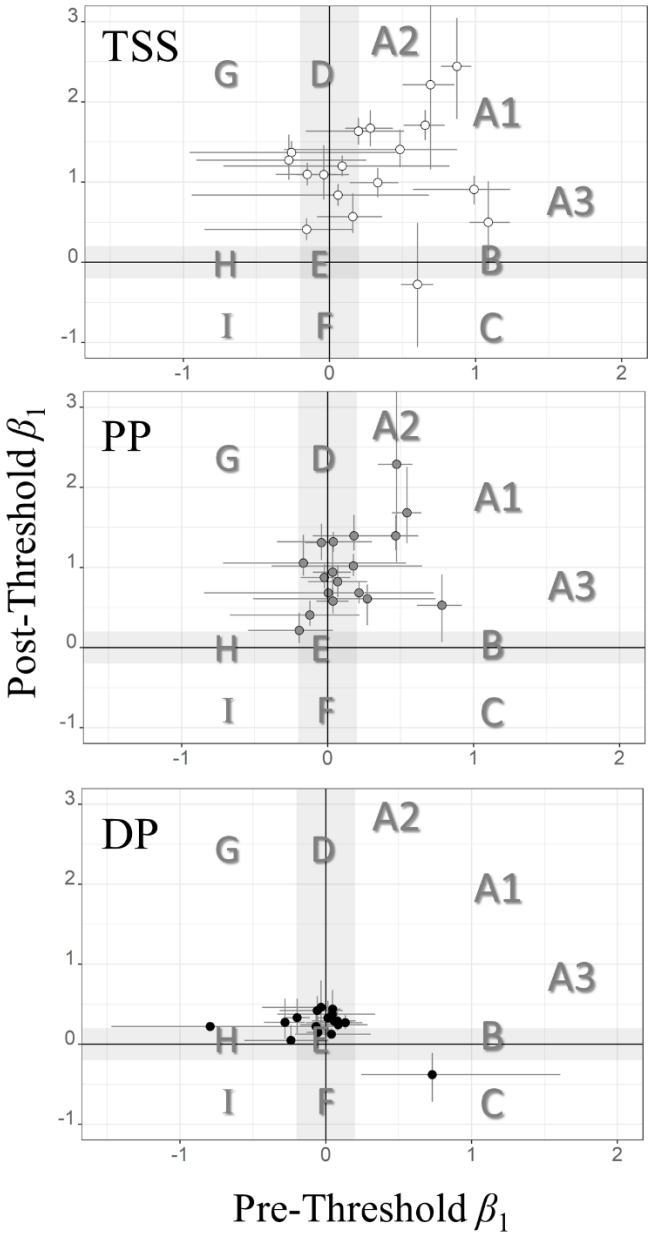

Figure 2.S3. Bivariate plots of post-threshold vs. pre-threshold regression slope (β_1) for Total Suspended Solids (top), Particulate Phosphorus (middle), and Dissolved Phosphorus (bottom). Vertical and horizontal whiskers indicate the 95% credible interval on the estimate of the mean value of the regression slope parameter derived from Bayesian Linear Regression. Gray shading indicates range from zero to $\beta_1 = |0.2|$ - defined by previous researchers as a "cutoff" value defining the difference between accretionary (or dilutionary) C-Q response and a stable response. Letters define model types after Figure 3 of the main manuscript.

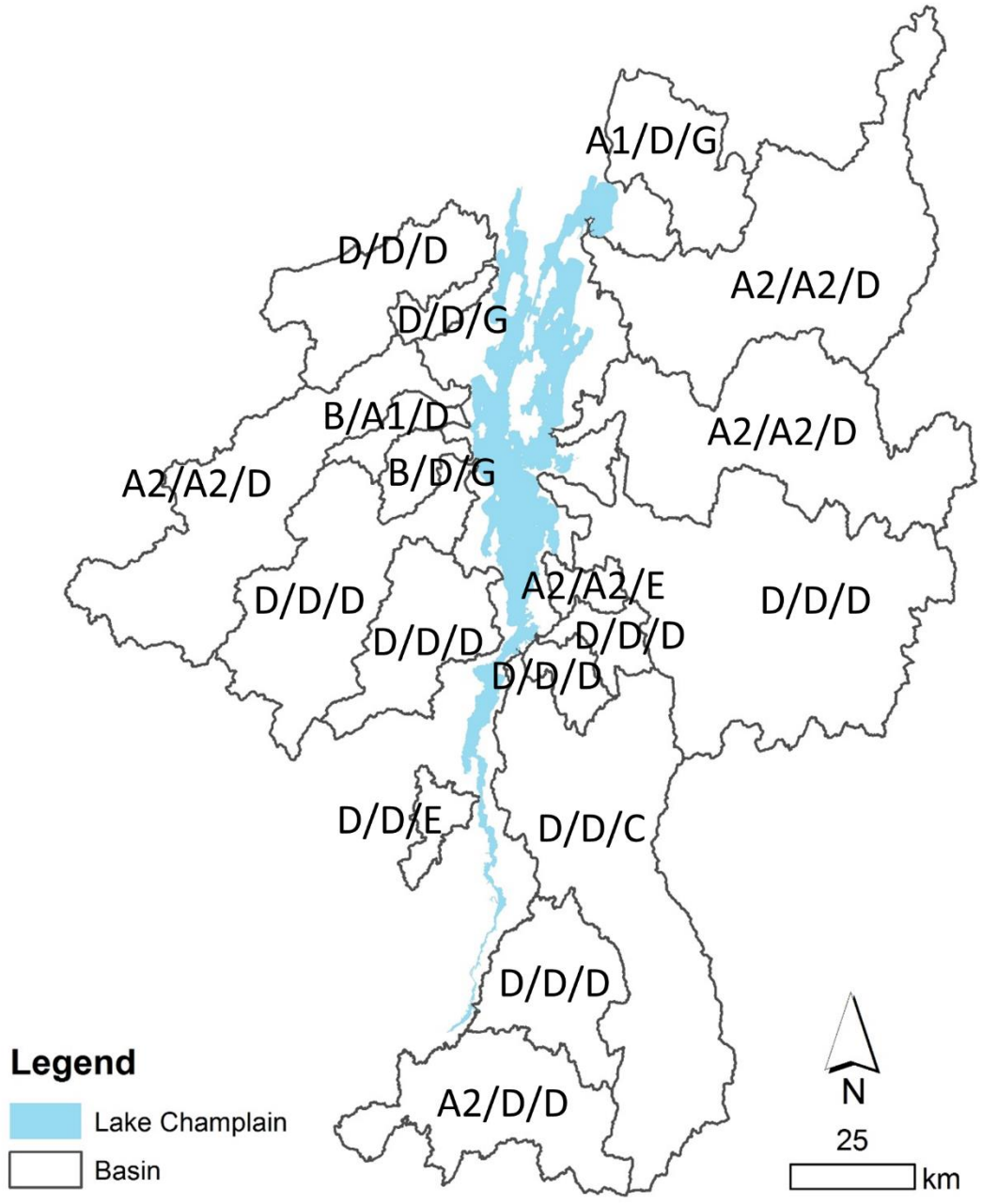

Figure 2.S4. Location of 18 study area basins in the Lake Champlain region, with C-Q model types assigned, using Bayesian Linear Regression for Total Suspended Solids/ Particulate Phosphorus/ Dissolved Phosphorus. Model types are defined in Figure 3 of the main manuscript.

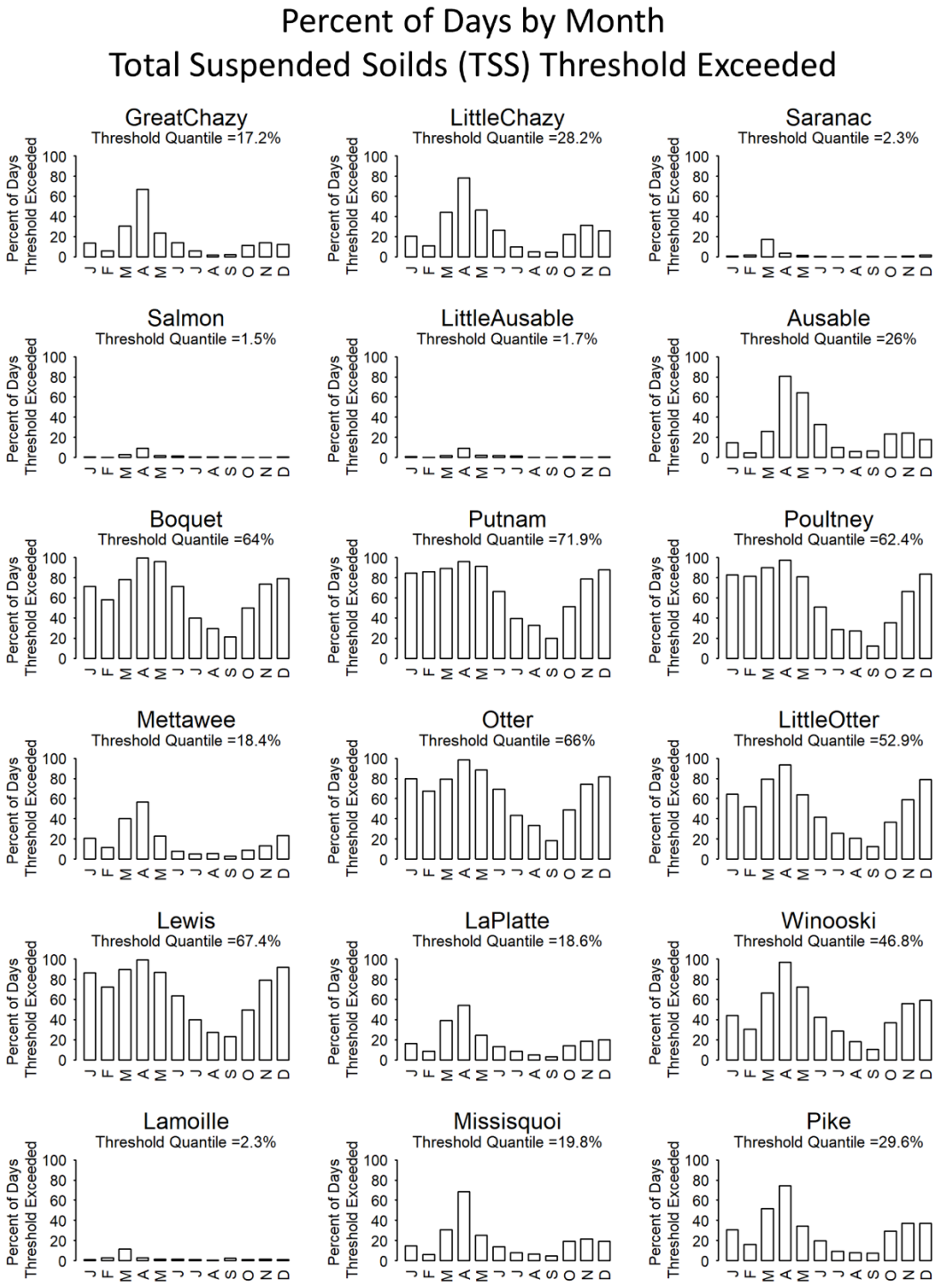

Figure 2.S5a. Monthly distribution of daily mean flows exceeding the basin-specific threshold defined using Bayesian Linear Regression of $\log_{10}$Concentration vs $\log_{10}$Discharge for 18 study area basins: Total Suspended Solids.

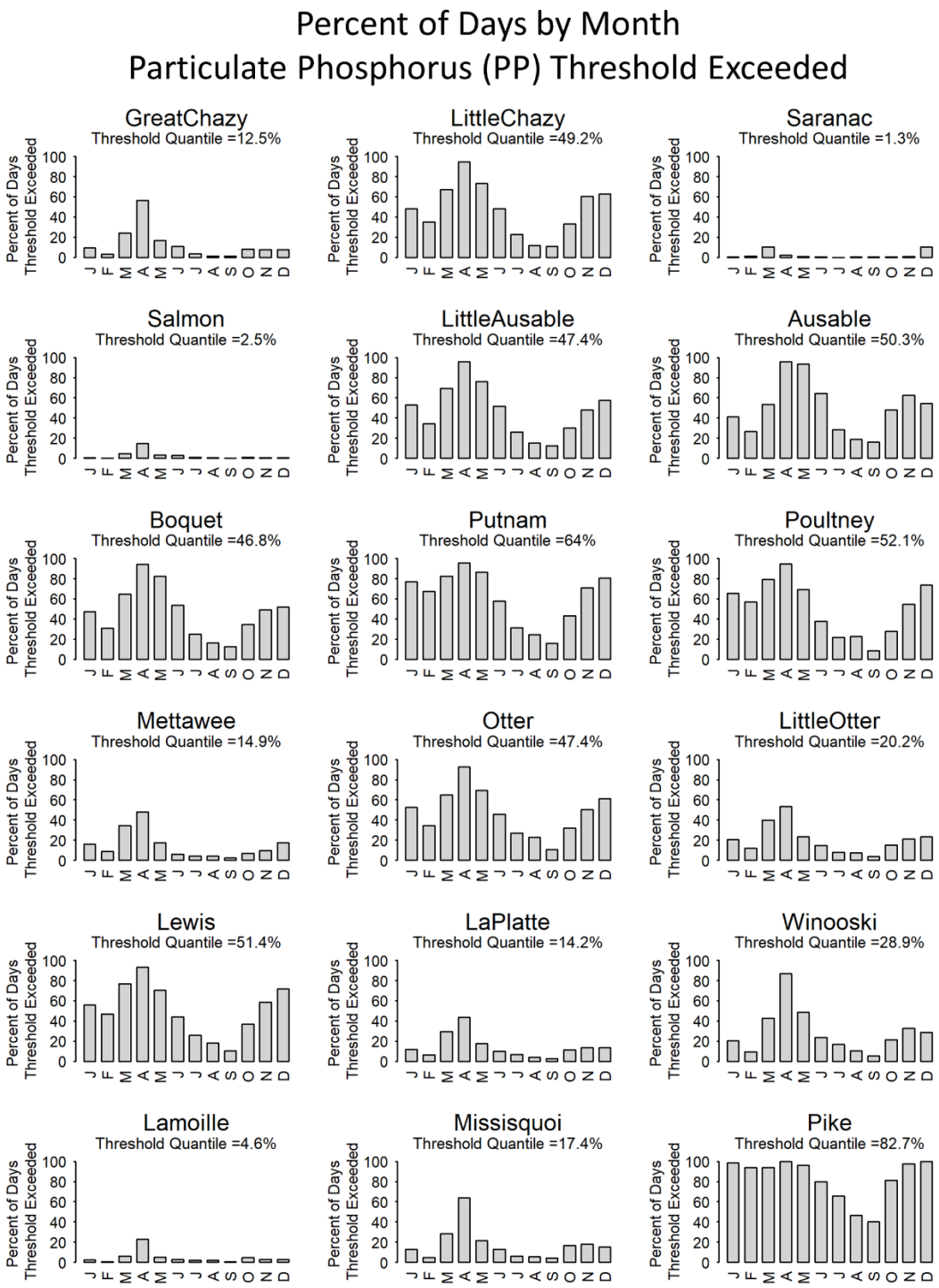

Figure 2.S5b. Monthly distribution of daily mean flows exceeding the basin-specific threshold defined using Bayesian Linear Regression of $\log_{10}$Concentration vs $\log_{10}$Discharge for 18 study area basins: Particulate Phosphorus.

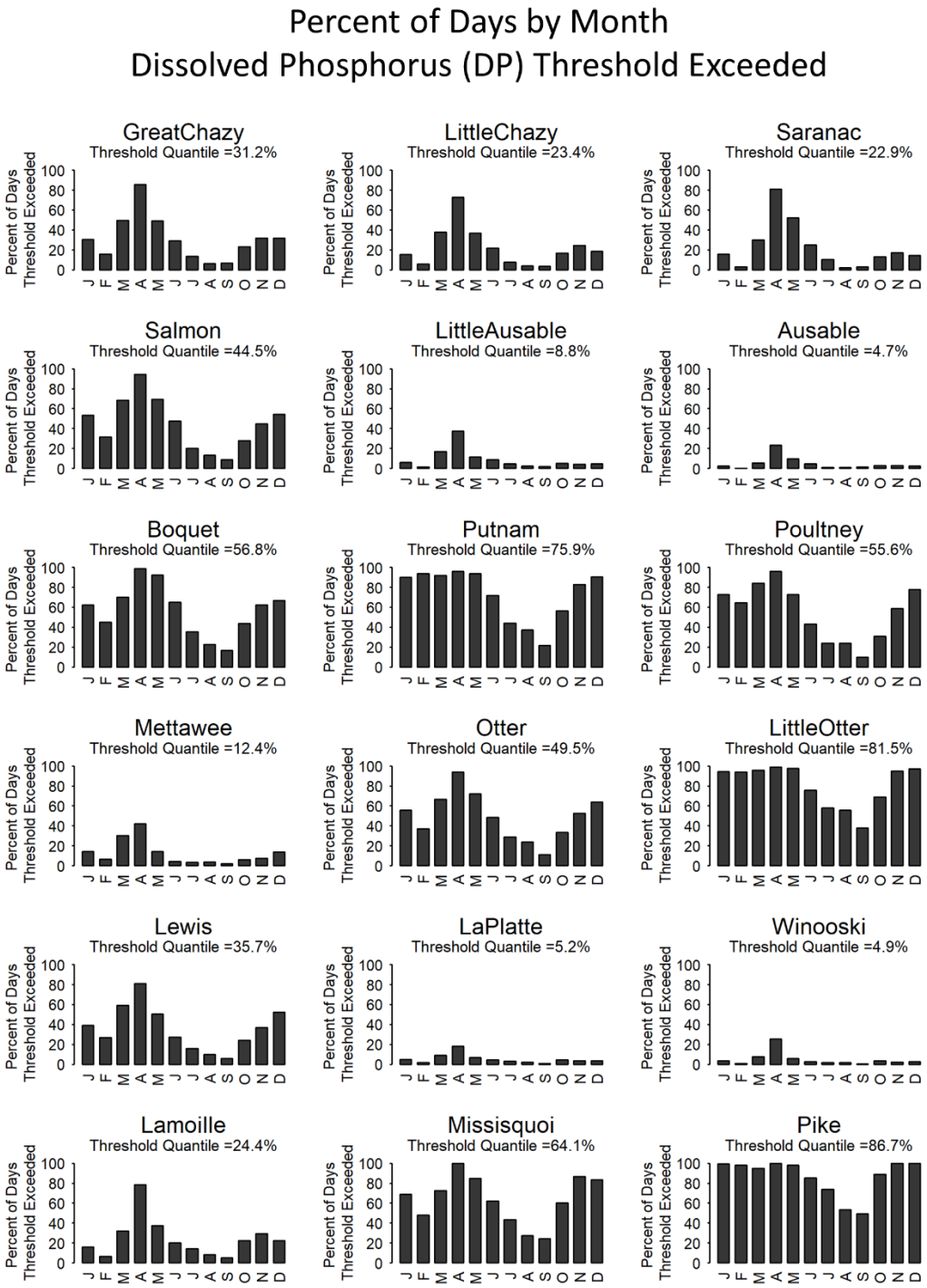

Figure 2.S5c. Monthly distribution of daily mean flows exceeding the basin-specific threshold defined using Bayesian Linear Regression of $\log_{10}$Concentration vs $\log_{10}$Discharge for 18 study area basins: Dissolved Phosphorus.

References

Alameddine, I., S. S. Qian, and K. H. Reckhow (2011), A Bayesian changepoint-threshold model to examine the effect of TMDL implementation on the flow-nitrogen concentration relationship in the Neuse River basin, *Water Res.*, 45, 51–62, doi:10.1016/j.watres.2010.08.003.

Alvarez-Guerra, M., C. González-Piñuela, A. Andrés, B. Galán, and J. R. Viguri (2008), Assessment of Self-Organizing Map artificial neural networks for the classification of sediment quality, *Environment International*, 34(6), 782-790, doi:10.1016/j.envint.2008.01.006.

Anderson, M. J. (2001), A new method for non-parametric multivariate analysis of variance, *Austral Ecology*, 26, 32-46, doi:10.1111/j.1442-9993.2001.01070.pp.x.

Asselman, N. E. M. (2000), Fitting and interpretation of sediment rating curves, *J. Hydrology*, 234, 228-248, doi:10.1016/S0022-1694(00)00253-5.

Baker, V. R. (1977), Stream-channel response to floods, with examples from central Texas, *GSA Bulletin*, 88, 1057-1071.

Basu, N. B., G. Destouni, J. W. Jawitz, S. E. Thompson, N. V. Loukinova, A. Darracq, S. Zanardo, M. Yaeger, M. Sivapalan, A. Rinaldo, and P. Suresh C. Rao (2010), Nutrient loads exported from managed catchments reveal emergent biogeochemical stationarity, *Geophys. Res. Lett.*, 37, L23404, doi:10.1029/2010GL045168.

Basu, N. B., S. E. Thompson, and P. S. C. Rao (2011), Hydrologic and biogeochemical functioning of intensively managed catchments: A synthesis of top-down analyses, *Water Resour. Res.*, 47, W00J15, doi:10.1029/2011WR010800.

Benda, L., and T. Dunne (1997), Stochastic forcing of sediment supply to channel networks from landsliding and debris flow, *Water Resour. Res.*, 33, 2849-2863.

Bende-Michl, U., K. Verburg, and H. P. Creswell (2013), High-frequency nutrient monitoring to infer seasonal patterns in catchment source availability, mobilization and delivery, *Environ. Monit. Assess.*, 185, 9191-9219.

Bieroza, M. Z. and A. L. Heathwaite (2015), Seasonal variation in phosphorus concentration–discharge hysteresis inferred from high-frequency in situ monitoring, *J. Hydrology*, 524, 333-347, doi:10.1016/j.hydrol.2015.02.036.

Boano, F., J. W. Harvey, A. Marion, A. I. Packman, R. Revelli, L. Ridolfi, and A. Wörman (2014), Hyporheic flow and transport processes: Mechanisms, models, and biogeochemical implications, *Rev. Geophys.*, 52, 603–679, doi:10.1002/2012RG000417.

Centre d'expertise hydrique Québec (2016), Fiche signalétique de la station 030424: Centre d'expertise hydrique Québec Hydrometric Network level and flow history station database, accessed May 4, 2016 at http://www.cehq.gouv.qc.ca/hydrometrie/historique_donnees/fiche_station.asp?NoStation=030424.

Cereghino, R. and Y.-S. Park (2009), Review of the Self-Organizing Map (SOM) approach in water resources: Commentary, *Environmental Modelling and Software*, 24, 945-947.

Denwood, M. J. (2016), runjags: An R Package Providing Interface Utilities, Model Templates, Parallel Computing Methods and Additional Distributions for MCMC Models in JAGS, *J. Stat. Softw*., 71(9), 1-25, doi:10.18637/jss.v071.i09.

Doyle, M. W., E. H. Stanley, D. L. Strayer, R. B. Jacobson, and J. C. Schmidt (2005), Effective discharge analysis of ecological processes in streams, *Water Resour. Res.*, 41, W11411, doi:10.1029/2005WR004222.

Dunne, T. and R. D. Black (1970), Partial Area Contributions to Storm Runoff in a Small New England Watershed, *Water Resour. Res.*, 6(5), 1296-1311.

Fisher, S.G., N. B. Grimm, E. Martı´, R. M. Holmes, and J. B. Jones, Jr. (1998), Material Spiraling in Stream Corridors: A Telescoping Ecosystem Model, *Ecosystems*, 1, 19-34, doi:10.1007/s100219900003.

Franzi, D. A., R. D. Fuller, and S. R. Kramer (2009), A preliminary study of nonpoint source runoff in the Little Chazy River watershed, northeastern New York, New York State Department of Environmental Conservation and The Nature Conservancy, http://www.lcbp.org/techreportPDF/chazy-npsrunoffJun09.pdf.

Fytilis, N. and D. M. Rizzo (2013), Coupling self-organizing maps with a Naıve Bayesian classifier: Stream classification studies using multiple assessment data, *Water Resour. Res.*, 49, 7747–7762, doi:10.1002/2012WR013422.

Gall, H. E., J. Park, C. J. Harman, J. W. Jawitz, P. S. C. Rao (2013), Landscape filtering of hydrologic and biogeochemical responses in managed catchments, *Landscape Ecology*, 28, 651–664, doi:10.1007/s10980-012-9829-x.

Gelman, A., and D. B. Rubin (1992), Inference from iterative simulation using multiple sequences, *Statistical Science*, 7, 457-472.

Gelman, A., Carlin, J. B., Stern, H. S., Rubin, D. B. (2004), *Bayesian Data Analysis*, Chapman & Hall/CRC, Boca Raton, FL.

Giles, C. D., P. D. F. Isles, T. Manley, Y. Xu, G. K. Druschel, and A. W. Schroth (2016), The mobility of phosphorus, iron, and manganese through the sediment–water continuum of a shallow eutrophic freshwater lake under stratified and mixed water-column conditions, *Biogeochemistry*, 127, 15–34, doi:10.1007/s10533-015-0144-x.

Godsey, S. E., J. W. Kirchner, D. W. Clow (2009), Concentration–discharge relationships reflect chemostatic characteristics of US catchments, *Hydrol. Processes*, 23, 1844-1864, doi: 10.1002/hyp.7315.

Guilbert, J., B. Beckage, J. M. Winter, R. M. Horton, T. Perkins, and A. Bomblies (2014), Impacts of projected climate change over the Lake Champlain Basin in Vermont, *J. Appl. Meteorol. Climatol.*, 53, 1861-1875, doi:10.1175/JAMC-D-13-0338.1.

Guilbert, J., A. K. Betts, D. M. Rizzo, B. Beckage, and A. Bomblies (2015), Characterization of increased persistence and intensity of precipitation in the Northeastern United States, *Geophys. Res. Lett.*, 42, 1888–1893, doi:10.1002/2015GL063124.

Harvey, J., and M. Gooseff (2015), River corridor science: Hydrologic exchange and ecological consequences from bedforms to basins, *Water Resour. Res*., 51, 6893–6922, doi:10.1002/2015WR017617.

Harvey, J. W., J. D. Drummond, R. L. Martin, L. E. McPhillips, A. I. Packman, D. J. Jerolmack, S. H. Stonedahl, A. F. Aubeneau, A. H. Sawyer, L. G. Larsen, and C. R. Tobias (2012),

Hydrogeomorphology of the hyporheic zone: Stream solute and fine particle interactions with a dynamic streambed, *J. Geophys. Res*., 117, G00N11, doi:10.1029/2012JG002043.

Heathwaite, A. L., A. N. Sharpley, and W. J. Gburek (2000), A conceptual approach for integrating phosphorus and nitrogen management at catchment scales, *J. Environ. Qual*, 29, 158-166.

Hicks, D. M., B. Gomez, N. A. Trustrum (2000), Erosion thresholds and suspended sediment yields, Waipaoa River Basin, New Zealand, *Water Resour. Res*., 36(4), 1129-1142, doi:10.1029/1999WR900340.

Hirsch, R.M., D. L. Moyer, and S. A. Archfield (2010), Weighted Regressions on Time, Discharge, and Season (WRTDS), with an Application to Chesapeake Bay River Inputs, *J. Am. Water Resour. Assoc.*, 46(5), 857-880, doi:10.1111/j.1752-1688.2010.00482.x.

Isles, P. D. F., C. D. Giles, T. A. Gearhart, Y. Xu, G. K. Druschel, and A. W. Schroth (2015), Dynamic internal drivers of a historically severe cyanobacteria bloom in Lake Champlain revealed through comprehensive monitoring, *J. Great Lakes Res.*, 41(3), 818–829, doi:10.1016/j.jglr.2015.06.006.

Isles, P. D. F., Y. Xu, J. Stockwell, A. W. Schroth (2017), Climate-driven changes in energy and mass inputs systematically alter nutrient concentration and stoichiometry in deep and shallow regions of Lake Champlain, *Biogeochemistry*, 133, 201–217, doi:10.1007/s10533-017-0327-8.

Jackson W. L., R. L. Beschta (1982), A model of two-phase bedload transport in an Oregon Coast Range stream, *Earth Surf. Process. Landf*., 7, 517–527, doi: 10.1002/esp.3290070602.

Karwan, D. L. and J. E. Saiers (2009), Influences of seasonal flow regime on the fate and transport of fine particles and a dissolved solute in a New England stream, *Water Resour. Res.*, 45, W11423, doi:10.1029/2009WR008077.

Karymbalis, E., K. Gaki-Papanastassiou and M. Ferentinou (2010), Fan deltas classification coupling morphometric analysis and artificial neural networks: The case of NW coast of Gulf of Corinth, Greece, *Hellenic Journal of Geosciences*, 45, 133-146.

Kennard, M. J., S. J. Mackay, B. J. Pusey, J. D. Olden and N. Marsh (2010), Quantifying Uncertainty in Estimation of Hydrologic Metrics for Ecohydrological Studies, *River Res. Appl.*, 26, 137-156, doi:10.1002/rra.1249.

Kline, M., and B. Cahoon (2010), Protecting River Corridors in Vermont, *Journal of the American Water Resources Association*, 46(2), 227-236, doi:10.1111／j.1752-1688.2010.00417.x.

Koch, R. W., and G. M. Smillie (1986), Bias in hydrologic prediction using log-transformed regression models, *Water Resources Bulletin*, 22(5), 717–723, doi:10.1111/j.1752-1688.1986.tb00744.x.

Kohonen, T. (1990), The Self-Organizing Map, *Proceedings of the IEEE*, 78(9), 1464-1480.

Kohonen, T. (2001), *Self-organizing maps* (3rd ed.), Springer, Berlin–Heidelberg, Germany.

Kohonen, T. (2013), Essentials of the Self-Organizing Map, *Neural Networks*, 37, 52-65, doi:10.1016/j.neunet.2012.09.018.

Kondolf, G. M. (1997), PROFILE: Hungry Water: Effects of Dams and Gravel Mining on River Channels, *Environmental Management*, 21(4), 533-551, doi:10.1007/s002679900048.

Krishnaswamy, J., M. Lavine, D. D. Richter, and K. Korfmacher (2000), Dynamic modeling of long term sedimentation in the Yadkin River Basin, *Adv. Water Resourc.*, 23(8), 881-892, doi:10.1016/S0309-1708(00)00013-0.

Kruschke, J. K. (2015), *Doing Bayesian Data Analysis: A Tutorial with R, JAGS, and Stan* (2nd Ed.), Academic Press / Elsevier, Boston, MA.

Lawler, D. M., G. E. Petts, I. D. L. Foster, and S. Harper (2006), Turbidity dynamics during spring storm events in an urban headwater river system: The Upper Tame, West Midlands, UK, *Sci Total Environ.*, 360, 109-126, doi:10.1016/j.scitotenv.2005.08.032.

Ley, R., M. C. Casper, H. Hellebrand, and R. Merz (2011), Catchment classification by runoff behaviour with self-organizing maps (SOMs), *Hydrol. Earth Syst. Sci.*, 15, 2947-2962, doi:10.5194/hess-15-2947-2011.

Lloyd, C. E., J. E. Freer, P. J. Johnes, and A. L. Collins (2016), Using hysteresis analysis of high-resolution water quality monitoring data, including uncertainty, to infer controls on nutrient and sediment transfer in catchments, *Sci Total Environ.*, 543(Pt A), 388-404. doi: 10.1016/j.scitotenv.2015.11.028.

Lumia, R., D. A. Freehafer, and M. J. Smith (2006), Magnitude and Frequency of Floods in New York, *Scientific Investigations Report 2006–5112*, U.S. Geological Survey, Washington, D.C.

Mangiameli, P., S. K. Chen, and D. West (1996), A comparison of SOM neural network and hierarchical clustering methods, *Eur. J. Oper. Res*., 93(2), 402–417, doi:10.1016/0377-2217(96)00038-0.

McClain, M. E, E. W. Boyer, C. L. Dent, S. E. Gergel, N. B. Grimm, P. M. Groffman, S. C. Hart, J. W. Harvey, C. A. Johnston, E. Mayorga, W. H. McDowell, and G. Pinay (2003), Biogeochemical Hot Spots and Hot Moments at the Interface of Terrestrial and Aquatic Ecosystems, *Ecosystems*, 6, 301-312, doi:10.1007/s10021-003-0161-9.

McDonnell, J. J., M. Sivapalan, K. Vache´, S. Dunn, G. Grant, R. Haggerty, C. Hinz, R. Hooper, J. Kirchner, M. L. Roderick, J. Selker, and M. Weiler (2007), Moving beyond heterogeneity and process complexity: A new vision for watershed hydrology, *Water Resour. Res*., 43, W07301, doi:10.1029/2006WR005467.

Meade, R. H. (1982), Sources, sinks and storage of river sediment in the Atlantic drainage of the United States, *J. of Geology*, 90, 235-252.

Medalie, L. (2013), Concentration, flux, and the analysis of trends of total and dissolved phosphorus, total nitrogen, and chloride in 18 tributaries to Lake Champlain, Vermont and New York, 1990–2011, *Scientific Investigations Report 2013–5021*, U.S. Geological Survey, Washington, D. C., http://pubs.usgs.gov/sir/2013/5021/.

Medalie, L. (2014), Concentration and flux of total and dissolved phosphorus, total nitrogen, chloride, and total suspended solids for monitored tributaries of Lake Champlain, 1990–2012, *Open-File Report 2014–1209*, U.S. Geological Survey, Washington, D. C., doi:10.3133/ofr20141209.

Medalie, L., R. M. Hirsch, and S. A. Archfield (2012), Use of flow-normalization to evaluate nutrient concentration and flux changes in Lake Champlain tributaries, 1990–2009, *J. Great Lakes Res.*, 38, 58-67, doi:10.1016/j.jglr.2011.10.002.

Meybeck, M., and F. Moatar (2012), Daily variability of river concentrations and fluxes: indicators based on the segmentation of the rating curve, *Hydrol. Processes*, 26, 1188-1207, doi:10.1002/hyp.8211.

Moatar, F., B. W. Abbott, C. Minaudo, F. Curie, and G. Pinay (2017), Elemental properties, hydrology, and biology interact to shape concentration-discharge curves for carbon, nutrients, sediment, and major ions, *Water Resour. Res.*, 53, 1270–1287, doi:10.1002/2016WR019635

Moyeed, R. A., and R. T. Clark (2005), The use of Bayesian methods for fitting rating curves, with case studies, *Adv. Water Resourc.*, 28, 807-818, 10.1016/j.advwatres.2005.02.005.

Mulholland, P. J., E. R. Marzolf, J. R. Webster, D. R. Hart, and S. P. Hendricks (1997), Evidence that hyporheic zones increase heterotrophic metabolism and phosphorus uptake in forest streams, *Limnol. Oceanogr*., 42(3), 443–451.

Musolff, A., C. Schmidt, B. Selle, and J. H. Fleckenstein (2015), Catchment Contols on Solute Export, *Adv. Water Resourc.*, 86, 133-146, doi:10.1016/j.advwatres.2015.09.026.

Nanson, G. C. (1986), Episodes of vertical accretion and catastrophic stripping — a model of disequilibrium floodplain development, *Geol. Soc. Am. Bull*., 97, 1467–1475, doi:10.1130/0016-7606(1986)97<1467:EOVAAC>2.0.CO;2.

Nash, D. B. (1994), Effective Sediment-Transporting Discharge from Magnitude-Frequency Analysis, *J. Geology*, 102(1), 79-95, doi:10.1086/629649.

Oksanen, J., F. G. Blanchet, M. Friendly, R. Kindt, P. Legendre, D. McGlinn, P. R. Minchin, R. B. O'Hara, G. L. Simpson, P. Solymos, M. Henry, H. Stevens, E. Szoecs and H. Wagner, (2017), vegan: Community Ecology Package. R package version 2.4-3, https://CRAN.R-project.org/package=vegan.

Olson, S. A. (2014), Estimation of flood discharges at selected annual exceedance probabilities for unregulated, rural streams in Vermont, *with a section on* Vermont regional skew regression, by Veilleux, A. G., *Scientific Investigations Report 2014–5078*, U.S. Geological Survey, Washington, D. C., doi:10.3133/sir20145078.

Park, Y.-S., R. Cereghino, A. Compin, and S. Lek (2003), Applications of artificial neural networks for patterning and predicting aquatic insect species richness in running waters, *Ecological Modelling*, 160, 265-280, doi:10.1016/j.ecoinf.2015.08.011.

Pearce, A. R., D. M. Rizzo, and P. J. Mouser (2011), Subsurface characterization of groundwater contaminated by landfill leachate using microbial community profile data and a non-parametric decision making process, *Water Resour. Res*., 47(6), W06511, doi:10.1029/2010WR009992.

Pearce, A. R., D. M. Rizzo, M. C. Watzin, and G. K. Druschel (2013), Unraveling Associations between Cyanobacteria Blooms and In-Lake Environmental Conditions in Missisquoi Bay, Lake Champlain, USA, Using a Modified Self-Organizing Map, *Environ. Sci. Technol.*, 47, 14267−14274, doi:10.1021/es403490g.

Pizzuto, J. E. (2014), Long-term storage and transport length scale of fine sediment: Analysis of a mercury release into a river, *Geophys. Res. Lett*., 41, 5875–5882, doi:10.1002/2014GL060722.

Plummer, M. (2003), JAGS: A program for analysis of Bayesian graphical models using Gibbs sampling. In *Proceedings of the 3rd international workshop on distributed statistical computing (dsc 2003), Vienna, Austria*. ISSN 1609-395X.

Plummer, M. (2016), Rjags: Bayesian Graphical Models using MCMC. R package version 4-6. URL: https://CRAN.R-project.org/package=rjags.

Plummer, M., N. Best, K. Cowles, and K. Vines (2006), CODA: Convergence Diagnosis and Output Analysis for MCMC, *R News*, 6, 7-11, https://www.r-project.org/doc/Rnews/Rnews_2006-1.pdf.

Qian, S. S., K. H. Reckhow, J. Zhai, and G. McMahon (2005), Nonlinear regression modeling of nutrient loads in streams: A Bayesian approach, *Water Resour. Res*., 41, W07012, doi:10.1029/2005WR003986.

Qian, S. S., and C. J. Richardson (1997), Estimating the long-term phosphorus accretion rate in the Everglades: a Bayesian approach with risk assessment, *Water Resour. Res*., 33, 1681-1688, doi:10.1029/97WR00997.

Qian, S. S, and T. F. Cuffney (2012), To threshold or not to threshold? That's the question, *Ecological Indicators*, 15, 1–9, doi:10.1016/j.ecolind.2011.08.019.

R Core Team, (2016), R: A language and environment for statistical computing. R Foundation for Statistical Computing, Vienna, Austria, ISBN 3-900051-07-0, URL: http://www.R-project.org/.

Randall, A. D. (1996), Mean annual runoff, precipitation, and evapotranspiration in the glaciated northeastern United States, 1951–1980, *Open-File Report 96-395*, U.S. Geological Survey, Washington, D.C.

Reid, I., J. C. Bathurst, P. A. Carling, D. E. Walling, B. W. Webb (1997), Sediment erosion, transport and deposition, in *Applied fluvial geomorphology for river engineering and management*: edited by C. R. Thorne, R. D. Hey, G. P. Williams, pp. 95–135, John Wiley, New York, NY.

Ries, K. G. and P. J. Friesz (2000), Methods for Estimating Low-Flow Statistics for Massachusetts Streams, *Water-Resources Investigations Report 00-4135*, U S. Geological Survey, Washington, D.C., https://pubs.usgs.gov/wri/wri004135/.

Roy, N. G. and R. Sinha (2014), Effective discharge for suspended sediment transport of the Ganga River and its geomorphic implication, *Geomorphology*, 227, 18-30, doi:10.1016/j.geomorph.2014.04.029.

Ryan, S. E., L. S. Porth, C. A. Troendle (2002), Defining phases of bedload transport using piecewise regression, *Earth Surf. Process. Landf*., 27, 971-990, doi:10.1002/esp.387.

Schmelter, M. L., S. O. Erwin, P. R. Wilcock (2012), Accounting for uncertainty in cumulative sediment transport using Bayesian statistics, *Geomorphology*, 175-176(15), 1-13, doi: 10.1016/j.geomorph.2012.06.012.

Smeltzer, E., A. D. Shambaugh, P. Stangel (2012), Environmental change in Lake Champlain revealed by long-term monitoring, *J. of Great Lakes Research*, 38, 6–18, doi:10.1016/j.jglr.2012.01.002.

Shanley, J. B., and J. C. Denner (1999), The hydrology of the Lake Champlain Basin, in *Lake Champlain in transition-From research toward restoration*, edited by T. O. Manley, P. L.

Manley, pp. 41-66, American Geophysical Union, Washington, D.C., doi: 10.1029/WS001p0041.

Shanley, J. B., W. H. McDowell, and R. F. Stallard (2011), Long-term patterns and short-term dynamics of stream solutes and suspended sediment in a rapidly weathering tropical watershed, *Water Resour. Res*., 47, W07515, doi:10.1029/2010WR009788.

Skalak, K., and J. Pizzuto (2010), The distribution and residence time of suspended sediment stored within the channel margins of a gravel-bed bedrock river, *Earth Surf. Process. Landf*., 35, 435–446, doi:10.1002/esp.1926.

Spiegelhalter, D. J., N. G. Best, B. P. Carlin, and A. van der Linde (2002), Bayesian measures of model complexity and fit (with discussion), *J. R. Statist. Soc.*, 64, 583–639, doi: 10.1111/1467-9868.00353.

Stewart, D. P. and P. MacClintock (1969), The Surficial Geology and Pleistocene History of Vermont, *Bulletin No. 31*, Vermont Geological Survey, Montpelier, VT.

Stojkovica, M., V. Simic, D. Milosevic, D. Mancev, T. Penczak (2013), Visualization of fish community distribution patterns using the self-organizing map: A case study of the Great Morava River system (Serbia), *Ecological Modelling*, 248, 20-29, doi:10.1016/j.ecolmodel.2012.09.014.

Stow, C. A., K. H. Reckhow, and S. S. Qian (2006), A Bayesian Approach to Retransformation Bias in Transformed Regression, *Ecology*, 87(6), 1472–1477, doi:10.1890/0012-9658(2006)87[1472:ABATRB]2.0.CO;2.

Syvitski, J. P., M. D. Morehead, D. B. Bahr, and T. Mulder (2000), Estimating Fluvial Sediment Transport: The Rating Parameters, *Water Resour. Res.*, 36(9), 2747-2760, 10.1029/2000WR900133.

Thompson, S. E., N. B. Basu, J. Lascurain Jr., A. Aubeneau, and P. S. C. Rao (2011), Relative dominance of hydrologic versus biogeochemical factors on solute export across impact gradients, *Water Resour. Res*., 47, W00J05, doi:10.1029/2010WR009605.

Todini, E. (2007), Hydrological catchment modelling: past, present, and future, *Hydrol. Earth Syst. Sci*., 11(1), 468-482, doi:10.5194/hess-11-468-2007.

Toone, J., S. Rice, and H. Piégay (2014), Spatial discontinuity and temporal evolution of channel morphology along a mixed bedrock-alluvial river, upper Drôme River, southeast France: Contingent responses to external and internal controls, *Geomorphology*, 205, 5–16, doi:10.1016/j.geomorph.2012.05.033.

Tran, L. T., C. G. Knight, R. V. O'Neill, E. R. Smith, and M. O'Connell (2003), Self-Organizing Maps for Integrated Environmental Assessment of the Mid-Atlantic Region, *Environmental Management*, 31(6), 822-835.

Trimble, S. W. (1997), Contribution of stream channel erosion to sediment yield from an urbanizing watershed, *Science*, 278, 1442–1444, doi:10.1126/science.278.5342.1442.

Troy, A., D. Wang, D. Capen, J. O'Neil-Dunne, and S. MacFaden (2007), Updating the Lake Champlain Basin Land Use Data to Improve Prediction of Phosphorus Loading, *Technical Report No. 54*, Lake Champlain Basin Program, Grand Isle, VT, http://www.lcbp.org/techreportPDF/54_LULC-Phosphorus_2007.pdf.

USGS (2016), National Water Information System, http://waterdata.usgs.gov/vt/nwis/rt.

Vesanto, J. and E. Alhoniemi (2000), Clustering of the Self-Organizing Map, *IEEE Transactions on Neural Networks,* 11(3), 586-600.

Vesanto, J., J. Himberg, E. Alhoniemi, and J. Parhankangas (2000), SOM Toolbox for Matlab 5. *Technical Report A57*, Neural Networks Research Centre, Helsinki University of Technology, Helsinki, Finland.

Vigiak, O., and U. Bende-Michl (2013), Estimating bootstrap and Bayesian prediction intervals for constituent load rating curves, *Water Resour. Res*., 49, 8565–8578, doi:10.1002/2013WR013559.

Vogel, R. M., B. E. Rudolph, and R. P. Hooper (2005), Probabilistic Behavior of Water-Quality Loads, *J. Environ. Eng.*, 131(7),1081-1089, doi:10.1061/(ASCE)0733-9372(2005)131:7(1081).

VTDEC (2015), Lake Champlain Long-term Water Quality and Biological Monitoring Program: Program Description, accessed at: https://anrweb.vermont.gov/dec/_dec/LongTermMonitoringTributary.aspx.

Walling, D. E. (1977), Assessing the accuracy of suspended sediment rating curves for a small basin, *Water Resour. Res.*, 13, 531–538.

Walling, D. E. (1983), The sediment delivery problem, *J. of Hydrology,* 65, 209-237, doi:10.1016/0022-1694(83)90217-2.

Walling, D. E., and Q. He (1999), Using fallout lead-210 measurements to estimate soil erosion on cultivated land, *Soil Sci. Soc. Am. J*., 63, 1404–1412, doi:10.2136/sssaj1999.6351404x.

Walling, D. E., P. N. Owens, G. J. L. Leeks (1999), Fingerprinting suspended sediment sources in the catchment of the River Ouse, Yorkshire, UK, *Hydrol. Processes*, 13, 955–975.

Wang, H., Z. Yang, Y. Wang, Y. Saito, and J.P. Liu (2008), Reconstruction of sediment flux from the Changjiang (Yangtze River) to the sea since the 1860s, *J. Hydrology*, 349, 318-332, doi:10.1016/j.jhydrol.2007.11.005.

Ward, J. V. (1989), The four-dimensional nature of lotic ecosystems, *J. N. Am. Benthol. Soc.*, 8, 2-8, doi:10.2307/1467397.

Warrick, J. A. (2014), Trend analyses with river sediment rating curves, *Hydrol. Process*., 29(6), 936–949, doi:10.1002/hyp.10198.

Watson, K., T. Ricketts, G. Galford, S. Polasky, J. O'Niel-Dunne, (2016), Quantifying flood mitigation services: The economic value of Otter Creek wetlands and floodplains to Middlebury, VT, *Ecological Economics*, 130(16-24), doi:10.1016/j.ecolecon.2016.05.015.

Wehrens, R., and L. M. C. Buydens (2007), Self- and Super-organising Maps in R: the kohonen package. *J. Stat. Softw*. 21 (5), 1-19, https://www.jstatsoft.org/index.

Williams, G. P., and M. G. Wolman (1984), Downstream effects of dams on alluvial rivers, *Professional Paper 1286*, United States Geological Survey, Washington, D. C.

Withers, P. J. A. and H. P. Jarvie (2008), Delivery and cycling of phosphorus in rivers: A review, *Sci. Total. Environ.,* 400, 379-395, doi:10.1016/j.scitotenv.2008.08.002.

Wohl, E., and N. D. Beckman (2014), Leaky rivers: Implications of the loss of longitudinal fluvial disconnectivity in headwater streams, *Geomorphology*, 205, 27-35, doi:10.1016/j.geomorph.2011.10.022.

Wolman, M. G., and R. Gerson (1978), Relative scales of time and effectiveness of climate in watershed geomorphology, *Earth Surf. Process. Landf.*, 3, 189-208, doi: 10.1002/esp.3290030207.

Wolman, M. G. and J. P. Miller (1960), Magnitude and Frequency of Forces in Geomorphic Processes, *J. Geology*, 68(1), 54-74, doi:10.1086/626637.

Xu, Y., A. W. Schroth, P. D. F. Isles, D. M. Rizzo (2015a), Quantile regression improves models of lake eutrophication with implications for ecosystem-specific management, *Freshw. Biol*., 60, 1841–1853, doi:10.1111/fwb.12615.

Xu, Y., A. W. Schroth, D. M. Rizzo (2015b), Developing a 21st century framework for lake-specific eutrophication assessment using quantile regression, *Limnol. Oceanogr*., 13, 237–249, doi:10.1002/lom3.10021.

Yellen, B., J. D. Woodruff, L. N. Kratz, S. B. Mabee, J. Morrison, A. M. Martini (2014), Source, conveyance and fate of suspended sediments following Hurricane Irene. New England, USA, *Geomorphology*, 226, 124-134, doi:10.1016/j.geomorph.2014.07.028.

Zhang, Q., C. J. Harman, and W. P. Ball (2016), An improved method for interpretation of riverine concentration-discharge relationships indicates long-term shifts in reservoir sediment trapping, *Geophys. Res. Lett*., 43, 10,215–10,224, doi:10.1002/2016GL069945.

Zia, A, A. Bomblies, A. W. Schroth, C. Koliba, P. D. F. Isles, Y. Tsai, I. N. Mohammed, G. Bucini, P. J. Clemins, S. Turnbull, M. Rodgers, A. Hamed, B. Beckage, J. Winter, C. Adair, G. L. Galford, D. Rizzo and J. Van Houten (2016), Coupled impacts of climate and land use change across a river–lake continuum: insights from an integrated assessment model of Lake Champlain's Missisquoi Basin, 2000–2040, *Environ. Res. Lett*., 11, 114026, doi:10.1088/1748-9326/11/11/114026.

CHAPTER 3. A BAYESIAN UN-MIXING MODEL TO DISCERN SUSPENDED SEDIMENT SOURCES IN A GLACIALLY-CONDITIONED CATCHMENT

Abstract

The effectiveness of mitigation measures for sediment impairment of our waterways is improved with information pertaining to sediment source types and locations, and the transport mechanisms which deliver sediment to receiving waters. Statistically-based tools such as sediment un-mixing models are one method for discerning the relative proportions of sediment source groups that may be contributing to suspended sediment flux. We applied a Bayesian un-mixing model to discern between surface and subsurface sources of suspended sediment and to quantify uncertainty on source apportionment estimates. Our study area was the Mad River watershed (360 km^2), a glacially-conditioned, montane catchment located in the humid temperate northeastern US. Using fallout radionuclides as fingerprints (^{137}Cs, excess ^{210}Pb), the model apportioned the relative contributions of four source groups (agricultural topsoils, forested topsoils, roads, and streambanks) for each of three suspended-sediment targets: (1) a catchment-scale sampling of two sequential summer 2015 storm events; (2) a sampling of the same storm events from three tributaries comprising 31% of the total catchment drainage area; and (3) a sampling of autumn 2015 storms from the same tributaries. Interpretation was supported by analysis of synoptically-measured suspended-sediment load quantified from regression models relying on continuous turbidity and discharge monitored at the outlets of the Mad River catchment and each tributary. Un-mixing model results suggest that suspended sediment load at the catchment outlet during two summer storms was generated primarily from subsurface sources characterized as

erosion from roads (36%) and stream banks/ gullies (40%), and that tributary source proportions during the same storms did not differ appreciably. Findings were substantiated by separate studies of channel change from multi-date lidar and unmanned aerial system surveys, as well as observations of road and road-ditch erosion during intense precipitation events during the study period. Limited seasonal comparison of tributary sediment flux suggested a greater proportion of sediment was sourced from agricultural surface soils in the autumn. Future work will explore the flexibility of the Bayesian model framework to model source ascription variability in space and time through explicit consideration of transport processes and use of informative priors based on distribution of storm hysteresis patterns over a given target-sample deployment.

Introduction

The effectiveness of mitigation measures for sediment impairment of our waterways is improved with information pertaining to sediment source types, locations and transport mechanisms. A better understanding of sediment dynamics would help identify critical catchment locations and time periods responsible for disproportionate fluxes of sediment and associate pollutants. Knowledge of these so called "hot spots" and "hot moments" (McClain et al., 2003; Heathwaite et al., 2000) would help to inform best management practices for reductions in sediment and nutrient loading. Physically-based, distributed models are able to forecast sediment concentration and flux; but the accuracy and calibration are resource-intensive, making such models typically less transferable among watersheds or regions (Todini, 2007). On the other hand, data-driven statistical models can be more readily implemented and have the appeal of representing system complexity in simple ways (McDonnell et al., 2007).

Sediment tracer studies (or un-mixing models) are a class of statistically-based models that have been developed over the years to unravel the disparate sources of sediment production and transport in catchments (Collins & Walling, 2002; Walling, 2013). To estimate the relative proportions of various terrestrial sediment sources contributing to the load of suspended sediment at a catchment outlet, un-mixing models use tracer constituents (or fingerprints) that behave in a conservative manner under the timeframe of interest. A conservative fingerprint maintains a consistent signature during its travel route from source region to catchment outlet, and is not degraded, transformed in chemical composition, attenuated or proliferated along the way (Walling, 2013). Researchers have utilized a wide variety of tracer types, from geochemical constituents

(Collins et al., 1997), to fallout radionuclides (Walling & Woodward, 1992), to sediment color (Martinez-Carreras, 2010), to stable isotopes of C and N (Fox & Papanicolaou, 2008), or a combination of multiple types in a "composite fingerprint" (Walling et al., 1993; Koiter et al., 2013). Typically, a subset of tracers with power to differentiate between sources is identified using a Kruskal-Wallis-*H* test followed by stepwise discriminant function analysis (Collins et al. 1997). A multivariate un-mixing model is then employed to: (i) link the tracer signature of the suspended sediment transported to the outlet (target material) back to the tracer signature(s) of the source-type sediments; and in so doing, (ii) determine the relative proportions of each sediment source (i.e., source apportionment).

With a linear un-mixing model, mass balance equations can be used to solve for n +1 sediment sources using a given number of tracer fingerprints, n. Due to the complexity of natural systems, however, it is often the case that more than $n + 1$ sediment sources contribute to the target composition of suspended sediment, and solution of the linear mixing model solution becomes indeterminate (Moore & Simmons, 2008). Certain frequentist approaches have been developed to solve the overdetermined matrix, including error minimization using least-squares (Collins et al., 1997). Linear mixing models have also improved through the application of Monte Carlo techniques to sample from fingerprint source and target distributions, and develop confidence intervals for source proportions (Davis & Fox, 2009), or to permit consideration of multiple targets (Phillips & Gregg, 2003). Still, the frequentist approaches are constrained to use of tracers that are not correlated, and assume that model residuals follow a Gaussian distribution (Davis & Fox, 2009).

Bayesian approaches using Markov Chain Monte Carlo (MCMC) integration methods, have emerged from the ecology and water resources fields to solve the overdetermined matrix. Bayesian methods applied to un-mixing models allow for > n +1 sediment sources, permit explicit accounting for sources of uncertainty, and allow for existing knowledge about the system in question to be included as prior information in source ascription estimates (Moore & Simmons, 2008; Abban et al., 2016). Additional advantages of the Bayesian framework include the ability to incorporate changing source-area contributions to a given outlet signal due to differential erosion and transport processes (Fox & Papanicolauo, 2008).

Bayesian un-mixing models have increased in their application, particularly with the emergence of open-source software including Stable Isotope Analysis in R (SIAR; Parnell et al., 2010) and a recent update (MixSIAR; Stock and Semmens, 2016) and MixSIR in MATLAB (Semmens and Moore, 2008). SIAR models have been used extensively in the ecology fields for assessing dietary composition in predator-prey relationships (Trapp et al., 2017; Reum et al., 2017) or in anthropology (Gordón, et al., 2017). In recent years, these models have had increasing application in the fields of hydrology and hydrogeology (Barbeta and Peñuelas, 2017; Zhao et al., 2018) and the study of sediment source apportionment (Koiter et al., 2013; Barthod et al., 2015). In a recent comparison, Bayesian un-mixing models were demonstrated to have better discriminatory power than frequentist approaches (Collins, et al., 2014).

In this work, we applied a Bayesian un-mixing model framework to discern the relative contribution of surface versus subsurface sources of erosion in a glacially-conditioned watershed of the temperate-humid northeastern US; the Mad River watershed

located in north-central Vermont. An additional goal was to provide a framework for validating previously-generated estimates from this watershed of suspended sediment flux at an annual scale using a process-based rainfall-runoff model (Stryker et al., 2017). Un-mixing model interpretation was supported by analysis of synoptically-measured suspended-sediment load quantified from regression models relying on continuous turbidity and discharge monitored at the outlets of the Mad River catchment and three principal tributaries (Hamshaw, 2018; Hamshaw et al., 2018).

Study Area

The Mad River watershed is located in central Vermont in the northeastern US (Figure 3.1), a region of ongoing international research efforts to monitor phosphorus and sediment contributions to Lake Champlain (Smeltzer, et al, 2012) and to reduce nutrient loading to mitigate the occurrence of harmful algal blooms (Isles, et al., 2015). Several small catchments in this region have been examined across a range of land covers, and the Mad River watershed has been studied for its end-member status as a forested, mountainous catchment with a "flashy" and turbid runoff signal. Several previous investigations have characterized its geology (Dunn et al., 2007; Whelan, 1998) and its hydrology and sediment dynamics (Wemple, et al., 2017; Stryker et al., 2017; Hamshaw et al., 2017; Hamshaw et al., 2018; Ross et al., in review).

The Mad River drains a 373 km^2 (144 mi^2) land area and flows north to join the Winooski River, a tributary to Lake Champlain. Elevations in the catchment range from 1,232 m (4,042 ft) to 166 m (544 ft) at the USGS streamflow gaging station (#04288000) at Moretown, which monitors a 360 km^2 (139 mi^2) area, and is located approximately 6

km upstream of the Mad River confluence with the Winooski River. The climate is characterized as humid temperate, with mean annual precipitation of 1300 mm (51.2 in). Mean annual runoff is estimated as 52% of precipitation, amounting to 671 mm (26.4 in; Olson, 2014). The catchment exhibits variable hydrologic source areas attributed to saturation-excess flow regimes (Dunne & Black, 1970). Within a typical year, a majority of the runoff from the Mad River occurs between ice-out and late spring (Shanley & Denner, 1999; USGS, 2018). Flooding often results from snow melt or rain-on-snow events, but can also be associated with convective storms or tropical systems in summer or fall. In recent years, the Mad River has been impacted by extreme events, including an approximate 2% annual exceedance probability (AEP) event in June 1998 and Tropical Storm Irene in August 2011 (estimated 0.2% AEP).

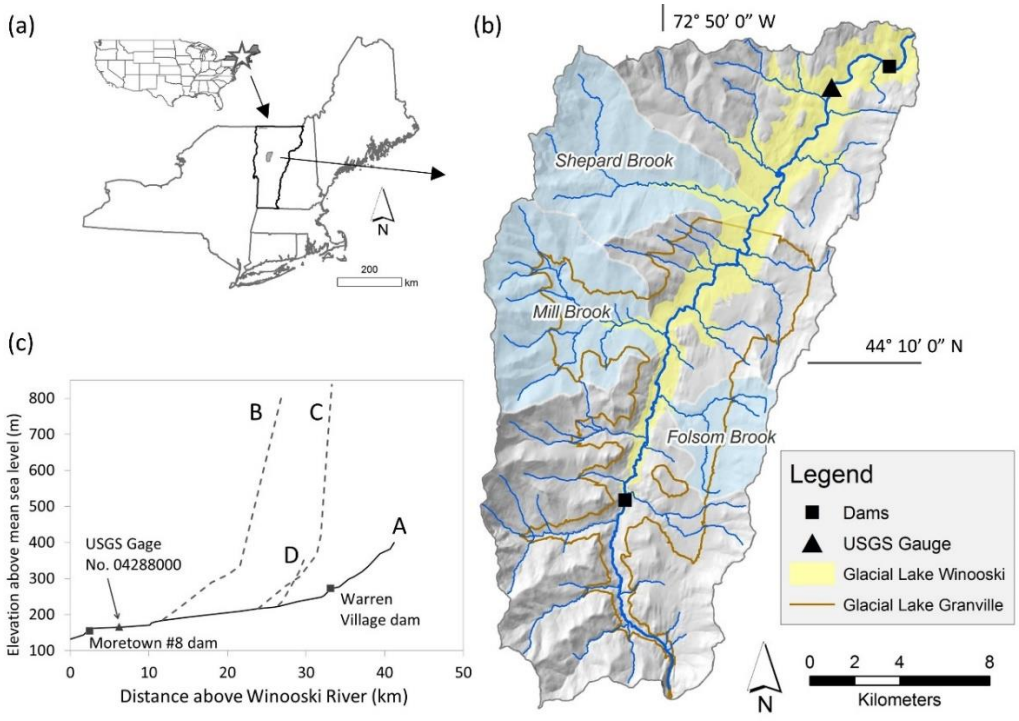

Figure 3.1. Location of study area including (a) US and Northeastern US context; (b) Mad River watershed; and (c) longitudinal profile of the main stem and three sampled tributaries. Capital letters A through D are keyed to supplementary Table 3.S3.

The Mad River is located entirely within the Northern Green Mountain geophysical province (Stewart & MacClintock, 1969). The main stem is oriented subparallel with the regional bedrock strike and flows north through a semi-confined to unconfined, moderate- to low-gradient valley flanked by the Green Mountains to the west and the Northfield Mountains to the east. The river flows through alluvial deposits, punctuated along their length by bedrock-controlled valley constrictions or channel-spanning bedrock exposures, grading from dominantly bedrock channels in the headwaters to mixed alluvial and bedrock channels in the lowlands.

Surficial deposits in the Mad River watershed reflect a Pleistocene glacial history. Upland slopes are dominated by shallow- to moderate thickness glacial till deposits overlying bedrock, with alluvial sands, gravels and cobbles found locally in stream corridors. These till deposits are typically a dense mixture of sediment sizes from silts to cobbles and boulders; the till sediments are typically cohesive and of low permeability (Stewart & MacClintock, 1969; Dunn et al., 2007). Kame terrace deposits of sands, gravels and cobbles developed at the marginal contact between the glaciers and the mountain slopes (Dunn et al., 2007). Silt- and fine-sand glaciolacustrine deposits are exposed along the valley margins and underlie the alluvial deposits along the mid to lower main stem and along the lower reaches of the major tributaries; these deposits were associated with two more persistent glacial meltwater lake stages that filled the Mad River valley for discrete time intervals: Glacial Lake Granville and Glacial Lake Winooski (Stewart and MacClintock, 1969, Larsen, 1987; Whalen, 1998) (Figure 3.1b). Through subsequent erosion and deposition cycles, the current Mad River has established an active floodplain along the lower main stem and occasionally impinges on valley walls

composed of glacial till or terraces composed of glaciolacustrine deposits (Dunn et al., 2007; Whalen, 1998; Larsen, 1987).

At a catchment scale, land cover is largely forested (86%), with lesser percentages of agricultural (5%) and urban (3%) land uses (Troy *et al*., 2007). At a river-corridor scale, however, the watershed is characterized by larger percentages of agricultural (28.6%) and developed (21.2%) uses, considering just those areas along the valleys of the main stem and principal tributaries using a GIS to buffer the stream centerline at fixed widths that ascend by stream order (Strahler, 1957). Included in the developed land use category are approximately 454 km of roads that traverse the watershed including 344 km of unpaved surfaces; and many of these road segments are connected to the stream network via bridge or culvert crossings (Wemple et al., 2017).

One in-service dam exists on the main stem within the Mad River study area, located approximately 43 km (27 mi) upstream of the streamflow gaging station at Moretown (Figure 3.1b, c). This dam impounds a negligible area of the channel and operates in run-of-river mode. Historically, additional dams were in service along the main stem and in headwater tributaries to service mill operations (Beers, 1873). They have since been breached during flood events, but may have historically contributed to upstream accumulation of legacy sediments (Walter & Merrits, 2008) or downstream incision (William & Wolman, 1984; Magilligan et al., 2003).

Methods

Un-mixing Model Overview and Fingerprint Selection

The un-mixing model involves selection of conservative fingerprints (Walling, 2013a), followed by sample collection from the study watershed for analysis of those fingerprints. Target samples (i.e., suspended sediments) are also gathered for analysis of the same tracers from the outlet of the study catchment – integrating over a time period sufficient to capture reasonable sediment volumes and in consideration of the particular study objectives. In the Bayesian modeling approach, a "prior" probability distribution (of source contributions) is combined with a "likelihood" (i.e., study area data) to derive new estimates on the source group proportions in the form of a "posterior" probability distribution. An informed prior is possible; however, we used an uninformed prior (Dirichlet distribution) so that model predictions would be driven by the data themselves (Gelman, 2004). We did not correct for organic matter content or particle size distribution of source and target samples, consistent with Martínez-Carreras et al. (2010), Smith and Blake (2014), and Koiter et al. (2013).

For potential fingerprints, we have used three fallout radionuclides (FRN): naturally-occurring ^{7}Be (with a half-life, $t_{1/2}$, equal to 53.3 days) and $^{210}Pb_{xs}$ ($t_{1/2}$ = 22.3 years); and anthropogenic FRN ^{137}Cs ($t_{1/2}$ = 30.2 yrs.). ^{7}Be is continuously produced in the atmosphere by cosmic ray spallation of oxygen and nitrogen atoms (Walling, 2013b). ^{210}Pb is also continuously produced, as a by-product of the decay of terrestrial uranium-238. ^{238}U decays through a series of very-short-lived radionuclides to ^{226}Ra ($t_{1/2}$ = 1600 yrs.), then subsequently to ^{222}Rn, a noble gas. Some of the ^{222}Rn escapes to the atmosphere and further decays to ^{210}Pb which is then deposited on the land surface

through wet and dry deposition. A portion of the ^{222}Rn stays *in situ*, for this decay to ^{210}Pb. Total ^{210}Pb present in surficial sediments is thus produced by two processes: the *in-situ* process, termed "supported", contributes a more or less steady activity of ^{210}Pb with depth in a soil profile, whereas the atmospherically-derived (or "excess") supply of ^{210}Pb ($^{210}Pb_{xs}$) is deposited to the land surface and activity levels decline with depth in an undisturbed soil profile. Source ascription studies rely on this excess ^{210}Pb, which is quantified as: total ^{210}Pb minus supported ^{210}Pb (Walling and Woodward, 1992; Matisoff et al., 2002). Typically, the quantity of supported ^{210}Pb is estimated using the proxy radionuclide, ^{226}Ra, as was the case in our study.

On the other hand, ^{137}Cs is an anthropogenic radionuclide that was produced during nuclear testing in the middle 1900s, with a peak in fallout occurring in 1963 (Ritchie & McHenry, 1990; Walling, 2013b). In North America, no significant sources of ^{137}Cs have been introduced since approximately 1976 (Matisoff et al., 2002). Given this discrete time period of production, this FRN tends to exhibit a peak activity at depth in a undisturbed soil profile, and that peak in a full vertical inventory of this tracer can be interpreted as a marker to date soil accumulation or erosion (Matisoff et al., 2005). In cultivated soils, however, ^{137}Cs is homogenized across the tilled layer.

All three FRN sorb readily to atmospheric aerosols and fine sediments (Ritchie and McHenry, 1990; He and Walling, 1996; You et al., 1989). While these FRN are deposited on land surface sediments through both wet and dry deposition, wet deposition is the primary mechanism. The longer half-lives (slow decay rate) of $^{210}Pb_{xs}$ and ^{137}Cs means that spatial inventories (i.e., FRN activity per unit area of soil column) across a region of similar latitude and relatively similar annual precipitation amounts should be

relatively uniform in undisturbed soils. This is because any short-term spatial variability in their deposition (via precipitation) will be "smoothed" over longer time frames. On the other hand, inventories of ^{7}Be can be spatially more variant and contingent upon rainfall distribution patterns due to its much shorter half-life. Downward migration is limited, and activities of this FRN are typically confined to the upper 1 to 2 cm of recently tagged soils, with highest activities detected in the upper few millimeters (Wallbrink and Murray, 1993, Wallbrink et al., 1996; Matisoff et al., 2002). If soils are disturbed through cultivation, the activity of $^{210}Pb_{xs}$ and ^{137}Cs become homogenized within the plow layer (typically, 20 cm). The much shorter half-life of ^{7}Be (rapid decay rate) means that cultivation practices are not effective in homogenizing ^{7}Be through the plow layer (Brigham et al., 2001; Walling, 2013b). Plowing mixes ^{7}Be-deficient sublayers with the surface-most few millimeters, and for short time between rain events ^{7}Be activity would be diluted to non-detectable activity levels; however, future precipitation events quickly re-tag the surface-most few millimeters with a fresh supply of ^{7}Be. Thus, ^{7}Be is not particularly helpful at discriminating between surface erosion from cultivated versus non-cultivated soils (Walling, 2013b).

The activity of $^{210}Pb_{xs}$ and ^{137}Cs in all soils drops off considerably at depths below 30 cm. It is this property that has been exploited in un-mixing models to discern between topsoil sources of sediment export to rivers (e.g., sheet erosion and rill erosion) and subsoil sources of suspended sediment (e.g., streambank and gully erosion). Streambank sediments typically contain highest activities of these FRN in surface layers, but are devoid of activities in the lower profile. Thus, as sediments are eroded into the river from streambank collapse, the $^{210}Pb_{xs}$ and ^{137}Cs activities in these surface layers are diluted by

isotope-free lower layers, leading to a generally low activity overall for streambank-sourced sediments (Wethered et al., 2015). The degree of dilution would be lesser for streambank sediments sourced from smaller-order streams and shallow gullies, given their smaller bank heights.

In contrast, the activity of ^{7}Be is typically confined to the top 5 to 10 mm of tagged soils (Walling, 2013b). Given its short half-life, inventories of ^{7}Be in these shallow layers are very dynamic and dependent on magnitude and sequencing of rain events juxtaposed with the schedule of land use activities, such as field tilling or road grading. As an example, assume a soil surface (either developed, cultivated, or undisturbed) has been subjected to several moderate-sized, low-intensity rain events in recent weeks during which erosion was minimal and no human activities (e.g., tilling, grading) have disturbed the soil surface. The top 5 to 10 mm of that soil would be tagged, containing elevated activities of ^{7}Be. If a higher-magnitude, rain event then occurs sufficient to cause erosion, the resulting signal of ^{7}Be in the runoff from that catchment would vary depending upon the nature of erosion processes occurring and their relative proportions. If erosion is dominated by sheet erosion, affecting the top few mm of soil, activities of ^{7}Be would be high in the runoff. On the other hand, erosion occurring in shallow gullies and rills would quickly breach this very shallow surface layer and expose underlying sediments devoid of ^{7}Be. Thus, catchment runoff sourced primarily from shallow gullies and rills or streambanks would be highly diluted by ^{7}Be - dead sediments, and low or non-detectable in ^{7}Be activity (Walling, 2013b). A mix of erosion modes across the catchment will introduce additional complexity in the ^{7}Be signal of the catchment runoff, and investigations need to frequently update the

characterization of potential source areas for this tracer, with knowledge of ongoing land use activities, as well as seasonally changing vegetation patterns and their effect on the rainfall-runoff balance.

Still, the contrasting temporal dynamics of ^{7}Be make it a useful compliment to $^{210}Pb_{xs}$ and ^{137}Cs fingerprints for distinguishing sediment sources. For example, if catchment runoff is high in ^{7}Be activity while moderate to low in ^{137}Cs activity, this could be explained by sheet erosion from pasture or tilled fields, respectively (Walling, 2013b). Moderate ^{7}Be activity and low ^{137}Cs activity would be consistent with sediment sourced from road ditch runoff, where open-canopy road ditch surfaces are continually eroding and remain largely exposed for continual tagging by ^{7}Be as they move down-network toward receiving streams.

Once in the receiving stream, the ^{7}Be sorbed to stream sediments begins to decay, and is no longer susceptible to tagging through dry or wet deposition (Salant et al., 2007), unless these sediments are returned to the land surface through overbank flooding or stored transiently within the active river corridor and exposed above the water surface. The ratio of ^{7}Be to $^{210}Pb_{xs}$ is much less spatially variable than either ^{7}Be or $^{210}Pb_{xs}$ alone and has been used as an indicator of age of suspended sediments (Matisoff et al., 2005).

Target sample collection

Target samples comprised suspended solids collected from the Mad River catchment outlet and three tributary outlets (Fig. 3.1b; Table 3.S3). Suspended sediments were sampled seasonally using in-situ, time-integrating passive samplers. In the tributary watersheds (Fig. 3.2a), a passive sampler constructed after Phillips et al. (2000) was deployed. This passive sampler was constructed of Schedule 40 PVC one-meter in

length, 98 mm in diameter with a 4-mm inlet and outlet, secured with hose clamps to two 1.3-cm rebar posts installed vertically into the streambed (Fig. 3.2b). At select sites, the Phillips sampler was installed both at a low-flow setting (approximately one half the

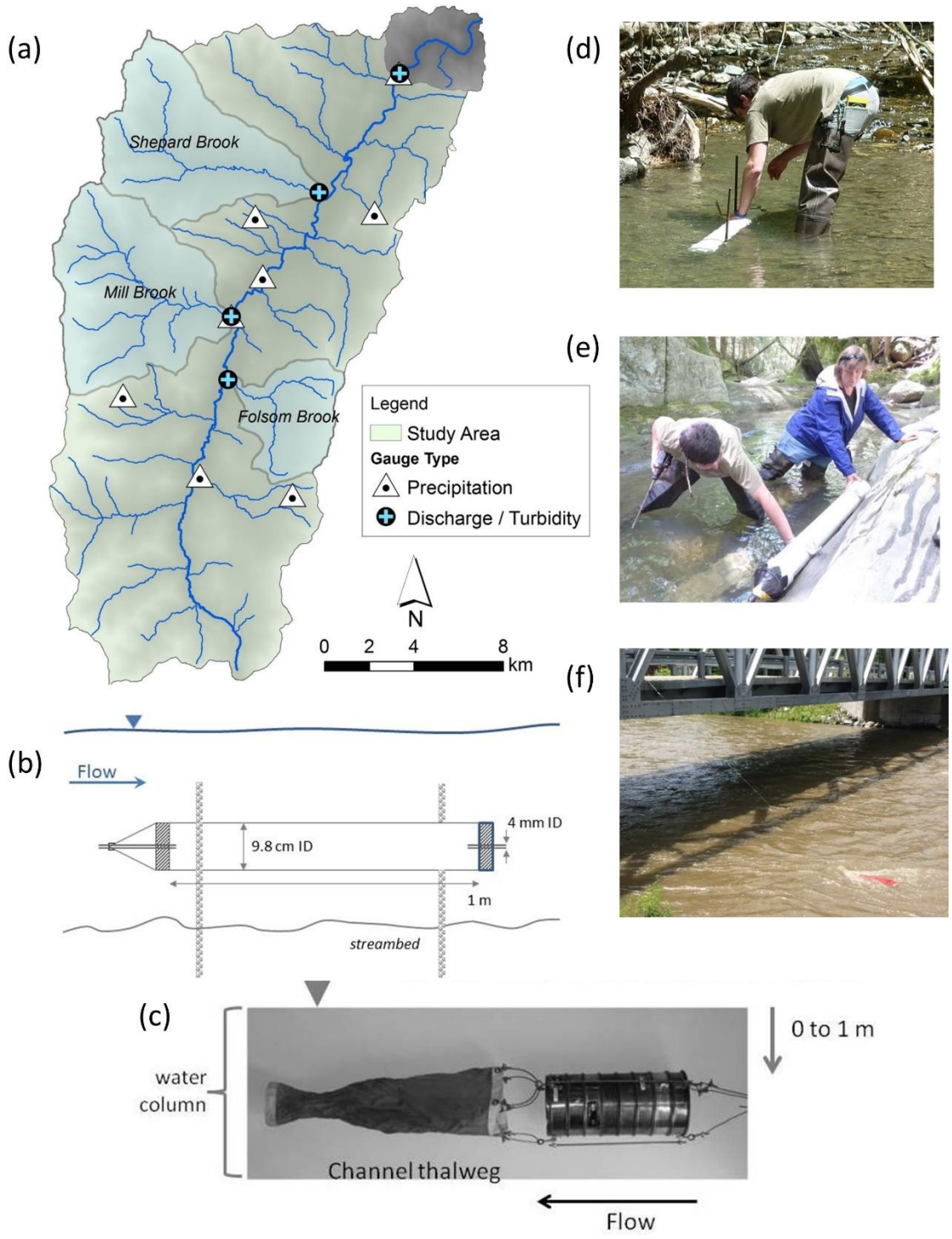

Figure 3.2. Location of target sampling sites in the (a) Mad River watershed using time-integrated passive samplers constructed after (b) Phillips et al., 2000 or (c) Borg, 2010. Example deployments of the (d) low-flow Phillips sampler, (e) high-flow Phillips sampler, and (f) Borg sampler.

vertical stage of a $Q_{1.5}$ flow) and at a high-flow setting (anchored to bedrock at an elevation approximately equal to a $Q_{1.5}$ stage) to characterize potential differences in suspended sediment characteristics vertically in the water column. In the larger-order main stem of the Mad River, a sampler modified after Borg (2010) was used to collect suspended sediment on a storm-event basis (Fig. 3.2c). This passive sampler was constructed from a stack of brass sieves in a sequence (from 500 to 53 μm), secured within a metal frame, and attached to a benthic sampler that acted as a rudder to stabilize the position of the sampler in the high-velocity water column. This "Borg" sampler was suspended from a bridge guardrail using 6.4-mm-diameter galvanized steel wire secured with a carabiner (Fig. 3.2f).

Source sample collection

Samples for fingerprint analysis were collected from four source groups determined *a priori* based on previous investigation and knowledge of the catchment (Wemple, 2013; Stryker, et al., 2017; Hamshaw, 2018): (1) forest surface soils (n = 47); (2) agricultural surface soils from hay/meadow/crop fields (n = 27); (3) road ditches (n = 5); and (4) streambank and gully subsoils (n = 15). Given the relatively sparse number of gullies, the streambank and gully samples were grouped together, in agreement with approaches of others (e.g., Collins et al., 2013; Wethered et al., 2015). This category would also be expected to include channel bed sediments newly exposed by vertical scour. We chose to group agricultural topsoil given generally lower occurrence of cultivated fields as compared to meadows, hay-fields and pastures in the Mad River watershed. Also, we anticipated that previous land uses may confound the expected separation between cultivated and non-cultivated fields in this study area, given the

common practice of rotating fields between tilled crops and hay or pasture. While FRN are effective at distinguishing between cultivated and non-cultivated fields (Matisoff et al., 2005), they also have been shown to discriminate more broadly between topsoil and subsoil (Wallbrink and Murray, 1993; Wethered et al., 2015). We anticipated that FRN may exhibit enhanced variance in an agricultural surface soil category that includes both cultivated and non-cultivated fields, but still expected the central tendency and variance of fingerprints in this source group to be distinguishable from that of forest surface soils, road ditches and subsoils, based on the work of other researchers (Collins et al., 2013; Wethered et al., 2015).

Source samples were collected during separate campaigns in the summers of 2013 through 2015; they were distributed across the Mad River catchment where landowner permission could be secured. Surface samples (< 5 cm) were each a composite of eight locations on a 30 m^2 grid (Figure 3.3), with each point sampled from a 15-cm^2 area excluding leaf litter and twigs. Streambank and gully samples were collected from actively eroding surfaces along the hydrologic network – a composite of between three and five vertical profiles (depending on the length of the exposure). Road ditch samples were retrieved in the headwaters of the catchment; select numbers of these road sites were sampled as part of the study conducted by Wemple (2013).

To quantify intra-grid variability in soil characteristics and tracer magnitude, a discrete sample from each of the eight grid points was collected at one meadow and one forest sample, and individually analyzed. Similarly, intra-profile variability was examined at one streambank site, by collecting discrete samples from individual soil horizons for analysis.

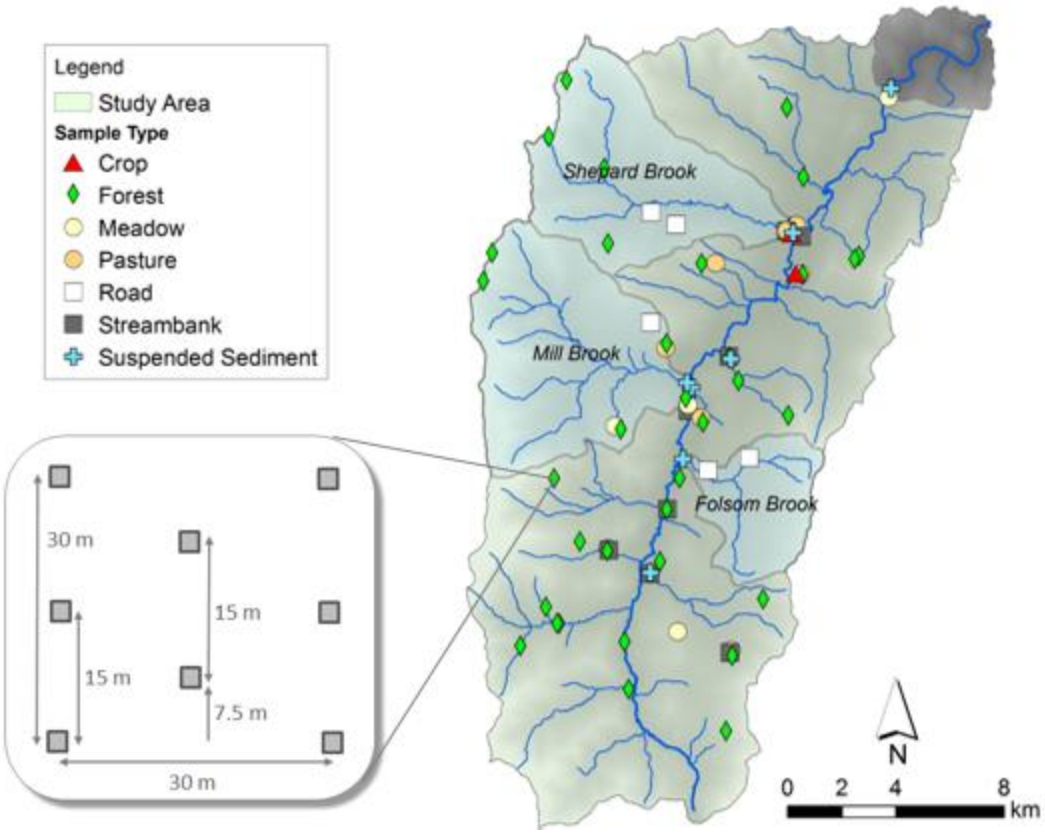

Figure 3.3. Location of fingerprint samples by source type collected in the Mad River watershed.

Meteorologic and hydrologic data collection

Precipitation data were collected at 7 stations distributed throughout the Mad River watershed (Figure 3.2) (Hamshaw, 2018). A meteorological station was established in Waitsfield village near the center of the watershed and collected precipitation, temperature, relative humidity, and soil moisture at 15-minute intervals. At six satellite meteorological stations, deployed from spring through early winter of each year, rainfall was measured using a HOBO Model RG-2 tipping bucket gage. Rainfall and temperature data were later aggregated to 15-minute intervals.

To characterize the hydrograph during passive-sampler target deployment, near-continuous discharge and turbidity data were collected at four surface water monitoring stations (Table 3.S3). For the Mad River main stem site, the study relied on discharge data from the existing USGS streamflow gaging station (#04288000) at Moretown. For each of the three tributary sites, a temporary flow gaging station was established, and a stage / discharge rating curve was developed from a log-log regression of the measured discharge on stage. Stage was monitored at 15-minute intervals using an ISCO 720 module pressure transducer from spring through early winter, since icing conditions prevented operation of the temporary gages over the winter months. Elevation of the transducer was surveyed with reference to a local benchmark to relate stage measurements between yearly deployments. Discharge was measured with a vertical-axis current meter by the area-velocity technique (USGS mid-section method; Rantz, et al, 1982). Rating curves were extended based on a HEC-RAS model of the discharge-monitoring station for stages that exceeded safe wading conditions (Hamshaw, 2018).

To characterize sedographs during passive sampler deployment, each site was instrumented with ISCO Model 6712 automated samplers and Forest Technology Systems Model DTS-12 instream turbidity sensors. Turbidity levels in Nephelometric Turbidity Units (NTUs) were captured at a 15-minute interval, and were related to Total Suspended Solids (TSS) concentrations by regressing TSS on Turbidity. TSS grab samples were collected at each station during a range of flow conditions to support development of a TSS-Turbidity rating curve (Hamshaw, 2018) that was relied upon for estimation of TSS flux during the time periods of passive-sampler deployment. TSS samples were analyzed at the Vermont Agricultural and Environmental Laboratory

(VAEL) via Standard Methods (21st ed.) 2540D, and at the Johnson State College laboratory (for additional samples collected at the Mad River gauge). Turbidity samples were also collected and analyzed via EPA Method 180.1 at VAEL as a check on the instream meter readings.

Analytical methods

Sediment samples (both target and source) were oven dried (<60°C), manually disaggregated using a mortar and pestle, and sieved to <63 μm to isolate the silt and clay fractions. Sediment samples for radionuclide analysis were packed into a uniformly-sized, round polyethylene container (105 mL), sealed with electrical tape. Where sample volumes were not sufficient to fill this standard container, as commonly occurred for suspended sediment samples, a 6.5-mL high-density polyethylene scintillation vial or 9.6-mL falcon petri dish was used. Samples were transported to the Dartmouth College Short-lived Isotope Lab for analysis of radionuclides by high-purity germanium Gamma detector (Canberra Industries, Meriden, CT). A duplicate sample was analyzed at a frequency of 10%; relative percent differences (RPD) of field duplicate pairs ranged from 0.2 to 9.9% for $^{210}Pb_{xs}$ and from 2.6 to 8.3% for ^{137}Cs.

Statistical analyses to finalize fingerprints

Consistent with guidance of Collins et al. (1997), conventional statistical tests were performed to identify tracers with significant discriminatory power. The non-parametric Kruskal-Wallis *H* test on ranks was applied to test the null hypothesis that different source groups of fingerprints were from distributions with the same mean. A pairwise test (Wilcoxan method) was then performed to identify that subset of fingerprints which demonstrated a significant difference between two or more of the

source groups. Selected fingerprints were then examined for conservative behavior by confirming that the range of values detected in the target samples (suspended sediments) was within the range of values reported for the source groups for each fingerprint – a "bracket" test (Nosrati et al., 2018).

Bayesian un-mixing model computation

Computation of the Bayesian un-mixing model was performed in a scripted version of the "MixSIAR" package (v.3.1.10, April 13, 2018) (Stock & Semmens, 2016). MixSIAR is a later incarnation of the Stable Isotope Analysis in R (SIAR) model, an open-source R code developed by Parnell et al. (2013) to support mixing model computation in the ecological fields. To parameterize the source observations, the MixSIAR modeling framework has options to use either: (a) the mean value and the standard deviation of sediment fingerprint properties; or (b) the raw data consisting of all available source observations; we used the raw data option. We used the default option of a non-informative prior (Dirichlet distribution). An informative prior based on existing knowledge of the system in question is also an option, and was explored in this study (see supplementary), but ultimately not used.

Parameter estimation was carried out using Markov-chain Monte Carlo (MCMC) methods. A Gibbs sampler (Geman and Geman, 1984) was used to obtain samples from the posterior distribution and estimate the mean, quantiles and credible intervals for proportions of each source group. MCMC sampling was implemented in R (R Core Development Team, 2018) using JAGS (v. 4.3.0) (Plummer, 2003). Sampling was conducted with three chains initialized with random number generators, for 50,000 iterations with a thinning factor of 25, after discarding the initial 25,000 iterations for

adaptation and burn-in phases. Convergence was confirmed by visual examination of trace plots and the Gelman-Ruben (1992) statistic - i.e., potential shrink reduction factor less than 1.05.

Consistent with other SIAR framework applications in sediment tracing studies (Koiter et al., 2013; Barthod et al., 2015), we omitted (i.e., set to zero) the trophic enrichment and concentration dependence factors commonly used in the model when applied to ecological investigations (Parnell et al., 2010). Source group proportion results were reported as the median value bounded by 25^{th} and 75^{th} quantiles of the posterior distribution, corresponding to a 50% credibility interval.

Results

Source and target sampling campaigns were carried out in the summers of 2013 and 2014 and the summer and fall of 2015, resulting in collection of 94 sediment samples (source) and 24 suspended sediment samples (target) (top portion of Table 3.1; Supplementary Table 3.S3). Given the elapsed time between sample collection and analysis, activities of the very-short-lived ^{7}Be radionuclide were not reported by the lab, resulting in reduced numbers of results available for this fingerprint, and for its ratio with $^{210}Pb_{xs}$, for three of the source groups.

Kruskal-Wallis-H tests revealed that ^{137}Cs and $^{210}Pb_{xs}$ had power to discriminate between two or more source groups ($p < 0.001$). Follow-up pairwise testing (Wilcoxan method) confirmed that source group means were statistically different for each FRN ($p<0.001$) except between streambanks and roads ($p=0.483$ for ^{137}Cs and $p=0.222$ for $^{210}Pb_{xs}$).

Table 3.1. Summary of radionuclide activities in source and target samples.

Source Samples		n	^{137}Cs	^{210}Pb$_{XS}$	n	^{7}Be	^{7}Be: ^{210}Pb$_{XS}$
Agricultural Topsoils	Mean	27	12.13	46.6	19	5.39	0.126
	SD		*7.15*	*13.6*		*5.34*	*0.165*
Forest Topsoils	Mean	47	31.85	85.5	37	6.01	0.074
	SD		*13.49*	*38.3*		*10.5*	*0.108*
Road Ditches	Mean	5	0.98	19.3	5	14.7	0.756
	SD		*0.88*	*21.7*		*12.2*	*1.326*
Streambanks	Mean	15	4.11	7.6	12	1.70	0.278
	SD		*4.61*	*12.6*		*2.33*	*0.39*
Target Samples		n	^{137}Cs	^{210}Pb$_{XS}$	n	^{7}Be	^{7}Be: ^{210}Pb$_{XS}$
Main stem Suspended Sediments	Mean	3	3.63	5.6	3	50.5	11.42
	SD		*0.28*	*3.7*		*1.56*	*7.26*
Tributary Suspended Sediments	Mean	21	6.04	31.7	21	81.8	3.87
	SD		*2.27*	*21.3*		*49.1*	*4.90*

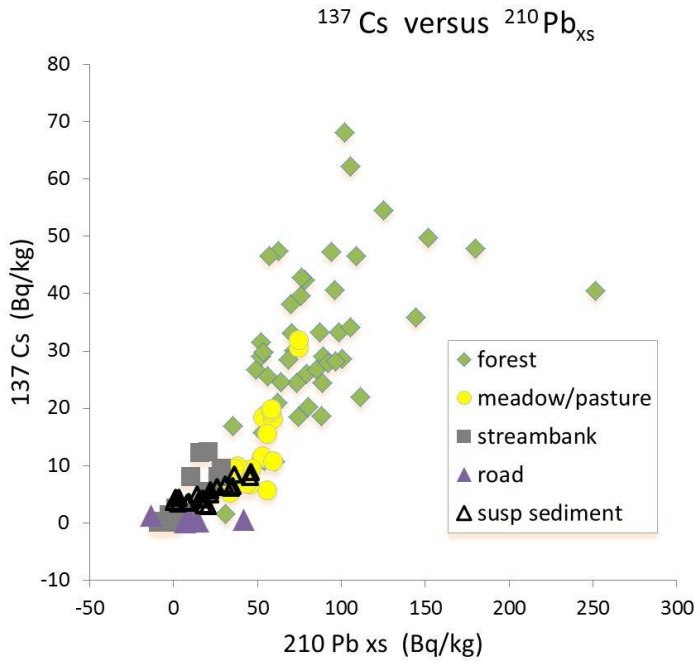

Figure 3.4. Bivariate plot of radionuclide activities by source group and target suspended sediments.

^{7}Be was able to discriminate between two or more source groups ($p<0.05$; Kruskal-Wallis-H), including between streambanks and each of the surface-soil groups (agricultural and forest topsoils) ($p<05$; Wilcoxan method); and this distinction was nearly significant between streambanks and roads ($p=0.102$). The group means for the ^{7}Be/ $^{210}Pb_{xs}$ ratio were not significantly different among source groups ($p = 0.095$).

While these results might suggest using ^{7}Be fingerprint as a complement to ^{137}Cs and $^{210}Pb_{xs}$ in the multivariate un-mixing model, a subsequent bracket test indicated that ^{7}Be was not suitable since the mean of suspended sediment ^{7}Be activities (representing the target) was positioned well outside the bracket of source group means on a bivariate plot of 7Be versus $^{210}Pb_{xs}$ (Fig. 3.5a). Suspended sediment activities for ^{137}Cs and $^{210}Pb_{xs}$, however, were within the bracket of source means, and these FRN were therefore selected as fingerprints in the un-mixing model, despite a low power to discriminate between the two subsurface source groups, roads and streambanks.

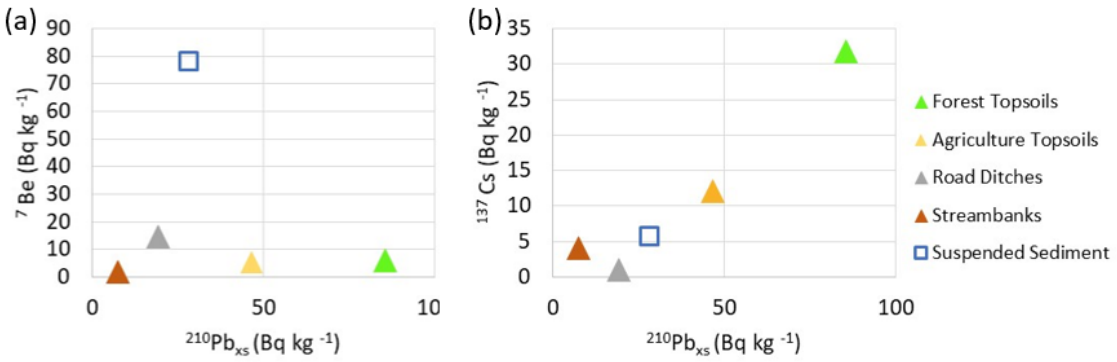

Figure 3.5. Bivariate plots of mean radionuclide activities by source group and target suspended sediment – bracket test to determine fingerprint suitability – pairing (a) 7Be and (b) 137Cs versus 210Pbxs.

Hydrologic characterization and specification of models

Years 2014 and 2015 represented near normal flow years based on mean annual discharge (MAQ) collected at the USGS Mad River streamflow gaging station (7.6 cms [269 cfs] and 7.5 cms [265 cfs], respectively). The average MAQ in the Mad River over the record from water year 1929 through 2015 was 7.7 cms (271 cfs) (USGS, 2018).

Suspended sediment samples were collected during the summer of 2014 and summer and fall of 2015. While the two years represented near-normal years on an annual scale, the two summer target deployments represented contrasting conditions. The summer 2014 deployment was a dry condition following a near-Q1.5 event, while the summer 2015 deployment occurred during wet conditions following a near-Q1.5 event (Figure 3.6). Autumn 2015 deployments were moderately wet following a prolonged dry period

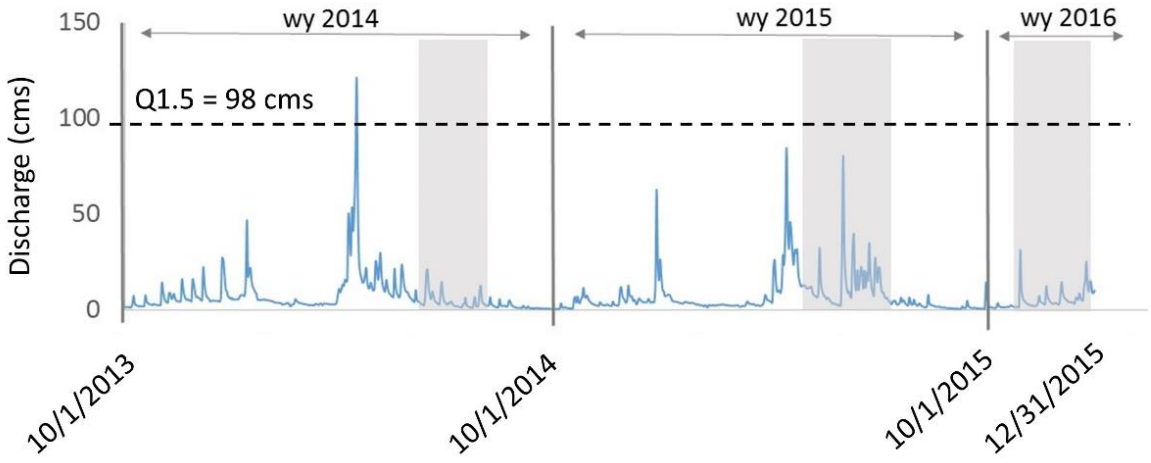

Figure 3.6. Daily mean flow during study period (water years 2014-2016) at USGS Gauging Station (#04288000) on Mad River at Moretown. Gray shading indicates time intervals of passive sampling for suspended sediments.

On the Mad River main stem, two discrete 24-hour storm events spaced approximately one week apart were captured with two sequential deployments of the

Borg sampler ending on June 25 and July 1 in 2015. On the three principal tributaries (Shepard, Folsom and Mill Brooks), time-integrating passive samplers were deployed for multi-week durations. This deployment schedule and the corresponding storm event schedule enabled un-mixing models to be developed for three separate scenarios (Figure 3.6), as detailed in the following sections: a catchment-scale, event-based mixing model (Model A) for the Mad River main stem monitoring station spanning the two June 2015 storms; and two tributary-scale models (B and C) for summer 2015 and autumn 2015, respectively.

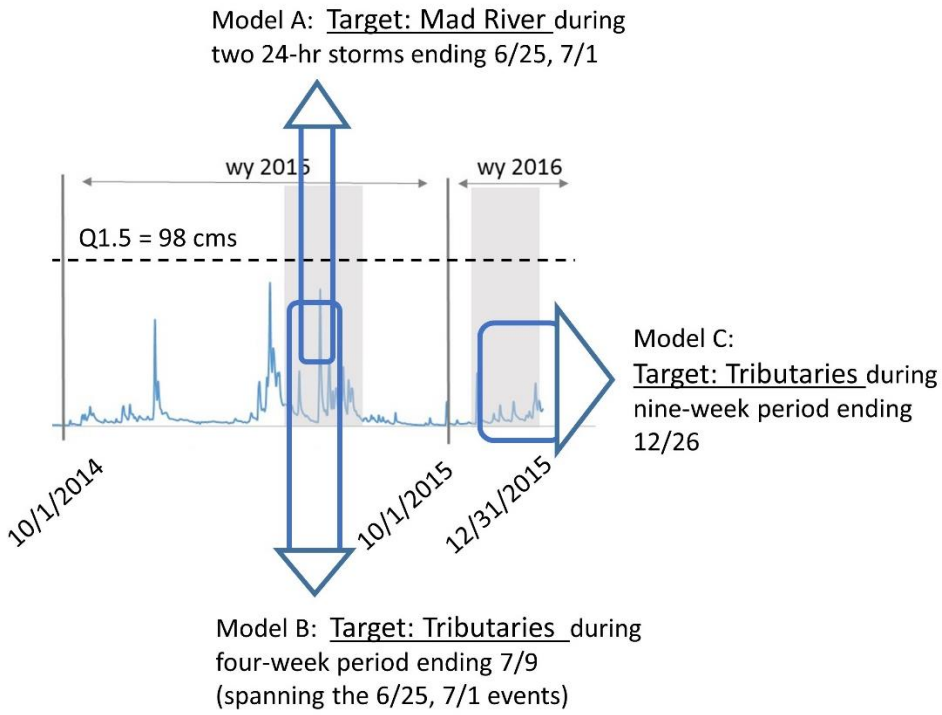

Figure 3.7. Un-mixing model scenarios involving separate suspended-sediment sampler deployments (i.e., targets). Additional model details provided in the text.

Catchment-scale, event-scale source ascription

Un-mixing Model A examined the contributing sources at a catchment scale to the Mad River main stem sampling location at the USGS streamflow gaging station during two sequential, 24-hour-duration streamflow events in late June 2015. Both events were characterized by relatively uniform rainfall across the watershed as measured at the seven rain gages, and above-average antecedent soil moisture levels (Supplementary Fig. 3.Sxa, b). Peak flows registered at 73 cms (storm ending 6/23) and 58 cms (storm ending 6/28), or approximately 74% and 59% of a Q1.5 event (98 cms). These two events had been preceded in the year by the annual spring runoff (in April) and a peak flow of 162 cms on 6/1 which flushed approximately 2,556 tonnes of suspended sediment, or 29% of the May to December 2015 load from the watershed (Hamshaw, 2018).

Un-mixing model results (Table 3.2 and Fig. 3.8) indicate that sediment during these two events was sourced predominantly from streambanks, accounting for approximately 40% of the suspended sediment (mean of the posterior distribution on the proportion estimate), followed by roads (36%) and lesser contributions from agricultural and forested surface soils (15% and 8%, respectively).

Table 3.2. Model A source apportionment results for Mad River main stem two June 2015 sequential storms; proportions by source group presented with 95% credible interval.

	Agricultural Topsoil	Forest Topsoil	Road Ditch	Streambank/ Gullies
Mean	0.155	0.084	0.358	0.403
Median	0.117	0.063	0.328	0.391
Lower 95%	0.005	0.003	0.017	0.022
Upper 95%	0.499	0.300	0.813	0.852

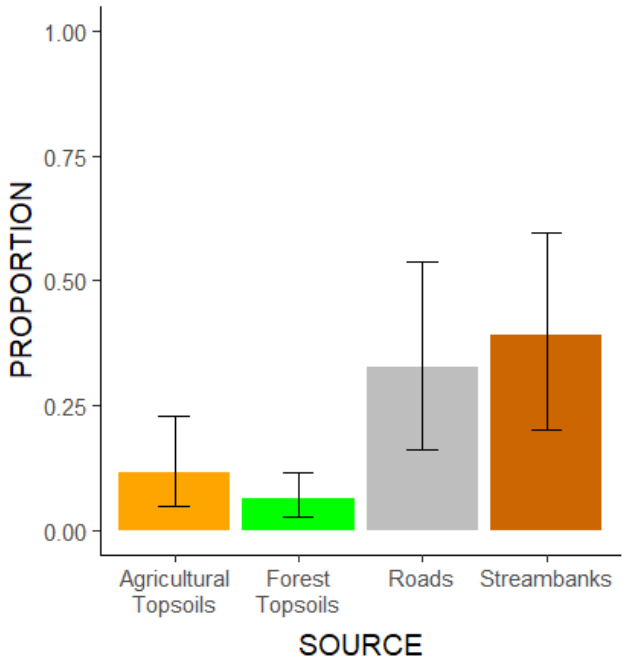

Figure 3.8. Source apportionment results for Mad River main stem target, **Model A**; spanning two 24-hour summer 2015 storm events; bars depict median value; whiskers denote 75th and 25th quartiles on posterior distribution of parameter estimate

Tributary-scale, Summer 2015 source ascription

Un-mixing Model B examined the suspended sediment passively captured at three principal tributaries (Shepard, Mill and Folsom Brooks) during a four-week deployment that spanned the two significant late June storm events captured on the main stem. Several storms were recorded on these tributaries during the month-long deployment. However, the two late June storms represented a large majority of the total deployment load in each of the three tributaries (38, 42 and 55%, respectively) based on TSS flux estimates generated from continuous Turbidity and discharge monitoring records at the outlet of each tributary (Hamshaw, 2018; Hamshaw et al., 2018). Model B results (Table 3.3, Figure 3.9) indicate that tributary sediments during these two events were sourced equally from streambanks and roads (33%), with lesser contributions from

agricultural and forested surface soils (23% and 11%, respectively). Thus, the proportion from subsurface sources in the tributary catchments (66%) would appear to be somewhat lesser than these source types in the main stem spanning the same storm events (76%), although this difference (10%) is likely within a margin of error of the model results.

Table 3.3. Model B source apportionment results for composite of Shepard, Mill, Folsom tributaries during four-week deployment spanning two June 2015 sequential storms; proportions by source group presented with 95% credibility interval.

	Agricultural Topsoil	Forest Topsoil	Road Ditch	Streambank/ Gullies
Mean	0.232	0.111	0.332	0.325
Median	0.200	0.096	0.311	0.308
Lower 95%	0.008	0.005	0.019	0.016
Upper 95%	0.609	0.305	0.746	0.736

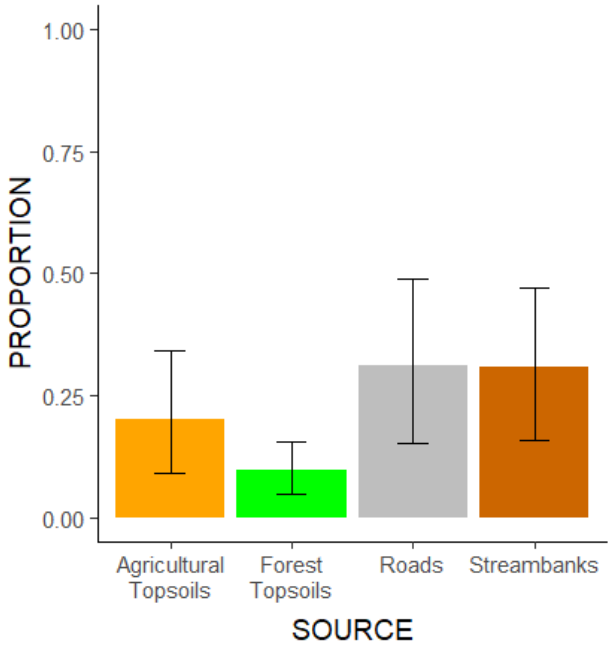

Figure 3.9. Source apportionment results for tributary target, summer 2015, **Model B**; bars depict median value; whiskers denote 75th and 25th quartiles on posterior distribution of parameter estimate

Tributary-scale, Autumn 2015 source ascription

Un-mixing Model C examined the suspended sediment passively captured at the same three principal tributaries (Shepard, Mill and Folsom Brooks) during a multi-week deployment from July 9 through December 26, 2015, but which principally captured sediment from small to moderate storm events occurring in late October through mid-December.

In contrast to the summer events, Model C results (Table 3.4, Figure 3.10) indicate that tributary sediments captured in the fall were sourced primarily from agricultural soils (32%) and roads (28%), followed by forests (21%) and streambanks (19%). Thus, surface sources of sediment from agriculture and forests (53%) appeared to play a more dominant role in overall sediment flux from these three tributaries in the autumn months of 2015. The significance of agricultural sources is underscored by the fact that this land use comprises a relatively small percentage of these tributaries on a catchment scale (3%, 7% and 15% for Shepard, Mill and Folsom, respectively). Interestingly, these percentages increase when considered on a river-corridor scale for Shepard (21%), but remain similar for Mill (14%), and decrease for Folsom (3%). This finding suggests that agricultural uses (while they are lower overall) may be more directly connected to the stream network in Shepard Brook tributary than the other two tributaries.

Table 3.4. Model C source apportionment results for composite of Shepard, Mill, Folsom tributaries during fall deployment from 7/9 to 12/26/15 sample recovery principally from storms in late Oct through Dec; proportions by source group presented with 95% credibility interval.

	Agricultural Topsoil	Forest Topsoil	Road Ditch	Streambank/ Gullies
Mean	0.317	0.210	0.279	0.194
Median	0.284	0.192	0.250	0.153
Lower 95%	0.013	0.012	0.009	0.006
Upper 95%	0.786	0.518	0.679	0.599

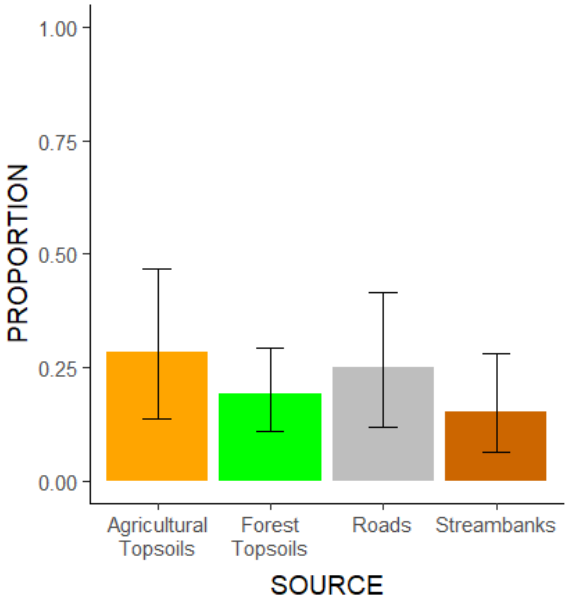

Figure 3.10. Source apportionment results for tributary target, autumn 2015, **Model** C bars depict median value; whiskers denote 75th and 25th quartiles on posterior distribution of parameter estimate.

Additional information from ratio of 7Be/210Pbxs

Given the spatial and temporal variability of 7Be inventories in soils over weekly to monthly time scales, driven in large part by stochastic meteorological inputs, and given our objectives of discerning sediment sources on a seasonal to annual time scale, it would be confounding to include 7Be alongside the FRNs of much longer half-life in our un-mixing model. The bracket test results (Figure 3.5a) underscores this. Nevertheless,

values of the $^{7}Be/\ ^{210}Pb_{xs}$ ratio can reveal something about the age of suspended sediments comprising our targets (Matisoff et al., 2002), and can be examined for consistency with source ascription results of the un-mixing model.

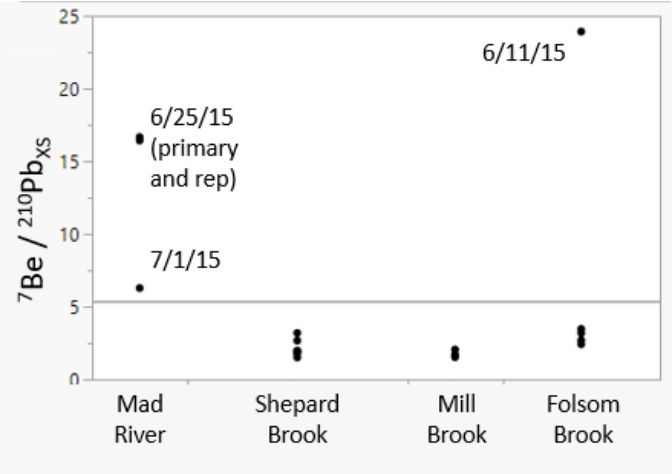

Figure 3.11. Ratios of $^{7}Be/\ ^{210}Pb_{xs}$ in suspended sediment targets collected using passive samplers from the Mad River and three tributaries. Indicated dates refer to deployment end dates. Horizontal line marks the overall mean ratio value

Elevated $^{7}Be/\ ^{210}Pb_{xs}$ ratios in suspended sediment samples were detected in the Mad River main stem during the storm deployment ending 6/25/15, and were less elevated in the next storm event to follow – i.e., deployment ending 7/1/15. This may suggest that a relatively newly-tagged source of surface sediments was mobilized in the first storm and was diluted by 7Be-dead sediments in the subsequent storm. A lower ratio $^{7}Be/\ ^{210}Pb_{xs}$ may be the result of dilution of the sample by 7Be-defficient sediment from either deeper layers of the stream bed or collapsing stream banks (Matisoff et al., 2005).

Discussion

Comparison to regional studies

The results of our source ascription modeling during a wet-summer, spanning two sequential near-Q1.5 events, are largely in accordance with regional estimates for contributions to suspended sediment flux from watersheds during flows on the order of a mean annual flood. The estimated event-scale contribution by roads to the Mad River main stem (36%) and the range of seasonal-scale contributions in the three tributaries (28 to 33%) are in agreement with regionally-derived annual-scale estimates of the contribution of roads to sediment flux from the larger Winooski River basin. Wemple et al. (2017) estimated that road erosion accounts for between 16% and 31% of the average annual TSS load from the Winooski River basin, relying in part on loading estimates from Medalie (2014). There are approximately 344 km of unpaved roads in the Mad River watershed, representing 76% of the total road network (Wemple et al., 2017). Based on estimates scaled up from field-based inventories of 3.4% of this unpaved road network, and in consideration of a GIS-based survey of the full watershed degree of road-stream connectedness, they estimated approximately 11,637 metrics tons of sediment were exported from roads to the Mad River stream network over the inventory period which approximated an annual cycle (Wemple et al. 2017). Among the eight tributary watersheds of the larger Winooski River basin, Mad River had the second highest mean volume of sediment eroded per km of road, and this factor was positively correlated to the median gradient of the watershed (Wemple et al., 2017). Our tributaries had similar road density as the Mad overall (1.32 km/km^2), but land cover categories may vary in their connectedness to the stream network.

Excessive streambank erosion has been documented along both tributary and main-stem segments of the Mad River (Fitzgerald Environmental Associates, 2008). Estimates of sediment flux volumes from streambank erosion have been conducted in recent years relying on terrestrial and airborne light detection and ranging surveys, unmanned aerial surveys, and historical imagery (Hamshaw, 2018; Ross et al., in review). Our mixing model results (19 to 40% from streambanks) generally corroborate findings from these other assessments, that streambanks are a significant source of sediment.

Given the admittedly low power of our tracers to discriminate between streambanks and roads, there is considerable uncertainty in our estimates of the relative contribution from each of these source groups, as reflected in the large 95% credibility intervals (Tables 3.2, 3.3, and 3.4). Still, subsurface sources (i.e., combined road and streambank sources) comprise a majority of the load (76% at the catchment-scale, Model A). This finding is generally consistent with results from a process-based rainfall-runoff model of the Mad River watershed that incorporated a module for simulation of streambank instability (Stryker et al., 2017, 2018). Model runs calibrated to USGS streamflow records for the year 2012 estimated that 96% of the total annual sediment load was sourced from subsurface sources (i.e., streambanks and roads), while only 4% was derived from overland runoff processes (Stryker, et al., 2018). Their modeled estimates of streambank (89%) and road (7%) contributions differ from our catchment-scale estimates (40% and 36%, respectively), and a number of factors could account for the disparity, beyond simple differences in modeling approaches. Most importantly, our study modeled streambank and road contributions during two moderate-sized summer storm events, while the process-based model estimates are annual average contributions.

Our two sampled events generated sediment loads that represented a large contribution of the estimated annual load for 2012 (Hamshaw, 2018), but would not be representative in terms of quantity, or perhaps quality (source contributions), of the annual spring runoff period of the year which has been documented to deliver greatest loads in a near-normal year (Leopold et al., 1995), and which was included in the Stryker et al. (2018) modeled estimate for 2012. The studies were conducted in different years that, while similar in terms of their cumulative flow patterns and near-normal mean annual flows (USGS, 2018), had different antecedent conditions. Year 2012 followed an unusually wet year in 2011 characterized by spring flooding and Tropical Storm Irene in August which was a 0.2% AEP event in the watershed (USGS, 2018). This extreme event was responsible for a shift in suspended sediment rating curves in rivers of the region, due to increased streambank erosion and mass wasting rates (Dethier et al., 2016). We would expect, therefore, that contributions from streambank erosion in a year following such an extreme event would be elevated relative to a timeframe four years out from the event. Finally, just as our estimates have associated uncertainty, the values for streambank and road contributions from the process-based model were reported with upper and lower bounds. Streambank proportions ranged from 75 to 95%, and road proportions ranged from 2 to 18% (Stryker et al., 2018).

Agricultural and forest sources of sediment erosion and transport to the Mad River watershed have been less studied, and our un-mixing model results are one of the first to quantify the relative contributions of these sectors to water quality in the watershed, although on a very limited basis. Our tributary results hinted at the higher significance of agricultural surface sources in autumn storms, and the importance of land

cover/ land use as a driver when considered at a corridor scale rather than a tributary watershed scale.

Our source apportionment results are reflective of hydrometeorological conditions, vegetative states and land use practices that prevailed during the summer and autumn of 2015, a year characterized as having near-average mean annual flow (USGS, 2018). We would expect source apportionment to vary under alternate seasons and in response to more extreme hydrological events that may access different lateral extents of hydrologically-connected land areas (i.e., effective catchment areas of Harvey [2002]; or expanded variable source areas of Dunne and Black [1970]). During extreme events suspended sediments may be preferentially sourced from the headwater regions of the catchment where hillslopes are more closely coupled to the stream and road networks, and are dominantly in forest cover. For example, suspended sediments were disproportionately sourced from reinitiated landslides and mass wasting sites in the Mad River watershed following Tropical Storm Irene (Dethier et al., 2016), similar to conditions encountered in the Connecticut River valley during the same event (Yellen, et al., 2014).

Uncertainties and Limitations

Caution should be applied to the interpretation of these results. While the distribution of rainfall amounts across the watershed during the autumn deployment period was reasonably uniform, autumn deployment lengths were somewhat different across the tributaries, because sample recovery was insufficient in the sampler from Shepard collected on 12/26/15. In the fall months, leaves often blocked the sampler inlet.

An upstream rebar "trash rack" was somewhat effective at keeping the inlet open, but its influence on flow dynamics and sample recovery was not evaluated.

Practical considerations including steep and remote topography, as well as landowner permission, precluded a rigorous, statistically-based, random sampling of all representative source groups in the catchment. Bracket results for the main stem suspended sediment samples were located near the extremes of a polygon enclosing source groups. However, flexibility of the Bayesian un-mixing model framework allows explicit estimation and visualization of uncertainties that may be introduced by inadequate characterization (Fox & Papanicilauo, 2008) - otherwise known as "source fitting error" (Ward et al., 2010; Stock & Semmens, 2016).

Given results of the "bracket test" we assumed that potential transformation of the tracers during transport from source area to the catchment or tributary outlets was minimal and did not influence the source apportionment results – i.e., the tracers behaved conservatively. Our un-mixing model did not explicitly consider potential delayed transport of suspended sediment due to transient storage within the active river corridor. The magnitude of the storm events during sampler deployments suggests that overbank deposition would not have been a significant issue. But sediment sourcing proportions could have been influenced by fines in channel storage since the previous event(s). Mad River is a steep watershed, and therefore storage within tributaries is expected to be relatively minimal; however, storage along the main stem river corridor could have been measurable.

Results of statistical analyses suggested less discriminatory power between streambank and road sources than between streambanks and the other surface source

groups (agricultural and forest). Some discrimination between streambank and roads was offered by ^{7}Be ($p = 0.102$) which was reflected also in the ^{7}Be / $^{210}Pb_{xs}$ ratio values, although insufficient reported numbers for this very-short-half-life FRN precluded its inclusion in the un-mixing model. It is possible that geochemical parameters reflective of bedrock and overburden parent materials would better distinguish between road and streambank/gully sources.

Management Implications

Conveniently, the four source groups identified in our un-mixing model represent management sectors with relevance to local and state stakeholders for consideration of appropriate management strategies to reduce sediment erosion and transport, as well as nutrients or other constituents that may be strongly correlated to sediment. Erosion along unpaved roads can be reduced through the use of structures that slow velocities of stormwater runoff, including turnouts, use of stone lining in ditches, and energy-dissipating structures at culvert outlets (Turton et al., 2009; Wear et al., 2013). In the Winooski River basin study region, road segments with greater percentages of these best management practices were associated with lower frequencies of erosional features (Wemple et al., 2017).

A better understanding of the contribution of streambanks will also inform efforts to reduce phosphorus loading. Streambank erosion has been documented as a source of phosphorus to receiving waters both globally (Sharpley et al., 2013) and regionally (DeWolfe et al., 2004; Langendoen, et al., 2012; Ishee et al., 2016). And phosphorus loading has been correlated to TSS loading in the Mad River watershed (Hamshaw, 2018; Ross et al., manuscript in review). Furthermore, coarse sediment sourced from headwater

regions can become deposited in lesser-gradient, lowland reaches of the river, driving lateral migration of channel banks and erosion of floodplain sediments that may be relatively more concentrated in phosphorus due to land use amendments. Thus, having better information about 'hot spots' of sediment erosion at a catchment scale can aid in implementing corrective measures that not only directly mitigate erosion at those hot spots but also indirectly help to mitigate downstream erosion and phosphorus loading. A future phase of this mixing model analysis will include phosphorus which was analyzed alongside geochemical parameters in source and target samples collected in the original field work.

The greater percentage of agricultural source groups in the fall samples from the tributaries may reflect the fact that cultivated fields are often tilled in that season, or be an indication of the reduced interception and surface roughness offered by vegetation as plants enter a dormant phase in autumn months. These results hint at the importance of seasonal differences in sediment sourcing throughout the watershed, as well as times of the year where best management practices may be especially warranted.

Future research directions

Future work will expand on this un-mixing model with the addition of geochemical tracer data (cations, trace metals, and phosphorus) collected synoptically with the short-term radionuclide data. It is expected that incorporation of these additional fingerprints will provide greater source discrimination, and may allow for consideration of additional or more refined source groups (e.g, distinction among crop/hay/pasture sources or distinction between subsurface sediments derived from glaciolacustrine vs alluvial or glacial till parent materials). This expanded analysis will be paired with

spatially-explicit data on streambank erosion, lateral and vertical channel stability, degree of floodplain (dis)connection, and channel evolution stage and trends supported by other studies (Ross et al., in review; Stryker et al.., 2016), to define hot spots of erosion.

This same source characterization data set could be leveraged for future sampling of event-based or time-integrated target distributions. Future storms in the watershed could be sampled for these same tracer constituents to enable estimates of source ascription under different seasons, storm magnitudes, hysteresis types, or antecedent conditions as well as expanded spatial sampling to further refine source ascription estimates by tributary. Future research of this team could explore the opportunities provided in MixSIAR to model random or fixed effects to explore how fingerprint signatures of various storms may deviate from the overall mean in a predictable way by continuous covariates (e.g., temperature, soil moisture, duration of flow above erosion threshold) or categorical covariates (e.g., season, tributary identification).

Since sediment sourcing is a complex function of not only the nature and magnitude of source regions but also transport processes and degree of source connectivity to the receiving stream network, modeling of source ascription variability in space and time can be improved through explicit consideration of transport processes. The Bayesian framework in general allows for this as demonstrated by Fox & Papanicolaou (2008) who specified deterministic mixing-model parameters that would account for spatial differences in sediment sourcing as well as temporal factors in sediment delivery such as residence time. Abban et al., (2016) later expanded on this work to include a probabilistic treatment of these erosion and transport parameters. The newly-released MixSIAR framework offers similar flexibility. In ecological modeling

applications, a fractionation error term can be introduced to the model to account for how "consumers differentially process source tissue" (Moore and Semmens, 2008; Stock and Semmens, 2016), and the effect that this has on variability of istopic levels in the consumers. Future research in MixSIAR applications to sediment tracer models could explore the use of this fractionation error term to account for how catchments differentially process sediments in sink to source transfers under various hydrologic and geomorphic conditions. Sources may also be more or less available at certain times of the year (as mediated by temperature and vegetation or land use activities) or at certain locations in a watershed (e.g., as governed by variable source area concept). This aspect of resource variability (Stock & Semmens, 2016) has been explored in mixing models in an ecological context (e.g., Yeakel et al., 2011), and could have similar applications to sediment un-mixing models.

Conclusions

A sediment tracer study was carried out in the Mad River catchment to discriminate between surface and subsurface sources of fine particulates (clay, silt, fine sand) carried in suspension by the river. Using fallout radionuclides as fingerprints (^{137}Cs, excess ^{210}Pb), a Bayesian un-mixing model apportioned the relative contributions of four source groups (agricultural topsoils, forested topsoils, roads, and streambanks) to suspended-sediments targets examined at the catchment outlet and from three principal tributaries that together comprised 31% of the total watershed. Interpretation was supported by analysis of synoptically-measured suspended-sediment load quantified from regression models relying on continuous turbidity and discharge monitored at the outlets of the Mad River catchment and each tributary.

Modeling results for the catchment-scale sampling of two sequential summer 2015 storm events suggested that suspended sediment load at the catchment outlet during two summer storms was generated primarily from subsurface sources characterized as erosion from roads (36%) and stream banks/ gullies (40%). Source proportions for the tributary-derived suspended-sampling of the same events did not differ appreciably from that of the catchment-scale, as roads and streambanks contributed 33% and 33% of the load, respectively. These findings were broadly supported by separate studies in the watershed of channel change from multi-date lidar and unmanned aerial system surveys, and fit within a range of estimates generated by a process-based rainfall-runoff model for year 2012 that estimated contributions of 89% from streambanks and 7% from roads.

A limited comparison of tributary sediment flux in the autumn months of 2015 suggested that source contributions vary with season. In the autumn, a greater proportion of sediment was sourced from agricultural surface soils than from the other three source groups in the three tributaries. Having better information about 'hot spots' and 'hot moments' of sediment erosion in the watershed will help to prioritize best management practices and corrective measures to address sediment and nutrient loading. Future work will explore the flexibility of the Bayesian model framework to model source ascription variability in space and time through explicit consideration of transport processes and use of informative priors based on distribution of storm hysteresis patterns over a given target-sample deployment.

Acknowledgements

Support to the authors was provided by Vermont EPSCoR with funds from the National Science Foundation Grant EPS-1101317. The authors are grateful to the United

States Geological Survey for hydrologic data sets used in this analysis. EPSCoR funds and Barrett Foundation grants provided intern support for data collection. The authors appreciate the help of EPSCoR and Barrett Foundation interns Jordan Duffy, Alex Morton, Marisa Rorabaugh, and Hanna Anderson who assisted with sample collection and processing. We thank Joshua Landis at the Dartmouth College Short-lived Isotope Lab for radionuclide analyses and interpretation. We are grateful to Joel Tilley at the Agricultural & Environmental Testing Lab Laboratory for oversight and quality assurance of ICP analyses. ICP laboratory assistance was provided Barrett Foundation intern Jordan Duffy and by REU intern Thomas Adler, funded through the UVM Civil & Environmental Engineering program. This work also benefited from previous characterizations of catchment geology (George Springston, Rick Dunn, Nathan Donahue) and fluvial geomorphology (Lori Barg, John Field, Evan Fitzgerald, Mary Nealon).

Supporting Information

This supplementary document contains additional tables and figures in support of Chapter 3 – A Bayesian Un-Mixing Model to Discern Suspended Sediment Sources in a Glacially-Conditioned Catchment. Items are presented in order of their introduction within the main manuscript.

- Text 3.S1. Development of informative priors from storm hysteresis data.
- Table 3.S1. Summary of sediment characteristics by storm hysteresis class.
- Table 3.S2. Source-group contribution coefficients by hysteresis class.
- Table 3.S3. Summary of physical characteristics of study area watersheds.
- Figure 3.S1a. Metrics for Mad River main stem storm ending 6/25/15.
- Figure 3.S1b. Metrics for Mad River main stem storm ending 7/1/15.

Our analysis explored the possibility of using information from synoptically monitored storm event data and hysteresis classifications to develop informative priors on the source group proportions for our time-integrated passive TSS deployments. Sampled storms can be examined in terms of hysteresis, a phenomenon where a different TSS concentration is evident for the same discharge, depending upon when a storm hydrograph is sampled. This disconnect is evident in a TSS-Q bivariate plot. Williams (1989) was one of the first to categorize styles of hysteresis exhibited in river systems as clockwise loops, counterclockwise loops, or figure 8 patterns as variants on a linear relationship that would be evident if the TSS and Q peaks coincided. He described possible driving factors that would manifest in these patterns, and additional characterization has been offered from wide-spread investigation of hysteresis patterns in subsequent decades (Asselman, 1999; Bowes, et al., 2015; Bieroza & Heathwaite, 2015; Buendia et al., 2016).

As an alternative to the non-informative prior, we developed an informative prior based on synoptically-generated classifications of storm hysteresis for the study area summarized by Hamshaw et al. (2018). For each passive sampler deployment, we summarized the distribution of storm events, their hysteresis pattern, antecedent moisture conditions, and suspended particulate matter flux by storm event (Table 3.S1). Total suspended solids (TSS) were estimated from TSS regressions on Turbidity, relying on continuous Turbidity and discharge monitoring records at the outlet of each tributary (Hamshaw, 2018; Hamshaw et al., 2018).

Hysteresis patterns of each storm event were classified after Williams (1989) and Hamshaw et al., (2017), and the expected predominance of contributing sediment sources by hysteresis class was based on a literature review summarized below in Table 3.S1. Based on the sediment sourcing and transport characteristics by hysteresis class, we hypothesized a relative contribution for each tracer-study source group (Table 3.S2). Note that for those classes where sources were indeterminate based on the literature review, equal source group proportions were assumed, corresponding to a non-informative prior ($\alpha = \{1, 1, 1, 1\}$).

The source-group contribution estimates by hysteresis class were then used to weight the proposed sediment source group proportions for a given passive-sampler deployment, based on the distribution of storm types encountered during deployment and their respective TSS flux. An informative prior was then developed for a given passive sampler deployment, given the proportional TSS flux by storm class.

Table 3.S1. Summary of sediment characteristics by storm hysteresis class.

Hysteresis Class	Sediment sources; Sediment delivery characteristics	Likely Source Groups
I (Linear, no significant hysteresis)	TSS peak aligns with Q peak Transport characteristics: Neither demonstrably supply-limited or transport-limited Seasonal effects: relatively infrequent occurrence overall in the study area (Hamshaw et al., 2018) in spring or late autumn/winter partly due to less vegetation or land use practices such as tillage (Asselman, 1999; Martin et al., 2014; Sherriff et al., 2016)	All Streambanks/ gullies/ Roads more weighted as with II
II (Clockwise)	Sources: Near- and within-stream TSS mobilized rapidly in response to hydrologic forcing (Asselman, 1999; Bowes, et al., 2015; Bieroza & Heathwaite, 2015; Buendia et al., 2016) including channel and gully erosion (Smith & Dragovich, 2009) and runoff from road-extended stream networks (Wemple, et al., 1996; Wemple et al., 2017) Pronounced-hysteresis sub-category: (2D and 2E of Hamshaw et al., 2018) Very-near, rainfall-activated, nonvegetated TSS sources - classic "first-flush" response including hydrologically-connected ditches, gullied sources very close to channel (Hamshaw et al., 2018) and road-ditch sediment via a road-extended hydrologic network (Wemple, et al., 1996; Wemple et al., 2017) Transport characteristics: Sediment exhaustion contributing to "first-flush" phenomenon (Walling & Webb, 1982) – i.e., supply-limited Soils: More common in catchments dominated by soils of limited infiltration capacity – i.e., poorly-drained (Sheriff et al., 2016) Hydrology: Wet antecedent conditions, leading to expanded and hydrologically-connected source area (Buendia et al., 2016; Hamshaw et al., 2018) and/or increased groundwater contributions manifesting in mid- to late-storm dilution (Walling & Webb, 1982; Bieroza & Heathwaite, 2015) Seasonal effects: more frequent in spring or late autumn/winter partly due to less vegetation or land use practices such as tillage (Asselman, 1999; Martin et al., 2014; Sherriff et al., 2016)	Streambanks/ Streambeds/ Gullies Roads/ Ditches/ Gullies

	Scale effects: more common at headwater monitoring sites (Asselman, 1999; Hamshaw et al., 2018)	
III (Counterclockwise)	Sources*: Previous research has not offered much information on sources other than to infer distal surface sources (Lawler et al., 2006). Given the transport and hydrologic characteristics below, and the dominance of forested land cover in the distal parts of our study area, we hypothesize forest surface soils as a dominant source for TSS –Q patterns exhibiting Type III hysteresis in our study area.* Transport characteristics: Delayed delivery of sediment from distal surface sources (Lawler et al. 2006; Bieroza & Heathwaite, 2015; Gellis, 2013) or hydrologically-driven breakup of armor layer or vegetation late in the storm or in a subsequent smaller storm due to progressive increases in shear stress leading to delayed delivery of TSS (Reid et al., 1997; Lawler et al. 2006; Bieroza & Heathwaite, 2015) – i.e., transport-limited Soils: More common in catchments dominated by soils of increased infiltration capacity – i.e., well-drained (Sheriff et al., 2016) Hydrology: More variable precipitation patterns across the catchment, with rainfall occurring distal from monitored outlet (Hamshaw et al., 2018) Scale effects: more common at low-land monitoring sites (Asselman, 1999; Hamshaw et al., 2018)	Forest Surface Soils Streambed and banks
IV (Complex)		Indefinite
V (Figure 8)	Sources: Some studies note stream bank and streambed sources (Eder et al., 2010; Megnounif et al., 2013; Seeger et al., 2004); May be complex with watershed-specific drivers. Transport characteristics: Delayed delivery of sediment from distal sources (Eder et al., 2010; Megnounif et al., 2013; Seeger et al., 2004 Hydrology: Conflicting evidence, occurring in both dry antecedent conditions (Hamshaw et al., 2018; Seeger et al 2004) and wet antecedent conditions with large events (Buenda et al., 2016)	Indefinite

Table 3.S2. Source-group contribution coefficients by hysteresis class.

Will-iams	Ham-shaw	Hysteresis Description	TSS Flux Character	Agricultural Topsoils	Forested Topsoils	Roads	Streambanks/ beds/ gullies
I II	1a, 1b, 2a	Linear to minor clockwise	Infrequent but responsible for majority of annual load	0.05	0.05	0.45	0.45
II	2b, 2c	Moderate clockwise	Late spring/ late autumn	0.05	0.05	0.45	0.45
II	2d, 2e	Pronounced clockwise		0.01	0.01	0.20	0.78
III	3's			0.10	0.55	0.10	0.25
IV	4's		Late autumn	0.25	0.25	0.25	0.25
V	5's	Figure 8		0.25	0.25	0.25	0.25

Table 3.S3. Summary of physical characteristics for study area watersheds.

	Sub-watershed	Stream Order	Drainage Area (km^2)	Percent of Basin Above 1200 ft Elevation [a] (%)	Mean Annual Precipitation [b] (mm)	Subwater-shed HSG C&D Soils [c] (%)	Corridor HSG C&D Soils [c] (%)	Subwatershed Land Use [d] Developed (%)	Agriculture (%)	Forest (%)
A	Mad River at Moretown	5	360.0	73.4	1300	78.3	63.1	8.0	4.7	85.5
B	Shepard Brook	4	44.5	81.8	1364	80.1	71.6	5.6	1.0	92.2
C	Mill Brook	4	49.7	85.9	1430	77.9	66.9	7.0	1.5	89.2
D	Folsom Brook	4	18.2	89	1295	88.7	78.1	8.8	12.7	77.6

a Vermont Streamstats

b PRISM data: 1981- 2010

c SSURGO soils and Table 20 attributes table

d Troy *et al*., 2007 (source date: 2001)

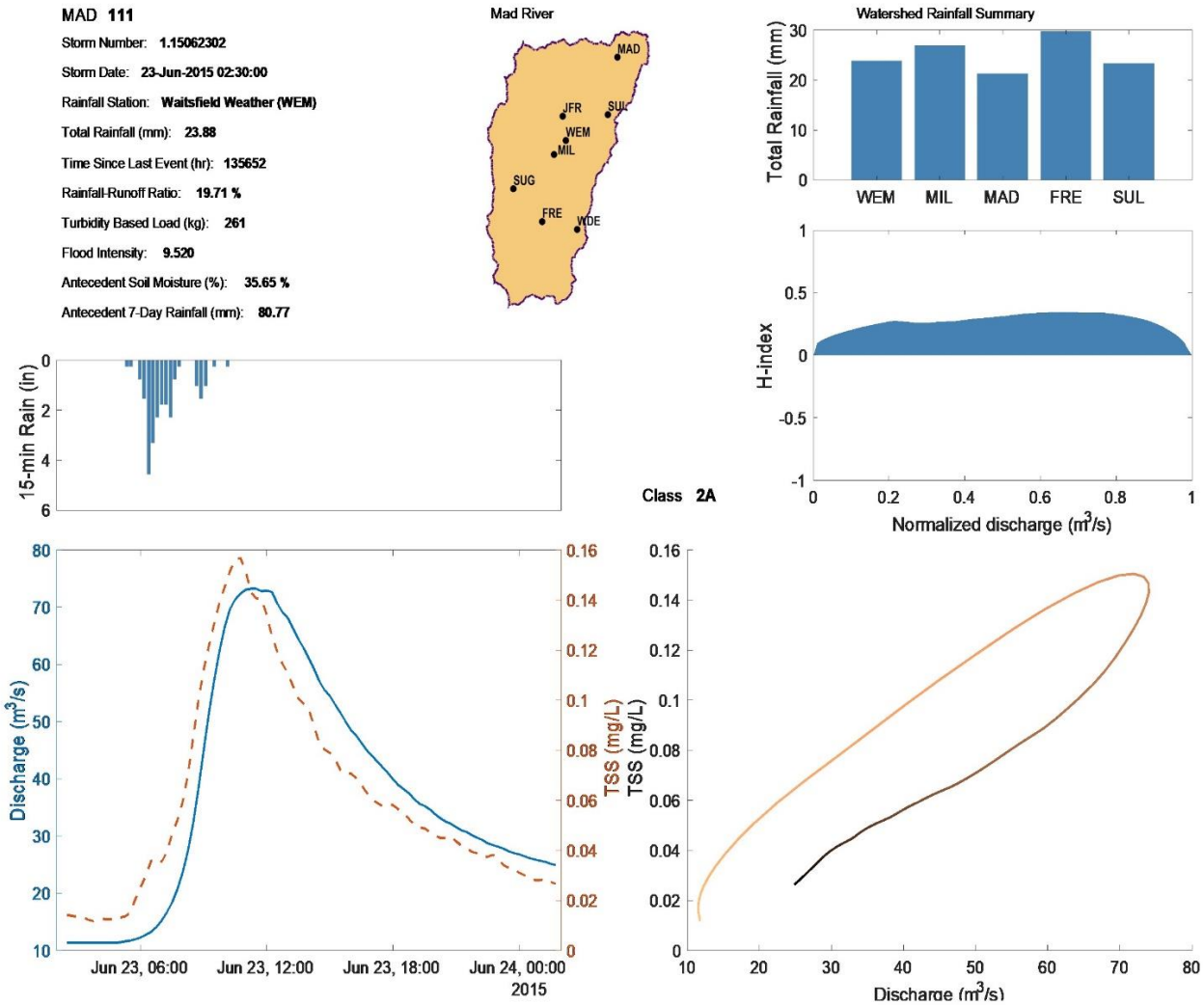

Figure 3.S1a. Metrics for Mad River main stem storm ending 6/25/15.

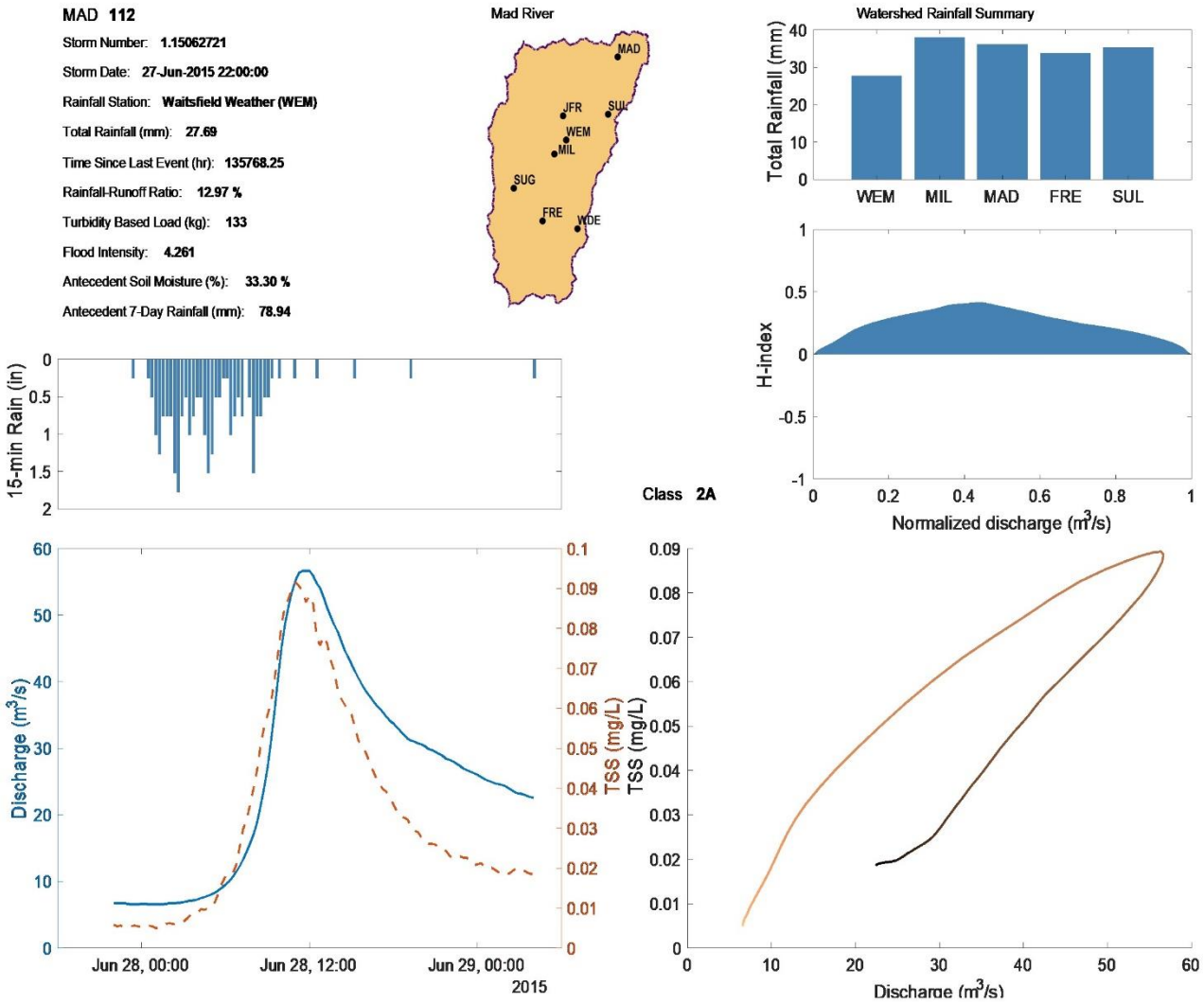

Figure 3.S1b. Metrics for Mad River main stem storm ending 7/1/15.

References

Abban, B., A. N. Papanicolaou, M. K. Cowles, C. G. Wilson, O. Abaci, K. Wacha, K. Schilling, and D. Schnoebelen (2016), An enhanced Bayesian fingerprinting framework for studying sediment source dynamics in intensively managed landscapes, *Water Resources Research*, 52, doi:10.1002/2015WR018030.

Anderson, I., D. M. Rizzo, D. R. Huston, and M. M. Dewoolkar (2017), Analysis of bridge and stream conditions of over 300 Vermont bridges damaged in Tropical Storm Irene, *Structure and Infrastructure Engineering*, 1-14, doi: 10.1080/15732479.2017.1285329.

Appleby, P., Oldfield, F., 1992. Application of 210Pb to sedimentation studies. In: Ivanovich, M., Harmon, R.S. (Eds.), Uranium Series Disequilibrium. Oxford University Press, Oxford, UK, pp. 731–778.

Ballantyne, Colin K., 2002, Paraglacial geomorphology. Quaternary Science Reviews, 21: 1935-2017.

Barbeta, A. J., Peñuelas (2017), Relative contribution of groundwater to plant transpiration estimated with stable isotopes, *Scientific Reports*, 7, 1, doi:10.1038/s41598-017-09643-x.

Barthod, L.R.M., Liu, K., Lobb, D.A., Owens, P.N., Martinez-Carreras, N., Koiter, A.J., Petticrew, E. L., McCullough, G.K., Liu, C., Gaspar, L., 2015, Selecting color-based tracers and classifying sediment sources in the assessment of sediment dynamics using sediment source fingerprinting. J. Environ. Qual., 44: 1605-1616.

Beers, F. W., 1873, Atlas of Washington County, Vermont.

Bierman, Paul, Andrea Lini, Paul Zehfuss, Amy Church, 1997, Postglacial Ponds and Alluvial Fans: Recorders of Holocene Landscape History. GSA Today, vol. 7, no. 10.

Borg, J. L. (2010), Streambank Stability and Sediment Tracing in Vermont Waterways, University of Vermont, Dept of Civil & Environmental Engineering, M.S. Thesis.

Brakenridge, G. Robert, Peter A. Thomas, Laura E. Conkey, Jane C. Schiferle, 1988. Fluvial Sedimentation in Response to Postglacial Uplift and Environmental Change, Missisquoi River, Vermont. Quaternary Research, vol. 30, p.190-203.

Brigham, M. E., C. J. McCullough and P. Wilkinson (2001), Analysis of suspended-sediment concentrations and radioisotope levels in the Wild Rice River Basin, Northwestern Minnesota, 1973–1998, *Water-Resources Investigations Rep. 01-4192*, U.S. Department of the Interior, U.S. Geological Survey.

Church, M. and J. Ryder, 1972, Paraglacial sedimentation: A consideration of fluvial processes conditioned by glaciation. Geological Society of America Bulletin, 83: 3059-3072.

Collins, A.L., and D. E. Walling (2002), Selecting fingerprint properties for discriminating potential suspended sediment sources in river basins, *J. Hydrology*, 261, 218.

Collins, A.L., D. E. Walling, G.J.L. Leeks (1997), Source type ascription for fluvial suspended sediment based on a quantitative fingerprinting technique, *Catena*, 29, 1–27, doi:10.1016/S0341-8162(96)00064-1.

Collins, A.L., Zhang, Y., Hickinbotham, R., Bailey, G., Darlington, S., Grenfell, S.E., Evans, R., Blackwell, M., (2013), Contemporary fine-grained bed sediment sources across the River Wensum Demonstration Test Catchment, UK. Hydrol. Process. 27, 857e884.

Cooper, R. J., T. Krueger, K. M. Hiscock, and B. G. Rawlins (2014), Sensitivity of fluvial sediment source apportionment to mixing model assumptions: A Bayesian model comparison, *Water Resour. Res*., 50, 9031–9047, doi:10.1002/2014WR016194.

Dethier, E., F. J. Magilligan, C. E. Renshaw, and K. H. Nislow (2016), The role of chronic and episodic disturbances on channel-hillslope coupling: the persistence and legacy of extreme floods, *Earth Surface Processes and Landforms*, *41*(10), 1437-1447, doi: 10.1002/esp.3958

DeWolfe, M. N., W. C. Hession, and M. C. Watzin (2004), Sediment and phosphorus loads from streambank erosion in Vermont, USA., in *Critical Transactions in Water and Environmental Resources Management*, edited by G. Sehlke, D. F. Hayes and D. K. Stevens, pp. 1-10, American Society of Civil Engineers, Reston, VA.

Dunn, R., Springston, G., and Donahue, N., 2007, Surficial Geologic Map of the Mad River Watershed, Vermont, Vermont Geological Survey Open File report, VG07-1.

Dunne, T. and R.D. Black, 1970, Partial Area Contributions to Storm Runoff in a Small New England Watershed. Water Resources Research, 6(5), 1296-1311.

Dutton, C., A.C. Ainsfield, H. Ernstburger. (2013). A novel sediment fingerprinting method using filtration: application to the Mara River, East Africa, J. Soils Sediments, 13: 1708-1723.

Fitzgerald Environmental Associates, 2008, Upper Mad River Corridor Plan, technical report prepared for Friends of the Mad River, available at: https://friendsofthemadriver.org/documents/FMR_Final_RCP_Report.pdf

Foster, D. R., and J. D. Aber, editors, 2004, Forests in Time: The Environmental Consequences of 1000 Years of Change in New England. Yale University Press, New Haven, CT.

Fox, J. F. & A. N. Papanicolaou (2008), An un-mixing model to study watershed erosion processes, *Advances in Water Resources*, 31, 96.

Gelman, A., & Rubin, D. B. (1992). Inference from iterative simulation using multiple sequences. *Statistical Science, 7*, 457-472.

Gelman, A., Carlin, J.B., Stern, H.S., Rubin, D.B., 2004. Bayesian Data Analysis. Chapman & Hall/CRC, Boca Raton, FL.

Geman, S., and D. Geman, (1984). Stochastic relaxation, Gibbs distributions, and the Bayesian restoration of images. *IEEE Transactions on Pattern Analysis and Machine Intelligence, 6*, 721-741.

Gordón, F., S. I. Perez, A. Hajduk, M. Lezcano and V. Bernal (2017), Dietary patterns in human populations from northwest Patagonia during Holocene: an approach using Binford's frames of reference and Bayesian isotope mixing models, *Archaeological and Anthropological Sciences*,.

Guilbert, J., A. K. Betts, D. M. Rizzo, B. Beckage, and A. Bomblies. 2015. Characterization of increased persistence and intensity of precipitation in the Northeastern United States. Geophysical Research Letters. DOI: 10.1002/2015GL063124.

Guilbert, J., B. Beckage, J. M. Winter, R. M. Horton, T. Perkins, and A. Bomblies. 2014. Impacts of projected climate change over the Lake Champlain Basin in Vermont. Journal of Applied Meteorology and Climatology 53: 1861-1875.

Hamshaw, S. D. (2018), Fluvial Processes in Motion: Measuring Bank Erosion and Suspended Sediment Flux using Advanced Geomatic Methods and Machine Learning, *Graduate College Dissertations and Theses*, https://scholarworks.uvm.edu/graddis/827

Hamshaw, S. D., Dewoolkar, M. M.,Schroth, A. W., Wemple, B. C., & Rizzo, D. M. (2018). A new machine-learning approach for classifying hysteresis in suspended-sediment discharge relationships using high-frequency monitoring data. Water Resources Research, 54, 4040–4058. doi: /10.1029/2017WR022238.

Hamshaw, S. D., T. Bryce, D. M. Rizzo, J. O'Neil-Dunne, J. Frolik, and M. M. Dewoolkar (2017), Quantifying streambank movement and topography using unmanned aircraft system photogrammetry with comparison to terrestrial laser scanning, *River Research and Applications*, *33*(8), 1354-1367, doi: 10.1002/rra.3183.

Harvey, A.M., 2002. Effective timescales of coupling within fluvial systems. Geomorphology 44, 175–201.

Harvey, J. W., J. D. Drummond, R. L. Martin, L. E. McPhillips, A. I. Packman, D. J. Jerolmack, S. H. Stonedahl, A. F. Aubeneau, A. H. Sawyer, L. G. Larsen, and C. R. Tobias (2012), Hydrogeomorphology of the hyporheic zone: Stream solute and fine particle interactions with a dynamic streambed, *J. Geophys. Res*., 117, G00N11, doi:10.1029/2012JG002043.

Hayhoe, K., Wake, C. P., Huntington, T. G., Luo, L., Schwartz, M., Sheffield, J., …Wolfe, D. (2007). Past and future changes in climate and hydrological indicators in the U.S. Northeast. *Climate Dynamics, 28*, 381-407

He, Q., Walling, D., 1996. Use of fallout Pb-210 measurements to investigate longerterm rates and patterns of overbank sediment deposition on the floodplains of lowland rivers. Earth Surface Processes and Landforms 21, 141–154.

Ishee ER, Ross DS, Garvey KM, Bourgault RR, Ford CR. 2015. Phosphorus characterization and contribution from eroding streambank soils of Vermont's Lake Champlain basin. Journal of Environmental Quality 44. DOI:10.2134/jeq2015.02.0108.

Isles, P.D.F., Giles, C.D., Gearhart, T.A, Xu, Y., Druschel, G.K., Schroth, A.W., 2015. Dynamic internal drivers of a historically severe cyanobacteria bloom in Lake Champlain revealed through comprehensive monitoring. Journal of Great Lakes Research. 41(3), 818–829.

Jones J. A., and G. E. Grant (1996), Peak flow responses to clear-cutting and roads in small and large basins, western Cascades, Oregon, *Water Resources Research*, 32, 959–974, doi:10.1029/95WR03493.

Karwan, D. L., and J. E. Saiers (2009), Influences of seasonal flow regime on the fate and transport of fine particles and a dissolved solute in a New England stream, Water Resour. Res., 45, W11423, doi:10.1029/2009WR008077.

Kline, M., and B. Cahoon (2010), Protecting river corridors in Vermont, *Journal of the American Water Resources Association*, 1(10), doi: 10.1111/j.1752-1688.2010.00417.x

Koiter, A.J., D.A. Lobb, P.N. Owens, E.L.Petticrew, K. Tiessen, S. Li (2013), Investigation the role of scale and connectivity in assessing the sources of sediment in an agricultural

watershed in the Canadian prairies using sediment source fingerprinting, J. Soils Sediments, 13: 1676-1691.

Kondolff, G. Mathias, 1997, PROFILE: Hungry Water: Effects of Dams and Gravel Mining on River Channels, Environmental Management, 21(4), 533-551.

Langendoen, E. J., A. Simon, L. Klimetz, N. Bankhead, and M. E. Ursic (2012), Quantifying sediment loadings from streambank erosion in selected agricultural watersheds draining to Lake Champlain, (Lake Champlain Basin Program Technical Report No. 72, 65 pp.). Burlington, VT.

Larsen, F.D., 1987. History of glacial lakes in the Dog River Valley, central Vermont: Westerman, D.S., ed., Guidebook for Field Trips in Vermont, Volume 2: New England Intercollegiate Geologic Conference, 79th annual meeting, Northfield, Vermont.

Lawler, D.M., Petts, G.E., Foster, I.D.L., Harper, S., 2006. Turbidity dynamics during spring storm events in an urban headwater river system: the Upper Tame, West Midlands, UK. Sci. Total Environ. 360 (1–3), 109–126.

Leopold, L.B.; M.G. Wolman, and J.P. Miller. 1995. Fluvial Processes in Geomorphology. Dover Publications. ISBN 0-486-68588-8Magilligan, F.J., Nislow, K.H., Graber, B.E., 2003. Scale-independent assessment of discharge reduction and riparian disconnectivity following flow regulation by dams. Geology. v. 31, no. 7, pp 569-572.

Martínez-Carreras, N., Krein A, Gallart F, Iffly JF, Pfister L, Hoffmann L, Owens PN (2010) Assessment of different colour parameters for discriminating potential suspended sediment sources and provenance: a multi-scale study in Luxembourg. Geomorphology 118:118–129.

Matisoff, G, E. C. Bonniwell and P.J. Whiting (2002), Soil erosion and sediment sources in an Ohio watershed using beryllium-7, cesium-137, and lead-210, *J. Environ. Qual.*, 31, 54–61.

Matisoff, G., C.G. Wilson and J. Whiting (2005), The $^{7}Be/^{210}Pb_{xs}$ ratio as an indicator of suspended sediment age or fraction new sediment in suspension, *Earth Surf. Processes Landforms*, 30, 1191–1201, doi: 10.1002/esp.1270.

Medalie, L. (2014), Concentration and flux of total and dissolved phosphorus, total nitrogen, chloride, and total suspended solids for monitored tributaries of Lake Champlain, 1990–2012, *Open-File Report 2014–1209*, U.S. Geological Survey, Washington, D. C., doi:10.3133/ofr20141209.

Moore, J. W., & Semmens, B. X. (2008). Incorporating uncertainty and prior information into stable isotope mixing models. Ecology Letters, 11(5), 470-480.

Mukundan, R., D.E. Radcliffe, J.C. Ritchie, L. M. Risse, R.A. McKinley (2010), Sediment fingerprinting to determine the source of suspended sediment in a southern Piedmont stream, *J. Environmental Quality*, 39, 1328–1337.

Noe, G. B. and C. R. Hupp (2005), Carbon, nitrogen, and phosphorus accumulation in floodplains of Atlantic coastal plain rivers, USA, *Ecological Applications*, 15(4), 1178-1190.

Nosrati, K., A. L. Collins, M. Madankan, 2018, Fingerprinting sub-basin spatial sediment sources using different multivariate statistical techniques and the Modified MixSIR model, *Catena*, 164, 32-43, doi: 10.1016/j.catena.2018.01.003.

Olson, S. A. (2014), Estimation of flood discharges at selected annual exceedance probabilities for unregulated, rural streams in Vermont, *with a section on* Vermont regional skew regression, by Veilleux, A. G., *Scientific Investigations Report 2014–5078*, U.S. Geological Survey, Washington, D. C., doi:10.3133/sir20145078.

Owens, P. N., W.H. Blake, L.Gaspar, D. Gateuille, A.J. Koiter, D.A. Lobb, E.L. Petticrew, D.G.Reiffarth, H.G. Smith, J.C. Woodward (2018), Fingerprinting and tracing the sources of soils and sediments: Earth and ocean science, geoarchaeological, forensic, and human health applications, Earth-Science Reviews, 162, 1-23, doi: 10.1016/j.earscirev.2016.08.012.

Parnell, A. C., R. Inger, S. Bearhop, and A. L. Jackson. 2010. Source partitioning using stable isotopes: coping with too much variation. PLoS ONE 5:e9672.

Pechenick AM, Rizzo DM, Morrissey LA, Garvey KM, Underwood KL, Wemple BC. 2014. A multi-scale statistical approach to assess the effects of connectivity of road and stream networks on geomorphic channel condition. Earth Surface Processes and Landforms 39: 1538–1549. DOI:10.1002/esp.3611.

Phillips, J.M., M.A. Russell, D.E. Walling, (2000), Time-integrated sampling of fluvial suspended sediment: a simple methodology for small catchments, *Hydrological Processes*, 14: 2589-2602.

Plummer, M. (2003). JAGS: A program for analysis of Bayesian graphical models using Gibbs sampling. In *Proceedings of the 3rd international workshop on distributed statistical computing (dsc 2003), Vienna, Austria*. ISSN 1609-395X.

R Core Team (2018). R: A language and environment for statistical computing. R Foundation for Statistical Computing, Vienna, Austria. ISBN 3-900051-07-0, URL: http://www.R-project.org/.

Randall, A. D. (1996). Mean annual runoff, precipitation, and evapotranspiration in the glaciated northeastern United States, 1951–1980. *U.S. Geological Open-File Report 96-395.*

Reid, I., J. C. Bathurst, P. A. Carling, D. E. Walling, B. W. Webb (1997), Sediment erosion, transport and deposition, in *Applied fluvial geomorphology for river engineering and management*: edited by C. R. Thorne, R. D. Hey, G. P. Williams, pp. 95–135, John Wiley, New York, NY.

Reum, J. C. P., G. D. Williams and C. J. Harvey (2017), Stable Isotope Applications for Understanding Shark Ecology in the Northeast Pacific Ocean, *Northeast Pacific Shark Biology, Research and Conservation Part A,* 10.1016/bs.amb.2017.06.003, 149-178).

Ridge, John C., 2003, The Last Deglaciation of the Northeastern United States: A Combined Varve, Paleomagnetic, and Calibrated 14C Chronology, in Geoarchaeology of Landscapes in the Glaciated Northeast. Cremeens, David L. and Hart, John P, Ed. Albany, NY: New York State Museum Bulletin 497.

Ritchie, J. C. and G. W. McHenry (1990), Application of radioactive fallout cesium-137 for measuring soil erosion and sediment accumulation rates and patterns: a review. J. Environ. Qual., 19, 215-233.

Ross, D. S., B. C. Wemple, L. J. Wilson, C. Balling, K. L. Underwood, and S. D. Hamshaw (2018), Impact of an Extreme Storm Event on River Corridor Bank Erosion and Phosphorus Mobilization in a Mountainous Watershed in the Northeastern USA, *J. Geophys. Res. Biogeosci.,* (under review).

Semmens, B. X. and J.W. Moore (2008), MixSIR: A Bayesian stable isotope mixing model, Version 1.0. http://www.ecologybox.org.

Shanley, J. B., & Denner, J. C. (1999). The hydrology of the Lake Champlain Basin. In T. O. Manley & P. L. Manley (Eds.), *Lake Champlain in transition-From research toward restoration* (Vol. 1, pp. 41-66): American Geophysical Union, Water Science and Application.

Sharpley, A., H. P. Jarvie, A. Buda, L. May, B. Spears, and P. Kleinman (2013), Phosphorus legacy: overcoming the effects of past management practices to mitigate future water quality impairment, *J Environ Qual*, *42*(5), 1308-1326, doi: 10.2134/jeq2013.03.0098.

Skalak, K., and J. Pizzuto (2010), The distribution and residence time of suspended sediment stored within the channel margins of a gravel-bed bedrock river, Earth Surf. Process. Landf., 35, 435–446, doi:10.1002/esp.1926.

Smith, H.G., and W.H. Blake. 2014. Sediment fingerprinting in agricultural catchments: A critical re-examination of source discrimination and data corrections. Geomorphology 204:177–191. doi:10.1016/j.geomorph.2013.08.003

Stewart, D. P. and P. MacClintock (1969), The Surficial Geology and Pleistocene History of Vermont, *Vermont Geological Survey Bulletin No. 31*, Montpelier, VT.

Stock, B. C. and B.X. Semmens (2016). MixSIAR GUI User Manual. Version 3.1. https://github.com/brianstock/MixSIAR. doi:10.5281/zenodo.1209993.

Stryker, J., B. Wemple, A. Bomblies, 2018, Modeling the impacts of changing climatic extremes on streamflow and sediment yield in a northeastern US watershed, Journal of Hydrology: Regional Studies, 17, 83-94.

Stryker, J., B. Wemple, A. Bomblies, 2017, Modeling sediment mobilization using a distributed hydrological model coupled with a bank stability model, *Water Resources Research*, 53, 2051–2073, doi:10.1002/2016WR019143.

Taylor, A., W. H. Blake, H. G. Smith, L. Mabit, M. J. Keith-Roach (2013), Assumptions and challenges in the use of fallout beryllium-7 as a soil and sediment tracer in river basins, Earth-Science Reviews, 126, 85-95, doi: 10.1016/j.earscirev.2013.08.002.

Trapp, S. E., W. P. Smith and E. A. Flaherty (2017), Diet and food availability of the Virginia northern flying squirrel (Glaucomys sabrinus fuscus): implications for dispersal in a fragmented forest, *Journal of Mammalogy*, 98(6), 1688-1696, doi: 10.1093/jmammal/gyx115.

Troy, A., D. Wang, D. Capen, J. O'Neil-Dunne, S. MacFaden, 2007. Updating the Lake Champlain Basin Land Use Data to Improve Prediction of Phosphorus Loading. Lake Champlain Basin Program Technical Report No. 54.

Turton DJ, Smolen MD, Stebler E. 2009. Effectiveness of BMPS in reducing sediment from unpaved roads in the Stillwater Creek, Oklahoma Watershed1. JAWRA Journal of the American Water Resources Association 45: 1343–1351. DOI:10.1111/j.1752-1688.2009.00367.x.

USGS, 2016, National Water Information System, http://waterdata.usgs.gov/vt/nwis/rt

VT Agency of Natural Resources, 2009, Stream Geomorphic Assessment Protocol Handbooks, Remote Sensing and Field Surveys Techniques for Conducting Watershed and Reach

Level Assessments. Available at: http://www.vtwaterquality.org/rivers/htm/rv_geoassesspro.htm

VTDEC Watershed Management Division, 2012, State of Vermont 2012 Water Quality Integrated Assessment Report, available at: www.waterquality.org

Voli, M., Wehmann, K., Bohnenstiehl, D., Leithold, E., Osburn, C., Polyakov, V.O. (2013), Fingerprinting the sources of suspended sediment delivery to a large municipal drinking water reservoir: Falls Lake, Neuse River, North Carolina, USA, *Journal of Soils and Sediments*, 3, 1692–1707, doi:10.1007/s11368-013-0758-3.

Wallbrink, P.J. and A.S. Murray (1993) Use of fallout radionuclides as indicators of erosion processes. Hydrol Process 7:297–304

Wallbrink PJ, Olley JM, Murray AS, Olive LJ (1996) The contribution of subsoils to sediment yield in the Murrumbidgee River basin, NSW, Australia, IAHS Publication no. 236. IAHS,Wallingford, pp 347–357

Walling DE (1983) Scale Problems in Hydrology The sediment delivery problem. Journal of Hydrology, 65, 209-237.

Walling, D.E. (2013a), The evolution of sediment source fingerprinting investigations in fluvial systems, *J. Soils Sediments*, 1310, 1658-1675.

Walling, D. E. (2013b), Beryllium-7: The Cinderella of fallout radionuclide sediment tracers? Hydrological Processes, 27, 837-844, doi:10.1002/hyp.9546.

Walling, D.E. and J.C. Woodward (1992), Use of radiometric fingerprints to derive information on suspended sediment sources. *In* Erosion and sediment transport monitoring programmes in river basins. Publ. 210. IAHS, Wallingford, UK.

Walling, D. E., Owens, P.N., Leeks, G.J.L., 1999. Fingerprinting suspended sediment sources in the catchment of the River Ouse, Yorkshire, UK. Hydrological Processes 13, 955–975.

Walter, R. and D. Merritts. 2008. Natural streams and the legacy of water-powered milling: Science v. 319, no. 5861, p. 299-304.

Wear LR, Aust WM, Bolding MC, Strahm BD, Dolloff CA. 2013. Effectiveness of best management practices for sediment reduction at operational forest stream crossings. Forest Ecology and Management, 289, 551–561. DOI: http://dx.doi.org/10.1016/j.foreco.2012.10.035

Wemple, B. C., 2013, Assessing the Effects of Unpaved Roads on Lake Champlain Water Quality. LCBP Technical Report No. 74. 67 pp. Available at: http://www.lcbp.org/wp-content/uploads/2013/07/74_Road-Study_revised_June2013.pdf.

Wemple BC, Jones JA, Grant GE (1996), Channel network extension by logging roads in two basins, Western Cascades, Oregon, *Water Resources Bulletin*, 32, 1195–1207.

Wemple, B. C., Clark, G. E., Ross, D. S., & Rizzo, D. M. (2017). Identifying the spatial pattern and importance of hydro-geomorphic drainage impairments on unpaved roads in the northeastern USA. Earth Surface Processes and Landforms, 42(11), 1652–1665, https://doi.org/10.1002/esp.4113

Wethered, A.S., Ralph, T.J., Smith, H.G., Fryirs, K.A., Heijnis, H., 2015. Quantifying fluvial (dis)connectivity in an agricultural catchment using a geomorphic approach and sediment source tracing. J. Soils Sediments. Doi:10.1007/s11368-015-1202-7.

Whalen, T.N., 1998, Post-glacial fluvial terraces in the Winooski Drainage Basin, Vermont. MS Thesis, University of Vermont.

Williams, G. P. (1989), Sediment concentration versus water discharge during single hydrologic events, Journal of Hydrology, 111, 89-106.

Williams, G. P., and Wolman, M.G., 1984. Downstream effects of dams on alluvial rivers. United States Geological Survey Professional Paper. 1286, 83.

Wolman, M. G., and Gerson, R., 1978, Relative scales of time and effectiveness of climate in watershed geomorphology: Earth Surface Processes and Landforms, v. 3, p. 189-208.

Yellen, B., J. D. Woodruff, L. N. Kratz, S. B. Mabee, J. Morrison, and A. M. Martini (2014), Source, conveyance and fate of suspended sediments following Hurricane Irene. New England, USA, *Geomorphology, 226*, 124-134, doi: 10.1016/j.geomorph.2014.07.028.

You, C., T. Lee, Y. Li (1989). The partition of Be between soil and water, *Chemical Geology*, 77, 105–118.

Zhao, X., F. Li, Z. Ai, J. Li and C. Gu (2018), Stable isotope evidences for identifying crop water uptake in a typical winter wheat–summer maize rotation field in the North China Plain, *Science of The Total Environment*, 618, 121-131, doi: 10.1016/j.scitotenv.2017.10.315.

CHAPTER 4. ANALYSIS OF REACH-SCALE SEDIMENT PROCESS DOMAINS IN GLACIALLY-CONDITIONED CATCHMENTS USING SELF-ORGANIZING MAPS

Abstract

Given that limited resources are available to manage erosion hazards and to address water quality impairment along rivers, stakeholders engaged in water resource management would benefit from tools to identify those river reaches most prone to adjustment and which disproportionately load sediment to receiving waters. The extent and rate of vertical and lateral channel adjustments in response to natural and human disturbances have been observed to vary considerably across space and time, and this complexity and nonlinearity introduce challenges for classification or modeling of river reaches using conventional statistical techniques. The Self-Organizing Map (SOM) is a data-driven computational tool with advantages for clustering or classification of multivariate observations and for exploratory data analysis and visualization of complex, nonlinear systems. We applied a SOM to cluster multivariate stream geomorphic assessment data into reach-scale sediment process domains for 193 river reaches in glacially-conditioned catchments of central and southern Vermont based on field- and GIS-derived hydraulic and geomorphic metrics gathered during stream geomorphic assessments. The reaches comprised a range of channel types from confined to unconfined, steep- to shallow-gradient, mid-to-high order, bedrock to alluvial channels. Fifteen variables were identified that meaningfully separated reaches into seven sediment regimes, following a two-stage application – i.e., a Coarse SOM followed by a Fine SOM. Sediment regime classifications are relied upon by the Vermont Agency of Natural Resources to

promote conservation and restoration strategies that reduce fluvial erosion losses to infrastructure, and restore water quality and improve instream and riparian habitats. This classification framework is transferable to other hydroclimate regions, with consideration of additional or alternate independent variables unique to those regions.

Introduction

River reaches undergoing excessive rates of adjustment pose hazards to infrastructure and public safety, and contribute to degraded water quality and compromised instream and riparian habitats. In glacially-conditioned, mountainous areas, rivers are naturally vulnerable to adjustment due to their topographic setting, close coupling of hillslope and channel processes, and reworking of glacial legacy sediments (Church & Ryder, 1972; Ballantyne, 2002). The geologic and glacial history have imparted longitudinal and lateral variations in valley setting and network position, as well as discontinuities in channel form and process (Rice et al., 1998; Toone et al., 2014; Phillips & Desloges, 2014) that influence the dynamics of sediment erosion, transport and deposition (Nanson & Croke, 1992; Fryirs et al., 2007). Human disturbances over the last 250 years have also altered patterns of water and sediment routing through the landscape (Leopold, 1994; Noe & Hupp, 2005; Walter & Merritts, 2008). Recovery times from these perturbations, and in response to extreme floods (Costa & O'Connor, 1995), may extend 100 years or more in humid temperate regions (Wolman and Gerson, 1978).

Water resource managers need tools to identify river reaches most prone to adjustment and which disproportionately load sediment to receiving waters. However, significant challenges exist for classification and prediction, given the complexity of sediment dynamics. Patterns of sediment flux and channel adjustment exhibit high variability across spatial and temporal scales (Walling, 1983; Fryirs, 2013), as a function of both watershed-level and reach-level processes that alter flow and sediment inputs, combined with reach-scale modifiers of stream power and boundary resistance. Many

factors, including the geologic setting, climate and hydrology, vegetation, and land use, combine in nonlinear ways (Benda & Dunne, 1997; Fryirs, 2013) to govern reach-scale adjustments in channel dimensions, profile and planform over time. The present channel form is the manifestation of various channel-floodplain processes occurring over a range of flows (Pickup & Rieger, 1979). Thus, both the spatial and temporal context (Wohl, 2018) are important determinants of the present channel-floodplain form and dominant adjustment process(es) that characterize a given process domain.

Over geologic and historic time frames, river reaches are subjected to natural and human disturbances, or stressors, that operate at both watershed and channel scales to influence the sediment source, transport and deposition conditions of these reaches. The sequence of vertical and lateral channel adjustments in response to natural and human stressors have been described in terms of channel evolution models (Schumm, *et al*., 1984; Simon and Hupp, 1986; Rosgen, 2006), which outline a trajectory of channel change that can be interpreted both in time and space. Common to each of these models is the possibility of a quasi-equilibrium state where the stream power produced by the volume and slope of the water come into balance with the resistance created by the quantity and caliber of the sediment under transport and that is offered by geologic and vegetative boundary conditions (Lane, 1955). Typically, channel evolution models are applied to alluvial or mixed alluvial-bedrock channels in unconfined to partly-confined settings, but they could be extended to include bedrock channels in confined, steep-gradient settings. In this case, the bedrock boundary conditions would be highly-resistant to lateral and vertical adjustment, and channels would be considered stable in response to most stressors in the current tectonic and hydrologic regimes. Bedrock channels would

have ample access to a floodplain; however, the floodplain in these settings may be longitudinally discontinuous or so minimal in extent as to be considered nonexistent (Wohl, 2000).

Channel evolution models most often describe stages of channel response to a single stressor or disturbance. In reality, rivers are integrating a myriad of stressors overlapping in time and space, and may adjust to an external stressor(s) in complex ways based on: the magnitude, intensity and duration of stressor; lag effects; intrinsic and extrinsic thresholds; self-reinforcing or self-limiting feedbacks; and the presence of antecedent conditions or contingencies (Bull, 1979; Chappell, 1983; Phillips, 2003; Toone et al., 2014). Despite these complexities and the uncertainty surrounding causal factors, the present channel-floodplain configuration warrants classification to highlight its sensitivity to change in the current hydrologic regime, and the associated consequences for flood erosion hazard, water quality and ecological integrity. Classification is also useful for estimating a probable trajectory of change in the face of projected increases in magnitude, frequency, and duration of extreme events (Collins, 2009; Guilbert et al., 2014; Guilbert et al., 2015) or additional human-caused watershed and channel disturbances.

Various field assessment techniques have been developed to classify river reaches in terms of their stability or sensitivity to adjustment, following the assumption that dominant adjustment process and degree of stability can be inferred from observations of channel form. (Pfankuch, 1975; Nanson & Croke, 1992; Rosgen, 1996; Montgomery & Buffington, 1997; Raven et al, 1998 [River Habitat Survey]; Brierley & Fryirs, 2005; Rinaldi *et al*., 2013). Insights gained from these assessments have led to the theory that

river networks comprise a longitudinal array of hydrogeomorphic units of relatively uniform composition, structure, and function, or "process domains" that differentially impact sediment connectivity (Montgomery, 1999; Brardonini & Hassan 2007; Lisenby and Fryirs, 2016).

Parametric statistical methods have been employed to examine correlations between dominant adjustment process and various geomorphic metrics, such as total or specific stream power (Bizzi & Lerner, 2013; Parker et al., 2014; Gartner et al., 2015; Lea & Legleiter, 2016; Yochum et al., 2017); valley confinement (Thompson & Croke, 2013; Surian et al., 2016; Ringhini et al., 2017; Weber and Pasternak, 2017); and channel geometry (Buraas et al., 2014). Availability of Geographic Information Systems (GIS) and high-resolution digital elevation models (DEMs) has enabled the development of remotely-sensed metrics to augment field-based assessment. Large, multi-parameter data sets have been examined to consider interactions among a suite of factors governing channel-floodplain form and process. Multivariate statistical techniques have been applied to channel and floodplain metrics for dimension reduction and classification of process domains including k-means, principal components analysis (PCA), discriminant analysis, logistic regression, and regression trees (Flores, 2006; Brardonini & Hassan, 2007; Phillips & Desloges, 2014; Livers & Wohl, 2015). However, these methods are predicated on linear relationships between variables, that often do not well describe geomorphic data. Moreover, their application assumes the data are normally distributed, while data sets of geomorphic variables often do not reliably conform to a Gaussian distribution.

Since multi-dimensional data govern sediment transport regimes in nonlinear and epistatic ways, Phillips (2003) advocated for the application of nonparametric, computational tools suited to nonlinear, complex dynamics. Artificial neural networks (ANNs) are well-suited for nonlinear processes, and handle nonparametric data of varying types (e.g., continuous, ordinal, nominal) and scales. A particular type of ANN, the Self-Organizing Map (SOM), has advantages for clustering or classification of multivariate observations and for exploratory data analysis and visualization (Kohonen, 2013). SOMs have demonstrated superior performance over parametric methods where data contain outliers or exhibit high variance (Mangiameli et al., 1996), and have particular advantages over other methods for data visualization and interpretation (Alvarez-Guerra, et al., 2008). SOMs have been used to classify or cluster multivariate environmental data, including instream species richness (Park et al., 2003), fish community distribution patterns (Stojkovica et al., 2013), lake chemistry data associated with harmful algal blooms (Pearce et al., 2011, 2013), and riverine habitats (Fytilis and Rizzo, 2013). Previous research (Besaw et al, 2009) applied the SOM to reach-based geomorphic assessment data to classify reach-level sensitivity, but the authors are not aware of research that has applied this nonparametric clustering tool to identify reach-based sediment regime.

In this work, we use SOMs to characterize and predict spatial variation in bedload erosion/deposition and fine-sediment export from glacially-conditioned catchments. The research objectives are to: (1) replicate an existing reach-scale classification system for fluvial process domains (Kline, 2010) using a non-parametric, clustering algorithm with a goal to refine the classification; and (2) assess and identify field- and GIS-derived

hydraulic and geomorphic metrics for prediction of the sediment regime; and (3) characterize the between-reach differences in net erosion or net deposition.

Study Area

Our study comprises 193 river reaches located in six catchments dispersed across the state of Vermont in the Lake Champlain, Connecticut River and Hudson River drainage basins (Figure 4.1). These rivers were chosen to represent a mix of biogeophysical regions (Stewart and MacClintock, 1969), and comprise relatively undeveloped drainages (≤ 5.3%; Table 4.S1). This previously-glaciated landscape consists of a mix of deposits ranging from Pleistocene glacial tills, glaciofluvial, and glaciolacustrine sediments and Holocene alluvial fans and stream terraces (Stewart and MacClintock, 1969). Generally, bedrock channels in the headwaters grade to mixed bedrock-alluvial and alluvial channels in the lowlands. However, longitudinal profiles can be complex and reflect discontinuities imparted by vertical and lateral bedrock controls and the downstream sequencing of glacial landforms. Historically, European settlement and the associated deforestation (Foster & Aber, 2004) generated high sediment yields from denuded hillslopes, leading to renewed aggradation in many alluvial reaches (Bierman et al, 1997; Brakenridge, et al., 1988). Subsequent reforestation has reduced sediment yields, contributing to channel incision and widening (Bierman, 2010, Schumm & Rea, 1995). Channelization, berming, armoring, and diversion of rivers during development, has locally disconnected river channels from the adjacent floodplain (Poff et al., 1997; Kline & Cahoon, 2010). Dams operated at bedrock knick-points in the headwaters to power local mills (Thompson & Sorenson, 2000); however, these small impoundments were typically breached during flood events of the 19th and 20th century.

At present, four dams remain on the studied reaches, but have limited impoundments and operate in run-of-river mode. Thus, hydrologic connectivity is maintained, but these grade controls may represent a sediment transport discontinuity to varying degrees. A substantial flood control dam operates within the Black River (basin 6 in Figure 4.1); however, studied reaches are more than 5.6 km upstream of this reservoir.

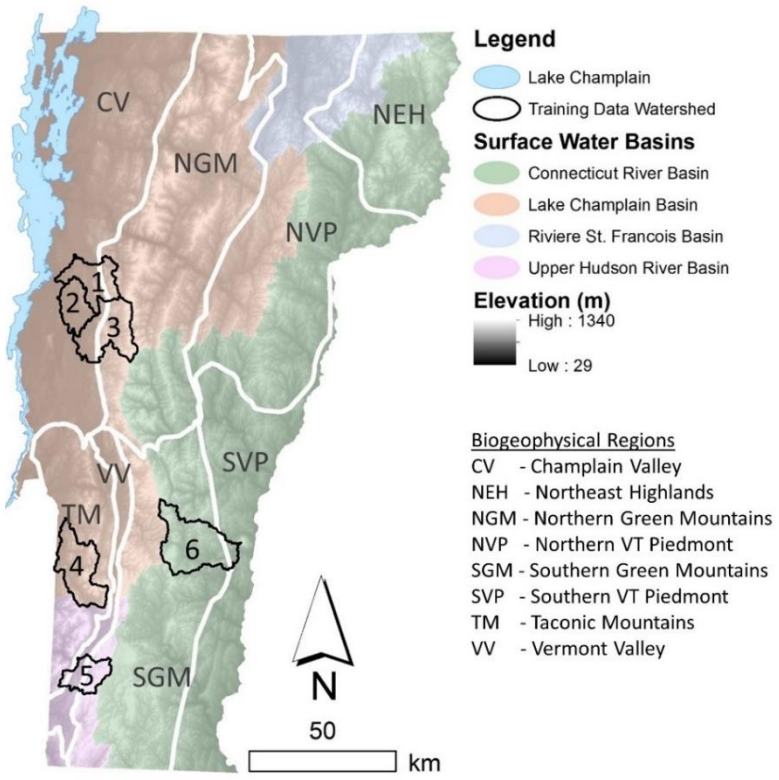

Figure 4.1. Location of study area watersheds across surface water basins and biogeophysical regions in Vermont. Watershed numbers are keyed to Supplementary Table 4.S1.

A humid temperate climate characterizes the region, with mean annual precipitation ranging from over 1,270 mm along the north-south trending spine of the Green Mountains to a low of 813 mm in the Champlain Valley (Randall, 1966). Spring and fall rains are common, and saturation-excess overland flow conditions dominate during these months, leading to variable hydrologic source areas (Dunne and Black,

1970). A majority of the total annual flow in the studied rivers occurs from ice-out to late spring in a typical year, due to the occurrence of spring rains falling on saturated or frozen ground, melting of the snow pack stored in higher elevations, and low evapotranspiration rates prior to leafing of deciduous vegetation (Shanley and Denner, 1999). The peak annual flow (1 to 1.5-year recurrence interval) most often occurs during the spring months, although occasionally in the fall or summer (USGS, 2018).

Methods

This research followed a mutli-phased approach consisting of: (1) geomorphic assessments to gather geomorphic and hydraulic variables; (2) assignment of sediment regime classification; (3) exploratory data analysis; and (4) the application of clustering algorithms to replicate and refine sediment regime classifications.

Assessment of geomorphic condition

Reach-scale geomorphic and hydraulic data were compiled from existing remote-sensing resources and field-based assessment for 193 river reaches in six catchments (Figure 4.1). Stream geomorphic assessments (SGAs) were conducted following protocols (Kline et al., 2009) developed by the Vermont Agency of Natural Resources (VTANR) relying on several resources (Wolman, 1954; Pfankuch, 1975; Nanson & Croke, 1992; Harrelson, et al., 1994; Rosgen, 1996; Montgomery & Buffington, 1997; Knighton, 1998). These quality-assured and peer-reviewed (Besaw *et al*., 2009; Somerville and Pruitt, 2004) protocols have been developed and applied to classify river reaches in terms of their dominant adjustment process, stage of channel evolution, and sensitivity to future adjustment (Kline *et al.,* 2009). Reaches are defined as lengths of channel of consistent confinement ratio (confined, semiconfined or unconfined) within

which other channel parameters (slope, sinuosity, and bedform) are generally more, rather than less, similar – a reach definition conforming to that employed by others (Brierly and Fryirs, 2005; Frissel *et al*., 1996; Rinaldi *et al*., 2013; Surian et al., 2016). Following initial identification through desk-top assessment of topographic resources, reach delineations were confirmed through direct observation, where sub-reaches of alternate slope or valley confinement may not have been apparent at the typical scale (1:24000) of remote-sensing resources. In some cases, field assessment also defined sub-reaches marked by discontinuities (e.g., bedrock grade controls or impoundments) or which demonstrated distinct differences in dominant substrate material or adjustment process (Kline et al., 2009). For clarity of presentation, these sub-reaches are simply referred to as reaches in this work. Various geomorphic and hydraulic metrics were compiled for each reach (including List A in Table 4.1) using a combination of remote-sensing and field-based assessment (see supplementary materials). Based on this information, each reach was classified by stream type (Montgomery & Buffington, 1997; Rosgen, 1996), dominant adjustment process (degradation, aggradation, widening, planform adjustment), and channel evolution model and stage (Schumm et al., 1984).

To supplement metrics gathered during geomorphic assessments, additional variables were derived for this study to evaluate their effectiveness to describe sediment regimes and cluster reaches of similar character (Supplementary text S1). Various estimates of stream power (Parker *et al.*, 2011; Parker *et al.*, 2014) and tractive force (Andrews, 1983; Ferguson, 2005) were computed relying on regional hydraulic geometry relationships (Jaquith & Kline, 2001; Jaquith & Kline, 2006) and pebble-count data from field assessment, to provide an indication of the capacity for sediment transport.

Table 4.1. Geomorphologic and hydraulic variables used to classify sediment regime.

A	B	C	Variable	Description	Units	Transformation
✓	✓	✓	Slope, S	Channel slope	[%]	† Log S
✓	✓		Valley Confinement, VC	Valley width / bankfull width	[-]	† Log VC
✓	✓	✓	Incision Ratio, IR	Low-bank height / bankfull channel height	[-]	‡ Log IR
✓	✓		Entrenchment Ratio, ER	Floodprone width / bankfull width	[-]	‡ Log ER
✓	✓	✓	Width $_{bkfl}$ to Depth $_{mn}$ ratio, W/D	Bankfull width / mean bankfull depth	[-]	‡ Log W/D
✓	✓	✓	Median grain size diameter, D50	Median grain size diameter from riffle or step pebble count, i.e., 50th percentile of the grain size distribution	[mm]	‡ $\sqrt{D50}$
✓	✓	✓	Percent Armoring, pArm	Length armoring normalized to reach length	[%]	‡ Arcsin(sqrt (pArm))
✓	✓		# Depositional Bars, nBars	Number of deposition bars normalized to reach length	[#/km]	‡ $\sqrt{nBars}$
✓	✓	✓	# Flood Chutes, nFCs	The number of flood chutes normalized to reach length	[#/km]	‡ $\sqrt{nFCs}$
	✓		Valley Confinement Ratio, VC rat	VC of subject reach / VC of upstream reach	[-]	† Log VCrat
	✓	✓	Grain Size Distribution, D84-D16	Range of two standard deviations around the median, computed as the 84th percentile minus the 16th percentile of the grain size distribution	[mm]	‡ Log D84-D16
	✓	✓	Specific Stream Power, SSP	Unit bed area steam power	[W m^{-2}]	‡ Log SSP
	✓		SSP Balance, SSP bal	SSP of subject reach / SSP of upstream reach	[-]	‡ Log SSP bal
		✓	Width ratio, Wrat	Regime bankfull width/ measured bankfull depth	[-]	‡ Wrat
		✓	Mean Depth ratio, Drat	Regime mean bankfull depth / measured mean bankfull depth	[-]	‡ Drat

† Normal distribution confirmed by Shapiro-Wilks test at α = 0.05; ‡ Nortmal distribution confirmed by histogram/normal quantile plot
List A variables used to assign sediment regime following criteria in Table 4.1; List B were inputs to the Coarse SOM (n=193);
List C were inputs to the Fine SOM (n=154).

Table 4.2. Geomorphic characteristics of sediment regime classes.
Class abbreviations are described in the text

Class	TR	CST	UST	FSTCD	CEFD	DEP
Color key						
Valley Confinement	< 6	< 6	≥ 4	≥ 4	≥ 4	≥ 6
Slope	> 2 %	> 2%	< 4%	< 2%	< 2%	< 2%
Incision Ratio	< 1.3	≥ 1.3	≥ 1.3	≥ 1.3	< 1.3	< 1.3
Entrenchment Ratio	< 1.4 1.4–2.2 (B)	> 2.2	> 2.2 1.4–2.2 (B)	> 2.2 1.4–2.2 (B)	> 2.2	> 2.2
Width/Depth Ratio	< 12 (A, G) > 12 (B, F)	< 12 (A, G) > 12 (B, F)	< 30 < 12 (E)	> 30 > 12 (E); > 40 (D)	< 30 <12 (E); < 40 (D)	> 30 (> 40, alluvial fan)
Common Channel Evolution Stage	I, V	II, III, IV	II, III	II, III, IV	I, V	
Rosgen (1996) Stream Type	A, B, G, F	A, B	G, F, B, E, C, Bc	E, C, Bc, F, D	C, E, D	C, D
D50	bedrock, boulder, cobble, (occas. gravel)	cobble, gravel, sand	cobble, gravel, sand	cobble, gravel, sand	cobble, gravel, sand, silt	cobble, gravel, sand, silt (occas. boulder)
Common Bedforms	cascade, step-pool	cascade, step-pool, plane bed	cobble/ gravel step-pool, plane bed, riffle-pool	gravel riffle-pool	gravel riffle-pool, sand/silt dune-ripple	gravel/ cobble/ boulder-braided
Planform	single-thread linear to sinuous imparted by bedrock structure	single-thread linear to sinuous imparted by bedrock or encroachments	single-thread	single-thread meandering, localized bifurcations	single-thread, meandering	multiple-thread, braided
Type	bedrock	mixed	mixed	alluvial	alluvial	alluvial

Assignment of sediment regime class

We then assigned one of six sediment regime classes to each study reach to describe the present regime for coarse and fine (<63 um) fluvial sediment (Kline, 2010) based on a combination of geomorphic metrics and observations (Table 4.2). The sediment regime classes lie on a continuum from supply-limited to transport-limited (Montgomery & Buffington, 1997) and classification focuses on sediment process domains operating at a temporal scale of 1 to 2 years, since metrics used as classification variables include dimensions (e.g., width, depth) relative to the bankfull stage, defined as the discharge with an approximate recurrence interval of 1.5 years, or $Q_{1.5}$ (Leopold, 1994).

This classification scheme (Figure 4.2) considers both the vertical and lateral dimensions of sediment (dis)connectivity in the context of varying degrees of channel confinement by valley walls (hillslope-channel coupling in narrowly-confined to semi-confined settings) and the vertical-lateral connectivity to floodplain (floodplain-channel coupling in unconfined settings). Three of the six sediment regimes describe channels that are vertically stable – i.e., not degraded appreciably below their floodplain (IR < 1.3), although the floodplain itself may be quite limited in areal extent (Figure 4.2a), while the other three classes are vertically-disconnected from the floodplain (IR ≥ 1.3) (Figure 4.2b).

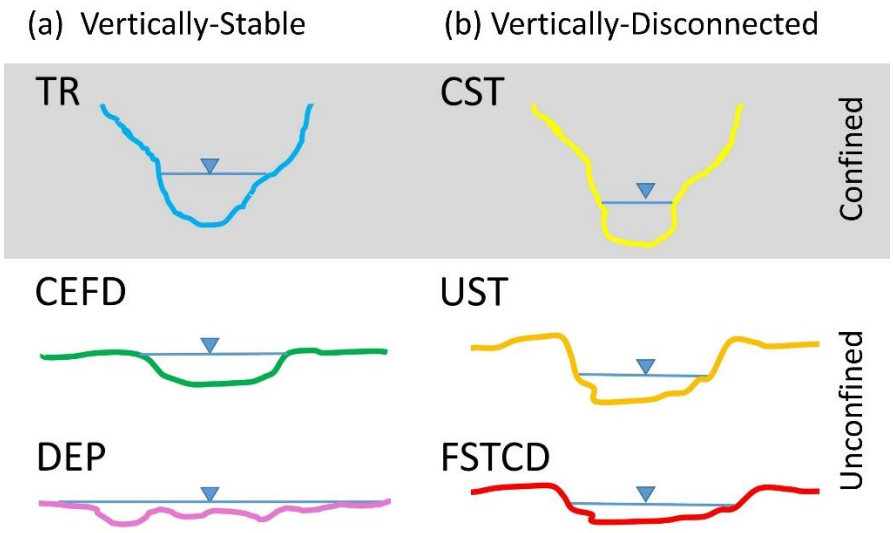

Figure 4.2. Schematic of typical cross section for six sediment regime classes. Class abbreviations are described in the text. Color scheme corresponds to Table 4.2.

In order from minor to major degree of lateral adjustment, representing bedrock-dominated to alluvial channel types, the three vertically-stable regime types (Figure 4.2a) include:

- Transport (TR) reaches are narrowly to semi-confined by their valley walls (VC < 6) and are supply-limited due to the boundaries and the relatively steep gradient (>2%). TR reaches are not considered a significant source of coarse and fine sediments (supply-limited) due to the high erosion resistance offered by channel boundaries typically composed of bedrock. Planform is controlled by the underlying bedrock structure, and floodplain areas for sediment storage are typically limited and discontinuous in areal extent (Wohl, 2000).

- Coarse Equilibrium and Fine Deposition (CEFD) reaches comprise alluvial self-formed (fully mobile) channels located in unconfined valley settings with low- to moderate-gradient (<2%; riffle-pool and dune-ripple bedforms, occasionally plane

bed). These channels are not incised (IR <1.3) and therefore deposit fine sediments (suspended load) in their floodplains during floods of ≥ 2- 5-year RI. A coarse-sediment quasi-equilibrium condition is inferred from the maintenance of no net change in meander belt width, profile and average channel dimensions over time.

- Deposition (DEP) reaches are relatively uncommon, but significant for their implications to erosion hazards. These reaches are often located at a sharp transition in valley confinement, from confined to unconfined, accompanied by a relaxation in gradient that can be expected to reduce stream competence. They are generally unconfined by valley walls, but may have moderate to steep slopes (2% to 6%) – e.g., Rosgen Ca or Cb stream types. Due to the relaxed valley confinement, these settings are expected to represent locations of increased deposition and lateral migration.

The remaining three categories (Table 4.2, Figure 4.2b) represent channel reaches that exhibit a moderate to major degree of floodplain disconnection (IR ≥ 1.3), resulting from either natural or human-induced conditions, or both. Consequently, the channel has become entrenched below an abandoned floodplain or terrace of glacial origin. Presented in order of increasing degree of lateral adjustment:

- Confined Source and Transport (CST) reaches exist in semi-confined to confined settings of moderate to steep gradient with more erosion-prone boundary conditions than TR reaches.

- Unconfined Source and Transport (UST) reaches occupy partly confined to unconfined valley settings of moderate to low gradient (< 4%) and are characterized by a moderate to high degree of vertical separation from the floodplain (1.5 < IR < 4). By virtue of this incision, the sediment regime has shifted from a deposition-dominated condition to a transport-dominated condition (channel evolution stage II or early III). Width/depth ratios are generally low but variable.

- Fine Source and Transport & Coarse Deposition (FSTCD) reaches are located in unconfined valley settings of low gradient (<2%) and are moderately to substantially incised (IR > 1.3). They are dominated by lateral adjustment processes including widening, planform adjustment accompanied by aggradation, typically in channel evolution stage III or IV.

Pre-processing input data for SOM training

The reach-scale geomorphic and hydraulic metrics (Table 4.S2) were then explored using conventional statistical methods (e.g., Pearson or Spearman Rank correlations and Principal Components Analysis [PCA]) to remove redundant variables (e.g., D84/D50 was closely correlated to SSP/D50) and select the subset of variables that would become inputs to the SOM (Lists B and C in Table 4.1). Additionally, transformed variables were examined to discern which variables had statistical power to differentiate between expert-assigned sediment regime classes using One-way Analysis of Variance (ANOVA) followed by Tukey Honest Significant Differences (HSD) tests between individual group means. For those variables (or their transformations) that were

not normally distributed, nonparametric methods were applied (Kruskal-Wallis). Data were also examined to help determine the appropriate SOM lattice configuration and size. A PCA was run on transformed variables, following the heuristic of Cereghino and Park (2009) that the optimal lattice column-to-row ratio approximates the ratio of the first two principal components. Statistical tests were performed in JMP (v. 12.0, SAS Institute, Cary, North Carolina).

Clustering algorithm

We used an unsupervised machine-learning algorithm – a Self-Organizing Map (SOM; Kohonen, 1990) - to cluster our reaches; the data set has *p* observations of *n* independent variables. The "unsupervised" descriptor means that data were presented to the clustering algorithm without their expert-assigned sediment regime classifications, and without a predetermined number of clusters (i.e., sediment regime classes) specified as an outcome. Like conventional clustering techniques that are also data-driven (e.g., k-means) and unsupervised (e.g., hierarchical clustering), the SOM will aggregate *p* observations into *k* groups, each with internally similar values for the *n* independent variables. However, certain features unique to the SOM technique (described below) ensure that this clustering proceeds in a manner that is more robust to outliers, non-continuous data types, and data that are not normally distributed (the latter two conditions being underlying assumptions of traditional clustering techniques). Similar to traditional methods such as PCA, regression trees, and logistic regression, the SOM is useful for reducing the dimensionality of data and for selecting variables that strongly influence clustering or classification (i.e., feature selection). Yet, the SOM has advantages over

these traditional methods for exploratory data analysis and visualization (Eshgi et al., 2011).

The SOM reduces a multidimensional data space into to a lower-dimension space. Typically, data are projected to a 2-D plane, or lattice, having a number of individual nodes, also called a feature map or a Kohonen map (Kohonen, 2013). The outcome of a converged lattice is such that observations introduced to the SOM self-organize into "a kind of similarity diagram" (Kohonen, 2013) where similar observations map to a similar location on the lattice/map. Each of the independent variables may also be viewed on the converged lattice in what is known as a "component plane" where values of each component, or variable, can be observed to vary monotonically.

Typically, input data to the SOM are normalized so that select variables of high magnitude do not overly dominate the clustering process. Our variables were each range-normalized to a value between 0 and 1 before beginning SOM training (Alvarez-Guerra et al., 2008):

$$norm(x_i) = \frac{(x_i - \min(x_i))}{(\max(x_i) - \min(x_i))}.$$

A hexagonal lattice topology (Figure 4.3) was selected, given the potential for conditional bias between input variables (Kohonen, 2001). At the initial state of the lattice, each node is assigned a vector, **m**, of random values (i.e., weights) ranging from 0 to 1; the vector length is equal to the number of input variables, *n*. One of the *p* observations is then selected at random from the data set, and its vector **X** of *n* variables $\{X_{p,1}, X_{p,2}, X_{p,3}, \ldots X_{p,n}\}$ is presented to the vector of weight values $\{m_{y,1}, m_{y,2}, m_{y,3}, m_{y,4}, \ldots m_{y,n}\}$ in each lattice node, y. The distance, or dissimilarity, between the

observation vector and each weight vector for each lattice node (y_1, y_2,… y_y) is computed. Euclidean distance is commonly used (Kohonen, 2013), and was also used in this study. The SOM works through a competitive ("winner-takes-all") algorithm, to ensure that the node whose weight vector is most similar to the observation vector is selected. This Best Matching Unit (BMU), along with a user-defined neighborhood of nodes (N_c) around the BMU, are made more similar to the input vector by incrementally adjusting the weights. This user-defined neighborhood of nodes is one of the features that distinguishes the SOM from other more common methods of clustering, such as k-means (which updates weights of a single node, only).

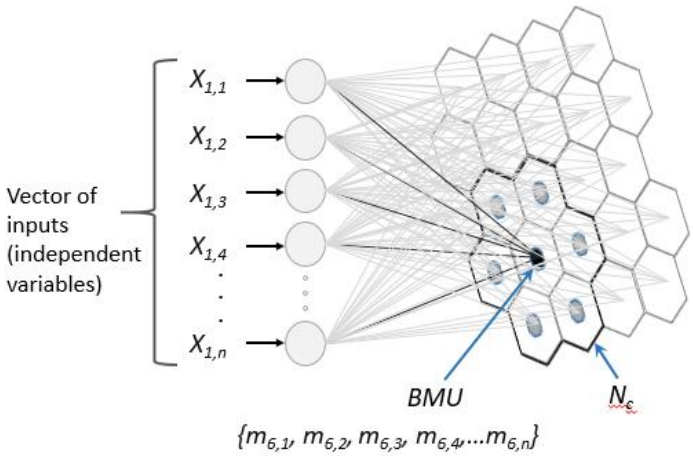

Figure 4.3. Architecture of Self-Organizing Map illustrating the competitive algorithm. Weights of the best matching unit (BMU) and lattice nodes within a user-specified neighborhood (N_c) surrounding the BMU are updated to make them more similar to values of the input vector.

The weights of the BMU and neighborhood units are adjusted gradually by a distance that amounts to a small fraction of the total distance between the input vector and each weight vector. This fractional distance is applied in accordance with a user-specified learning rate parameter. A next observation vector is then selected at random from the data set and compared to the weight vectors of each lattice node; a BMU is

identified, and its weights and that of its neighbor nodes are adjusted, as the process is repeated in each successive iteration. Commonly, both the size of the updating neighborhood and the learning rate are decreased linearly with progressive iterations, moving from a coarse to fine tuning process. As multiple iterations are executed, the lattice weights are adjusted by smaller and smaller amounts, and the algorithm converges (self-organizes). At convergence, the adjusted weight vectors will closely reflect the input vectors and will be monotonically arranged across the lattice such that similar stream reach observations are aggregated together. The distance (or dissimilarity) between weight vectors at convergence is then examined to define clusters of nodes containing similar weights. Several methods are possible to define clusters of the converged weights; often hierarchical clustering is used (Vesanto and Alhoniemi, 2000) as was the case in this study.

SOM computation, training and cluster validation

The above algorithm was implemented in R applying the "kohonen" package (*Wehrens and Buydens*, 2007, v. 3.0.2 released 2017). SOM training was performed in 900 iterations. The learning rate was set initially at 0.05 and decreased linearly to 0.01. The neighborhood size decreased linearly from a radius encompassing two-thirds of the lattice, to a value of 0 at one-third of the iterations - at which point, the algorithm was only updating the BMU (analogous to k-means clustering).

For a given data set, several multi-iteration SOM runs were performed utilizing lattices with varying configurations and numbers of nodes. Column-to-row configurations were chosen to closely approximate the ratio of the first two principal components of the transformed variables (Cereghino and Park, 2009). As an additional

constraint, the final grid size (*y* nodes) approximated a value of $5\sqrt{y}$ following the heuristic of Vesanto et al. (2000), yet did not exceed the number of input variables. For each converged lattice configuration, clusters of similar weights were identified using hierarchical clustering specifying *k* groups, where $k = \{3, 4, \ldots 8\}$. We identified the "optimal" number of clusters for a given input data set by quantifying between-cluster variance (or cluster separation) and within-cluster variance (or compactness of clusters), to maximize a nonparametric F statistic (Anderson, 2001), computed as the ratio of between-cluster to within-cluster variance. At the same time quantization error (QE) was minimized to identify the number and configuration of lattice nodes with best resolution (Kohonen, 2001), achieving a local minimization of QE (Cereghino and Park, 2009). Cluster validation was evaluated using the nonparametric F statistic (*Anderson*, 2001) aided by the "adonis" function in the "vegan" package in R (*Oksanen et al*., 2017).

Clusters were also examined *post hoc* to better understand variables driving the clustering. For each input variable, the intra-cluster mean (on a normalized scale) was plotted against the overall mean, and the magnitude and direction relative to the overall mean were examined. For select clusters with sufficient member numbers, we compared the means of (transformed) reach variables by cluster using one-way ANOVA/Tukey HSD methods on transformed variables in JMP. Several data sets (i.e., lists of geomorphic and hydraulic variables) were run through the SOM to arrive at a parsimonious list of input variables.

Results

Geomorphic condition

Geomorphic assessment data were finalized for 193 reaches assessed between 2004 and 2011 along confined to unconfined, steep- to shallow-gradient, mid-to-high order channels that ranged from bedrock to alluvial in nature (Table 4.3; Supplemental Table 4.Sx). Not included in assessments were those reaches in which fluvial processes were affected by impoundments (artificial or beaver-constructed) or wetland conditions. Study reaches ranged in elevation from 29 to 573 meters above sea level. Drainage areas to the studied reaches ranged in size from 0.93 to 302 km^2 and represented varying physiographic regions (Fig. 4.1) and land cover / land use conditions, although all catchments were reasonably undeveloped (< 6%; Tab. 4.Sx). Bedforms most commonly encountered included step pool, plane bed, riffle pool and dune ripple (Figure 4.4a).

Table 4.3. Characteristics of study area reaches.

	Elevation (m)	Length (m)	Drainage Area (km^2)	Slope (%)	Valley Confinement (ratio)	D50 (mm)
Min	29	95	0.93	0.03	1.1	0.06
Max	573	4,724	302	10.7	104	303
Mean	203	997	83.5	1.5	11.5	75

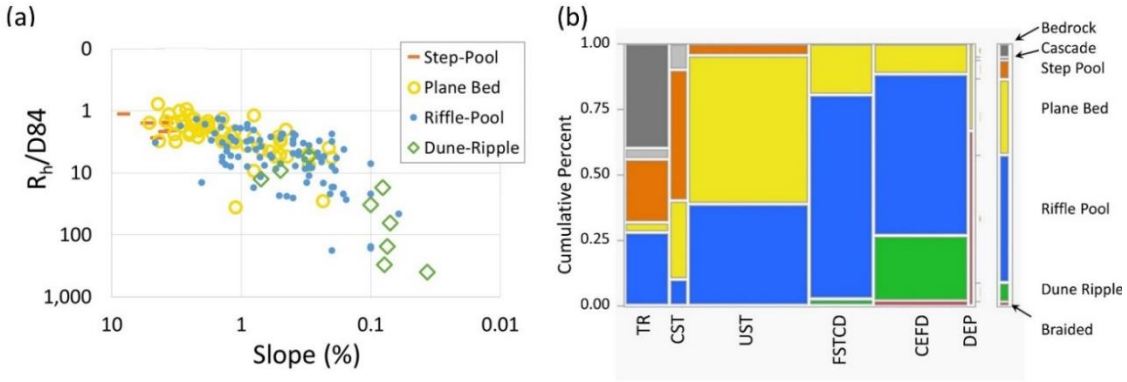

Figure 4.4. Distribution of bedforms by: (a) slope – relative roughness plot; and (b) sediment regime class (n=193). Braided and cascade bedforms omitted from panel a.

Sediment regime classification

Sediment regimes assigned to the 193 study reaches included representatives from each of the six categories (Fig. 4.4b, Tab. 4.Sx). Classifications generally conformed to VTANR guidance (Table 4.2), but included some variation illustrating the fuzziness of these classifications, particularly where classification rules conflict. Thirty-five of the assessed reaches were in confined settings (TR, CST), while the remaining reaches (158; 82%) were in naturally-unconfined settings. Drainage area, reach length, and elevation did not vary considerably between classes (Fig. 4.S1-a, b, c), although CST reaches tended to be located in headwater reaches characterized by smaller drainage areas and higher elevation. The DEP class had a small sample size in the studied reaches (n=3; 1.6%), and this is a typical representation for this class, at least in Vermont. One DEP reach was located at the transition from a 4th-order channel to a downstream reservoir delta; the remaining two reaches were located in alluvial fan settings. Sediment deposition at these alluvial fan locations was probably much more active in earlier post-glacial environments (1,000s of years before present), under more intense hydrologic and sediment regimes, just after glaciation and prior to vegetation of the landscape. These locations may also have seen renewed sedimentation and lateral adjustments during widespread deforestation of upland slopes in the 1800s (Bierman *et al*, 1997).

The TR and CST classes had valley confinement (VC) values below 6 (Fig. 4.S1-d), consistent with their confined status, while the remaining classes had VC values generally >6. Some exceptions were noted for UST and FSTCD reaches where human encroachments (e.g., road embankments, berms) were driving lower-than-expected VC for these reaches in unconfined settings. The VC ratio (subject reach to upstream reach

VC) was generally above 1 for the unconfined classes, reflecting the prevalence of increasing valley and channel widths with downstream distance in a river network (Schumm, 1984). However, some reaches had values below 1, indicative of longitudinal variability and discontinuities imparted by bedrock and glacial deposits. The laterally-confined TR and CST reaches generally had lower VC values than their upstream reach, reflecting the co-location of these sediment regimes with local valley pinch points. The confined reaches (TR, CST) were generally found in steeper settings (> 2%); however, a few reaches of gradient < 2% were classified in either TR (12 of 25) or CST (2 of 10) where bedrock boundary conditions controlled the valley confinement. In a longitudinal context, bedrock reaches are recognized for their role as vertical grade controls, or points of fixed elevation in the overall river network (over recent geologic history).

The CST, UST, FSTCD, and CEFD classes exhibited a wide range of D50 values centered in the cobble- to gravel-dominated categories, with mean D50 decreasing across these four sediment regimes (Fig. 4.S1-h). CST and FSTCD categories each had some reaches with a boulder-sized D50 value, due to the influence of artificial armoring materials or natural glacial outwash materials and erratics. As expected, D50 was positively correlated to slope (ρ = 0.599) and to SSP (ρ = 0.771), and negatively correlated to VC (ρ = -0.461; transformed variables, $p < 0.05$), reflecting the general trend of decreasing sediment caliber with downstream distance in catchments. The mean differential between D84 and D16 sediment sizes (Fig. 4.S1-i) was significantly lower for CEFD reaches than for CST, UST, and FSTCD reaches (ANOVA/Tukey HSD on log-transformed values, $p<0.001$), indicating the prevalence of well-graded, fine-grained bed sediments (silt, sand and fine gravel) in many of the CEFD reaches.

The distribution of Incision Ratio (IR) values across sediment regime classes (Fig. 4.5a) showed strong conformance to the VTANR guidance (Table 4.2). TR, CEFD and DEP reaches had IR values < 1.3 and the remaining classes had IR ≥ 1.3, signifying a degree of vertical separation from the floodplain (statistically-significant differences between class means, ANOVA/Tukey HSD on log-transformed variables, $p<0.001$). The timescale of degradation processes resulting in loss of floodplain connection may be highly variable. The assessment protocols do not include a determination of timing beyond a subjective classification of active, historic or post-glacial; to do so would require surficial geologic investigation beyond the scope of a rapid stream geomorphic assessment. Degradation may have resulted from direct manipulation of the channel such as straightening, windrowing, selective removal of large boulders and woody debris, gravel mining, armoring, or berming, often implemented to achieve land drainage or during flood recovery efforts to protect nearby infrastructure (Kline and Cahoon, 2010). Incision may also have happened in response to processes or conditions in adjacent reaches (e.g., sediment-starved conditions downstream of historic mill dams or flood control dams (Magilligan et al., 2008); upstream knick-point migration from a modified or dam-breach reach; tributary rejuvenation) or as a result of more dispersed disturbances operating at catchment scales (e.g., increased runoff due to urbanization, deforestation, or climate change) (Booth, 1990). For several reaches, we inferred a complex history of degradation, with active or historic incision overprinted on post-glacial incision.

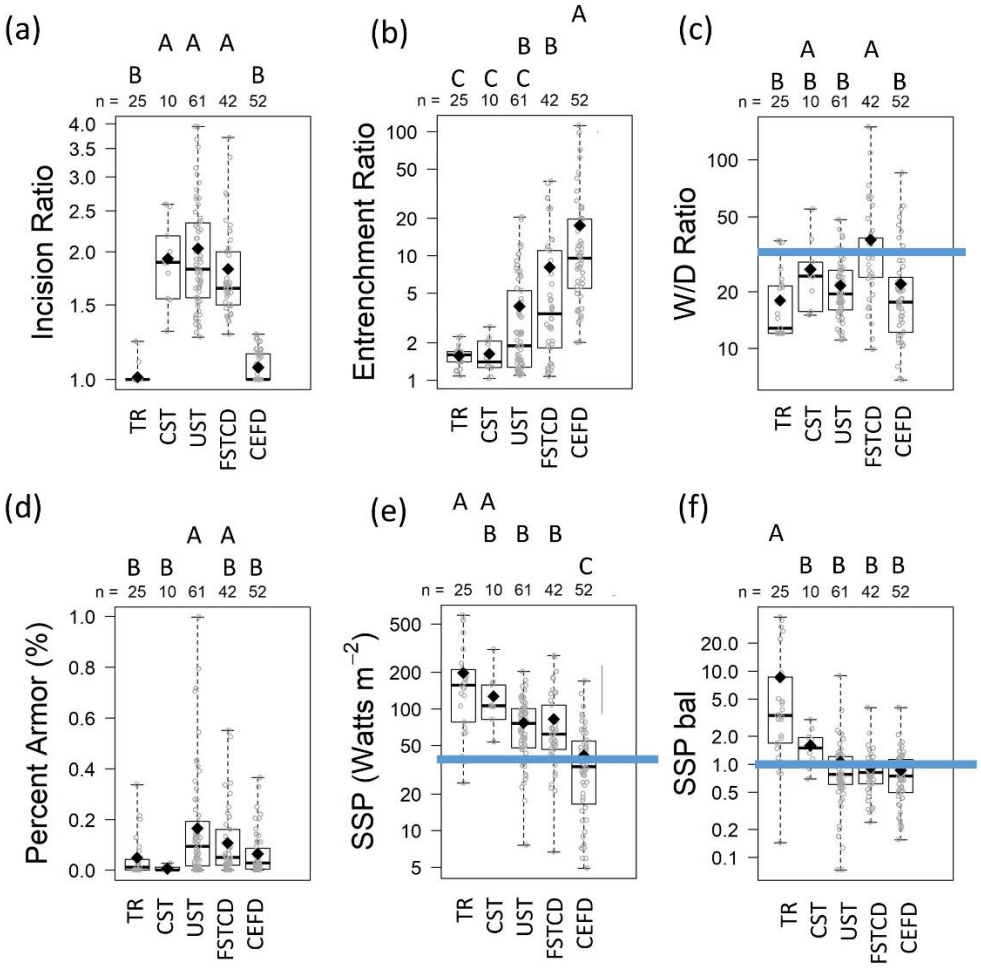

Figure 4.5. Box plots displaying range and central tendency of geomorphic and hydraulic variables by assigned sediment regime class. Solid, black horizontal line depicts median value; diamond symbol depicts arithmetic mean of non-transformed values. Blue horizontal lines depict threshold values discussed in the text. Unique letters indicate statistically-significant differences between class means by ANOVA/Tukey HSD on transformed variables.

Consistent with their naturally-confined status, TR and CST reaches had a low Entrenchment Ratio (ER; Fig. 4.5b), below a value of 2.7. This generally conformed to VTANR guidance (<2.2 +/- 0.2), and in the case of CST reaches existed despite a degree of incision (up to a maximum of IR =2.6). Due to the negligible floodplain and steep slopes of TR and CST reaches, we infer both fine and coarse sediment fractions are

exported through these reaches. Elevated values of SSP (Fig. 4.5e) would support this interpretation, although it would take a flood event greater in magnitude than the Q1.5 to exceed the critical SSP required to mobilize the D85 particles or larger, as suggested by the SSPcr ratio (Fig. 4.SXu). Where channel boundaries are less erosion-resistant (CST reaches), close-coupling to hillslopes can lead to lateral inputs of sediment during higher-magnitude flows when erosion at the toe of the slopes induces mass wasting from the valley wall or terraces positioned well above the active channel (Dethier, et al, 2016). Depending on the nature of the hillslope parent material (commonly glacial till, glaciolacustrine or outwash), imported sediment can range in particle size from very fine silt and clays to coarse boulders. The ten CST reaches assessed in this study were found in headwater settings where forest cover dominated the riparian area, and trees heights were comparable to channel widths (on the order of 1 to 10 m). LWD recruitment and presence of debris jams were observed coincident with localized widening and flood chute development creating discontinuous, narrow pockets of flood plain. Channel-spanning debris jams induced localized sediment aggradation where the valley confinement and gradient otherwise govern net supply-limited conditions at the reach-wide scale. Generally, artificial armoring was relatively sparse on the ten CST reaches assessed during this study (Fig. 4.5d).

Reaches in the unconfined classes had elevated ERs (generally, >2.2), except for those reaches in the UST and FSTCD classes where degradation had led to vertical disconnection from the floodplain to a degree that had depressed the ER (to values as low as 1.1). VTANR guidance anticipates that a high degree of incision will lead to lower-than-expected ER values in unconfined settings, and allows for low ER values in UST

classifications. But an ER<2.2 would represent an outlier status for FSTCD, except for Rosgen Bc reaches. Due to the reduced floodplain access and enhanced velocities of the incised and entrenched cross section of UST reaches, we infer both fine and coarse sediment fractions are exported through these reaches. The SSP values presented in Figure 4.5e and 4.5f are generated from regional hydraulic geometry relationships and would not necessarily reflect the influence on SSP of stressor-induced cross section modifications. Various channel-boundary conditions provided erosion resistance that has likely moderated the degree of lateral adjustment, including natural features (e.g., presence of woody riparian buffers, cohesive channel bed and bank sediments, lateral exposures of bedrock) or human-constructed features (e.g., bank armoring or road encroachments).

FSTCD reaches had a statistically-significant, higher mean value of Width-to-Depth (W/D) ratio (Fig. 4.5c) than UST or CEFD reaches (ANOVA/Tukey HSD on log-transformed values, $p<0.001$). Mean W/D values for vertically-disconnected UST and CST reaches were not significantly different from that of vertically-stable CEFD reaches ($p>0.10$), likely due to the presence of natural (e.g., bedrock, glacial terraces, mature woody vegetation) or constructed features (e.g., road embankments) that would be expected to limit lateral adjustments. VTANR guidance suggests a threshold of W/D = 30 to distinguish FSTCD reaches from the other two classes (Table 4.2). Interquartile ranges of the UST and CEFD classes were each below a value of 30, while the median value for FSTCD reaches was equivalent to 30 (Fig. 4.5c). However, approximately half of the FSTCD reaches had recorded W/D values below this value. This outcome likely reflects the lumping of disparate stream types within this class (e.g., Rosgen E channel,

commonly with W/D < 12). A threshold value of W/D = 30 may be sufficient to describe a departure from a CEFD to FSTCD regime for a gravel-to cobble-bedded channel that has a reference channel configuration of W/D >12 (e.g., Rosgen C channel). However, it may be too high a threshold for a highly-sinuous, sand- to silt-dominated channel (e.g., Rosgen E channel) characterized by a lower reference condition for W/D (i.e, <12).

Percent armoring (Fig. 4.5d) was highest in the UST reaches, and this class mean was significantly different (ANOVA/Tukey HSD on arcsin-transformed values, $p<0.01$) from the mean value for CEFD reaches. However, percent armoring was not particularly helpful in discerning between UST and FSTCD classes (means not significantly different, $p=0.491$). Moreover, the classification threshold of 50% (Table 4.2) for distinguishing between these two classes may be too high, since a much lower percentage was typically associated with UST reaches (in the studied catchments). A mean of 17% armoring was recorded for the UST reaches, with an interquartile range from 1 to 20%, while the corresponding mean and range for FSTCD reaches were 11% and 2 to 17%, respectively.

Reach-scale Specific Stream Power (SSP; Fig. 4.5e) had reasonable power to distinguish between the TR class, which had higher SSP values than UST and FSTCD reaches, which each had higher SSP values than the CEFD class (statistically-significant differences in class means for log-transformed variables, ANOVA/Tukey HSD, $p<0.001$). The unconfined, vertically- and laterally-stable CEFD reaches exhibited a mean and median SSP of 41 and 34 Watt m^{-2}, respectively, with an interquartile range from 16 to 55 Watts m^{-2}. This central tendency is similar to stability thresholds identified by others in humid temperate regions. For catchments in the United Kingdom (UK), Bizzi & Lerner (2013) identified an unconfined-channel stability threshold of 34 Watts

m^{-2} separating erosion-dominated reaches from those in a quasi-equilibrium state. Brookes (1987) working in Denmark and the UK identified a similar threshold at 35 Watts m^{-2} marking a transition between erosion-dominated and deposition-dominated channels. Notably, the SSP interquartile ranges for our unstable, unconfined UST and FSTCD reaches were each above this threshold, consistent with the predominance of both vertical and lateral adjustments and CES II – IV that are characteristic of reaches in these classes.

The Specific Stream Power balance (SSP_{bal}) appeared to distinguish TR reaches from the remaining sediment regime classes (ANOVA/Tukey HSD on log transformed values, $p<0.0001$, except CST: $p=0.02$), but means were not significantly different between other classes ($p>0.05$). Notably, the means of SSP_{bal} for reaches in the CST and UST classes were greater than 1, the threshold suggested by Parker et al (2014) and Gartner et al (2015) that would be expected to distinguish erosion-dominated conditions (>1) from deposition-dominated conditions (<1) in alluvial reaches. However, several UST reaches and 2 of 10 CST reaches had values below 1. Similarly, select reaches in the FSTCD and CEFD classes had SSP_{bal} values above 1, while the mean values and majority of scores were below 1.

Clustering outcomes

The above expert-assigned classifications may include human error, and are somewhat subjective, particularly where classification rules conflict or data do not conform to thresholds. To determine whether the above-assigned sediment regime classes could be replicated by a data-driven, unsupervised clustering algorithm where the above class assignments were with-held, we introduced a variety of geomorphic and

hydraulic variables to the SOM, but with-held the above class assignments. Exploratory data analysis and provisional clustering outcomes indicated that a two-stage implementation of clustering was warranted to control for different scales of classification - essentially, a coarse-tuning SOM for all 193 reaches ranging in character from steep bedrock channels to alluvial channels, followed by a fine-tuning SOM applied to the subset of 154 reaches comprising unconfined, low-gradient (<2%), self-formed alluvial channels. The coarse-tune SOM was trained using largely reach-scale geomorphic variables, while the fine-tune SOM was trained using the addition of channel-scale hydraulic variables reflecting stream competence as affected by channel-floodplain configurations.

Coarse-tune SOM

The coarse-screen SOM was trained using List B of input variables (Table 4.1). Input data self-organized into seven clusters, broadly corresponding to the six sediment regime classifications proposed by Kline (2010). The multivariate input data for the 193 training reaches were reduced to a two-dimensional 6 x 13 lattice for visualization (Figure 4.6a). The column-to-row ratio for this lattice (2.2) approximated the ratio of the first two principal components of the (transformed) input data (4.6/1.9), as per Cereghino and Park (2009). To illustrate an advantage of SOM methods over other multivariate statistical techniques for pattern visualization, component planes for a select number of the SOM input variables are provided in Figure 4.6b (see also Fig. 4.S2). The multivariate reach observations self-organized on the SOM lattice during training, such that reaches with similar variable sets aggregated together, and logical groupings of these observations were partitioned into clusters. Each input variable can be viewed on the

converged lattice in these component planes, where the range-normalized values can be observed to vary in magnitude with direction across the lattice. For example, reach observations that aggregated to Cluster 4 in the upper-left corner of the lattice, are characterized by high values of slope relative to other observations, as illustrated by the warmer tones in that region of the component plane for slope. These are also vertically-stable reaches, as suggested by the low values (cool tones) in the same region of the component plane for IR. Reach observations that aggregated to Cluster 7 of the SOM lattice are also vertically-stable (low values for IR), but are characterized by low slope values, and higher values than other reaches for VC and ER.

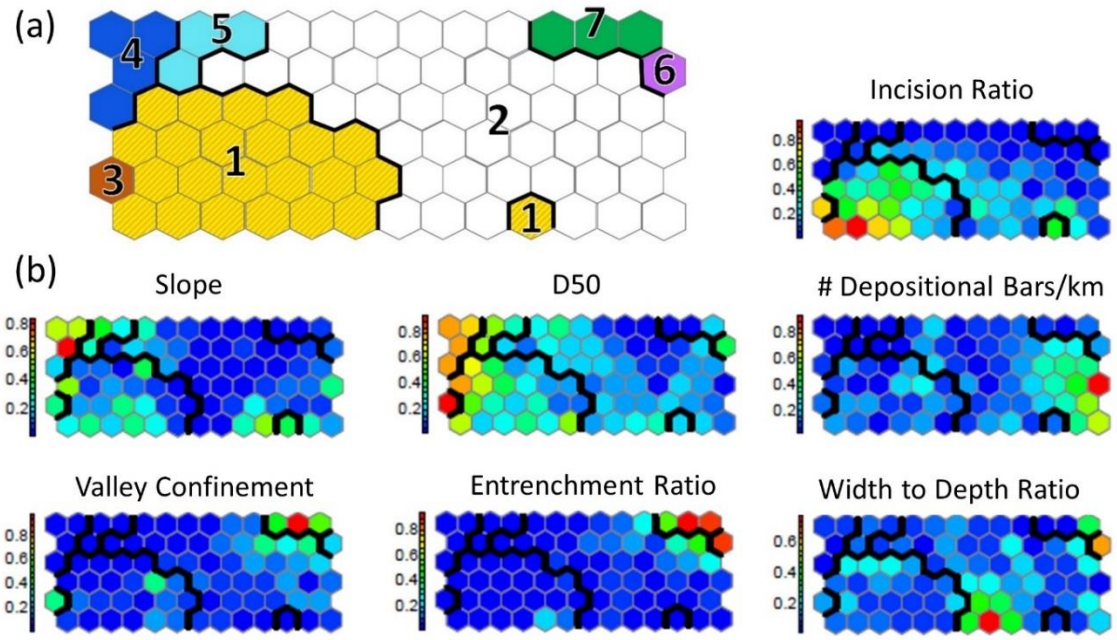

Figure 4.6. Coarse-tune SOM clustering outcomes for study area reaches, including **(**a**)** converged SOM lattice; and (b) component planes for select input variables, in which the color scheme represents a "heat map" grading from low (cool blue tones) to high (warmer red tones) range-normalized values for each independent variable. Component planes for additional variables are presented in Supplementary Figure S2.

Bar plots of intra-cluster means (on a normalized scale) relative to overall means for each parameter suggest which variables are important in defining the sediment regimes clusters (Figure 4.7a). Two TR clusters (4 and 5) comprised vertically-stable reaches confined by valley walls (Figure 4.7b). These reaches were characterized by steeper-than-average slopes, greater-than-average SSP, and coarser bedload (dominated by bedrock in each case). Cluster 5 reaches were distinguished from Cluster 4 by a high SSP_{bal} value (>1; see Supplementary data). While this condition might suggest the propensity for incision, the bedrock boundary conditions would be expected to offer resistance in the present hydrologic regime. Therefore, in this data set (n=193) and our study area (which includes reaches from a range of topographic settings), SSP_{bal} is a variable with ability to discern bedrock-controlled knickpoints at a transition from a lesser-gradient upstream reach.

At the opposite end of the sediment transport continuum, representing transport-limited conditions, two clusters (6 and 7) in unconfined settings were characterized by larger-than-average VC and ER values (Figure 4.7c). Cluster 6 (DEP) reaches comprise coarser-than-average bedload and very high W/D ratios (braided channels). Cluster 7 (CEFD) reaches, however, were distinguished by their lower-than-average W/D ratios, lesser slopes and finer-grained bed material. These reaches were further characterized by a marked transition to a much more open valley setting compared to the upstream reach (i.e., high VC ratio). In our study region, Cluster 7 reaches were located along the edge of post-glacial Lake Vermont, a higher-stage pre-cursor to Lake Champlain (Stewart & MacClintock, 1969), and channel boundaries were composed of cohesive glaciolacustrine silts and silty-sands with varying percentages of clay (dune-ripple bedforms).

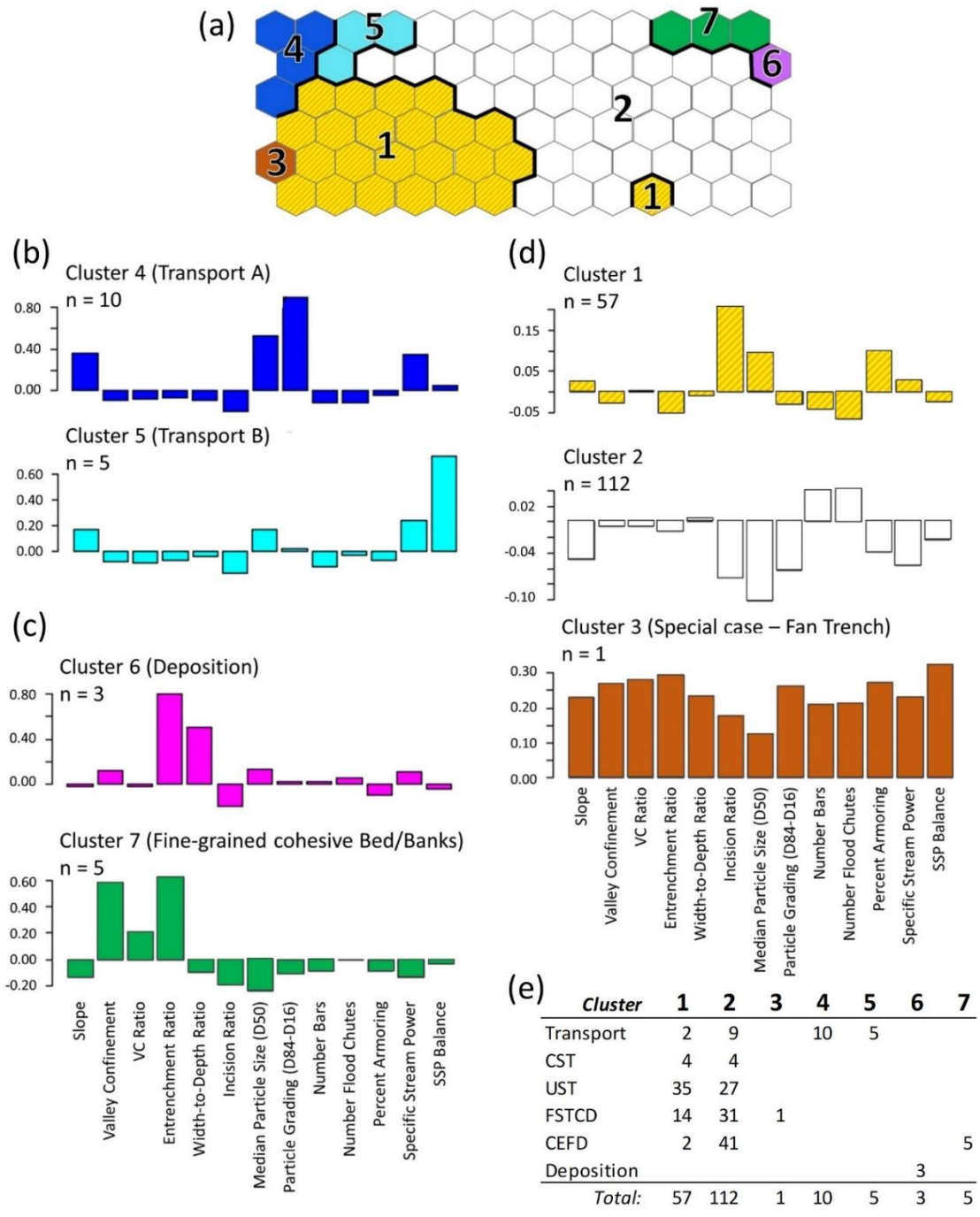

(e)

Cluster	1	2	3	4	5	6	7
Transport	2	9		10	5		
CST	4	4					
UST	35	27					
FSTCD	14	31	1				
CEFD	2	41					5
Deposition						3	
Total:	57	112	1	10	5	3	5

Figure 4.7. Coarse-tune SOM clustering outcomes for study area reaches, including **(**a**)** converged SOM lattice; and variable bar plots by cluster for (b) vertically-stable reaches in confined settings, Clusters 4 and 5; (c) vertically-stable reaches in unconfined settings, Clusters 6 and 7; (d) vertically-disconnected reaches in unconfined settings, Clusters 1, 2 and 3 (n = number of reaches per cluster; y-axis represents range-normalized values); (e) summary of expert-assigned sediment regimes by cluster.

The remaining reach observations in this coarse-tune SOM aggregated to three clusters of vertically-disconnected reaches in unconfined settings (Figure 4.7d). In general, Class 1 contained reaches associated with a higher-than-average IR, lower-than-average ER and coarser-grained, well-graded, bed material. Class 2 reaches, however, were much less incised (on average), and exhibited greater ER values, lower slopes, and finer-grained, well-sorted, bed materials. Variables including number of depositional bars, number of flood chutes, percent armoring, and SSP were useful in distinguishing between Clusters 1 and 2, as the cluster means for these factors trended in opposite directions from the overall average. Cluster 3 comprised one reach that was a special case of an alluvial fan head trench (Schumm, 2005) that likely formed under post-glacial times related to base-level lowering as proglacial lakes impounding downstream reaches were drained (DeSimone, 2000).

Surprisingly, ratios of SSP to measures of bedload (D95, D84, D50) and to critical SSP incorporating these coarse sediment fraction metrics, were not particularly useful in defining clusters – that is why the final list of input parameters did not include them. Similar results were found by Brardinoni and Hassan (2007).

To evaluate the utility of the coarse-tune SOM for partitioning reaches into sediment regimes, we have summarized by cluster (Figure 4.7e) the sediment regime classifications assigned to reach observations in Section 5.2. We have also overlaid reach observation numbers on the lattice nodes to which they clustered, color-coded by the assigned sediment regime classification (Figure 4.8). Based on 13 independent variables (list B in Table 4.1), the coarse-tune SOM was able to distinguish reasonably well between sediment regimes at the extremes of the lateral-confinement continuum for

vertically-stable reaches (Figure 4.8a). Clusters 4 and 5 are two variations of the TR regime, with the latter representing local knickpoints. Cluster 6 contains the DEP reaches, while Cluster 7 represents a subset of the CEFD classification comprised of fine-grained, cohesive channel types. Thus, along the lattice-horizontal dimension, the reach observations have self-organized into a configuration that is suggestive of the continuum of reach types from supply-limited (figure-left) to transport-limited (figure-right), as proposed by Montgomery & Buffington (1997). Along the lattice-vertical dimension, an increasing gradient of vertical disconnection from the floodplain is evident (Fig. 4.8b). An increasing degree of channel or catchment stressors may also be suggested by the distribution of parameter values that can be visualized on the component planes for IR, ER, percent armoring, and numbers of depositional bars and flood chutes (Fig. 4.S2).

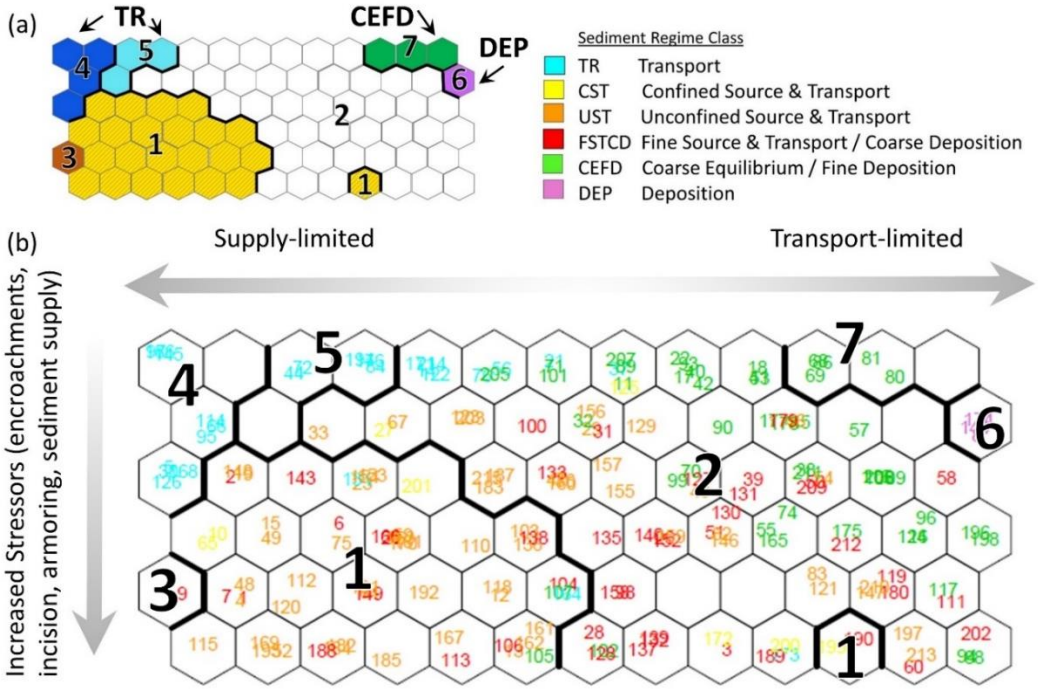

Figure 4.8. Reach observation numbers color-coded by expert-assigned sediment transport regime (see key above) plotted to SOM to visualize where observations clustered on the coarse-tune SOM.

Clusters 1 and 2 reaches, on the other hand, each have a mix of expert-assigned sediment regimes (Figure 4.7e), although the former is dominantly represented by UST, and the latter by CEFD regimes. Thus, governing variables used in the coarse-tune SOM may have only moderate power to discern between sediment regimes, particularly in the context of the full range of stream types from bedrock-cascade to silt-dune-ripple channels. Therefore, a second fine-tune SOM was applied to cluster observations from only the unconfined, low-gradient (<2%), self-formed alluvial channels.

Fine-tune SOM

The fine-tune SOM was trained on the subset of 154 reach observations consisting of both geomorphic and hydraulic input variables (list C of Table 4.1). These reaches were unconfined, low-gradient (<2%) channels predominantly alluvial in nature, although characterized by the occasional bedrock grade controls or valley pinch points. Multivariate (p = 10) input data for the 154 training reaches reduced to a two-dimensional 6 x 12 lattice, with a column-to-row ratio (2.0) similar to the ratio of the first two principal components of the (transformed) input data (4.1/2.2). Non-transformed, but range-normalized, input data mapped to three clusters (Fig. 9a) that are characterized by different combinations of input variables (Fig. 4.9b).

The fine-tune SOM has closely replicated the expert-assigned sediment regimes (Fig. 4.9c), and performed better than the coarse-tune SOM for these unconfined CEFD, UST and FSTCD classes. Variable plots (Fig. 4.9b) illustrate that CEFD (Cluster 1) reaches were differentiated from the other two classes, principally by their lower-than-average IR (< 1.3), and lower slopes and SSP. The FSTCD (Cluster 3) reaches were discerned from their UST counterparts (Cluster 2), by elevated values for width ratio and

W/D ratio, a higher incidence of flood chutes, and lower-than-average mean depth ratio, reflecting the "wide-and-shallow" nature of these channels. If the expert-assigned regimes are taken as "correct", the fine-tune SOM resulted in a correct classification rate of 64%, overall, with slightly higher classification rates for UST and CEFD classes (66% and 65%, respectively) than the FSTCD class (60%).

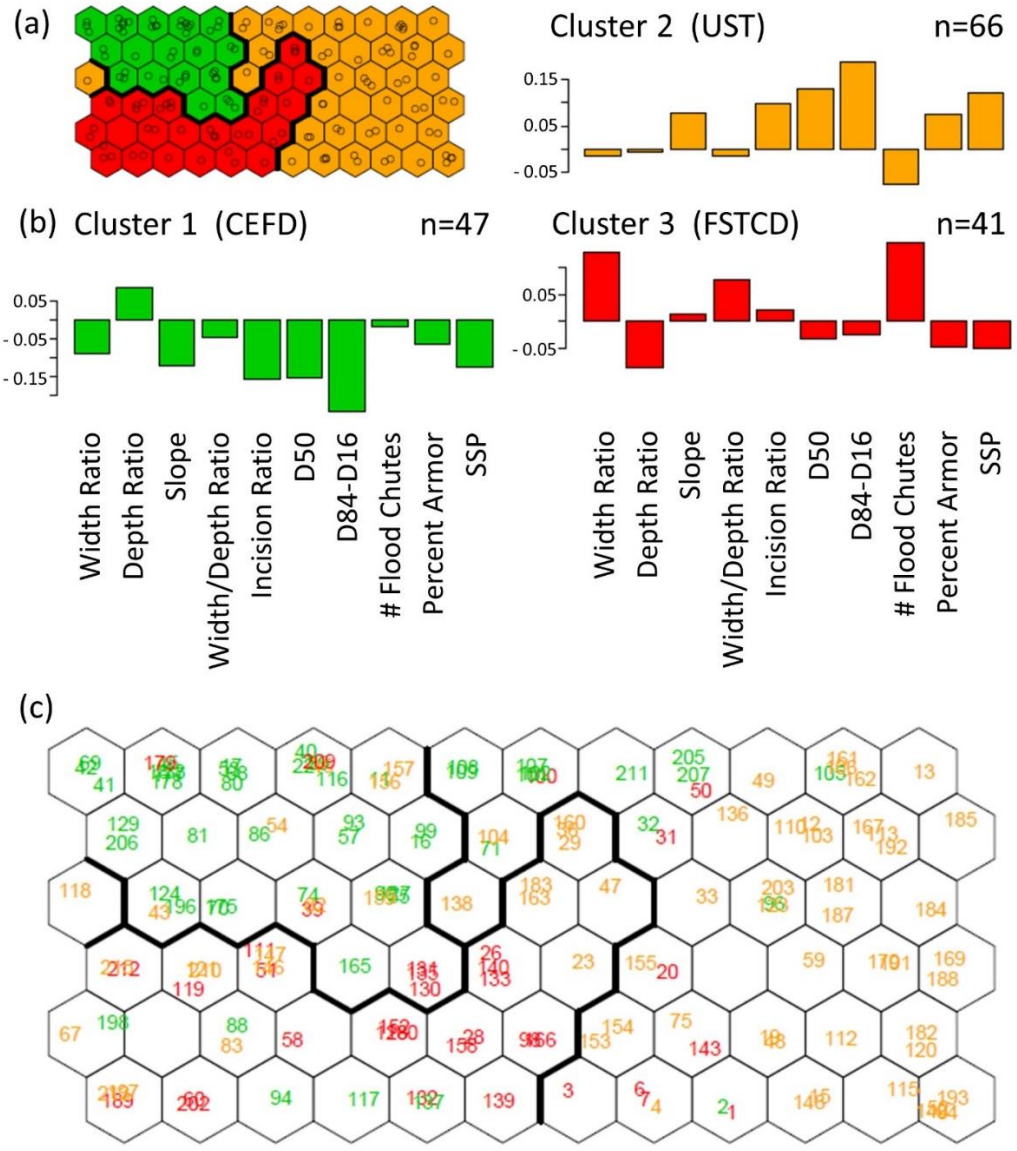

Figure 4.9. Fine-tune SOM clustering outcomes for study area reaches, including **(**a**)** converged SOM lattice; (b) variable bar plots by cluster; and (c) reach observation numbers plotted to lattice, color-coded by expert-assigned sediment transport regime.

Discussion

Refinement of sediment regime classifications

Multivariate SGA data for 193 Vermont stream reaches self-organized into seven clusters (sediment regimes). The resulting clusters broadly replicated and refined six classifications offered in a VTANR River Corridor Planning Guide utilized for management in Vermont rivers (Kline, 2010). Similar to findings of others (Costa and O'Connor, 1995), a stream's current sediment regime is a function of both geomorphic and hydraulic variables operating at the cross-section scale (e.g., relative roughness, depth) and reach-scale (e.g., valley confinement, slope). While these metrics are based largely on observations of channel and floodplain form, form reflects process; thus the identified sediment regimes reflect the spatial and temporal context of processes that manifest the present condition (Wohl, 2018). These sediment regime classes are analogous to reach-scale fluvial process domains (Montgomery, 1999; Brardonini & Hassan, 2007; Lisenby and Fryirs, 2016), and can be superimposed on the continuum of stream types proposed for montane systems by Montgomery & Buffington (1997).

Our approach represents an extension of earlier work that typically applied parametric, multivariate statistics to infer process domains from large data sets of geomorphic and hydraulic variables. For example, Brardonini & Hassan (2007) applied multivariate discriminant analysis (DA) paired with PCA to channel and floodplain metrics for dimension reduction and classification of process domains, identifying a variation on the downstream continuum of stream types of Montgomery & Buffington (1997), related to legacy glacial landforms in British Columbia. Phillips and Desloges (2014) used k-means clustering, PCA, and DA to analyze geomorphic parameters and

classify alluvial channels from a glacially-conditioned setting in southern Ontario. Their analysis (limited to low-gradient, single-thread, channels in unconfined settings) identified four broad channel-floodplain types (corresponding generally to C3, C4, E5, and E6 stream types of Rosgen, 1996). Importantly, their analysis also identified channel entrenchment (or degree of vertical disconnection from the floodplain) as a factor contributing to within-class variability (Phillips and Desloges, 2014). Our study captured this condition as IR; and it was shown to distinguish between sediment regime classes, underscoring the importance of vertical-lateral connectivity as a modifier of sediment regime. Channel incision and entrenchment occur naturally, but also commonly result from human activity. As such, these are aspects of channel-floodplain form that society can influence as we manage toward course sediment equilibrium and fine sediment storage.

Uncertainty in sediment regime classifications

While application of nonlinear, clustering approaches has merit for differentiating between sediment process domains, there is some fuzziness in the clustered outcomes. The noted overlap between clusters may have several reasons. First, there is variability amongst the spatial scales of the metrics used to apply this reach-scale classification (i.e., cross-section to reach scales). The hierarchical nature of spatial scales in a catchment suggests that processes and features identified at a cross section scale can be relied upon to infer processes characteristic of the reach scale (Frissel et al., 1986), provided the reach length is appropriately delineated to reflect relatively homogeneous characteristics. Whereas, the VT SGA protocols stress the importance of guarding against this, there is the potential that reach-scale conditions are not well-described by the cross section

chosen to represent the reach. For example, a cross section with an outlier parameter (e.g., elevated W/D ratio due to a localized effect such as adjacency to a crossing structure that may have induced upstream aggradation), may not be representative of the reach as a whole, while other parameters (such as IR, D50, ER) may well characterize the reach. In other words, geomorphic and hydraulic parameters obtained at the cross section may reflect processes operating at a more granular scale than is characteristic of the reach as a whole (Lea & Legleiter, 2016).

A second spatial-context source of uncertainty may involve the broad range of stream types (bedrock-cascade to silt-dune-ripple) treated with classification. Coarse SOM results for the lumped range of stream types, and List B input variables, indicate that certain sediment regimes are more predictable (e.g., TR, DEP), while remaining regimes have more uncertainty. The latter group may represent reaches closer to thresholds and "more vulnerable to small perturbations" (Phillips, 2003). Executing a two-stage SOM helped address these different scales for classification. Using only the subset of reach data observed from unconfined settings (i.e., controlling for valley confinement and slope), the Fine SOM and a slightly different set of input variables (List C) were better able to differentiate between sediment regime classes.

A third source of uncertainty is linked to the above consideration of spatial scale – namely, the temporal scale of our observations within this relatively broad spatial context (i.e., bedrock to alluvial reaches). The nature of a channel's connection to the adjacent floodplain will vary as a function of flood stage (Weber and Pasternack, 2017) and flood intensity and duration (Magilligan et al., 2015). In alluvial to semi-alluvial channels, relatively frequent, moderate recurrence-interval flow events (i.e., dominant discharge)

are important in governing channel-floodplain form and transporting a majority of the sediment from the watershed (Wolman & Miller, 1960). In contrast, in steeper, bedrock-controlled headwaters, extreme events play a more dominant role in shaping the channel and transporting sediment (Wolman and Gerson, 1978; Lenzi et al., 2006). While the metrics used in our sediment regime classification (e.g., W/D ratio, IR, SSP) are derived for bankfull (Q1.5) stage, and the sediment classifications constitute the continuum of regimes that will be characteristic of higher-frequency, low- to moderate-magnitude discharge (Q2 to Q50), we recognize that extreme events (> Q100) can exert significant controls on channel and floodplain response – both in terms of the event itself, and by influencing channel change through post-flood recovery phases (Wolman & Gerson, 1978). Extreme events have legacy impacts on channel adjustment that can persist long after the event itself by altering boundary conditions including valley slopes, source sediment volumes, landscape and streambank vegetation conditions, and instream large woody debris densities (Dethier et al, 2016). The current sediment regime may be a manifestation of recovery from a past extreme event, more so than characteristic of the bankfull-flow regime (Dethier et al., 2016).

Thus, varying states of reach recovery from past disturbance may have introduced uncertainty in both our expert classifications and SOM clustering outcomes. River reaches were assessed during a relatively quiescent period (2004 through 2011) between significant flood events. The six study area catchments were affected by a state-wide flood of significance (RI ranging from 25 to 500+ years) in August 2011 during Tropical Storm Irene (USGS, 2018). Except for three of the reaches (1.6%), geomorphic data from our 193 reaches were collected before this extreme event, and these three reaches

were located in a catchment (#6 in Fig. 4.1) where Irene generated only a 50-yr RI flood. Prior to Tropical Storm Irene, the largest floods of regional to state-wide significance (>50 yr RI) were the floods of 1973, 1938 and 1927 (Paulson et al., 1989).

There are no sharp boundaries ("edges") between sediment regimes; rather, these classifications reflect a continuum of change, both temporally as well as spatially. It is likely that some reaches are in transition between sediment regimes as the channel evolves in response to past floods and other natural and human disturbance(s). Notably, the "outliers" (i.e., mis-classified reach observations) of the coarse and fine SOMs (Figures 4.8b and 4.9c, respectively) are generally positioned at the boundaries, or transition, between clusters.

Fourth, the nature or number of input variables may not have been sufficient to adequately discern between sediment regime classes. For example, an additional category may be suggested by the broad range of values under the CEFD class. Select reach observations classified as CEFD (Obs. 2, 137, 94, 117, etc.) were observed aggregating to FSTCD or (less commonly) UST clusters of the Fine SOM. These are reaches that have IR < 1.3 (in contrast to FSTCD and UST classes), but exhibit differences from the coarse-sediment quasi-equilibrium condition inferred for CEFD reaches. They are typically over-widened as signified by elevated values for W/D ratio and W_{rat} (similar to their lattice neighborhood of FSTCD reaches); and occasionally, these reaches have reduced ER values due to floodplain encroachments that resulted in clustering with UST reaches. These outlier reaches might instead be classified as Coarse Deposition Fine Deposition (C**D**FD), constituting a subclass of CEFD, as they were usually dominated by aggradation and planform adjustment (late stage IV). They often

exhibited braided or plane-bed bedforms, or riffle-pool bedforms characterized by reduced pool depths, and an elevated incidence of flood chutes. C**D**FD reaches (IR < 1.3) would be distinguished from DEP reaches (IR = 1.0) by their slight degree of incision. Greater separation of reaches into clusters that included this proposed C**D**FD class might have been achieved by calculating W_{rat} and considering W/D stratified by stream type. For example, some reference Rosgen E stream types (sinuous channels composed of silt-rich bed and banks) that had departed to a C stream type by virtue of active widening may arguably have been C**D**FD reaches, but their W/D and W_{rat} values would be too low to flag them as such, unless considered with respect to lower reference values of these metrics for E channels. Vermont RHGCs are based on C and B stream types, and over-represent channel widths for reference E stream types (Jaquith & Kline, 2006). Therefore, W_{rat} values calculated based on these RHGCs would be underestimated for these reference E channels. If RHGCs were developed for E stream types and used to estimate regime W values used in the calculation of W_{rat}, these mis-classified reaches would have a somewhat higher W_{rat} that would help them to cluster better with other C**D**FDs.

Finally, some uncertainty in sediment regime classifications may simply be a reflection of the nonlinear, complexity of river systems (Phillips, 2009). Natural variability in our glacially-conditioned landscape characterized by a mixture of bedrock and alluvial river types, means that more than one set of governing variables may yield the same system state. For example, an unconfined setting would normally suggest slopes < 2%. Yet, our data set also includes unconfined reaches with steeper slopes in headwater settings where shallow, underlying bedrock has controlled topography. These

reaches were classified in a UST sediment regime with a non-conforming slope. Similarly, it would be conceivable to observe more than one system state in response to the same set of governing variables.

SOM advantages for visualization

The SOM and its component planes have advantages over traditional statistical methods when attempting to visualize the multivariate features that interact in nonlinear ways to manifest in a given fluvial process domain. The reduction of multi-dimensional data to a two-dimensional lattice for each of the Coarse and Fine SOMs (Fig. 4.8b and 4.9c, respectively), simplified the data analysis. The component planes (Fig. 4.6b and 4.Sx) and bar plots (Fig. 4.7b-d and 4.9b) provide insight into which variable (or combinations of variables) may be a governing factor(s) in any particular cluster (i.e., sediment regime).

By applying a space-for-time substitution, the converged lattice also represents a kind of process domain space (Montgomery, 1999) that can be used to visualize the transition of a channel reach from one sediment regime to another as it progresses through channel evolution stages in response to a stressor (Figure 4.10). For example, consider a low-gradient, gravel-dominated, riffle-pool reach with good connection to its floodplain (i.e., IR<1.3) - all conditions that suggest a quasi-equilibrium state (CES stage I) characterized by a CEFD sediment regime. If this reach was subjected to channelization and dredging that lead to channel incision (IR > 1.3) and floodplain disconnection, it would move to stage II, characterized by a UST and FSTCD regimes (Figure 4.10a and 4.10c). The individual component planes for IR and W/D ratio demonstrate monotonic trends in the lattice-vertical and lattice-horizontal dimensions that

are consistent with this idea. The pre-disturbance reach would plot near the top-center of the lattice. Upon dredging, this same reach would shift vertically downward and right on the lattice to areas characterized by higher IR values. With subsequent widening, this reach would move lattice-left to a region typified by higher W/D ratios (and greater numbers of depositional bars; Fig. 4.Sx). As channel widening reduces stream competence leading to progressive aggradation, this reach might transition toward a more transport-limited state – moving further lattice-left and -up toward a region characterized by increasing numbers of depositional bars and lower W/D ratio. Finally, with progressive channel-narrowing, the channel may return to a quasi-equilibrium state (stage V) and return once again to the top-center of the lattice. Thus, the SOM lattice provides a way to explicitly consider and "map" the trajectory of shifting geomorphic process domains with time.

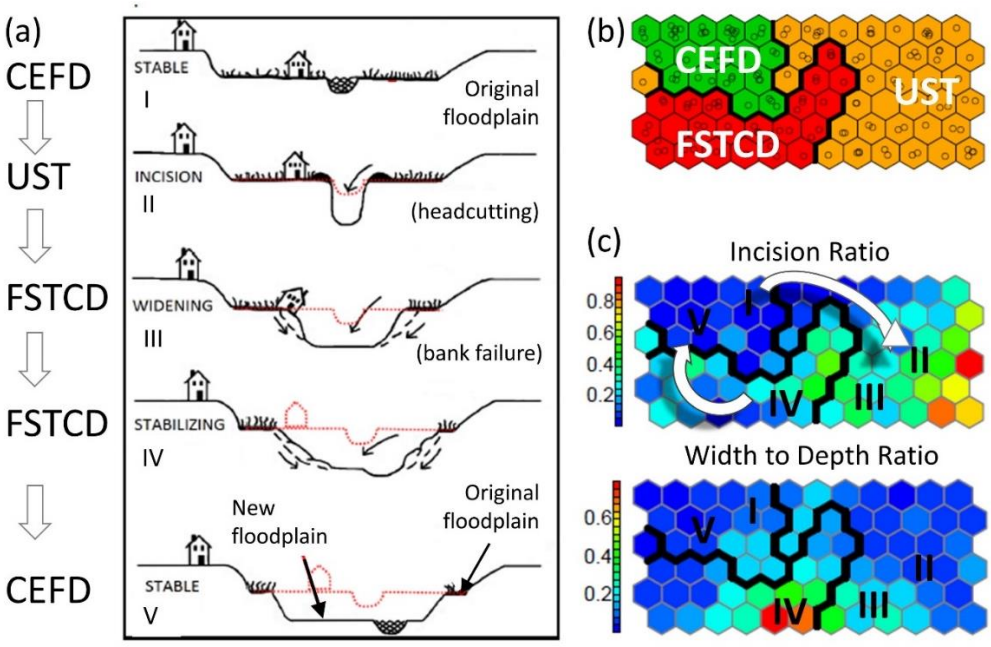

Figure 4.10. Representation of (a) sediment regime classes by channel evolution stage (Schumm et al., 1984) superimposed on (b) the fine-tune SOM lattice; and (c) SOM component planes.

Management implications

Classifying the current sediment regime of river reaches is of value for water resource managers to highlight the potential for impacts to property, water quality and habitat, and to inform prioritization schemes for allocation of limited resources (Kline & Cahoon, 2010). Vertically-disconnected reaches have greater propensity for vertical and lateral channel adjustments with the potential to impact adjacent built infrastructure. In confined settings of the glacially-conditioned Northeast, roads, rail berms, bridges and culverts are commonly located within narrow, steep river valleys and are at enhanced risk of damage during moderate to extreme events (Anderson et al., 2016). In unconfined reaches, varying degrees of vertical disconnection from the floodplain would subject a channel to increased varying magnitudes of SSP, with implications for enhanced erosion. Figure 4.11 is based upon a case of contiguous reaches in the Mad River watershed in central Vermont, where reach A (UST) has been subjected to historic dredging, channel straightening and berming to the extent that it has become disconnected from the floodplain (IR = 2.6). While a nearby downstream reach of similar drainage area (reach B; CEFD) remained relatively unmodified and well connected to the floodplain (IR=1.0). A range of storm flows was modeled using 1D HEC-RAS for a regional flood study provided by Dubois & King, Inc., and main channel SSP was computed as the product of average shear stress and average velocity. At the 2.3-year RI peak discharge, the relative difference in channel SSP between reaches A and B is largely the result of differences in channel configurations. In the entrenched cross section (reach A), a steeper slope and slightly greater hydraulic radius (more efficient cross section) minimizes friction (due to smaller wetted perimeter) leading to higher velocities and greater SSP. For the range of

flows above a 2.3-year RI, however, the channel relationship to floodplain becomes most important. Since modeled flood flows of all stages above Q2.3 were able to access the floodplain in the non-entrenched reach B, the channel-bed SSP has much lower magnitude across the array of peak flows than the entrenched cross section of reach A. Conversely, given the degree of incision and entrenchment at reach A, SSP continues to rise steadily until overtopping of the bank occurs somewhere between a Q100 and Q500 flood peak. Magnitudes of SSP at the reach A cross section greatly exceed the 300 W m^{-2} value suggested by Magilligan (1992) as a threshold for major channel adjustment. Figure 4.11 illustrates the enhanced potential of incised and entrenched (i.e., UST) channels to serve as a source of sediment to downstream reaches.

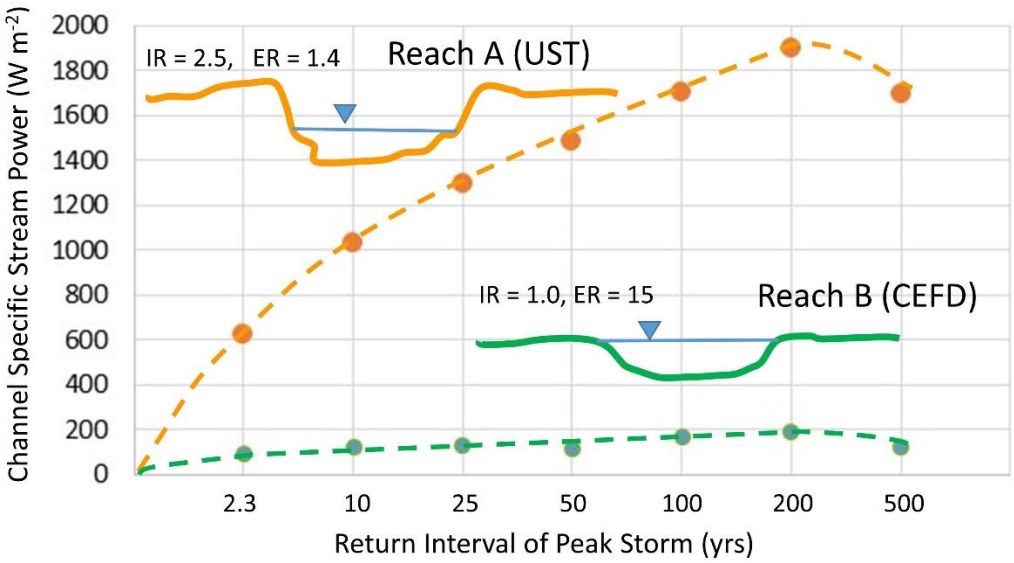

Figure 4.11. Channel-bed SSP estimated for a range of modeled return interval storms in contiguous reaches of the Mad River, VT with differing channel configurations (IR, ER).

CEFD reaches that are well-connected with the floodplain can be prioritized for corridor protection strategies in municipal or regional planning and zoning to maintain their floodplain storage function. On the other hand, FSTCD reaches that are presently

disconnected with the floodplain may be prioritized for conservation easements to curtail river management and allow the unfolding channel evolution process to create new floodplain as an "attenuation asset" (Kline, 2010). Particularly, where such reaches are located upstream of developed areas with a greater degree of channel encroachment, they may be targeted for protection and worthy of public investment for the attenuation of flood peaks and associated reduction in flooding hazards to downstream communities (Kline and Cahoon, 2010; Watson et al., 2016).

In a changing climate, where magnitude, frequency and intensity of extreme events is projected to increase (Guilbert et al., 2014), vertically-disconnected channels will have an enhanced potential to serve as a source of sediment to downstream reaches. CST reaches are vulnerable to increased fine sediment export under extreme events where these channels impinge upon hillslopes and high terraces comprised of glaciolacustrine or glacial till deposits (Yellen, et al., 2014; Dethier, et al., 2016). Since, the trajectory of SSP rise with storm recurrence interval is much steeper for incised and entrenched UST and FSTCD reaches, it can be inferred that they will have greater potential to export sediment than CEFD reaches. Coarse sediment will have the potential to aggrade and drive lateral adjustments and avulsions in downstream reaches, while fine sediments will be carried to receiving waters and further degrade water quality.

To address water quality concerns on a river network scale, this sediment regime classification approach could be used to identify reaches that are disproportionately responsible for loading of coarse and fine sediments. For example, streambank erosion has been identified as a source of phosphorus contributing to harmful algal blooms in Lake Champlain in the northwestern region of Vermont (Isles et al., 2015). In the Total

Maximum Daily Load plan, estimates of phosphorus loading from streambanks are based on the dominant reach-based channel evolution stage at a HUC 12 scale (USEPA, 2016). Our algorithm could be used to refine estimates of streambank sediment loading at a more granular scale to identify "hot spots" (McClain et al 2003) and to optimize best management practices for the reduction of sediment and nutrient loading.

Taken collectively, reaches of a similar sediment process domain may also constitute a "functional process zone" of Thorp and others (2006, 2008) for consideration of ecosystem services rendered and to manage for optimal ecological integrity of the active river area.

Conclusions

Multivariate stream geomorphic assessment data have been clustered into sediment process domains that constitute net sources or sinks of coarse and fine sediment on a mean annual temporal scale (i.e., Q1.5 discharge) using a two-stage Self-Organizing Map (SOM). The iterative process of streamlining input parameters and training the SOM identified a parsimonious set of geomorphic and hydraulic variables that meaningfully separated reaches into these sediment regimes. Working with the domain experts also served to elicit information regarding the relative importance of these geomorphic and hydraulic drivers of sediment erosion and deposition, helping to refine the classification scheme for the Vermont study area.

While this classification scheme has been applied to characterize sensitivity of its rivers to historic and future watershed and channel stressors common to the glacially-conditioned and mountainous areas of Northeastern US, the framework should be transferable to other regions (utilizing additional or alternate independent variables). The

geomorphic and hydraulic variables used to cluster our reaches were similar to parameters commonly inventoried during assessment protocols in widespread use (e.g., Nanson & Croke, 1992; Rosgen, 1996; Montgomery & Buffington, 1997; Raven et al, 1998; Brierley & Fryirs, 2005; Rinaldi *et al*., 2013). As channels evolve over time in response to stressors or management practices, these data-driven, nonparametric clustering tools can be quite easily updated with new assessment results, supporting an adaptive approach to river corridor management.

To our knowledge, this current study is the first application of a neural network to examine geomorphic data for a range of stream types and to classify a reach-based sediment regime that explains the nature of the adjustment (vertical, lateral) within the trajectory of channel evolution. Our results extend the supply-limited to transport-limited continuum of reach types suggested by Montgomery & Buffington (1997), through the additional dimension of a channel's increasing degree of vertical disconnection from the floodplain that can result from a variety of natural and human disturbances. Through its effect on channel stream power, this vertical-lateral connectivity condition can influence the sediment transport regime in channels and has implications for inundation and erosion flooding hazards, as well as water quality and ecological integrity in the active river corridor.

Future work will explore automation of this algorithm, and linkage to existing state-wide stream geomorphic assessment data in a GIS to enable model predictions statewide and the examination of potential autocorrelation in governing variables. This anticipated framework will facilitate scenario testing to evaluate how sediment transport regimes of a given reach (or river network) might shift in the event of future channel and

floodplain manipulation or restoration, or in response to regional changes in climate. The GIS framework could also be used to forecast estimates of channel adjustment to optimize best management practices for the reduction of sediment and nutrient loading from streambanks.

Acknowledgements

This material is based upon work supported by the National Science Foundation under Vermont EPSCoR Grant Nos. EPS-1101317 and NSF OIA 1556770. Any opinions, findings, and conclusions or recommendations expressed in this material are those of the author(s) and do not necessarily reflect the views of the National Science Foundation or Vermont EPSCoR. Original geomorphic assessments completed by the first author were supported in part by FEMA Hazard Mitigation grants, Lake Champlain Basin Program grants, and the Vermont Agency of Natural Resources. The authors are grateful to Dr. John Field of Field Geology Services, for assessment data from two reaches, and to Dubois & King, Inc. for HEC-RAS modeling results underlying Figure 4.11.

Supporting Information

This supplementary document contains text, figures and tables to further explain and document the manuscript's methodological framework for the assessment, classification and clustering of geomorphic and hydraulic variables from 193 river reaches located in 6 catchments in central and southern Vermont, northeast USA. Items are presented in order of their introduction within the main manuscript.

- Text 4.S1 provides a description of methods used to compile geomorphic variables used for sediment regime classifications and as inputs for training the Self-Organizing Maps.
- Table 4.S1 provides a summary of study area watershed characteristics.
- Figure 4.S1 summarizes geomorphic and hydraulic variables in box plots by expert-assigned sediment regime class.
- Figure 4.S2 provides component planes for each of the input variables to the coarse-tune SOM.
- Figure 4.S3 provides component planes for each of the input variables to the fine-tune SOM.

4.S1 Geomorphic and Hydraulic Variables

Channel slope (S) was calculated as the difference in elevation interpolated from 1:24000 USGS topographic maps at the upstream and downstream ends of the delineated reach, divided by the channel length between end points depicted on the Vermont Hydrography Dataset (high-resolution NHD) (VCGI, 2013). Field-based measurements of bankfull channel dimensions were made with a tape and rod at a cross section considered representative of the reach, based on observations along the entire reach. Cross section measurements were entered into a spreadsheet modified with permission after Ohio DNR (Kline et al., 2009). Bankfull discharge was defined as the discharge with an approximate recurrence interval of 1.5 years (Leopold, 1994), and was identified by reference to various field features, including a break in bank slope, transition to perennial vegetation, and bench-like deposits of finer-grained sediments (Harrelson, et al., 1994; Kline et al, 2009).

Width-to-depth ratio (W/D) was generated as the bankfull width (W_{bfl}) divided by mean depth (D_{mn}) for a representative reach cross section measured at a riffle bedform. W_{bfl} was the channel top width at bankfull stage. D_{mn} was defined as the cross-sectional area of the channel divided by the maximum depth, D_{mx}, which itself is defined as the vertical distance from the bankfull stage to the channel thalweg, or deepest part of the channel cross section. Valley confinement was defined as the field-truthed valley width estimated from 1:24000 topography divided by the W_{bfl} and was classified into five possible categories: ranging from narrowly-confined (< 2), semi-confined (≥2 < 4), narrow (≥4 < 6), broad (≥6 < 10) and very broad (≥10). In a few cases (xx % of reaches/segments), where bedrock gorge conditions precluded field assessment, W_{bfl}

measurements were estimated from remote-sensing or regional hydraulic geometry curves (Jaquith and Kline, 2006). Entrenchment ratio (ER) was defined as the ratio of the floodprone width to W_{bfl}, where floodprone width is estimated as the distance between valley walls calculated at an elevation that is two times the maximum bankfull channel depth (Kline et al., 2009). This metric is intended to reflect the aerial extent of the floodplain inundated by a flooding event with an annual exceedance probability of 0.02%. Incision ratio (IR) was calculated as the ratio of the low-bank height above the channel thalweg over the maximum bankfull depth, D_{max}, and reflects the degree of vertical disconnection of the river from its adjacent floodplain. Dominant channel-bed grain size for each reach was defined as the median grain size, or D50, based on a pebble count (Wolman, 1954) of channel materials spanning bankfull stage at each riffle cross section. The number of depositional features normalized to the length of reach (i.e., # / km) was estimated, including point, mid-channel, and side bars, as well as tributary junction bars. Higher values for this metric are hypothesized to suggest net depositional conditions. The number of flood chutes normalized to reach length was also compiled to indicate active widening and planform adjustment that may also suggest an imbalance in driving versus resisting forces and net deposition of bedload. The proportion of the reach that has been armored using stone or other hard bank materials (e.g., retaining walls) was included as percent armoring. Similarly, we calculated the percent of the reach length that had been historically straightened, based on historical accounts, historical photographs, aerial imagery and maps, and proximity of encroaching infrastructure. These latter two metrics were included to reflect human encroachments and modifications with a tendency to lead to bed degradation or downstream (within-reach)

bank erosion. A bankfull W ratio, Wrat, was computed as the quotient of measured bankfull W and regime bankfull W. A D ratio, Drat, was calculated as the ratio of measured to regime mean D. Regime bankfull W and mean D were estimated from published regional hydraulic geometry relationships for non-urbanized catchments (Jaquith & Kline, 2001; Jaquith & Kline, 2006):

$$Q_{1.5} = 0.18\ A^{1.08} \quad (n = 14;\ r^2 = 0.81) \qquad (1)$$

$$W_{1.5} = 2.62\ A^{0.44} \quad (n = 20;\ r^2 = 0.91) \qquad (2)$$

$$D_{1.5} = 0.22\ A^{0.30} \quad (n = 20;\ r^2 = 0.87) \qquad (3)$$

where drainage area (A) was expressed in km^2, and the coefficients and exponents of these power-law relationships were derived from linear regression of empirically-derived data.

Peak specific stream power (SSP) was computed as $\omega = \gamma QS/W$, where ω is the SSP (W m^{-2}), γ is the specific weight of water (9810 N m^{-3}), Q is discharge ($m^3\ s^{-1}$), W is the channel top width (m), and S is the energy slope of the stream for which the convention is to substitute the channel slope (m m^{-1}) under assumptions of uniform, steady flow. SSP is the rate at which potential energy is supplied to a unit area of the stream wetted perimeter (Bagnold, 1966), and stream power calculations were based on a discharge with an approximate recurrence interval of 1.5 years. $Q_{1.5}$ ($m^3\ s^{-1}$) and $W_{1.5}$ were estimated from published regional hydraulic geometry relationships for non-urbanized catchments (Jaquith & Kline, 2001; Jaquith & Kline, 2006) (see Supplementary).

An additional stream power metric was defined as the ratio of subject-reach SSP to upstream-reach SSP, or SSP_{bal} (Parker *et al.,* 2014). An $SSP_{bal} < 1$ would indicate a

downstream reduction in stream power, with an expected inducement of sediment deposition. Conversely, an $SSP_{bal} > 1$ would indicate a downstream increase in stream power, and the associated likelihood for stream bed and bank erosion (Bizzi and Lerner, 2013; Gartner *et al*, 2015; Parker et al., 2014).

These SSP calculation methods employing variables gathered through remote-sensing and regional hydraulic geometry relationships (S, Q, W) may under- or over-estimate actual SSP, and may not reflect on-the-ground conditions at present where catchments and rivers have undergone watershed-scale or reach-scale modifications that resulted in channel and floodplain adjustments (Kline & Cahoon, 2010; Noe and Hupp, 2005). Nonetheless, they represent catchment-scale estimates of power relationships and erosion / deposition potential driven by topography and valley-scale metrics. We hypothesized that anthropogenic enhancements of (or decreases in) reach-scale SSP due to channel narrowing (or widening) would then be captured in our analysis by field-measured morphologic metrics including incision ratio (IR), entrenchment ratio (ER) and width/depth ratio (W/D), as well as additional variables of measured bankfull width and mean depth expressed as ratios to regime width and depth (Wrat and Drat, respectively).

A set of tractive force parameters was also developed, but was limited to that subset of reaches that were dominantly alluvial and in unconfined settings, since calculation methods for these parameters (Andrews, 1983; Ferguson, 2005) are empirically-derived and apply generally to gravel- and cobble-bedded streams of low to moderate gradient. To assess threshold effects of particle movement incorporating hiding and protrusion effects, we defined the critical SSP, ω_{ci} (in units of W m^{-2}), required to entrain a bed particle size of interest, *i*. as:

$$\omega_{ci} = 0.113\, D_{50}^{1.5}\, log\left[\frac{0.73}{S} * \left(\frac{D_i}{D_{50}}\right)^{0.4}\right]\left(\frac{D_i}{D_{50}}\right)^{0.6} \quad (4)$$

where S refers to channel slope, D_i is the diameter of the particle size of interest (in mm), and D_{50} is the median grain size of channel bed materials (in mm) (Ferguson, 2005; Andrews, 1983). We computed critical SSP (SSP_{cr}) for entrainment of two particle sizes represented by the 84th percentile (i.e., D_i = D84) and the 95th percentile (D95). Ratios of SSP_{cr} for each particle size were then constructed as SSP/ SSP_{cr}.

We estimated two additional inverse measures of channel-boundary resistance to stream power: (1) a ratio of SSP to D50; and (2) a ratio of hydraulic radius, R_h, to D84, consistent with the definition of relative roughness by Leopold, Wolman & Miller (1964). These are each inverse measures; therefore, lower values of SSP/D50 or R_h /D84 would indicate increased hydraulic roughness due to coarser bedload or wide-and-shallow channel configurations, or both.

Finally, three additional hydraulic parameters were calculated to capture the variability in boundary conditions of the bankfull channel and its potential influence on transport capacity: (1) the range of grain size (in mm) for two standard deviations spanning the median (i.e., D84 minus D16); (2) D84/D50; and (3) D95/D50. The sediment transport capacity is expected to be different when comparing a well-sorted riffle (i.e., low values of these parameters) to that of a poorly-sorted riffle (high values). In post-glacial terrain, very large grain sizes may persist from previous glacial transport (e.g., outwash or ice-rafted boulders in glaciolacustrine environments), and these largest grain sizes may be considered immobile under the present hydrologic regime, offering stability to the channel (Phillips & Desloges, 2014).

Table 4.S1. Physical characteristics of study area watersheds.

Map Key	Watershed	Study Region Drainage Area [a] (km^2)	Percent Above 366 m Elev. [a] (%)	Mean Annual Precip-itation[b] (mm)	Percent Storage [c] (%)	Land Use [d]			
						Water/ Wetland (%)	Forest (%)	Agri-culture (%)	Dev-eloped (%)
1	Lewis Creek	205	21.7	1069	5.9	8	61	26	5
2	Little Otter Creek	149	0.2	975	4.8	9	41	46	4
3	New Haven River	303	62.6	1186	2.1	5	76	15	4
4	Mettawee River	285	47.5	1293	3.9	6	74	16	4
5	Battenkill River	139	67.1	1509	3.9	5	86	5	4
6	Black River	386	73.9	1265	2.3	4	88	2	5

a USGS Streamstats (https://water.usgs.gov/osw/streamstats/) and Olson (2014)
b PRISM data for 1981 - 2010 obtained through a
c Water bodies and wetlands from NLCD 2006 obtained through a
d Developed includes industrial, commercial and residential; forest incl. brush; https://anrweb.vt.gov/DEC/SGA/Default.aspx

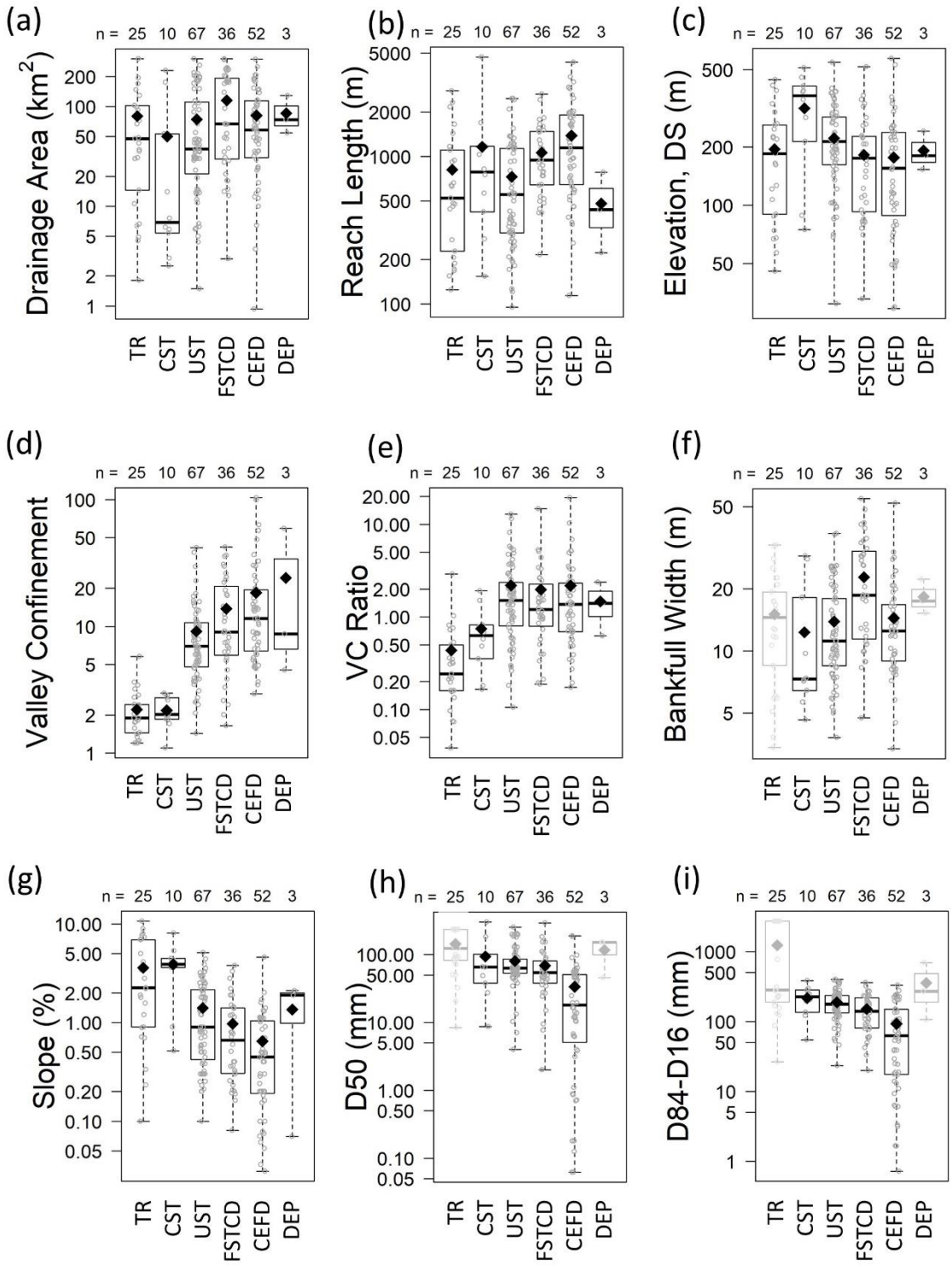

Figure 4.S1. Box plots of reach geomorphic variables by expert-assigned sediment regime class.

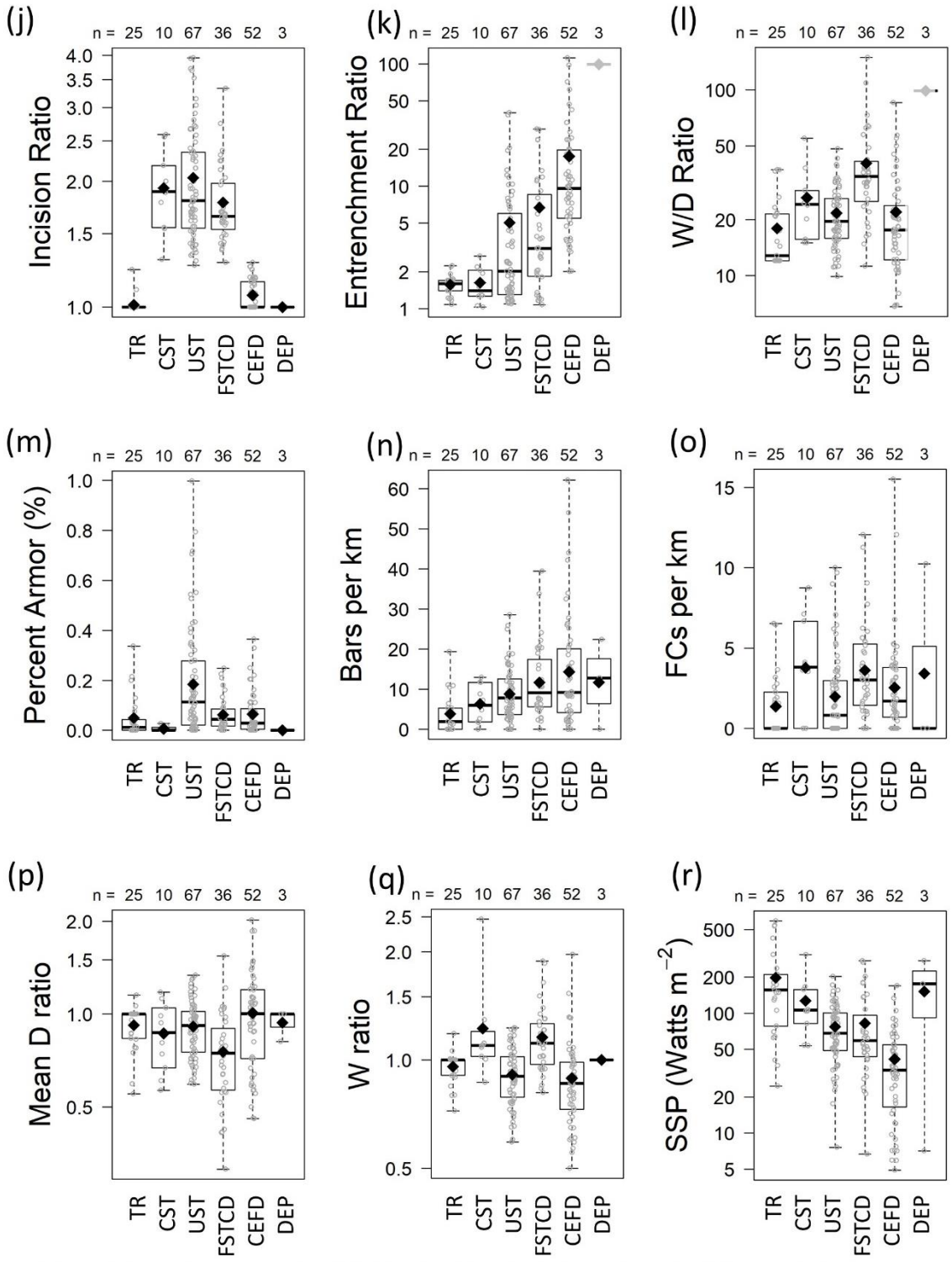

Figure 4.S1. (Continued) Box plots of reach geomorphic variables by expert-assigned sediment regime class.

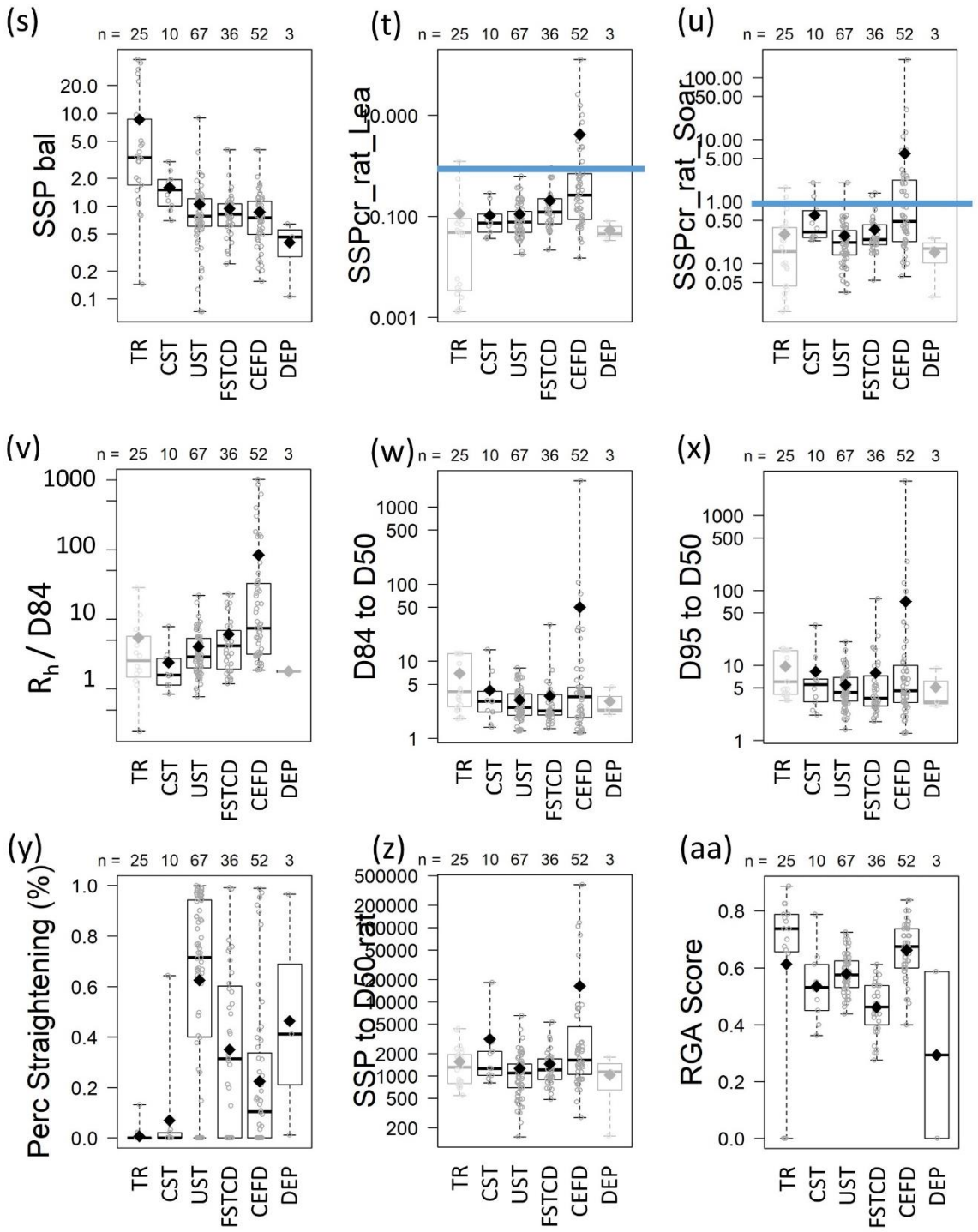

Figure 4.S1. (Continued) Box plots of reach geomorphic variables by expert-assigned sediment regime class.

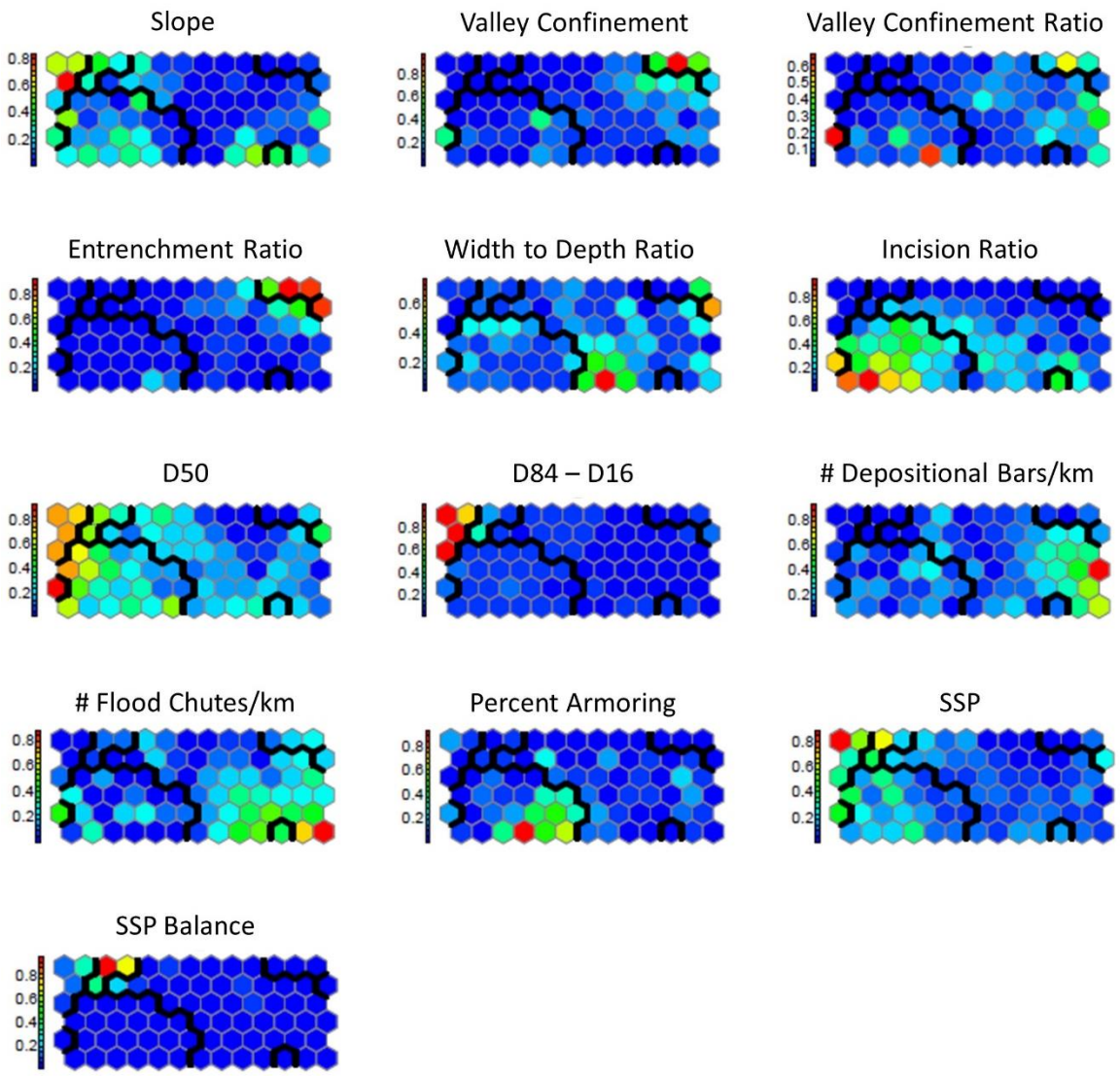

Figure 4.S2. Component planes for each of the 13 input variables to the coarse-tune SOM. Color scheme represents a "heat map" grading from low (cool blue tones) to high (warmer red tones) range-normalized values for each independent variable.

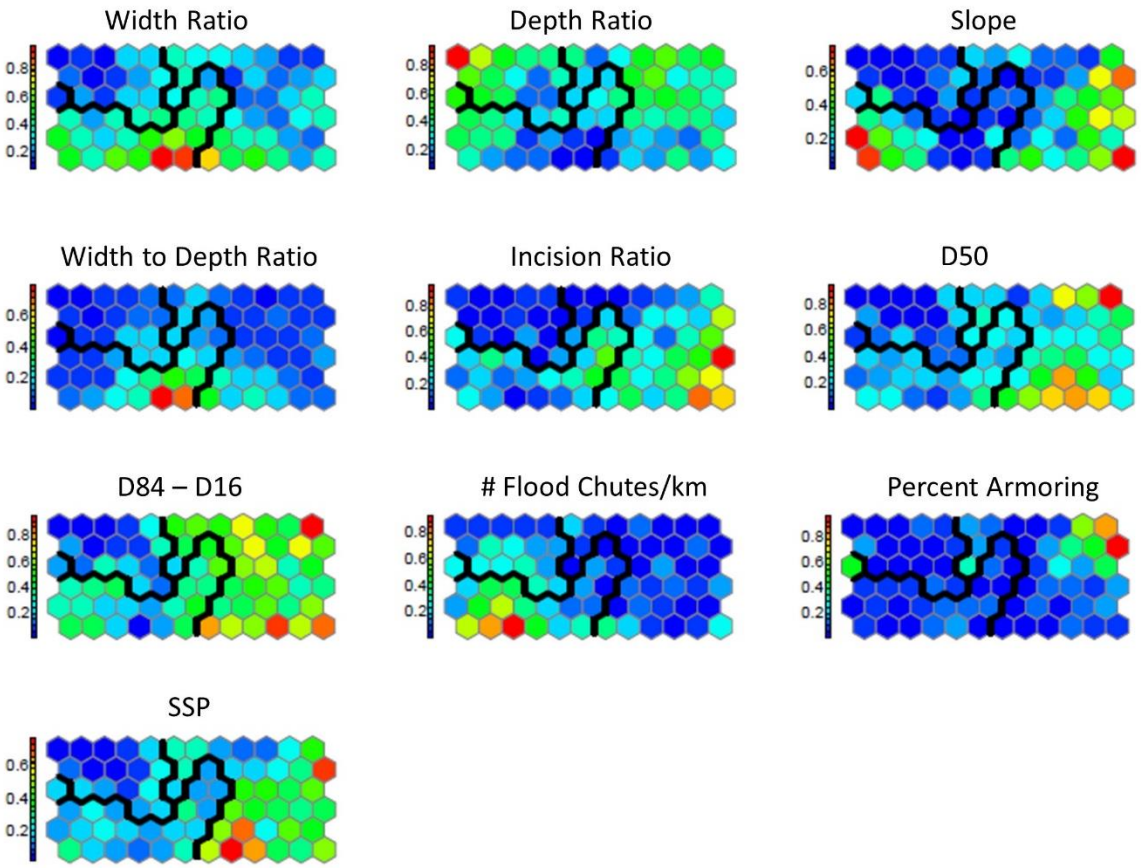

Figure 4.S3. Component planes for each of the 10 input variables to the fine-tune SOM. Color scheme represents a "heat map" grading from low (cool blue tones) to high (warmer red tones) range-normalized values for each independent variable.

References

Alvarez-Guerra, M., C. González-Piñuela, A. Andrés, B. Galán, and J. R. Viguri (2008), Assessment of Self-Organizing Map artificial neural networks for the classification of sediment quality, *Environment International*, 34(6), 782-790, doi:10.1016/j.envint.2008.01.006.

Anderson, M. J. (2001), A new method for non-parametric multivariate analysis of variance, *Austral Ecology*, 26, 32-46, doi:10.1111/j.1442-9993.2001.01070.pp.x.

Anderson, I. , D. M. Rizzo, D. R. Huston, M. M. Dewoolkar, 2016, Stream Power application for bridge damage probability mapping based on empirical evidence from Tropical Storm Irene, *Bridge Engineering* (in print).

Andrews, E.D., 1983, Entrainment of gravel from naturally sorted riverbed material. Geol. Soc. Amer. Bull. 94, 1225–1231.

Bagnold, R.A., 1966. An Approach to the Sediment Transport Problem from General Physics. USGS Professional Paper, vol. 422-J. Washington, DC.

Ballantyne, Colin K., 2002, Paraglacial geomorphology. Quaternary Science Reviews, 21: 1935-2017.

Benda L, Dunne T (1997) Stochastic forcing of sediment supply to channel networks from landsliding and debris flow. Water Resources Research, 33, 2849-2863.

Besaw, L. E., D.M. Rizzo, M. Kline, K.L. Underwood, J.J. Doris, L.A. Morrissey, K. Pelletier, (2009), Stream classification using hierarchical artificial neural networks: A fluvial hazard management tool, *Journal of Hydrology*, 373, 34-43, doi:10.1016/j.jhydrol.2009.04.007.

Bierman PR (2010) Clearcutting, Reforestation, and the coming of the Interstate: Vermont's Photographic Record of Landscape Use and Response In: *Repeat Photography: Methods and Applications in the Geological and Ecological Sciences.* (eds Webb RH, Boyer DE, Turner RM) pp Page., Cambridge University Press

Bierman, P.,Lini, A.,Zehfuss, P.,Church, A.,Davis, P.T.,Southon, J.,Baldwin, L., 1997. Postglacial ponds and alluvial fans: recorders of Holocene landscape history. GSA Today 7(10), 1–8.

Bizzi, S., and Lerner, D.N., (2013), The use of stream power as an indicator of channel sensitivity to erosion and deposition processes, *River Research and Applications*, 31, 16–27, doi:10.1002 /rra.2717.

Bizzi S, Demarchi L, Grabowski RC, Weissteiner CJ, Bund W (2015) The use of remote sensing to characterise hydromorphological properties of European rivers. Aquatic Sciences, 78, 57-70.

Booth, D.B., (1990), Stream-channel incision following drainage basin urbanization. *Water Resour. Bull. Am. Water Resour. Assoc*. 26 (3), 407–417, doi: 10.1111/j.1752-1688.1990.tb01380.x

Brakenridge, G. R., P. A. Thomas, L. E. Conkey, J. C. Schiferle, (1988) Fluvial Sedimentation in Response to Postglacial Uplift and Environmental Change, Missisquoi River, Vermont. *Quaternary Research*,30: 190-203, doi: 10.1016/0033-5894(88)90023-3.

Brardinoni, F., Hassan, M.A., (2007), Glacially induced organization of channel-reach morphology in mountain streams. *J. Geophys. Res*., 112, F03013, doi:10.1029/2006JF000741

Brardinoni, F., and M. A. Hassan (2006), Glacial erosion, evolution of river long profiles, and the organization of process domains in mountain drainage basins of coastal British Columbia, *J. Geophys. Res*., 111, F01013, doi:10.1029/2005JF000358.

Brierley, G.J., K. A. Fryirs, (2005), Geomorphology and River Management: Applications of the River Style Framework. Blackwell, Oxford, p. 398.

Brookes A. (1987), The distribution and management of channelized streams in Denmark, *Regulated Rivers*, 1: 3–16.

Bull, W.B. (1979), Threshold of critical power in streams. *Bull. Geol. Soc. Am*., 90, 453–464.

Buraas, E.M.,Magilligan, F.J., Renshaw, C.E., Dade, W.B., (2014), Impact of reach geometry on stream channel sensitivity to extreme floods. *Earth Surf. Process. Landf*. http://dx.doi.org/10.1002/esp.3562.

Cereghino, R. and Y.-S. Park (2009), Review of the Self-Organizing Map (SOM) approach in water resources: Commentary, *Environmental Modelling and Software*, 24, 945-947.

Chappell, J. (1983), Thresholds and lags in geomorphologic changes, *Australian Geographer*, 15, 358–66.

Church, M. and J. Ryder, 1972, Paraglacial sedimentation: A consideration of fluvial processes conditioned by glaciation. Geological Society of America Bulletin, 83: 3059-3072.

Collins, M. J. (2009). Evidence for Changing Flood Risk in New England Since the Late 20th Century. *Journal of the American Water Resources Association*, *45*(2), 279-290. doi: DOI: 10.1111/j.1752-1688.2008.00277.x

Costa, J.E. and J. E. O'Connor (1995), Geomorphically effective floods. In Natural and Anthropogenic Influences in Fluvial Geomorphology, Costa JE, Miller AJ, Potter KW, Wilcock PR (eds). American Geophysical Union: Washington, DC; 45–56.

Death, R. G., I. C. Fuller, and M. G. Macklin (2015), Resetting the river template: the potential for climate-related extreme floods to transform river geomorphology and ecology, *Freshwater Biology*, *60*(12), 2477-2496, doi: 10.1111/fwb.12639.

Dethier, E., F. J. Magilligan, C. E. Renshaw, and K. H. Nislow (2016), The role of chronic and episodic disturbances on channel-hillslope coupling: the persistence and legacy of extreme floods, *Earth Surface Processes and Landforms*, *41*(10), 1437-1447, doi: 10.1002/esp.3958

Dunne, T. and R. D. Black (1970), Partial Area Contributions to Storm Runoff in a Small New England Watershed, *Water Resour. Res.*, 6(5), 1296-1311.

Eshghi, A., Haughton, D., Legrand, P., Skaletsky, M., Woolford, S. (2011). Identifying Groups: A Comparison of Methodologies, Journal of Data Science, 9, 271-291.

Ferguson, R.I., (2005), Estimating critical stream power for bedload transport calculations in gravel-bed rivers, *Geomorphology*, 70 (1–2), 33–41.

Flores, A.N., Bledsoe, B.P., Cuhaciyan, C.O., Wohl, E.E., (2006), Channel-reach morphology dependence on energy, scale, and hydroclimatic processes with implications for

prediction using geospatial data. *Water Resour. Res*, 42, doi: 10.1029/2005WR004226 W06412.

Foster, D.R. & Aber, J.D. (2004). Forests in Time: The Environmental Consequences of 1,000 Years of Change in New England. New Haven, CT: Yale University Press. 477 pp. ISBN: 0–300–09235–0.

Frissell CA, Liss WJ,Warren CE, Hurley MD. 1986. A hierarchical framework for stream habitat classification: viewing streams in a watershed context. Environmental Management 10: 199–214.

Fripp, J. B. and Diplas, P., (1993), Surface Sampling in Gravel Streams. *ASCE Journal of Hydraulic Engineering*, 119, 473-490.

Fryirs K. (2013) (Dis)Connectivity in catchment sediment cascades: a fresh look at the sediment delivery problem. Earth Surface Processes and Landforms, 38, 30-46.

Fryirs, K. A. (2017), River sensitivity: A lost foundation concept in fluvial geomorphology, Earth Surf. Processes Landforms, doi:10.1002/esp.3940,

Fryirs, K.A., G.J.Brierley, N. J. Preston, and M. Kasai (2007), Buffers, barriers and blankets: The (dis)connectivity of catchment-scale sediment cascades, *Catena*, 70 (49-67).

Fytilis, N. and D. M. Rizzo, 2013, Coupling self-organizing maps with a Naıve Bayesian classifier: Stream classification studies using multiple assessment data. *Water Resources Research*, 49: 7747–7762, doi:10.1002/2012WR013422.

Gartner, J. D., W. B. Dade, C.E. Renshaw, F.J. Magilligan and E. M. Buraas (2015), Gradients in stream power influence lateral and downstream sediment flux in floods, *Geology*, 43(11), 983-986, doi:10.1130/G36969.1.

Gellis, A.C., C.R. Hupp, M.J. Pavich, J.M. Landwehr, W.S.L. Banks, B.E. Hubbard, M.J. Langland, J.C. Ritchie, and J.M. Reuter. 2009. Sources, Transport, and Storage of Sediment at Selected Sites in the Chesapeake Bay Watershed. Scientific Investigations Report 2008– 5186. U.S. Geological Survey, Reston, VA.

Giles, C. D., P. D. F. Isles, T. Manley, Y. Xu, G. K. Druschel, and A. W. Schroth (2016), The mobility of phosphorus, iron, and manganese through the sediment–water continuum of a shallow eutrophic freshwater lake under stratified and mixed water-column conditions, *Biogeochemistry*, 127, 15–34, doi:10.1007/s10533-015-0144-x.

Grossberg, S., 1972. A neural theory of punishment and avoidance: II. Quantitative theory. Mathematical Biosciences 15, 253–285.

Guilbert, J., A. K. Betts, D. M. Rizzo, B. Beckage, and A. Bomblies. 2015. Characterization of increased persistence and intensity of precipitation in the Northeastern United States. Geophysical Research Letters. DOI: 10.1002/2015GL063124.

Guilbert, J., B. Beckage, J. M. Winter, R. M. Horton, T. Perkins, and A. Bomblies (2014), Impacts of projected climate change over the Lake Champlain Basin in Vermont, *J. Appl. Meteorol. Climatol.*, 53, 1861-1875, doi:10.1175/JAMC-D-13-0338.1.

Hack, J.T., 1957, Studies of longitudinal stream profiles in Virginia and Maryland, *in* Shorter contributions to general geology: U.S. Geological Survey Professional Paper 294B, p. 45–97.

Harrelson, Cheryl C., C.L. Rawlins, and J. Potyondy. 1994. Stream channel reference sites: an illustrated guide to field technique. General Technical Report RM-245. Fort Collins, CO:

U.S. Department of Agriculture, Forest Service, Rocky Mountain Forest and Range Experiment Station. 61p. https://www.fs.fed.us/rm/pubs_rm/rm_gtr245.pdf

Hecht-Nielson, R. (1987), Counterpropagation Networks, *Applied Opt*., 26(23).

Hodgkins, G. A., & Dudley, R. W. (2005). Changes in the magnitude of annual and monthly streamflows in New England, 1902 – 2002. *US Geological Survey Scientific Investigations Report 2005-5235*.

Hooke, J.M. and Redmond, C.E. 1992: Causes and nature of river planform change. In Billi, P., Hey, R.D., Thorne, C.R. and Taccont, P., editors, *Dynamics of gravel-bed rivers*. Chichester: John Wiley, 559–71.

Howarth, R.W., G. Billen, D. Swaney, A. Townsend, N. Jaworski, K. Lajtha, J.A. Downing, E.R. Elmgren, N. Caraco, T. Jordan, F. Berendse, J. Freney, V. Kudeyarov, P. Murdoch, H. Zhaoliang, and H. Zhu. 1995. Regional nitrogen budgets and riverine N & P fluxes for the drainages to the North Atlantic Ocean: Natural and human influences. Biogeochemistry 35(1):75-139.

Isles, P. D. F., C. D. Giles, T. A. Gearhart, Y. Xu, G. K. Druschel, and A. W. Schroth (2015), Dynamic internal drivers of a historically severe cyanobacteria bloom in Lake Champlain revealed through comprehensive monitoring, *J. Great Lakes Res.*, 41(3), 818–829, doi:10.1016/j.jglr.2015.06.006.

Isles, P. D. F., Y. Xu, J. Stockwell, A. W. Schroth (2017), Climate-driven changes in energy and mass inputs systematically alter nutrient concentration and stoichiometry in deep and shallow regions of Lake Champlain, *Biogeochemistry*, 133, 201–217, doi:10.1007/s10533-017-0327-8.

James, L. A. (2013). Legacy sediment: Definitions and processes of episodically produced anthropogenic sediment. *Anthropocene, 2*, 16–26.

Jaquith, S., and M. Kline, 2001, Vermont regional hydraulic geometry curves: Waterbury, VT, Vermont Water Quality Division, accessed March 6, 2003 (http://www.anr.state.vt.us/dec/waterq/rivers/docs/rv_hydraulicgeocurves.pdf),.

Jaquith, S., and M. Kline, 2006, Vermont regional hydraulic geometry curves: Waterbury, VT, Vermont Water Quality Division, accessed November 21, 2017: http://dec.vermont.gov/sites/dec/files/wsm/rivers/docs/assessment-protocol-appendices/J-Appendix-J-06-Hydraulic-Geometry-Curves.pdf.

Karymbalis, E., K. Gaki-Papanastassiou and M. Ferentinou (2010), Fan deltas classification coupling morphometric analysis and artificial neural networks: The case of NW coast of Gulf of Corinth, Greece, *Hellenic Journal of Geosciences*, 45, 133-146.

Kline, M. 2010. Vermont ANR River Corridor Planning Guide: to Identify and Develop River Corridor Protection and Restoration Projects, 2nd edition. Vermont Agency of Natural Resources. Waterbury, Vermont.

Kline, M., C. Alexander, S. Pytlik, S. Jaquith, and S. Pomeroy, 2009. Vermont Stream Geomorphic Assessment Protocol Handbooks. Vermont Agency of Natural Resources, Waterbury, Vermont. http://dec.vermont.gov/watershed/rivers/river-corridor-and-floodplain-protection/geomorphic-assessment

Kline, M., & Cahoon, B. (2010). Protecting River Corridors in Vermont. *Journal of the American Water Resources Association, 1*(10). doi: 10.1111/j.1752-1688.2010.00417.x

Knighton, D., 1998, Fluvial Forms and Processes. New York, NY: Routledge, 383 pp.

Kohonen, T. (1990), The Self-Organizing Map, *Proceedings of the IEEE*, 78(9), 1464-1480.

Kohonen, T. (2001), *Self-organizing maps* (3rd ed.), Springer, Berlin–Heidelberg, Germany.

Kohonen, T. (2013), Essentials of the Self-Organizing Map, *Neural Networks*, 37, 52-65, doi:10.1016/j.neunet.2012.09.018.

Lane, E.W. 1955. The Importance of Fluvial Morphology in Hydraulic Engineering, American Society of Civil Engineering, Proceedings, 81, paper 745: 1-17.

Lea, D.M.; Legleiter, C.J. Mapping spatial patterns of stream power and channel change along a gravel-bed river in northern Yellowstone. Geomorphology 2016, 252, 66–79.

Lenzi, M.A., Mao, L., Comiti, F., (2006), Effective discharge for sediment transport in a mountain river: computational approaches and geomorphic effectiveness. *J. Hydrol.* 326, 257–276.

Leopold, L. B., (1994), A View of the River, Cambridge, Massachusetts: Harvard University Press.

Leopold, L.B., M.G. Wolman and J.P. Miller, (1995), Fluvial Processes in Geomorphology. Dover Publications. ISBN 0-486-68588-8.

Lisenby, P. E., and K. Fryirs (2016), Catchment- and reach-scale controls on the distribution and expectation of geomorphic channel adjustment, *Water Resour. Res*., 52, 3408–3427, doi:10.1002/2015WR017747.

Livers, B. and E. Wohl (2015), An evaluation of stream characteristics in glacial versus fluvial process domains in the Colorado Front Range, *Geomorphology*, 231, 72–82.

Magilligan, F.J., 1992. Thresholds and the spatial variability of flood power during extreme floods. Geomorphology 5, 373–390.

Magilligan, F., Haynie, H., Nislow, K., 2008. Channel adjustments to dams in the Connecticut River basin: implications for forested mesic watersheds. Ann. Assoc. Am. Geogr. 98, 267–284.

Magilligan, F.J., E.M. Buraas, C.E. Renshaw, 2015. The efficacy of streampower and flow duration on geomorphic responses to catastrophic flooding. Geomorphology, 228, 175-188.

Mangiameli, P., S. K. Chen, and D. West (1996), A comparison of SOM neural network and hierarchical clustering methods, *Eur. J. Oper. Res*., 93(2), 402–417.

McClain, M. E, E. W. Boyer, C. L. Dent, S. E. Gergel, N. B. Grimm, P. M. Groffman, S. C. Hart, J. W. Harvey, C. A. Johnston, E. Mayorga, W. H. McDowell, and G. Pinay (2003), Biogeochemical Hot Spots and Hot Moments at the Interface of Terrestrial and Aquatic Ecosystems, *Ecosystems*, 6, 301-312, doi:10.1007/s10021-003-0161-9.

Miller, A.J., 1990. Flood hydrology and geomorphic effectiveness in the Central Appalachians. Earth Surf. Process. Landf. 15, 119–134.

Montgomery, D. R. (1999), Process domains and the river continuum, *Journal of the American Water Resources Association*, 35(2), 397–410.

Montgomery, D.R. and Buffington, J.M., (1997), Channel-reach morphology in mountain drainage basins, *Geological Society of America Bulletin*, 109 (5), 596-611.

Nanson, G.C. and J.C. Croke (1992), A genetic classification of floodplains, *Geomorphology*, 4(6), 459-486.

Noe, Gregory B. and Cliff R. Hupp, 2005, Carbon, Nitrogen, and Phosphorus Accumulation in Floodplains of Atlantic Coastal Plain Rivers, USA. Ecological Applications, 15(4): 1178-1190.

Oksanen, J., F. G. Blanchet, M. Friendly, R. Kindt, P. Legendre, D. McGlinn, P. R. Minchin, R. B. O'Hara, G. L. Simpson, P. Solymos, M. Henry, H. Stevens, E. Szoecs and H. Wagner, (2017), vegan: Community Ecology Package. R package version 2.4-3, https://CRAN.R-project.org/package=vegan.

Olson, S. A. (2014), Estimation of flood discharges at selected annual exceedance probabilities for unregulated, rural streams in Vermont, *with a section on* Vermont regional skew regression, by Veilleux, A. G., *Scientific Investigations Report 2014–5078*, U.S. Geological Survey, Washington, D. C., doi:10.3133/sir20145078

Park, Y.-S., R. Cereghino, A. Compin, and S. Lek (2003), Applications of artificial neural networks for patterning and predicting aquatic insect species richness in running waters, *Ecological Modelling*, 160, 265-280, doi:10.1016/j.ecoinf.2015.08.011.

Parker, C., C.R. Thorne, and N. J. Clifford (2014), Development of ST:REAM: a reach-based stream power balance approach for predicting alluvial river channel adjustment, *Earth Surface Processes and Landforms*, doi: 10.1002/esp.3641.

Parker, C., Clifford, N.J., Thorne, C.R., (2011), Understanding the influence of slope on the threshold of coarse grain motion: revisiting critical stream power, *Geomorphology*, 126, 51–65.

Paulson, R. W., E.B. Chase, R.S. Roberts, D.W. Moody, 1989, National Water Summary 1988-89—Hydrologic Events and Floods and Droughts. USGS Water-Supply Paper 2375, https://pubs.usgs.gov/wsp/2375/report.pdf.

Pearce, A. R., D. M. Rizzo, and P. J. Mouser (2011), Subsurface characterization of groundwater contaminated by landfill leachate using microbial community profile data and a non-parametric decision making process, *Water Resour. Res*., 47(6), W06511, doi:10.1029/2010WR009992.

Pearce, A. R., D. M. Rizzo, M. C. Watzin, and G. K. Druschel (2013), Unraveling Associations between Cyanobacteria Blooms and In-Lake Environmental Conditions in Missisquoi Bay, Lake Champlain, USA, Using a Modified Self-Organizing Map, *Environ. Sci. Technol.*, 47, 14267−14274, doi:10.1021/es403490g.

Pfankuch, D. J. (1975), Stream reach inventory and channel stability evaluation. U.S. Department of Agriculture Forest Service. Region 1. Missoula, Montana.

Phillips, J.D. (2003), Sources of nonlinearity and complexity in geomorphic systems. *Progress in Physical Geography*, 26, 339–361, doi:10.1191/0309133303pp340ra.

Phillips, R.T.J., J. R. Desloges (2014a), Glacially conditioned specific stream powers in low-relief river catchments of the southern Laurentian Great Lakes, *Geomorphology*, 206, 271–287, doi:10.1016/j.geomorph.2013.09.030.

Phillips, R.T.J., J. R. Desloges (2014b), Alluvial floodplain classification by multivariate clustering and discriminant analysis for low-relief glacially conditioned river catchments, *Earth Surf. Process. Landforms*, doi:10.1002/esp.3681.

Pickup, G., Rieger, W.A., 1979. A conceptual model of the relationship between channel characteristics and discharge. Earth Surface Processes 4, 37–42.

Poff, N. L., J. D. Allan, M. B. Bain, J. R. Karr, K. L. Pres-tegaard, B. D. Richter, R. E. Sparks, and J. C. Stromberg. 1997. The natural flow regime: a paradigm for river con-servation and restoration. BioScience 47:769-784.

Pringle, C. (2003). What is hydrologic connectivity and why is it ecologically important? *Hydrological Processes*, *17*, 2685–2689.

R Core Team, (2017), R: A language and environment for statistical computing. R Foundation for Statistical Computing, Vienna, Austria, ISBN 3-900051-07-0, URL: http://www.R-project.org/.

Randall, A. D. (1996), Mean annual runoff, precipitation, and evapotranspiration in the glaciated northeastern United States, 1951–1980, *Open-File Report 96-395*, U.S. Geological Survey, Washington, D.C.

Raven, P.J., N. Holmes, F.H. Dawson, P.J.A. Fox, M. Everard, I.R. Fozzard, K.J. Rouen (1998), River Habitat Quality: the physical character of rivers and streams in the UK and Isle of Man. River Habitat Survey Report No. 2, Environment Agency.

Rice, S.P., Church, M., 1996, Sampling surficial fluvial gravels: the precision of size distribution percentile estimates. Journal of Sedimentary Research. 66(3): 654-665.

Rice, S.P., Church, M., 1998. Grain size along two gravel-bed rivers: Statistical variation, spatial pattern and sedimentary links. Earth Surface Processes and Landforms 23: 345-363.

Righini, M., Surian, N.,Wohl, E., Marchi, L., Comiti, F., Amponsah, W., Borga, M., 2017. Geomorphic response to an extreme flood in two Mediterranean rivers (northeastern Sardinia, Italy): analysis of controlling factors. Geomorphology 290:184–199, doi:10.1016/j.geomorph.2017.04.014.

Rinaldi, M., N. Surian, F. Comiti, M. Bussettini (2013), A method for the assessment and analysis of the hydromorphological condition of Italian streams: the Morphological Quality Index (MQI), *Geomorphology*, 180-181, 96–108.

Rosgen, D. (1996), Applied Fluvial Morphology, Wildland Hydrology Books, Pagosa Springs, CO. ISBN 0 965 32890 2.

Rosgen, D., (2006), Watershed Assessment for River Stability and Sediment Supply, WARSSS. Wildland Hydrology Books, Ft. Collins, CO, ISBN 13: 978-0979130809.

Schumm, S.A. (1984), The Fluvial System. New York, NY: John Wiley and Sons.

Schumm, S.A. (2005), River Variability and Complexity, New York, NY: Cambridge University Press.

Schumm, S.A., Harvey, M.D., and Watson, C.C., (1984), Incised Channels Morphology, Dynamics and Control. Water Resources Publications: Littleton, CO.

Schumm SA, Rea DK (1995), Sediment yield from disturbed earth systems, *Geology*, 23, 391-394.

Shanley, J. B., and J. C. Denner (1999), The hydrology of the Lake Champlain Basin, in *Lake Champlain in transition-From research toward restoration*, edited by T. O. Manley, P. L. Manley, pp. 41-66, American Geophysical Union, Washington, D.C., doi: 10.1029/WS001p0041.

Simon, A. and Hupp, C., 1986, Channel evolution in modified Tennesee channels in Proceedings of the 4th Federal Interagency Sedimentation Conference, Las Vegas US Government Printing Office, Washington, DC, 571-582.

Simon, A. and Rinaldi M, 2006. Disturbance, stream incision, and channel evolution: the roles of excess transport capacity and boundary materials in controlling channel response . Geomorphology 79 361–83.

Simon, A., Doyle, M., Kondolf, M., Shields Jr., F., Rhoads, B., & Mcphillips, M. (2007). Critical evaluation of how the Rosgen Classification and associated "Natural Channel Design" methods fail to integrate and quantify fluvial processes and channel response. *Journal of the American Water Resources Association*, 1117-1131.

Somerville, D.E. and B.A. Pruitt, 2004. Physical Stream Assessment: A Review of Selected Protocols for Use in the Clean Water Act Section 404 Program. September 2004. Prepared for the U.S. Environmental Protection Agency, Office of Wetlands, Oceans, and Watersheds, Wetlands Division (Order No. 3W-0503-NATX). Washington, D.C., 213 pp.

Stewart, D. P. and P. MacClintock (1969), The Surficial Geology and Pleistocene History of Vermont, *Bulletin No. 31*, Vermont Geological Survey, Montpelier, VT.

Stojkovica, M., V. Simic, D. Milosevic, D. Mancev, T. Penczak (2013), Visualization of fish community distribution patterns using the self-organizing map: A case study of the Great Morava River system (Serbia), *Ecological Modelling*, 248, 20-29, doi:10.1016/j.ecolmodel.2012.09.014.

Surian, N., Righini, M., Lucía, A, Nardi, L., Amponsah, W., Benvenuti, M., Borga, M., Cavalli, M., Comiti, F., Marchi, L., Rinaldi, M., Viero. A., 2016, Channel response to extreme floods: Insights on controlling factors from six mountain rivers in northern Apennines, Italy. *Geomorphology*, 272: 78-91. doi:10.1016/j.geomorph.2016.02.002

Surian, N., Mao, L., Giacomin, M., Ziliani, L., 2009. Morphological effects of different channel forming discharges in a gravel-bed river. Earth Surf. Process. Landf. 34, 1093–1107.

Thayer, J. B., R. T. J. Phillips, J. R. Desloges, 2016. Downstream channel adjustment in a low-relief, glacially conditioned watershed, Geomorphology, 262: 101-111. http://dx.doi.org/10.1016/j.geomorph.2016.03.019.

Thompson CJ, Croke JC. 2013. Geomorphic effects, flood power, and channel competence of a catastrophic flood in confined and unconfined reaches of the upper Lockyer valley, southeast Queensland, Australia. Geomorphology 197: 156–169. DOI: 10.1016/j.geomorph.2013.05.006

Thompson, E. H. and Sorenson, E. R., 2000, Wetland, Woodland, Wildland: A guide to the natural communities of Vermont, Hanover, NH: University Press of New England.

Toone, J., S. Rice, and H. Piégay (2014), Spatial discontinuity and temporal evolution of channel morphology along a mixed bedrock-alluvial river, upper Drôme River, southeast France: Contingent responses to external and internal controls, *Geomorphology*, 205, 5–16, doi:10.1016/j.geomorph.2012.05.033.

U.S. Environmental Protection Agency (2016) Phosphorus TMDLs for Vermont Segments of Lake Champlain. Available at: https://www.epa.gov/tmdl/lake-champlain-phosphorus-tmdlcommitment-clean-water

USGS (2018), National Water Information System, http://waterdata.usgs.gov/vt/nwis/rt.

Vesanto, J. and E. Alhoniemi (2000), Clustering of the Self-Organizing Map, *IEEE Transactions on Neural Networks*, 11(3), 586-600.

Vesanto, J., J. Himberg, E. Alhoniemi, and J. Parhankangas (2000), SOM Toolbox for Matlab 5. *Technical Report A57*, Neural Networks Research Centre, Helsinki University of Technology, Helsinki, Finland.

Vocal Ferencevic M, Ashmore P. 2012. Creating and evaluating digital elevation model-based stream-power map as a stream assessment tool. River Research and Applications 28: 1394–1416.

VT Agency of Natural Resources (2011), Vermont Clean and Clear Action Plan 2010 Annual Report, submitted to the Vermont General Assembly, February 1, 2011.

[dataset] VT Agency of Natural Resources, Stream Geomorphic Assessment Data Management System, 2017, https://anrweb.vt.gov/DEC/SGA/Default.aspx

Vermont Department of Environmental Conservation, 2016, Vermont Rivers & Roads Field Manual: A Guide for Considering the River and Habitat in the Design, Construction and Maintenance of Transportation Infrastructure in Vermont, available at: http://dec.vermont.gov/sites/dec/files/wsm/rivers/docs/2016_ RiverAndRoadFieldManual.pdf.

Walling DE (1983) Scale Problems in Hydrology The sediment delivery problem. Journal of Hydrology, 65, 209-237.

Walter, R.C.,Merritts, D.J., 2008. Natural streams and the legacy of water-powered mills. Science. 319 (5861), 299–304.

Weber, M. D. and G. B. Pasternack (2017), Valley-scale morphology drives differences in fluvial sediment budgets and incision rates during contrasting flow regimes, *Geomorphology*, 288, 39-51, doi:10.1016/j.geomorph.2017.03.018.

Wehrens, R., and L. M. C. Buydens (2007), Self- and Super-organising Maps in R: the kohonen package. *J. Stat. Softw*. 21 (5), 1-19, https://www.jstatsoft.org/index.

Wohl, E. (2018), Geomorphic context in rivers, *Progress in Physical Geography*, 1–17, doi: 10.1177/0309133318776488.

Wohl, E. (2010), A brief review of the process domain concepts and its application to quantifying sediment dynamics in bedrock canyons, *Terra Nova*, 22, 411–416.

Yellen, B., J. D. Woodruff, L. N. Kratz, S. B. Mabee, J. Morrison, A. M. Martini (2014), Source, conveyance and fate of suspended sediments following Hurricane Irene. New England, USA, *Geomorphology*, 226, 124-134, doi:10.1016/j.geomorph.2014.07.028.

CHAPTER 5. CONCLUSIONS AND FUTURE DIRECTIONS

This dissertation has followed an earlier career focused on river conservation and restoration projects in service to landowners, municipalities, nonprofit groups, and state and federal agencies. During previous assessment work to evaluate river sensitivity to various natural and human perturbations, I observed the complex and nonlinear behavior of rivers, and noted that available assessment tools were limited in their ability to adequately model this complexity. Consequently, I was motivated to return to graduate study to learn more about machine-learning approaches and advanced statistical methods to aid water resource management and decision-making.

The overarching objective of this work was to improve the understanding of sediment cascades in glacially-conditioned humid temperate regions using Vermont catchments as a test bed. In particular, this dissertation has focused on the application of data-driven methods and Bayesian statistics to sediment dynamics at three spatial scales ranging from the basin, to catchment, to reach levels.

In Chapter 2, I examined concentration-discharge dynamics, using the Lake Champlain Basin as a test bed by first applying Bayesian regression methods to long-term water quality and streamflow data from 18 tributary basins. The probability distribution on pre- and post-threshold regression slopes from a segmented regression model was interpreted to discern between "hydrologically-driven" stages of constituent export and "reactive" stages that were more dominated by biogeochemical cycling. I then applied a nonparametric clustering and data visualization approach, using a Self-Organizing Map (SOM), that identified two unique basin clusters of high sediment and

phosphorus flux. In the first group, sediment and particulate phosphorus flux was hydrologically-driven and disproportionately occurring during relatively infrequent, high-magnitude runoff events – generating an acute response that may be more consequential in the context of loading to the lake (e.g., TMDLs and sediment budgets). In the second group, the sourcing and mobilization of sediment and nutrients were more bimodal, resulting from both hydrologic processes at post-threshold discharges and reactive processes (such as nutrient cycling or lateral/vertical exchanges of fine sediment) that dominate at pre-threshold discharges. This latter functional stage generates a more chronic concentration response that may be of greater concern in the context of ecological balance in the receiving waters, and important for the prediction of harmful algal blooms. Future work will involve application of Bayesian hierarchical analysis to examine temporal trends of these hydrologic-driven and reactive stages in constituent export, on a seasonal to multi-year time scale.

At the catchment scale (Chapter 4) I illustrated the application of a flexible Bayesian un-mixing model, utilizing statistical techniques to discriminate between surface and subsurface sources of fine particulates (clay, silt, fine sand) carried in suspension by the river. Results suggested that, at a catchment scale, runoff is dominated by subsurface sources of sediment including erosional gullies, failing streambanks, and eroding roads and road ditches. This work has set the stage for future exploration of the Bayesian model framework to model source ascription variability in space and time through explicit consideration of transport processes and use of informative priors based on distribution of storm hysteresis patterns over a given target-sample deployment. Having additional information about ‘hot spots’ and ‘hot moments’ of sediment erosion

in the watershed will help to prioritize best management practices and corrective measures to address sediment and nutrient loading.

Finally, I applied a two-stage SOM to river metrics (Chapter 5) to characterize spatially-variable sediment erosion and deposition at a reach scale in response to natural and human perturbations. The SOM clustered multivariate geomorphic assessment data for 193 Vermont stream reaches into seven sediment process domains that constitute net sources or sinks of coarse and fine sediment on a mean annual temporal scale (i.e., Q1.5 discharge). Results have broadly replicated and refined six classifications currently in use by river managers in Vermont. The iterative process of training these neural networks, in consultation with stakeholders, has identified geomorphic and hydraulic drivers of significance operating at the cross-section scale (e.g., relative roughness) and reach-scale (e.g., valley confinement, slope). Our approach represents an extension of earlier work that has typically applied parametric, multivariate statistical methods to infer process domains from large data sets of geomorphic and hydraulic variables. In future, this computational framework utilizing nonparametric, smart classifiers can be linked to a geographic information system to automate the prediction of sediment transport regimes in response to various channel and catchment modifications, supporting adaptive management of rivers, While the driving variables, and resultant sediment process domains, may vary by geographic region, I expect the overall statistical framework to be transferable to other catchments in humid temperate regions.

COMPREHENSIVE BIBLIOGRAPHY

Abban, B., A. N. Papanicolaou, M. K. Cowles, C. G. Wilson, O. Abaci, K. Wacha, K. Schilling, and D. Schnoebelen (2016), An enhanced Bayesian fingerprinting framework for studying sediment source dynamics in intensively managed landscapes, *Water Resources Research*, 52, doi:10.1002/2015WR018030.

Alameddine, I., S. S. Qian, and K. H. Reckhow (2011), A Bayesian changepoint-threshold model to examine the effect of TMDL implementation on the flow-nitrogen concentration relationship in the Neuse River basin, *Water Res.*, 45, 51–62, doi:10.1016/j.watres.2010.08.003.

Alvarez-Guerra, M., C. González-Piñuela, A. Andrés, B. Galán, and J. R. Viguri (2008), Assessment of Self-Organizing Map artificial neural networks for the classification of sediment quality, *Environment International*, 34(6), 782-790, doi:10.1016/j.envint.2008.01.006.

Anderson, M. J. (2001), A new method for non-parametric multivariate analysis of variance, *Austral Ecology*, 26, 32-46, doi:10.1111/j.1442-9993.2001.01070.pp.x.

Anderson D.M., Glibert P.M., Burkholder J.M. (2002), Harmful algal blooms and eutrophication: nutrient sources, composition, and consequences, *Estuaries*, 25, 704–726

Anderson, I., D. M. Rizzo, D. R. Huston, and M. M. Dewoolkar (2017), Analysis of bridge and stream conditions of over 300 Vermont bridges damaged in Tropical Storm Irene, *Structure and Infrastructure Engineering*, 1-14, doi: 10.1080/15732479.2017.1285329.

Andrews, E.D., 1983, Entrainment of gravel from naturally sorted riverbed material. Geol. Soc. Amer. Bull. 94, 1225–1231.

Appleby, P., Oldfield, F., 1992. Application of 210Pb to sedimentation studies. In: Ivanovich, M., Harmon, R.S. (Eds.), Uranium Series Disequilibrium. Oxford University Press, Oxford, UK, pp. 731–778.

Asselman, N. E. M. (2000), Fitting and interpretation of sediment rating curves, *J. Hydrology*, 234, 228-248, doi:10.1016/S0022-1694(00)00253-5.

Bagnold, R.A., 1966. An Approach to the Sediment Transport Problem from General Physics. USGS Professional Paper, vol. 422-J. Washington, DC.

Baker, V. R. (1977), Stream-channel response to floods, with examples from central Texas, *GSA Bulletin*, 88, 1057-1071.

Ballantyne, C. K. (2002), Paraglacial geomorphology, *Quaternary Science Reviews*, 21, 1935-2017.

Barbeta, A. J., Peñuelas (2017), Relative contribution of groundwater to plant transpiration estimated with stable isotopes, *Scientific Reports*, 7, 1, doi:10.1038/s41598-017-09643-x.

Barthod, L.R.M., Liu, K., Lobb, D.A., Owens, P.N., Martinez-Carreras, N., Koiter, A.J., Petticrew, E. L., McCullough, G.K., Liu, C., Gaspar, L., 2015, Selecting color-based tracers and classifying sediment sources in the assessment of sediment dynamics using sediment source fingerprinting. J. Environ. Qual., 44: 1605-1616.

Basu, N. B., G. Destouni, J. W. Jawitz, S. E. Thompson, N. V. Loukinova, A. Darracq, S. Zanardo, M. Yaeger, M. Sivapalan, A. Rinaldo, and P. Suresh C. Rao (2010), Nutrient

loads exported from managed catchments reveal emergent biogeochemical stationarity, *Geophys. Res. Lett.*, 37, L23404, doi:10.1029/2010GL045168.

Basu, N. B., S. E. Thompson, and P. S. C. Rao (2011), Hydrologic and biogeochemical functioning of intensively managed catchments: A synthesis of top-down analyses, *Water Resour. Res.*, 47, W00J15, doi:10.1029/2011WR010800.

Beers, F. W., 1873, Atlas of Washington County, Vermont.

Benda, L., and T. Dunne (1997), Stochastic forcing of sediment supply to channel networks from landsliding and debris flow, *Water Resour. Res.*, 33, 2849-2863.

Benda, L., M. A. Hassan, M. Church, and C. L. May (2005), Geomorphology of steepland headwaters: the transition from hillslopes to channels, *Journal of the American Water Resources Association*, 41(4), 835-851.

Bende-Michl, U., K. Verburg, and H. P. Creswell (2013), High-frequency nutrient monitoring to infer seasonal patterns in catchment source availability, mobilization and delivery, *Environ. Monit. Assess.*, 185, 9191-9219.

Bennett, G.L., P. Molnar, B.W. McArdell, and P. Burlando (2014), A probabilistic sediment cascade model of sediment transfer in the Illgraben, *Water Resources Research*, 50, 1225-1244.

Besaw, L. E., D.M. Rizzo, M. Kline, K.L. Underwood, J.J. Doris, L.A. Morrissey, K. Pelletier, (2009), Stream classification using hierarchical artificial neural networks: A fluvial hazard management tool, *Journal of Hydrology*, 373, 34-43, doi:10.1016/j.jhydrol.2009.04.007.

Bierman PR (2010) Clearcutting, Reforestation, and the coming of the Interstate: Vermont's Photographic Record of Landscape Use and Response In: *Repeat Photography: Methods and Applications in the Geological and Ecological Sciences.* (eds Webb RH, Boyer DE, Turner RM) pp Page., Cambridge University Press

Bierman, P., A. Lini, P. Zehfuss and A. Church, 1997, Postglacial ponds and alluvial fans: recorders of holocene landscape history, *GSA Today*, 7(10), 1-8.

Bieroza, M. Z. and A. L. Heathwaite (2015), Seasonal variation in phosphorus concentration–discharge hysteresis inferred from high-frequency in situ monitoring, *J. Hydrology*, 524, 333-347, doi:10.1016/j.hydrol.2015.02.036.

Bizzi, S., and Lerner, D.N., (2013), The use of stream power as an indicator of channel sensitivity to erosion and deposition processes, *River Research and Applications*, 31, 16–27, doi:10.1002 /rra.2717.

Bizzi S, Demarchi L, Grabowski RC, Weissteiner CJ, Bund W (2015) The use of remote sensing to characterise hydromorphological properties of European rivers. Aquatic Sciences, 78, 57-70.

Boano, F., J. W. Harvey, A. Marion, A. I. Packman, R. Revelli, L. Ridolfi, and A. Wörman (2014), Hyporheic flow and transport processes: Mechanisms, models, and biogeochemical implications, *Rev. Geophys.*, 52, 603–679, doi:10.1002/2012RG000417.

Booth, D.B., (1990), Stream-channel incision following drainage basin urbanization. *Water Resour. Bull. Am. Water Resour. Assoc*. 26 (3), 407–417, doi: 10.1111/j.1752-1688.1990.tb01380.x

Borg, J. L. (2010), Streambank Stability and Sediment Tracing in Vermont Waterways, University of Vermont, Dept of Civil & Environmental Engineering, M.S. Thesis.

Borselli, L., P. Cassi, D. Torri (2008), Prolegomena to sediment and flow connectivity in the landscape: A GIS and field numerical assessment, *Catena*, 75, 268-277.

Bracken, L. J., L. Turnbull, J. Wainwright, P. Bogaart (2014), Sediment connectivity: a framework for understanding sediment transfer at multiple scales, *Earth Surf. Process. Landforms*, doi: 10.1002/esp.3635.

Bracken, L .J. and J. Croke (2007), The concept of hydrological connectivity and its contribution to understanding runoff-dominated geomorphic systems, *Hydrological Processes*, 21, 1749-1763, doi: 10.1002/hyp.6313.

Brakenridge, G. R., P. A. Thomas, L. E. Conkey, J. C. Schiferle, (1988) Fluvial Sedimentation in Response to Postglacial Uplift and Environmental Change, Missisquoi River, Vermont. *Quaternary Research*,30: 190-203, doi: 10.1016/0033-5894(88)90023-3.

Brardinoni, F., Hassan, M.A., (2007), Glacially induced organization of channel-reach morphology in mountain streams. *J. Geophys. Res*., 112, F03013, doi:10.1029/2006JF000741

Brardinoni, F., and M. A. Hassan (2006), Glacial erosion, evolution of river long profiles, and the organization of process domains in mountain drainage basins of coastal British Columbia, *J. Geophys. Res*., 111, F01013, doi:10.1029/2005JF000358.

Brierley, G.J., K. A. Fryirs, (2005), Geomorphology and River Management: Applications of the River Style Framework. Blackwell, Oxford, p. 398.

Brigham, M. E., C. J. McCullough and P. Wilkinson (2001), Analysis of suspended-sediment concentrations and radioisotope levels in the Wild Rice River Basin, Northwestern Minnesota, 1973–1998, *Water-Resources Investigations Rep. 01-4192*, U.S. Department of the Interior, U.S. Geological Survey.

Brookes A. (1987), The distribution and management of channelized streams in Denmark, *Regulated Rivers*, 1: 3–16.

Bull, W.B. (1979), Threshold of critical power in streams. *Bull. Geol. Soc. Am*., 90, 453–464.

Buraas, E.M.,Magilligan, F.J., Renshaw, C.E., Dade, W.B., (2014), Impact of reach geometry on stream channel sensitivity to extreme floods. *Earth Surf. Process. Landf*. http://dx.doi.org/10.1002/esp.3562.

Burt T. and R. Allison (2010), Sediment cascades: an integrated approach. New York, NY: John Wiley & Sons.

Cavalli, M., S. Trevisani, F. Comiti, L. Marchi, 2013. Geomorphometric assessment of spatial sediment connectivity in small Alpine catchments. Geomorphology, 188 (31-41).

Centre d'expertise hydrique Québec (2016), Fiche signalétique de la station 030424: Centre d'expertise hydrique Québec Hydrometric Network level and flow history station database, accessed May 4, 2016 at http://www.cehq.gouv.qc.ca/hydrometrie/historique_donnees/fiche_station.asp?NoStation=030424.

Cereghino, R. and Y.-S. Park (2009), Review of the Self-Organizing Map (SOM) approach in water resources: Commentary, *Environmental Modelling and Software*, 24, 945-947.

Chappell, J. (1983), Thresholds and lags in geomorphologic changes, *Australian Geographer*, 15, 358–66.

Church, M. and J. Ryder, 1972, Paraglacial sedimentation: A consideration of fluvial processes conditioned by glaciation. Geological Society of America Bulletin, 83: 3059-3072.

Church, M., O. Slaymaker (1989), Disequilibrium of Holocene sediment yield in glaciated British Columbia, Nature, 337, 452-454.

Clark, G.M., D.K. Mueller, and M.A Mast. 2000. Nutrient concentrations and yields in undeveloped stream basins of the United States. Journal of the American Water Resources Association 36(4):849–860.

Collins, M. J. (2009). Evidence for Changing Flood Risk in New England Since the Late 20th Century. *Journal of the American Water Resources Association*, *45*(2), 279-290. doi: DOI: 10.1111/j.1752-1688.2008.00277.x

Collins, A.L., and D. E. Walling (2002), Selecting fingerprint properties for discriminating potential suspended sediment sources in river basins, *J. Hydrology*, 261, 218.

Collins, A.L., D. E. Walling, G.J.L. Leeks (1997), Source type ascription for fluvial suspended sediment based on a quantitative fingerprinting technique, *Catena*, 29, 1–27, doi:10.1016/S0341-8162(96)00064-1.

Collins, A.L., Zhang, Y., Hickinbotham, R., Bailey, G., Darlington, S., Grenfell, S.E., Evans, R., Blackwell, M., (2013), Contemporary fine-grained bed sediment sources across the River Wensum Demonstration Test Catchment, UK. Hydrol. Process. 27, 857e884.

Cooper, R. J., T. Krueger, K. M. Hiscock, and B. G. Rawlins (2014), Sensitivity of fluvial sediment source apportionment to mixing model assumptions: A Bayesian model comparison, *Water Resour. Res*., 50, 9031–9047, doi:10.1002/2014WR016194.

Costa, J.E. and J. E. O'Connor (1995), Geomorphically effective floods. In Natural and Anthropogenic Influences in Fluvial Geomorphology, Costa JE, Miller AJ, Potter KW, Wilcock PR (eds). American Geophysical Union: Washington, DC; 45–56.

Croke, J., Mockler, S., Fogarty, P. and Takken, I., 2005. Sediment concentration changes in runoff pathways from a forest road network and the resultant spatial pattern of catchment connectivity. Geomorphology, 68, 257-268.

Croke, J., K. Fryirs, C. Thompson, 2013. Channel-floodplain connectivity during an extreme flood event: implications for sediment erosion, deposition, and delivery. Earth Surface Processes and Landforms, 38 (1444-1456).

Clark, G.M., D.K. Mueller, and M.A Mast. 2000. Nutrient concentrations and yields in undeveloped stream basins of the United States. Journal of the American Water Resources Association 36(4):849–860.

Denwood, M. J. (2016), runjags: An R Package Providing Interface Utilities, Model Templates, Parallel Computing Methods and Additional Distributions for MCMC Models in JAGS, *J. Stat. Softw*., 71(9), 1-25, doi:10.18637/jss.v071.i09.

Death, R. G., I. C. Fuller, and M. G. Macklin (2015), Resetting the river template: the potential for climate-related extreme floods to transform river geomorphology and ecology, *Freshwater Biology*, *60*(12), 2477-2496, doi: 10.1111/fwb.12639.

Dethier, E., F. J. Magilligan, C. E. Renshaw, and K. H. Nislow (2016), The role of chronic and episodic disturbances on channel-hillslope coupling: the persistence and legacy of

extreme floods, *Earth Surface Processes and Landforms*, *41*(10), 1437-1447, doi: 10.1002/esp.3958

DeWolfe, M. N., W. C. Hession, and M. C. Watzin (2004), Sediment and phosphorus loads from streambank erosion in Vermont, USA., in *Critical Transactions in Water and Environmental Resources Management*, edited by G. Sehlke, D. F. Hayes and D. K. Stevens, pp. 1-10, American Society of Civil Engineers, Reston, VA.

Dietrich, W.E. and T. Dunne, 1978. Sediment budget for a small catchment in mountainous terrain. *Zeitschrift für Geomorphologie, Supplementeband*, 29 (191-206).

Doyle, M. W., E. H. Stanley, D. L. Strayer, R. B. Jacobson, and J. C. Schmidt (2005), Effective discharge analysis of ecological processes in streams, *Water Resour. Res.*, 41, W11411, doi:10.1029/2005WR004222.

Dubrovsky, N.M., Burow, K.R., Clark, G.M., Gronberg, J.M., Hamilton P.A., Hitt, K.J., Mueller, D.K., Munn, M.D., Nolan, B.T., Puckett, L.J., Rupert, M.G., Short, T.M., Spahr, N.E., Sprague, L.A., and Wilber, W.G. 2010. The quality of our Nation's waters—Nutrients in the Nation's streams and groundwater, 1992–2004: U.S. Geological Survey Circular 1350.

Dunn, R., Springston, G., and Donahue, N., 2007, Surficial Geologic Map of the Mad River Watershed, Vermont, Vermont Geological Survey Open File report, VG07-1.

Dunne, T. and R.D. Black (1970), Partial Area Contributions to Storm Runoff in a Small New England Watershed, *Water Resources Research*, 6(5), 1296-1311.

Dutton, C., A.C. Ainsfield, H. Ernstburger. (2013). A novel sediment fingerprinting method using filtration: application to the Mara River, East Africa, J. Soils Sediments, 13: 1708-1723.

Eshghi, A., Haughton, D., Legrand, P., Skaletsky, M., Woolford, S. (2011). Identifying Groups: A Comparison of Methodologies, Journal of Data Science, 9, 271-291.

Ferguson, R.I. (1981), Channel forms and channel changes. In British Rivers, Lewin J. (ed). Allen and Unwin: London: 90-125.

Ferguson, R.I., (2005), Estimating critical stream power for bedload transport calculations in gravel-bed rivers, *Geomorphology*, 70 (1–2), 33–41.

Finlayson, D. P., and D. R. Montgomery (2003), Modeling large-scale fluvial erosion in geographic information systems, *Geomorphology*, 53(1): 147-164. doi:10.1016/S0169-555X(02)00351-3

Fisher, S.G., N. B. Grimm, E. Martı´, R. M. Holmes, and J. B. Jones, Jr. (1998), Material Spiraling in Stream Corridors: A Telescoping Ecosystem Model, *Ecosystems*, 1, 19-34, doi:10.1007/s100219900003.

FISRWG. 1998. Stream Corridor Restoration: Principles, Processes, and Practices. Federal Interagency Stream Restoration Working Group, U.S. Department of Commerce, National Technical Information Service. http://www.nrcs.usda.gov/technical/stream_restoration.

Fitzgerald Environmental Associates, 2008, Upper Mad River Corridor Plan, technical report prepared for Friends of the Mad River, available at: https://friendsofthemadriver.org/documents/FMR_Final_RCP_Report.pdf

Flores, A.N., Bledsoe, B.P., Cuhaciyan, C.O., Wohl, E.E., (2006), Channel-reach morphology dependence on energy, scale, and hydroclimatic processes with implications for

prediction using geospatial data. *Water Resour. Res*, 42, doi: 10.1029/2005WR004226 W06412.

Foster, D.R. & Aber, J.D. (2004). Forests in Time: The Environmental Consequences of 1,000 Years of Change in New England. New Haven, CT: Yale University Press. 477 pp. ISBN: 0–300–09235–0.

Fox, J. F. & A. N. Papanicolaou (2008), An un-mixing model to study watershed erosion processes, *Advances in Water Resources*, 31, 96.

Franzi, D. A., R. D. Fuller, and S. R. Kramer (2009), A preliminary study of nonpoint source runoff in the Little Chazy River watershed, northeastern New York, New York State Department of Environmental Conservation and The Nature Conservancy, http://www.lcbp.org/techreportPDF/chazy-npsrunoffJun09.pdf.

Frissell CA, Liss WJ,Warren CE, Hurley MD. 1986. A hierarchical framework for stream habitat classification: viewing streams in a watershed context. Environmental Management 10: 199–214.

Fripp, J. B. and Diplas, P., (1993), Surface Sampling in Gravel Streams. *ASCE Journal of Hydraulic Engineering*, 119, 473-490.

Frumhoff, P. C., McCarthy, J. J., Melillo, J. M., Moster, S. C., & Wuebbles, D. G. (2007). *Confronting Climate Change in the U.S. Northeast: Science, Impacts, and Solutions*. Cambridge, MA: Union of Concerned Scientists

Fryirs, K, 2013. (Dis)Connectivity in catchment sediment cascades: a fresh look at the sediment delivery problem. Earth Surface Processes and Landforms, 38, 30-46.

Fryirs, K. A. (2017), River sensitivity: A lost foundation concept in fluvial geomorphology, Earth Surf. Processes Landforms, doi:10.1002/esp.3940,

Fryirs, K.A., G.J.Brierley, N. J. Preston, and M. Kasai (2007), Buffers, barriers and blankets: The (dis)connectivity of catchment-scale sediment cascades, *Catena*, 70 (49-67).

Fytilis, N. and D. M. Rizzo (2013), Coupling self-organizing maps with a Naıve Bayesian classifier: Stream classification studies using multiple assessment data, *Water Resour. Res.*, 49, 7747–7762, doi:10.1002/2012WR013422.

Gall, H. E., J. Park, C. J. Harman, J. W. Jawitz, P. S. C. Rao (2013), Landscape filtering of hydrologic and biogeochemical responses in managed catchments, *Landscape Ecology*, 28, 651–664, doi:10.1007/s10980-012-9829-x.

Gartner, J. D., W. B. Dade, C.E. Renshaw, F.J. Magilligan and E. M. Buraas (2015), Gradients in stream power influence lateral and downstream sediment flux in floods, *Geology*, 43(11), 983-986, doi:10.1130/G36969.1.

Gellis, A.C., C.R. Hupp, M.J. Pavich, J.M. Landwehr, W.S.L. Banks, B.E. Hubbard, M.J. Langland, J.C. Ritchie, and J.M. Reuter. 2009. Sources, Transport, and Storage of Sediment at Selected Sites in the Chesapeake Bay Watershed. Scientific Investigations Report 2008– 5186. U.S. Geological Survey, Reston, VA.

Gelman, A., and D. B. Rubin (1992), Inference from iterative simulation using multiple sequences, *Statistical Science*, 7, 457-472.

Gelman, A., Carlin, J. B., Stern, H. S., Rubin, D. B. (2004), *Bayesian Data Analysis*, Chapman & Hall/CRC, Boca Raton, FL.

Geman, S., and D. Geman, (1984). Stochastic relaxation, Gibbs distributions, and the Bayesian restoration of images. *IEEE Transactions on Pattern Analysis and Machine Intelligence*, *6*, 721-741.

Giles, C. D., P. D. F. Isles, T. Manley, Y. Xu, G. K. Druschel, and A. W. Schroth (2016), The mobility of phosphorus, iron, and manganese through the sediment–water continuum of a shallow eutrophic freshwater lake under stratified and mixed water-column conditions, *Biogeochemistry*, 127, 15–34, doi:10.1007/s10533-015-0144-x.

Godsey, S. E., J. W. Kirchner, D. W. Clow (2009), Concentration–discharge relationships reflect chemostatic characteristics of US catchments, *Hydrol. Processes*, 23, 1844-1864, doi: 10.1002/hyp.7315.

Gordón, F., S. I. Perez, A. Hajduk, M. Lezcano and V. Bernal (2017), Dietary patterns in human populations from northwest Patagonia during Holocene: an approach using Binford's frames of reference and Bayesian isotope mixing models, *Archaeological and Anthropological Sciences*,.

Groisman, P. Y., Knight, R. W., & Karl, T. R. (2001). Heavy Precipitation and High Streamflow in the Contiguous United States: Trends in the 20th Century. *Bulletin of the American Meteorological Society*, *82*(2), 219-246Harvey, A. M., 2002. Effective timescales of coupling within fluvial systems. Geomorphology, 44, 175-201.

Grossberg, S., 1972. A neural theory of punishment and avoidance: II. Quantitative theory. Mathematical Biosciences 15, 253–285.

Guilbert, J., B. Beckage, J. M. Winter, R. M. Horton, T. Perkins, and A. Bomblies (2014), Impacts of projected climate change over the Lake Champlain Basin in Vermont, *J. Appl. Meteorol. Climatol.*, 53, 1861-1875, doi:10.1175/JAMC-D-13-0338.1.

Guilbert, J., A. K. Betts, D. M. Rizzo, B. Beckage, and A. Bomblies (2015), Characterization of increased persistence and intensity of precipitation in the Northeastern United States, *Geophys. Res. Lett.*, 42, 1888–1893, doi:10.1002/2015GL063124.

Hack, J.T., 1957, Studies of longitudinal stream profiles in Virginia and Maryland, *in* Shorter contributions to general geology: U.S. Geological Survey Professional Paper 294B, p. 45–97.

Hamshaw, S. D. (2018), Fluvial Processes in Motion: Measuring Bank Erosion and Suspended Sediment Flux using Advanced Geomatic Methods and Machine Learning, *Graduate College Dissertations and Theses*, https://scholarworks.uvm.edu/graddis/827

Hamshaw, S. D., Dewoolkar, M. M.,Schroth, A. W., Wemple, B. C., & Rizzo, D. M. (2018). A new machine-learning approach for classifying hysteresis in suspended-sediment discharge relationships using high-frequency monitoring data. Water Resources Research, 54, 4040–4058. doi: /10.1029/2017WR022238.

Hamshaw, S. D., T. Bryce, D. M. Rizzo, J. O'Neil-Dunne, J. Frolik, and M. M. Dewoolkar (2017), Quantifying streambank movement and topography using unmanned aircraft system photogrammetry with comparison to terrestrial laser scanning, *River Research and Applications*, *33*(8), 1354-1367, doi: 10.1002/rra.3183.

Harrelson, Cheryl C., C.L. Rawlins, and J. Potyondy. 1994. Stream channel reference sites: an illustrated guide to field technique. General Technical Report RM-245. Fort Collins, CO: U.S. Department of Agriculture, Forest Service, Rocky Mountain Forest and Range Experiment Station. 61p. https://www.fs.fed.us/rm/pubs_rm/rm_gtr245.pdf

Harvey, A.M., 2002. Effective timescales of coupling within fluvial systems. Geomorphology 44, 175–201.

Harvey, J., and M. Gooseff (2015), River corridor science: Hydrologic exchange and ecological consequences from bedforms to basins, *Water Resour. Res*., 51, 6893–6922, doi:10.1002/2015WR017617.

Harvey, J. W., J. D. Drummond, R. L. Martin, L. E. McPhillips, A. I. Packman, D. J. Jerolmack, S. H. Stonedahl, A. F. Aubeneau, A. H. Sawyer, L. G. Larsen, and C. R. Tobias (2012), Hydrogeomorphology of the hyporheic zone: Stream solute and fine particle interactions with a dynamic streambed, *J. Geophys. Res*., 117, G00N11, doi:10.1029/2012JG002043.

Hayhoe, K., Wake, C. P., Huntington, T. G., Luo, L., Schwartz, M., Sheffield, J., . . . Wolfe, D. (2007). Past and future changes in climate and hydrological indicators in the U.S. Northeast. *Climate Dynamics, 28*, 381-407.

He, Q., Walling, D., 1996. Use of fallout Pb-210 measurements to investigate longerterm rates and patterns of overbank sediment deposition on the floodplains of lowland rivers. Earth Surface Processes and Landforms 21, 141–154.

Heathwaite, A. L., A. N.Sharpley, and W. J. Gburek. 2000. Integrating phosphorus and nitrogen management at catchment scales. J. Environ. Qual 29:158-166.

Hecht-Nielson, R. (1987), Counterpropagation Networks, *Applied Opt*., 26(23).

Hicks, D. M., B. Gomez, N. A. Trustrum (2000), Erosion thresholds and suspended sediment yields, Waipaoa River Basin, New Zealand, *Water Resour. Res*., 36(4), 1129-1142, doi:10.1029/1999WR900340.

Hirsch, R.M., D. L. Moyer, and S. A. Archfield (2010), Weighted Regressions on Time, Discharge, and Season (WRTDS), with an Application to Chesapeake Bay River Inputs, *J. Am. Water Resour. Assoc.*, 46(5), 857-880, doi:10.1111/j.1752-1688.2010.00482.x.

Hodgkins, G. A., & Dudley, R. W. (2005). Changes in the magnitude of annual and monthly streamflows in New England, 1902 – 2002. *US Geological Survey Scientific Investigations Report 2005-5235*.

Hodgkins, G. A., & Dudley, R. W. (2011). Historical summer base flow and stormflow trends for New England rivers. *Water Resources Research, 47*. doi: 10.1029/2010WR009109.

Hooke, J., 2003. Coarse sediment connectivity in river channel systems: a conceptual framework and methodology. Geomorphology, 56 (79-94).

Hooke, J.M. and Redmond, C.E. 1992: Causes and nature of river planform change. In Billi, P., Hey, R.D., Thorne, C.R. and Taccont, P., editors, *Dynamics of gravel-bed rivers*. Chichester: John Wiley, 559–71.

Howarth, R.W., G. Billen, D. Swaney, A. Townsend, N. Jaworski, K. Lajtha, J.A. Downing, E.R. Elmgren, N. Caraco, T. Jordan, F. Berendse, J. Freney, V. Kudeyarov, P. Murdoch, H. Zhaoliang, and H. Zhu. 1995. Regional nitrogen budgets and riverine N & P fluxes for the drainages to the North Atlantic Ocean: Natural and human influences. Biogeochemistry 35(1):75-139.

Huntington, T. G., Sheffield, J., & Hayhoe, K. (2007). *Impacts of Climate Change on Wintertime Precipitation, Snowmelt Regime, Surface Runoff and Infiltration in the Northeastern USA during the 21st Century*. Paper presented at the 64th Eastern Snow Conference, St. John's, Newfoundland, Canada.

Huntington, T. G., Richardson, A. D., McGuire, K. J., & Hayhoe, K. (2009). Climate and hydrological changes in the northeastern United States: recent trends and implications for forested and aquatic ecosystems. *Canadian Journal of Forest Research, 39*, 199-212.

Huntington, T. G., Sheffield, J., & Hayhoe, K. (2007). *Impacts of Climate Change on Wintertime Precipitation, Snowmelt Regime, Surface Runoff and Infiltration in the Northeastern USA during the 21st Century*. Paper presented at the 64th Eastern Snow Conference, St. John's, Newfoundland, Canada.

Intergovernmental Panel on Climate Change, 2014, Climate Change 2014: Impacts, Adaptation and Vulnerability: Summary for Policymakers, downloaded from: http://ipcc-wg2.gov/AR5/images/uploads/WG2AR5_SPM_FINAL.pdf

Ishee ER, Ross DS, Garvey KM, Bourgault RR, Ford CR. 2015. Phosphorus characterization and contribution from eroding streambank soils of Vermont's Lake Champlain basin. Journal of Environmental Quality 44. DOI:10.2134/jeq2015.02.0108.

Isles, P. D. F., C. D. Giles, T. A. Gearhart, Y. Xu, G. K. Druschel, and A. W. Schroth (2015), Dynamic internal drivers of a historically severe cyanobacteria bloom in Lake Champlain revealed through comprehensive monitoring, *J. Great Lakes Res.*, 41(3), 818–829, doi:10.1016/j.jglr.2015.06.006.

Isles, P. D. F., Y. Xu, J. Stockwell, A. W. Schroth (2017), Climate-driven changes in energy and mass inputs systematically alter nutrient concentration and stoichiometry in deep and shallow regions of Lake Champlain, *Biogeochemistry*, 133, 201–217, doi:10.1007/s10533-017-0327-8.

Jackson W. L., R. L. Beschta (1982), A model of two-phase bedload transport in an Oregon Coast Range stream, *Earth Surf. Process. Landf.*, 7, 517–527, doi: 10.1002/esp.3290070602.

James, L. A. (2013). Legacy sediment: Definitions and processes of episodically produced anthropogenic sediment. *Anthropocene*, *2*, 16–26.

Jaquith, S., and M. Kline, 2001, Vermont regional hydraulic geometry curves: Waterbury, VT, Vermont Water Quality Division, accessed March 6, 2003 (http://www.anr.state.vt.us/dec/waterq/rivers/docs/rv_hydraulicgeocurves.pdf),.

Jaquith, S., and M. Kline, 2006, Vermont regional hydraulic geometry curves: Waterbury, VT, Vermont Water Quality Division, accessed November 21, 2017: http://dec.vermont.gov/sites/dec/files/wsm/rivers/docs/assessment-protocol-appendices/J-Appendix-J-06-Hydraulic-Geometry-Curves.pdf.

Jarvie, H. P., M. D. Jurgens, R. J. Williams, C. Neal, J. J. L. Davies, C. Barrett, and J. White (2005), Role of river bed sediments as sources and sinks of phosphorus across two major eutrophic UK river basins: the Hampshire Avon and Herefordshire Wye, *J. Hydrology*, 304(1-4), 51-74, doi:10.1016/j.jhydrol.2004.10.002.

Jennings, K.L., 2001, Depositional Histories of Vermont Alluvial Fans: MS Thesis, University of Vermont, Burlington, VT.

Jones J. A., and G. E. Grant (1996), Peak flow responses to clear-cutting and roads in small and large basins, western Cascades, Oregon, *Water Resources Research*, 32, 959–974, doi:10.1029/95WR03493.

Karl, T. R., & Knight, R. W. (1998). Secular trends of precipitation amount, frequency, and intensity in the United States. *Bulletin of the American Meteorological Society, 79*, 231-241

Karwan, D. L. and J. E. Saiers (2009), Influences of seasonal flow regime on the fate and transport of fine particles and a dissolved solute in a New England stream, *Water Resour. Res.*, 45, W11423, doi:10.1029/2009WR008077.

Karymbalis, E., K. Gaki-Papanastassiou and M. Ferentinou (2010), Fan deltas classification coupling morphometric analysis and artificial neural networks: The case of NW coast of Gulf of Corinth, Greece, *Hellenic Journal of Geosciences*, 45, 133-146.

Kennard, M. J., S. J. Mackay, B. J. Pusey, J. D. Olden and N. Marsh (2010), Quantifying Uncertainty in Estimation of Hydrologic Metrics for Ecohydrological Studies, *River Res. Appl.*, 26, 137-156, doi:10.1002/rra.1249.

Kirchner, J. W. (2006), Getting the right answers for the right reasons: Linking measurements, analyses, and models to advance the science of hydrology, *Water Resour. Res*., 42, W03S04, doi:10.1029/2005WR004362.

Kirchner, J. W., X. H. Feng, C. Neal, and A. J. Robson (2004), The fine structure of water-quality dynamics: The (high-frequency) wave of the future, *Hydrol. Processes*, 18, 1353– 1359, doi:10.1002/hyp.5537.

Kline, M. 2010. Vermont ANR River Corridor Planning Guide: to Identify and Develop River Corridor Protection and Restoration Projects, 2nd edition. Vermont Agency of Natural Resources. Waterbury, Vermont.

Kline, M., & Cahoon, B. (2010). Protecting River Corridors in Vermont. *Journal of the American Water Resources Association, 1*(10). doi: 10.1111/j.1752-1688.2010.00417.x

Kline, M., C. Alexander, S. Pytlik, S. Jaquith, and S. Pomeroy, 2009. Vermont Stream Geomorphic Assessment Protocol Handbooks. Vermont Agency of Natural Resources, Waterbury, Vermont. http://dec.vermont.gov/watershed/rivers/river-corridor-and-floodplain-protection/geomorphic-assessment

Knighton, D., 1998, Fluvial Forms and Processes. New York, NY: Routledge, 383 pp.

Koch, R. W., and G. M. Smillie (1986), Bias in hydrologic prediction using log-transformed regression models, *Water Resources Bulletin*, 22(5), 717–723, doi:10.1111/j.1752-1688.1986.tb00744.x.

Kohonen, T. (1990), The Self-Organizing Map, *Proceedings of the IEEE*, 78(9), 1464-1480.

Kohonen, T. (2001), *Self-organizing maps* (3rd ed.), Springer, Berlin–Heidelberg, Germany.

Kohonen, T. (2013), Essentials of the Self-Organizing Map, *Neural Networks*, 37, 52-65, doi:10.1016/j.neunet.2012.09.018.

Koiter, A.J., D.A. Lobb, P.N. Owens, E.L.Petticrew, K. Tiessen, S. Li (2013), Investigation the role of scale and connectivity in assessing the sources of sediment in an agricultural watershed in the Canadian prairies using sediment source fingerprinting, J. Soils Sediments, 13: 1676-1691.

Kondolf, G. M. (1997), PROFILE: Hungry Water: Effects of Dams and Gravel Mining on River Channels, *Environmental Management*, 21(4), 533-551, doi:10.1007/s002679900048.

Krishnaswamy, J., M. Lavine, D. D. Richter, and K. Korfmacher (2000), Dynamic modeling of long term sedimentation in the Yadkin River Basin, *Adv. Water Resourc.*, 23(8), 881-892, doi:10.1016/S0309-1708(00)00013-0.

Kruschke, J. K. (2015), *Doing Bayesian Data Analysis: A Tutorial with R, JAGS, and Stan* (2nd Ed.), Academic Press / Elsevier, Boston, MA.

Lake Champlain Basin Program, 2012, State of the Lake and Ecosystem Indicators Report, downloaded from: http://www.lcbp.org/wp-content/uploads/2013/05/SOL2012-web.pdf

Lane, E.W. 1955. The Importance of Fluvial Morphology in Hydraulic Engineering, American Society of Civil Engineering, Proceedings, 81, paper 745: 1-17.

Langendoen, E. J., A. Simon, L. Klimetz, N. Bankhead, and M. E. Ursic (2012), Quantifying sediment loadings from streambank erosion in selected agricultural watersheds draining to Lake Champlain, (Lake Champlain Basin Program Technical Report No. 72, 65 pp.). Burlington, VT.

Larsen, F.D., 1987. History of glacial lakes in the Dog River Valley, central Vermont: Westerman, D.S., ed., Guidebook for Field Trips in Vermont, Volume 2: New England Intercollegiate Geologic Conference, 79th annual meeting, Northfield, Vermont.

Lawler, D. M., G. E. Petts, I. D. L. Foster, and S. Harper (2006), Turbidity dynamics during spring storm events in an urban headwater river system: The Upper Tame, West Midlands, UK, *Sci Total Environ.*, 360, 109-126, doi:10.1016/j.scitotenv.2005.08.032.

Lea, D.M.; Legleiter, C.J. Mapping spatial patterns of stream power and channel change along a gravel-bed river in northern Yellowstone. Geomorphology 2016, 252, 66–79.

Lenzi, M.A., Mao, L., Comiti, F., (2006), Effective discharge for sediment transport in a mountain river: computational approaches and geomorphic effectiveness. *J. Hydrol.* 326, 257–276.

Leopold, L. B., (1994), A View of the River, Cambridge, Massachusetts: Harvard University Press.

Leopold, L.B., Maddock, T., 1953. The Hydraulic Geometry of Stream Channels and Some Physiographic Implications. Professional Paper 252. US Geological Survey, Washington, DC.

Leopold, L.B., M.G. Wolman and J.P. Miller, (1995), Fluvial Processes in Geomorphology. Dover Publications. ISBN 0-486-68588-8.

Lisenby, P. E., and K. Fryirs (2016), Catchment- and reach-scale controls on the distribution and expectation of geomorphic channel adjustment, *Water Resour. Res*., 52, 3408–3427, doi:10.1002/2015WR017747.

Livers, B. and E. Wohl (2015), An evaluation of stream characteristics in glacial versus fluvial process domains in the Colorado Front Range, *Geomorphology*, 231, 72–82.

Ley, R., M. C. Casper, H. Hellebrand, and R. Merz (2011), Catchment classification by runoff behaviour with self-organizing maps (SOMs), *Hydrol. Earth Syst. Sci.*, 15, 2947-2962, doi:10.5194/hess-15-2947-2011.

Lisenby, P. E., and K. Fryirs (2016), Catchment- and reach-scale controls on the distribution and expectation of geomorphic channel adjustment, *Water Resour. Res*., 52, 3408–3427, doi:10.1002/2015WR017747.

Livers, B. and E. Wohl (2015), An evaluation of stream characteristics in glacial versus fluvial process domains in the Colorado Front Range, *Geomorphology*, 231, 72–82.

Lloyd, C. E., J. E. Freer, P. J. Johnes, and A. L. Collins (2016), Using hysteresis analysis of high-resolution water quality monitoring data, including uncertainty, to infer controls on nutrient and sediment transfer in catchments, *Sci Total Environ.*, 543(Pt A), 388-404. doi: 10.1016/j.scitotenv.2015.11.028.

Lumia, R., D. A. Freehafer, and M. J. Smith (2006), Magnitude and Frequency of Floods in New York, *Scientific Investigations Report 2006–5112*, U.S. Geological Survey, Washington, D.C.

Magilligan, F.J., 1992. Thresholds and the spatial variability of flood power during extreme floods. Geomorphology 5, 373–390.

Magilligan, F.J., Nislow, K.H., Graber, B.E., 2003. Scale-independent assessment of discharge reduction and riparian disconnectivity following flow regulation by dams. Geology. v. 31, no. 7, pp 569-572.

Magilligan, F., Haynie, H., Nislow, K., 2008. Channel adjustments to dams in the Connecticut River basin: implications for forested mesic watersheds. Ann. Assoc. Am. Geogr. 98, 267–284.

Magilligan, F.J., E.M. Buraas, C.E. Renshaw, 2015. The efficacy of streampower and flow duration on geomorphic responses to catastrophic flooding. Geomorphology, 228, 175-188.

Mangiameli, P., S. K. Chen, and D. West (1996), A comparison of SOM neural network and hierarchical clustering methods, *Eur. J. Oper. Res*., 93(2), 402–417, doi:10.1016/0377-2217(96)00038-0.

Martinez-Carreras, N., A. Krein, F. Gallart, J.F. Iffly, L. Pfister, L. Hoffmann, and P.N. Owens. 2010. Assessment of different colour parameters for discriminating potential suspended sediment sources and provenance: A multi-scale study in Luxembourg. Geomorphology 118:118–129. doi:10.1016/j.geomorph.2009.12.013

Matisoff, G, E. C. Bonniwell and P.J. Whiting (2002), Soil erosion and sediment sources in an Ohio watershed using beryllium-7, cesium-137, and lead-210, *J. Environ. Qual.,* 31, 54–61.

Matisoff, G., C.G. Wilson and J. Whiting (2005), The $^{7}Be/^{210}Pb_{xs}$ ratio as an indicator of suspended sediment age or fraction new sediment in suspension, *Earth Surf. Processes Landforms*, 30, 1191–1201, doi: 10.1002/esp.1270.

McClain, M.E, E. W. Boyer, C. L. Dent, S. E. Gergel, N. B. Grimm, P. M. Groffman, S. C. Hart, J. W. Harvey, C. A. Johnston, E. Mayorga, W. H. McDowell, and G. Pinay. 2003, Biogeochemical Hot Spots and Hot Moments at the Interface of Terrestrial and Aquatic Ecosystems, *Ecosystems*, 6: 301-312.

McDonnell, J. J., M. Sivapalan, K. Vache´, S. Dunn, G. Grant, R. Haggerty, C. Hinz, R. Hooper, J. Kirchner, M. L. Roderick, J. Selker, and M. Weiler (2007), Moving beyond heterogeneity and process complexity: A new vision for watershed hydrology, *Water Resour. Res*., 43, W07301, doi:10.1029/2006WR005467.

Meade, R.H., 1982. Sources, sinks and storage of river sediment in the Atlantic drainage of the United States. Journal of Geology, 90: 235-252.

Medalie, L. (2013), Concentration, flux, and the analysis of trends of total and dissolved phosphorus, total nitrogen, and chloride in 18 tributaries to Lake Champlain, Vermont and New York, 1990–2011, *Scientific Investigations Report 2013–5021*, U.S. Geological Survey, Washington, D. C., http://pubs.usgs.gov/sir/2013/5021/.

Medalie, L. (2014), Concentration and flux of total and dissolved phosphorus, total nitrogen, chloride, and total suspended solids for monitored tributaries of Lake Champlain, 1990–2012, *Open-File Report 2014–1209*, U.S. Geological Survey, Washington, D. C., doi:10.3133/ofr20141209.

Medalie, L., R. M. Hirsch, and S. A. Archfield (2012), Use of flow-normalization to evaluate nutrient concentration and flux changes in Lake Champlain tributaries, 1990–2009, *J. Great Lakes Res.*, 38, 58-67, doi:10.1016/j.jglr.2011.10.002.

Meybeck, M., and F. Moatar (2012), Daily variability of river concentrations and fluxes: indicators based on the segmentation of the rating curve, *Hydrol. Processes*, 26, 1188-1207, doi:10.1002/hyp.8211.

Michaelides ,K., A. Chappell, 2009, Connectivity as a concept for characterizing hydrological behavior. Hydrological Processes, 23 (517-522).

Miller, A.J., 1990. Flood hydrology and geomorphic effectiveness in the Central Appalachians. Earth Surf. Process. Landf. 15, 119–134.

Moatar, F., B. W. Abbott, C. Minaudo, F. Curie, and G. Pinay (2017), Elemental properties, hydrology, and biology interact to shape concentration-discharge curves for carbon, nutrients, sediment, and major ions, *Water Resour. Res*., 53, 1270–1287, doi:10.1002/2016WR019635

Montgomery, D. R. (1999), Process domains and the river continuum, *Journal of the American Water Resources Association*, 35(2), 397–410.

Montgomery, D.R. and Buffington, J.M., (1997), Channel-reach morphology in mountain drainage basins, *Geological Society of America Bulletin*, 109 (5), 596-611.

Moore, J. W., & Semmens, B. X. (2008). Incorporating uncertainty and prior information into stable isotope mixing models. Ecology Letters, 11(5), 470-480.

Moyeed, R. A., and R. T. Clark (2005), The use of Bayesian methods for fitting rating curves, with case studies, *Adv. Water Resourc.*, 28, 807-818, 10.1016/j.advwatres.2005.02.005.

Mukundan, R., D.E. Radcliffe, J.C. Ritchie, L. M. Risse, R.A. McKinley (2010), Sediment fingerprinting to determine the source of suspended sediment in a southern Piedmont stream, *J. Environmental Quality*, 39, 1328–1337.

Mulholland, P. J., E. R. Marzolf, J. R. Webster, D. R. Hart, and S. P. Hendricks (1997), Evidence that hyporheic zones increase heterotrophic metabolism and phosphorus uptake in forest streams, *Limnol. Oceanogr*., 42(3), 443–451.

Musolff, A., C. Schmidt, B. Selle, and J. H. Fleckenstein (2015), Catchment Contols on Solute Export, *Adv. Water Resourc.*, 86, 133-146, doi:10.1016/j.advwatres.2015.09.026.

Nanson, G. C. (1986), Episodes of vertical accretion and catastrophic stripping — a model of disequilibrium floodplain development, *Geol. Soc. Am. Bull*., 97, 1467–1475, doi:10.1130/0016-7606(1986)97<1467:EOVAAC>2.0.CO;2.

Nanson, G.C. and J.C. Croke (1992), A genetic classification of floodplains, *Geomorphology*, 4(6), 459-486.

Nash, D. B. (1994), Effective Sediment-Transporting Discharge from Magnitude-Frequency Analysis, *J. Geology*, 102(1), 79-95, doi:10.1086/629649.

National Research Council, 2000, Clean coastal waters understanding and reducing the effects of nutrient pollution: Washington, D.C., National Academy Press, 405 p.

National Research Council (2002), Riparian Areas: Functions and Strategies for Management, Natl. Acad. Press, Washington, D. C.

Nelder, J. A., and R. W. M. Wedderburn (1972), Generalized linear models, *Journal of the Royal Statistical Society: Series A (General)*, 135(3), 370-384.

Noe, G. B. and C. R. Hupp (2005), Carbon, nitrogen, and phosphorus accumulation in floodplains of Atlantic coastal plain rivers, USA, *Ecological Applications*, 15(4), 1178-1190.

Nosrati, K., A. L. Collins, M. Madankan, 2018, Fingerprinting sub-basin spatial sediment sources using different multivariate statistical techniques and the Modified MixSIR model, *Catena*, 164, 32-43, doi: 10.1016/j.catena.2018.01.003.

Oksanen, J., F. G. Blanchet, M. Friendly, R. Kindt, P. Legendre, D. McGlinn, P. R. Minchin, R. B. O'Hara, G. L. Simpson, P. Solymos, M. Henry, H. Stevens, E. Szoecs and H. Wagner, (2017), vegan: Community Ecology Package. R package version 2.4-3, https://CRAN.R-project.org/package=vegan.

Olson, S. A. (2014), Estimation of flood discharges at selected annual exceedance probabilities for unregulated, rural streams in Vermont, *with a section on* Vermont regional skew regression, by Veilleux, A. G., *Scientific Investigations Report 2014–5078*, U.S. Geological Survey, Washington, D. C., doi:10.3133/sir20145078.

Owens, P. N., W.H. Blake, L.Gaspar, D. Gateuille, A.J. Koiter, D.A. Lobb, E.L. Petticrew, D.G.Reiffarth, H.G. Smith, J.C. Woodward (2018), Fingerprinting and tracing the sources of soils and sediments: Earth and ocean science, geoarchaeological, forensic, and human health applications, Earth-Science Reviews, 162, 1-23, doi: 10.1016/j.earscirev.2016.08.012.

Park, Y.-S., R. Cereghino, A. Compin, and S. Lek (2003), Applications of artificial neural networks for patterning and predicting aquatic insect species richness in running waters, *Ecological Modelling*, 160, 265-280, doi:10.1016/j.ecoinf.2015.08.011.

Parker, C., C.R. Thorne, and N. J. Clifford (2014), Development of ST:REAM: a reach-based stream power balance approach for predicting alluvial river channel adjustment, *Earth Surface Processes and Landforms*, doi: 10.1002/esp.3641.

Parker, C., Clifford, N.J., Thorne, C.R., (2011), Understanding the influence of slope on the threshold of coarse grain motion: revisiting critical stream power, *Geomorphology*, 126, 51–65.

Parnell, A. C., R. Inger, S. Bearhop, and A. L. Jackson. 2010. Source partitioning using stable isotopes: coping with too much variation. PLoS ONE 5:e9672.

Paulson, R. W., E.B. Chase, R.S. Roberts, D.W. Moody, 1989, National Water Summary 1988-89—Hydrologic Events and Floods and Droughts. USGS Water-Supply Paper 2375, https://pubs.usgs.gov/wsp/2375/report.pdf.

Pearce, A. R., D. M. Rizzo, and P. J. Mouser (2011), Subsurface characterization of groundwater contaminated by landfill leachate using microbial community profile data and a non-

parametric decision making process, *Water Resour. Res*., 47(6), W06511, doi:10.1029/2010WR009992.

Pearce, A. R., D. M. Rizzo, M. C. Watzin, and G. K. Druschel (2013), Unraveling Associations between Cyanobacteria Blooms and In-Lake Environmental Conditions in Missisquoi Bay, Lake Champlain, USA, Using a Modified Self-Organizing Map, *Environ. Sci. Technol.*, 47, 14267−14274, doi:10.1021/es403490g.

Pechenick AM, Rizzo DM, Morrissey LA, Garvey KM, Underwood KL, Wemple BC. 2014. A multi-scale statistical approach to assess the effects of connectivity of road and stream networks on geomorphic channel condition. Earth Surface Processes and Landforms 39: 1538–1549. DOI:10.1002/esp.3611.

Pfankuch, D. J. (1975), Stream reach inventory and channel stability evaluation. U.S. Department of Agriculture Forest Service. Region 1. Missoula, Montana.

Phillips, J.D. (2003), Sources of nonlinearity and complexity in geomorphic systems. *Progress in Physical Geography*, 26, 339–361, doi:10.1191/0309133303pp340ra.

Phillips, R.T.J., J. R. Desloges (2014a), Glacially conditioned specific stream powers in low-relief river catchments of the southern Laurentian Great Lakes, *Geomorphology*, 206, 271–287, doi:10.1016/j.geomorph.2013.09.030.

Phillips, R.T.J., J. R. Desloges (2014b), Alluvial floodplain classification by multivariate clustering and discriminant analysis for low-relief glacially conditioned river catchments, *Earth Surf. Process. Landforms*, doi:10.1002/esp.3681.

Phillips, J.M., M.A. Russell, D.E. Walling, (2000), Time-integrated sampling of fluvial suspended sediment: a simple methodology for small catchments, *Hydrological Processes*, 14: 2589-2602.

Pickup, G., Rieger, W.A., 1979. A conceptual model of the relationship between channel characteristics and discharge. Earth Surface Processes 4, 37–42.

Pizzuto, J. E. (2014), Long-term storage and transport length scale of fine sediment: Analysis of a mercury release into a river, *Geophys. Res. Lett*., 41, 5875–5882, doi:10.1002/2014GL060722.

Plummer, M. (2003), JAGS: A program for analysis of Bayesian graphical models using Gibbs sampling. In *Proceedings of the 3rd international workshop on distributed statistical computing (dsc 2003), Vienna, Austria*. ISSN 1609-395X.

Plummer, M. (2016), Rjags: Bayesian Graphical Models using MCMC. R package version 4-6. URL: https://CRAN.R-project.org/package=rjags.

Plummer, M., N. Best, K. Cowles, and K. Vines (2006), CODA: Convergence Diagnosis and Output Analysis for MCMC, *R News*, 6, 7-11, https://www.r-project.org/doc/Rnews/Rnews_2006-1.pdf.

Poeppl, Ronald E., M. Keiler, K. Von El Verfeldt, I. Zweimueller, and T. Glade (2012), The Influence of Riparian Vegetation Cover on Diffuse Lateral Sediment Connectivity and Biogeomorphic Processes in a Medium-Sized Agricultural Catchment, Austria. Geografiska Annaler: Series A, Physical Geography, 94 (4), p 511-529.

Poff, N. L., J. D. Allan, M. B. Bain, J. R. Karr, K. L. Pres-tegaard, B. D. Richter, R. E. Sparks, and J. C. Stromberg. 1997. The natural flow regime: a paradigm for river con-servation and restoration. BioScience 47:769-784.

Pringle, C. (2003). What is hydrologic connectivity and why is it ecologically important? *Hydrological Processes, 17,* 2685–2689.

Prowse, T.D., J. M. Culp (2003), Ice breakup: a neglected factor in river ecology, *Can. J. Civ. Eng*., 30, 128–144, doi:10.1139/L02-040.

Qian, S. S, and T. F. Cuffney (2012), To threshold or not to threshold? That's the question, *Ecological Indicators*, 15, 1–9, doi:10.1016/j.ecolind.2011.08.019.

Qian, S. S., and C. J. Richardson (1997), Estimating the long-term phosphorus accretion rate in the Everglades: a Bayesian approach with risk assessment, *Water Resour. Res*., 33, 1681-1688, doi:10.1029/97WR00997.

Qian, S. S., K. H. Reckhow, J. Zhai, and G. McMahon (2005), Nonlinear regression modeling of nutrient loads in streams: A Bayesian approach, *Water Resour. Res*., 41, W07012, doi:10.1029/2005WR003986.

R Core Team, (2018), R: A language and environment for statistical computing. R Foundation for Statistical Computing, Vienna, Austria, ISBN 3-900051-07-0, URL: http://www.R-project.org/.

Randall, A. D. (1996), Mean annual runoff, precipitation, and evapotranspiration in the glaciated northeastern United States, 1951–1980, *Open-File Report 96-395,* U.S. Geological Survey, Washington, D.C.

Rapp C., Abbe T. (2003) A Framework for Delineating Channel Migration Zones. Washington State Department of Ecology & Washington State Department of Transportation: Ecology Final Draft Publication #03-06-027. https://fortress.wa.gov/ecy/publications/documents/0306027.pdf

Ratcliffe, N.M., Stanley, R.S, Gale, M.H., Thompson, P.J., and Walsh, G.J., 2011, Bedrock Geologic Map of Vermont: U.S. Geological Survey Scientific Investigations Map 3184,

Raven, P.J., N. Holmes, F.H. Dawson, P.J.A. Fox, M. Everard, I.R. Fozzard, K.J. Rouen (1998), River Habitat Quality: the physical character of rivers and streams in the UK and Isle of Man. River Habitat Survey Report No. 2, Environment Agency.

Reid, I., J. C. Bathurst, P. A. Carling, D. E. Walling, B. W. Webb (1997), Sediment erosion, transport and deposition, in *Applied fluvial geomorphology for river engineering and management*: edited by C. R. Thorne, R. D. Hey, G. P. Williams, pp. 95–135, John Wiley, New York, NY.

Reum, J. C. P., G. D. Williams and C. J. Harvey (2017), Stable Isotope Applications for Understanding Shark Ecology in the Northeast Pacific Ocean, *Northeast Pacific Shark Biology, Research and Conservation Part A,* 10.1016/bs.amb.2017.06.003, 149-178).

Rice, S.P., Church, M., 1996, Sampling surficial fluvial gravels: the precision of size distribution percentile estimates. Journal of Sedimentary Research. 66(3): 654-665.

Rice, S.P., Church, M., 1998. Grain size along two gravel-bed rivers: Statistical variation, spatial pattern and sedimentary links. Earth Surface Processes and Landforms 23: 345-363.

Ridge, John C., 2003, The Last Deglaciation of the Northeastern United States: A Combined Varve, Paleomagnetic, and Calibrated 14C Chronology, in Geoarchaeology of Landscapes in the Glaciated Northeast. Cremeens, David L. and Hart, John P, Ed. Albany, NY: New York State Museum Bulletin 497.

Ries, K. G. and P. J. Friesz (2000), Methods for Estimating Low-Flow Statistics for Massachusetts Streams, *Water-Resources Investigations Report 00-4135*, U S. Geological Survey, Washington, D.C., https://pubs.usgs.gov/wri/wri004135/.

Righini, M., Surian, N.,Wohl, E., Marchi, L., Comiti, F., Amponsah, W., Borga, M., 2017. Geomorphic response to an extreme flood in two Mediterranean rivers (northeastern Sardinia, Italy): analysis of controlling factors. Geomorphology 290:184–199, doi:10.1016/j.geomorph.2017.04.014.

Rinaldi, M., N. Surian, F. Comiti, M. Bussettini (2013), A method for the assessment and analysis of the hydromorphological condition of Italian streams: the Morphological Quality Index (MQI), *Geomorphology*, 180-181, 96–108.

Ritchie, J. C. and G. W. McHenry (1990), Application of radioactive fallout cesium-137 for measuring soil erosion and sediment accumulation rates and patterns: a review. J. Environ. Qual., 19, 215-233.

Rizzo, D. M. and D.E. Dougherty, 1994, Characterization of aquifer properties using artificial neural networks: Neural kriging. *Water Resources Research* 30 (2): 483-497.

Rosgen, D. (1996), Applied Fluvial Morphology, Wildland Hydrology Books, Pagosa Springs, CO. ISBN 0 965 32890 2.

Rosgen, D., (2006), Watershed Assessment for River Stability and Sediment Supply, WARSSS. Wildland Hydrology Books, Ft. Collins, CO, ISBN 13: 978-0979130809.

Ross, D. S., B. C. Wemple, L. J. Wilson, C. Balling, K. L. Underwood, and S. D. Hamshaw (2018), Impact of an Extreme Storm Event on River Corridor Bank Erosion and Phosphorus Mobilization in a Mountainous Watershed in the Northeastern USA, *J. Geophys. Res. Biogeosci.*, (under review).

Roy, N. G. and R. Sinha (2014), Effective discharge for suspended sediment transport of the Ganga River and its geomorphic implication, *Geomorphology*, 227, 18-30, doi:10.1016/j.geomorph.2014.04.029.

Ryan, S. E., L. S. Porth, C. A. Troendle (2002), Defining phases of bedload transport using piecewise regression, *Earth Surf. Process. Landf.*, 27, 971-990, doi:10.1002/esp.387.

Schmelter, M. L., S. O. Erwin, P. R. Wilcock (2012), Accounting for uncertainty in cumulative sediment transport using Bayesian statistics, *Geomorphology*, 175-176(15), 1-13, doi: 10.1016/j.geomorph.2012.06.012.

Schumm, S.A. (1984), The Fluvial System. New York, NY: John Wiley and Sons.

Schumm, S.A. (2005), River Variability and Complexity, New York, NY: Cambridge University Press.

Schumm, S.A., Harvey, M.D., and Watson, C.C., (1984), Incised Channels Morphology, Dynamics and Control. Water Resources Publications: Littleton, CO.

Schumm SA, Rea DK (1995), Sediment yield from disturbed earth systems, *Geology*, 23, 391-394.

Semmens, B. X. and J.W. Moore (2008), MixSIR: A Bayesian stable isotope mixing model, Version 1.0. http://www.ecologybox.org.

Shanley, J. B., & Chalmers, A. (1999). The effect of frozen soil on snowmelt runoff at Sleepers River, Vermont. *Hydrological Processes, 13*, 1843-1858.

Shanley, J. B., & Denner, J. C. (1999). The hydrology of the Lake Champlain Basin. In T. O. Manley & P. L. Manley (Eds.), *Lake Champlain in transition-From research toward restoration* (Vol. 1, pp. 41-66): American Geophysical Union, Water Science and Application.

Shanley, J. B., W. H. McDowell, and R. F. Stallard (2011), Long-term patterns and short-term dynamics of stream solutes and suspended sediment in a rapidly weathering tropical watershed, *Water Resour. Res*., 47, W07515, doi:10.1029/2010WR009788.

Sharpley, A., H. P. Jarvie, A. Buda, L. May, B. Spears, and P. Kleinman (2013), Phosphorus legacy: overcoming the effects of past management practices to mitigate future water quality impairment, *J Environ Qual*, *42*(5), 1308-1326, doi: 10.2134/jeq2013.03.0098.

Simon, A. and Hupp, C., 1986, Channel evolution in modified Tennesee channels in Proceedings of the 4th Federal Interagency Sedimentation Conference, Las Vegas US Government Printing Office, Washington, DC, 571-582.

Simon, A. and Rinaldi M, 2006. Disturbance, stream incision, and channel evolution: the roles of excess transport capacity and boundary materials in controlling channel response . Geomorphology 79 361–83.

Simon, A., Doyle, M., Kondolf, M., Shields Jr., F., Rhoads, B., & Mcphillips, M. (2007). Critical evaluation of how the Rosgen Classification and associated "Natural Channel Design" methods fail to integrate and quantify fluvial processes and channel response. *Journal of the American Water Resources Association*, 1117-1131.

Skalak, K., and J. Pizzuto (2010), The distribution and residence time of suspended sediment stored within the channel margins of a gravel-bed bedrock river, *Earth Surf. Process. Landf*., 35, 435–446, doi:10.1002/esp.1926.

Smeltzer, E., A. D. Shambaugh, P. Stangel (2012), Environmental change in Lake Champlain revealed by long-term monitoring, *J. of Great Lakes Research*, 38, 6–18, doi:10.1016/j.jglr.2012.01.002.

Smith, H.G., and W.H. Blake. 2014. Sediment fingerprinting in agricultural catchments: A critical re-examination of source discrimination and data corrections. Geomorphology 204:177–191. doi:10.1016/j.geomorph.2013.08.003

Somerville, D.E. and B.A. Pruitt, 2004. Physical Stream Assessment: A Review of Selected Protocols for Use in the Clean Water Act Section 404 Program. September 2004. Prepared for the U.S. Environmental Protection Agency, Office of Wetlands, Oceans, and Watersheds, Wetlands Division (Order No. 3W-0503-NATX). Washington, D.C., 213 pp.

Spiegelhalter, D. J., N. G. Best, B. P. Carlin, and A. van der Linde (2002), Bayesian measures of model complexity and fit (with discussion), *J. R. Statist. Soc.*, 64, 583–639, doi: 10.1111/1467-9868.00353.

Springston et al, 2011, Fluvial Geomorphology of the Middlebury River Watershed: Geologic Controls, Assessment of Stream Channel Stability, and River Corridor Restoration. Trip B5. Guidebook for Field Trips in Vermont and Adjacent New York. New England Intercollegiate Geological Conference.

Stewart, D.P. and P. MacClintock, 1969, The Surficial Geology and Pleistocene History of Vermont. Vermont Geological Survey Bulletin No. 31.

Stock, B. C. and B.X. Semmens (2016). MixSIAR GUI User Manual. Version 3.1. https://github.com/brianstock/MixSIAR. doi:10.5281/zenodo.1209993.

Stojkovica, M., V. Simic, D. Milosevic, D. Mancev, T. Penczak (2013), Visualization of fish community distribution patterns using the self-organizing map: A case study of the Great Morava River system (Serbia), *Ecological Modelling*, 248, 20-29, doi:10.1016/j.ecolmodel.2012.09.014.

Stow, C. A., K. H. Reckhow, and S. S. Qian (2006), A Bayesian Approach to Retransformation Bias in Transformed Regression, *Ecology*, 87(6), 1472–1477, doi:10.1890/0012-9658(2006)87[1472:ABATRB]2.0.CO;2.

Stryker, J., B. Wemple, A. Bomblies, 2018, Modeling the impacts of changing climatic extremes on streamflow and sediment yield in a northeastern US watershed, Journal of Hydrology: Regional Studies, 17, 83-94.

Stryker, J., B. Wemple, A. Bomblies, 2017, Modeling sediment mobilization using a distributed hydrological model coupled with a bank stability model, *Water Resources Research*, 53, 2051–2073, doi:10.1002/2016WR019143.

Surian, N., Righini, M., Lucía, A, Nardi, L., Amponsah, W., Benvenuti, M., Borga, M., Cavalli, M., Comiti, F., Marchi, L., Rinaldi, M., Viero. A., 2016, Channel response to extreme floods: Insights on controlling factors from six mountain rivers in northern Apennines, Italy. *Geomorphology*, 272: 78-91. doi:10.1016/j.geomorph.2016.02.002.

Syvitski, J. P., M. D. Morehead, D. B. Bahr, and T. Mulder (2000), Estimating Fluvial Sediment Transport: The Rating Parameters, *Water Resour. Res.*, 36(9), 2747-2760, 10.1029/2000WR900133.

Taylor, A., W. H. Blake, H. G. Smith, L. Mabit, M. J. Keith-Roach (2013), Assumptions and challenges in the use of fallout beryllium-7 as a soil and sediment tracer in river basins, Earth-Science Reviews, 126, 85-95, doi: 10.1016/j.earscirev.2013.08.002.

Thayer, J. B., R. T. J. Phillips, J. R. Desloges, 2016. Downstream channel adjustment in a low-relief, glacially conditioned watershed, Geomorphology, 262: 101-111. http://dx.doi.org/10.1016/j.geomorph.2016.03.019.

Thompson CJ, Croke JC. 2013. Geomorphic effects, flood power, and channel competence of a catastrophic flood in confined and unconfined reaches of the upper Lockyer valley, southeast Queensland, Australia. Geomorphology 197: 156–169. DOI: 10.1016/j.geomorph.2013.05.006

Thompson, E. H. and Sorenson, E. R., 2000, Wetland, Woodland, Wildland: A guide to the natural communities of Vermont, Hanover, NH: University Press of New England.

Thompson, S. E., N. B. Basu, J. Lascurain Jr., A. Aubeneau, and P. S. C. Rao (2011), Relative dominance of hydrologic versus biogeochemical factors on solute export across impact gradients, *Water Resour. Res*., 47, W00J05, doi:10.1029/2010WR009605.

Thoms, M.C., M. Parsons (2003), Identifying spatial and temporal patterns in the hydrological character of the Condamine-Balonne River, Australia, using multivariate statistics, *River Res. Applic*., 19, 443-457, doi: 10.1002/rra.737.

Thorp, J. H., M. C. Thoms, M. D. Delong (2006), The Riverine Ecosystem Synthesis: Biocomplexity in river networks across space and time, *River Res. Applic*., 22, 123-147, doi: 10.1002/rra.901.

Todini, E. (2007), Hydrological catchment modelling: past, present, and future, *Hydrol. Earth Syst. Sci*., 11(1), 468-482, doi:10.5194/hess-11-468-2007.

Toone, J., S. Rice, and H. Piégay (2014), Spatial discontinuity and temporal evolution of channel morphology along a mixed bedrock-alluvial river, upper Drôme River, southeast France: Contingent responses to external and internal controls, *Geomorphology*, 205, 5–16, doi:10.1016/j.geomorph.2012.05.033.

Tran, L. T., C. G. Knight, R. V. O'Neill, E. R. Smith, and M. O'Connell (2003), Self-Organizing Maps for Integrated Environmental Assessment of the Mid-Atlantic Region, *Environmental Management*, 31(6), 822-835.

Trapp, S. E., W. P. Smith and E. A. Flaherty (2017), Diet and food availability of the Virginia northern flying squirrel (Glaucomys sabrinus fuscus): implications for dispersal in a fragmented forest, *Journal of Mammalogy*, 98(6), 1688-1696, doi: 10.1093/jmammal/gyx115.

Trimble, S. W. (1997), Contribution of stream channel erosion to sediment yield from an urbanizing watershed, *Science*, 278, 1442–1444, doi:10.1126/science.278.5342.1442.

Troy, A., D. Wang, D. Capen, J. O'Neil-Dunne, and S. MacFaden (2007), Updating the Lake Champlain Basin Land Use Data to Improve Prediction of Phosphorus Loading, *Technical Report No. 54*, Lake Champlain Basin Program, Grand Isle, VT, http://www.lcbp.org/techreportPDF/54_LULC-Phosphorus_2007.pdf.

Turcotte, B., B. Morse, N. E. Bergeron, A. G. Roy, (2011), Sediment transport in ice-affected rivers, *J. Hydrology*, 409, 561-577, doi: 10.1016/j.jhydrol.2011.08.009.

Turton DJ, Smolen MD, Stebler E. 2009. Effectiveness of BMPS in reducing sediment from unpaved roads in the Stillwater Creek, Oklahoma Watershed1. JAWRA Journal of the American Water Resources Association 45: 1343–1351. DOI:10.1111/j.1752-1688.2009.00367.x.

US Department of Agriculture, 1986. *Urban hydrology for small watersheds*. Technical Release 55 (TR-55) (Second Edition ed.). Natural Resources Conservation Service, Conservation Engineering Division.

U.S. Environmental Protection Agency (2016) Phosphorus TMDLs for Vermont Segments of Lake Champlain. Available at: https://www.epa.gov/tmdl/lake-champlain-phosphorus-tmdlcommitment-clean-water

US Environmental Protection Agency, 2016, "National Summary of State Information" for available water quality data reported by the States to EPA under Section 305(b) and 303(d) of the Clean Water Act. Downloaded July 2016 from: https://iaspub.epa.gov/waters10/attains_nation_cy.control.

USGS (2016), National Water Information System, http://waterdata.usgs.gov/vt/nwis/rt.

de Vente, Joris, J. Poesen, M. Arabkhedri, G. Verstraeten, 2007, The Sediment Delivery Problem Revisited. Progress in Physical Geography, 31(2): 155-178.

VT Agency of Natural Resources, 2009, Stream Geomorphic Assessment Protocol Handbooks, Remote Sensing and Field Surveys Techniques for Conducting Watershed and Reach Level Assessments. Available at: http://www.vtwaterquality.org/rivers/htm/rv_geoassesspro.htm

[dataset] VT Agency of Natural Resources, Stream Geomorphic Assessment Data Management System, 2017, https://anrweb.vt.gov/DEC/SGA/Default.aspx

Vermont Department of Environmental Conservation, 2016, Vermont Rivers & Roads Field Manual: A Guide for Considering the River and Habitat in the Design, Construction and Maintenance of Transportation Infrastructure in Vermont, available at: http://dec.vermont.gov/sites/dec/files/wsm/rivers/docs/2016_ RiverAndRoadFieldManual.pdf.

VTDEC Watershed Management Division, 2012, State of Vermont 2012 Water Quality Integrated Assessment Report, available at: www.waterquality.org

VTDEC (2015), Lake Champlain Long-term Water Quality and Biological Monitoring Program: Program Description, accessed at: https://anrweb.vermont.gov/dec/_dec/ LongTermMonitoringTributary.aspx.

Vesanto, J. and E. Alhoniemi (2000), Clustering of the Self-Organizing Map, *IEEE Transactions on Neural Networks*, 11(3), 586-600.

Vesanto, J., J. Himberg, E. Alhoniemi, and J. Parhankangas (2000), SOM Toolbox for Matlab 5. *Technical Report A57*, Neural Networks Research Centre, Helsinki University of Technology, Helsinki, Finland.

Vigiak, O., and U. Bende-Michl (2013), Estimating bootstrap and Bayesian prediction intervals for constituent load rating curves, *Water Resour. Res*., 49, 8565–8578, doi:10.1002/2013WR013559.

Vocal Ferencevic M, Ashmore P. 2012. Creating and evaluating digital elevation model-based stream-power map as a stream assessment tool. River Research and Applications 28: 1394–1416.

Vogel, R. M., B. E. Rudolph, and R. P. Hooper (2005), Probabilistic Behavior of Water-Quality Loads, *J. Environ. Eng.*, 131(7),1081-1089, doi:10.1061/(ASCE)0733-9372(2005)131:7(1081).

Voli, M., Wehmann, K., Bohnenstiehl, D., Leithold, E., Osburn, C., Polyakov, V.O. (2013), Fingerprinting the sources of suspended sediment delivery to a large municipal drinking water reservoir: Falls Lake, Neuse River, North Carolina, USA, *Journal of Soils and Sediments*, 3, 1692–1707, doi:10.1007/s11368-013-0758-3.

Wang, H., Z. Yang, Y. Wang, Y. Saito, and J.P. Liu (2008), Reconstruction of sediment flux from the Changjiang (Yangtze River) to the sea since the 1860s, *J. Hydrology*, 349, 318-332, doi:10.1016/j.jhydrol.2007.11.005.

Ward, J.V., 1989. The four-dimensional nature of lotic ecosystems. Journal of the North American Benthological Society, 8, p. 2-8.

Wallbrink, P.J. and A.S. Murray (1993) Use of fallout radionuclides as indicators of erosion processes. Hydrol Process 7:297–304

Wallbrink PJ, Olley JM, Murray AS, Olive LJ (1996) The contribution of subsoils to sediment yield in the Murrumbidgee River basin, NSW, Australia, IAHS Publication no. 236. IAHS,Wallingford, pp 347–357

Walling, D. E. (1977), Assessing the accuracy of suspended sediment rating curves for a small basin, *Water Resour. Res.*, 13, 531–538.

Walling, D.E. (1983), The Sediment Delivery Problem, *J. Hydrology*, 65, 209-237.

Walling, D.E. (2013a), The evolution of sediment source fingerprinting investigations in fluvial systems, *J. Soils Sediments*, 1310, 1658-1675.

Walling, D. E. (2013b), Beryllium-7: The Cinderella of fallout radionuclide sediment tracers? Hydrological Processes, 27, 837-844, doi:10.1002/hyp.9546.

Walling, D. E., and Q. He (1999), Using fallout lead-210 measurements to estimate soil erosion on cultivated land, *Soil Sci. Soc. Am. J*., 63, 1404–1412, doi:10.2136/sssaj1999.6351404x.

Walling, D.E. and J.C. Woodward (1992), Use of radiometric fingerprints to derive information on suspended sediment sources. *In* Erosion and sediment transport monitoring programmes in river basins. Publ. 210. IAHS, Wallingford, UK.

Walling, D. E., P. N. Owens, G. J. L. Leeks (1999), Fingerprinting suspended sediment sources in the catchment of the River Ouse, Yorkshire, UK, *Hydrol. Processes*, 13, 955–975.

Walling, D.E., J. C. Woodward, A.P. Nicholas, (1993), A multiparameter approach to fingerprinting suspended sediment sources. In: Tracers in Hydrology, IAHS Publication No. 215, 329–338.

Walter, R.C.,Merritts, D.J., 2008. Natural streams and the legacy of water-powered mills. Science. 319 (5861), 299–304.

Wang, H., Z. Yang, Y. Wang, Y. Saito, and J.P. Liu (2008), Reconstruction of sediment flux from the Changjiang (Yangtze River) to the sea since the 1860s, *J. Hydrology*, 349, 318-332, doi:10.1016/j.jhydrol.2007.11.005.

Ward, J. V. (1989), The four-dimensional nature of lotic ecosystems, *J. N. Am. Benthol. Soc.*, 8, 2-8, doi:10.2307/1467397.

Warrick, J. A. (2014), Trend analyses with river sediment rating curves, *Hydrol. Process*., 29(6), 936–949, doi:10.1002/hyp.10198.

Watson, K., T. Ricketts, G. Galford, S. Polasky, J. O'Niel-Dunne, (2016), Quantifying flood mitigation services: The economic value of Otter Creek wetlands and floodplains to Middlebury, VT, *Ecological Economics*, 130(16-24), doi:10.1016/j.ecolecon.2016.05.015.

Wear LR, Aust WM, Bolding MC, Strahm BD, Dolloff CA. 2013. Effectiveness of best management practices for sediment reduction at operational forest stream crossings. Forest Ecology and Management, 289, 551–561. DOI: http://dx.doi.org/10.1016/j.foreco.2012.10.035

Weber, M. D. and G. B. Pasternack (2017), Valley-scale morphology drives differences in fluvial sediment budgets and incision rates during contrasting flow regimes, *Geomorphology*, 288, 39-51, doi:10.1016/j.geomorph.2017.03.018.

Wehrens, R., and L. M. C. Buydens (2007), Self- and Super-organising Maps in R: the kohonen package. *J. Stat. Softw*. 21 (5), 1-19, https://www.jstatsoft.org/index.

Wemple, B. C., 2013, Assessing the Effects of Unpaved Roads on Lake Champlain Water Quality. LCBP Technical Report No. 74. 67 pp. Available at: http://www.lcbp.org/wp-content/uploads/2013/07/74_Road-Study_revised_June2013.pdf.

Wemple BC, Jones JA, Grant GE (1996), Channel network extension by logging roads in two basins, Western Cascades, Oregon, *Water Resources Bulletin*, 32, 1195–1207.

Wemple, B. C., Clark, G. E., Ross, D. S., & Rizzo, D. M. (2017). Identifying the spatial pattern and importance of hydro-geomorphic drainage impairments on unpaved roads in the northeastern USA. Earth Surface Processes and Landforms, 42(11), 1652–1665, https://doi.org/10.1002/esp.4113

Wethered, A.S., Ralph, T.J., Smith, H.G., Fryirs, K.A., Heijnis, H., 2015. Quantifying fluvial (dis)connectivity in an agricultural catchment using a geomorphic approach and sediment source tracing. J. Soils Sediments. Doi:10.1007/s11368-015-1202-7.

Whalen, T.N., 1998, Post-glacial fluvial terraces in the Winooski Drainage Basin, Vermont. MS Thesis, University of Vermont.

Williams, G. P. (1989), Sediment concentration versus water discharge during single hydrologic events, Journal of Hydrology, 111, 89-106.

Williams, G.P., and Costa, J.E., 1998, Geomorphic measurements after a flood: *In* Baker, V.R., Kochel, R.C., and Patton, P.C., eds., Flood geomorphology: Wiley Interscience, NY: New York, p. 65-77.

Williams, G. P., and M. G. Wolman (1984), Downstream effects of dams on alluvial rivers, *Professional Paper 1286*, United States Geological Survey, Washington, D. C.

Withers, P. J. A. and H. P. Jarvie (2008), Delivery and cycling of phosphorus in rivers: A review, *Sci. Total. Environ.*, 400, 379-395, doi:10.1016/j.scitotenv.2008.08.002.

Wohl, E. (2018), Geomorphic context in rivers, *Progress in Physical Geography*, 1–17, doi: 10.1177/0309133318776488.

Wohl, E. (2010), A brief review of the process domain concepts and its application to quantifying Wohl, E., 2010b. Mountain Rivers Revisited. American Geophysical Union Press, Washington, D.C.

Wohl, E., and N. D. Beckman (2014), Leaky rivers: Implications of the loss of longitudinal fluvial disconnectivity in headwater streams, *Geomorphology*, 205, 27-35, doi:10.1016/j.geomorph.2011.10.022.

Wolman, M. G., and R. Gerson (1978), Relative scales of time and effectiveness of climate in watershed geomorphology, *Earth Surf. Process. Landf.*, 3, 189-208, doi: 10.1002/esp.3290030207.

Wolman, M. G. and J. P. Miller (1960), Magnitude and Frequency of Forces in Geomorphic Processes, *J. Geology*, 68(1), 54-74, doi:10.1086/626637.

Xu, Y., A. W. Schroth, P. D. F. Isles, D. M. Rizzo (2015a), Quantile regression improves models of lake eutrophication with implications for ecosystem-specific management, *Freshw. Biol*., 60, 1841–1853, doi:10.1111/fwb.12615.

Xu, Y., A. W. Schroth, D. M. Rizzo (2015b), Developing a 21st century framework for lake-specific eutrophication assessment using quantile regression, *Limnol. Oceanogr*., 13, 237–249, doi:10.1002/lom3.10021.

Yellen, B., J. D. Woodruff, L. N. Kratz, S. B. Mabee, J. Morrison, and A. M. Martini (2014), Source, conveyance and fate of suspended sediments following Hurricane Irene. New England, USA, *Geomorphology*, *226*, 124-134, doi: 10.1016/j.geomorph.2014.07.028.

Yochum, S. E., J. S. Sholtes, J. A. Scott, B. P. Bledsoe (2017), Stream power framework for predicting geomorphic change: The 2013 Colorado Front Range flood, *Geomorphology*, 292, 178-192, doi:10.1016/j.geomorph.2017.03.004.

You, C., T. Lee, Y. Li (1989). The partition of Be between soil and water, *Chemical Geology*, 77, 105–118.

Zhang, Q., C. J. Harman, and W. P. Ball (2016), An improved method for interpretation of riverine concentration-discharge relationships indicates long-term shifts in reservoir sediment trapping, *Geophys. Res. Lett*., 43, 10,215–10,224, doi:10.1002/2016GL069945.

Zhao, X., F. Li, Z. Ai, J. Li and C. Gu (2018), Stable isotope evidences for identifying crop water uptake in a typical winter wheat–summer maize rotation field in the North China Plain, *Science of The Total Environment*, 618, 121-131, doi: 10.1016/j.scitotenv.2017.10.315.

Zia, A, A. Bomblies, A. W. Schroth, C. Koliba, P. D. F. Isles, Y. Tsai, I. N. Mohammed, G. Bucini, P. J. Clemins, S. Turnbull, M. Rodgers, A. Hamed, B. Beckage, J. Winter, C. Adair, G. L. Galford, D. Rizzo and J. Van Houten (2016), Coupled impacts of climate and land use change across a river–lake continuum: insights from an integrated assessment model of Lake Champlain's Missisquoi Basin, 2000–2040, *Environ. Res. Lett*., 11, 114026, doi:10.1088/1748-9326/11/11/114026.